

Molecular biological investigations on the antagonistic effects of the  
probiotic *Escherichia coli* strain Nissle 1917 towards Shiga toxin  
producing *Escherichia coli*

Molekularbiologische Untersuchungen der antagonistischen Effekte  
des probiotischen *Escherichia coli* Stamms Nissle 1917 auf Shiga-  
Toxin produzierende *Escherichia coli* Stämme



**Doctoral thesis for a doctoral degree at the  
Graduate School of Life Sciences  
Julius-Maximilians-Universität Würzburg**

Section Infection and Immunity

submitted by

**Susanne Bury**

from Fürth

**Würzburg 2018**

**Submitted on:**

.....

**Office stamp**

Members of the *Thesis Committee*:

Chairperson: Prof. Dr. Thomas Dandekar

Primary Supervisor: Dr. Tobias Ölschläger, ADir

Supervisor (Second): PD Dr. Knut Ohlsen

Supervisor (Third): Dr. Ulrich Sonnenborn

**Date of Public Defence:**

**Date of Receipt of Certificates:**

### **Eidesstattliche Erklärung**

Hiermit erkläre ich an Eides statt, die Dissertation "Molekularbiologische Untersuchungen der antagonistischen Effekte des probiotischen Escherichia coli Stamms Nissle 1917 auf Shiga-Toxin produzierende Escherichia coli Stämme" eigenständig, d. h. insbesondere selbstständig und ohne Hilfe eines kommerziellen Promotionsberaters, angefertigt und keine anderen als die von mir angegebenen Quellen und Hilfsmittel verwendet zu haben.

Ich erkläre außerdem, dass die Dissertation weder in gleicher noch in ähnlicher Form bereits in einem anderen Prüfungsverfahren vorgelegen hat.

Würzburg,

*Für meine Familie*

## Danksagung

An dieser Stelle möchte ich meinen besonderen Dank nachstehenden Personen entgegenbringen, ohne deren Mithilfe die Anfertigung dieser Promotionsschrift niemals zustande gekommen wäre.

Ein ganz besonderer Dank gilt meinem Doktorvater Dr. Tobias Ölschläger (*Institut für Molekulare Infektionsbiologie, Universität Würzburg*). Er hat mir ein sehr interessantes Thema bereitgestellt, mir die Möglichkeit gegeben neue Ideen zu verfolgen und mich stets mit seinem fachlichen Rat und ständiger Diskussionsbereitschaft unterstützt. Darüber hinaus hat er mir die Teilnahme an mehreren nationalen sowie internationalen Symposien ermöglicht, auf welchen ich mich mit anderen Experten auf dem Gebiet austauschen konnte.

Des Weiteren möchte ich mich bei Herrn Dr. Ulrich Sonnenborn und Herrn PD Dr. Knut Ohlsen (*Institut für Molekulare Infektionsbiologie, Universität Würzburg*) für die Erstellung des Zweit-, und Drittgutachtens bedanken, sowie für deren Unterstützung durch neue Anregungen bezüglich der Fortführung meines Projekts und für ihren fachlichen Rat.

Ebenfalls bedanken möchte ich mich bei der Graduate School of Life Sciences (GSLs) für die Organisation des Graduiertenprogramms und die Möglichkeit der Teilnahme an abwechslungsreichen Workshops.

Frau Daniela Bunsen und Claudia Gehrig möchte ich für die Unterstützung bei der Elektronenmikroskopie danken.

Ich möchte mich auch bei unserem Techniker Josef Heger bedanken, dass er sich sofort Problemen angenommen hat und man sich stets auf ihn verlassen konnte.

Darüber hinaus möchte ich mich bei der AG Ölschläger bedanken. Insbesondere gilt mein Dank Srikanth Balasubramanian und Manonmani Soundararajan welche in den Jahren meiner Doktorandenzeit enge Freunde von mir geworden sind. Ihre Unterstützung durch Diskussionen über mögliche Experimente oder neue Strategien haben das Thema weit vorangetrieben. Die vielen Momente in denen wir zusammensaßen und lachen konnten haben die Doktorandenzeit zu einer außergewöhnlich schönen Erfahrung gemacht. Unsere Studentinnen Rebekka Kochilas, Juna Knop und Laura Hepp haben mit ihrer herzlichen Art ebenfalls unsere Gruppe bereichert. Der gesamten AG Ziebuhr danke ich für die vielen fröhlichen Momente in unserem Büro.

Meinen Eltern, meiner Schwester und meinen Brüdern möchte ich für die Unterstützung in all den Jahren danken. Es ist ein wundervoller Gedanke zu wissen, dass es Menschen gibt die ohne Wenn und Aber für dich da sind. Meinem Freund Marius Glogger möchte ich für all unsere wunderbaren Momente danken und dafür, dass er immer ein offenes Ohr für mich und meine Gedanken hat. All meinen Freunden (Bazingaaaaa Gruppe) danke ich dafür, dass sie die Jahre in Würzburg zu einer unvergesslichen Zeit für mich gemacht haben.

Abschließender Dank gilt der Ardeypharm GmbH und der Pharma-Zentrale GmbH für das großzügige Stipendium ohne das ich diese Arbeit nicht hätte realisieren können. Ich möchte mich auch bei den Mitarbeitern bedanken, mit denen ich das große Vergnügen hatte zusammenarbeiten zu dürfen. Hierbei sind vor allem Rudolf von Büнау, Birgit Klinkert, Silke Dubbert, Michael Magnus-Werner und Daniela Bunsen zu erwähnen.

## **List of contents**

<b>Summary .....</b>	<b>1</b>
<b>Zusammenfassung.....</b>	<b>3</b>
<b>1. Introduction .....</b>	<b>6</b>
<b>1.1. The human gut microbiota .....</b>	<b>6</b>
<b>1.2. Probiotics.....</b>	<b>7</b>
<b>1.3. <i>Escherichia coli</i> .....</b>	<b>7</b>
1.3.1. Phases of <i>E. coli</i> culture growth .....	8
1.3.2. <i>E. coli</i> categorization.....	8
<b>1.4. <i>E. coli</i> Nissle 1917.....</b>	<b>11</b>
1.4.1. Molecular characteristics of EcN.....	11
<b>1.5. Shiga toxin producing <i>E. coli</i>.....</b>	<b>13</b>
1.5.1. Shiga toxin mode of action .....	13
1.5.2. Clinical outcome of STEC infections .....	14
1.5.3. STEC outbreaks .....	16
1.5.4. O104:H4 outbreak strain.....	16
<b>1.6. Regulation of the Shiga toxin expression.....</b>	<b>17</b>
1.6.1. Lysogenic and lytic <i>stx</i> -phage cycle .....	17
<b>1.7. Bacteriophages .....</b>	<b>19</b>
1.7.1. Phage assembly.....	19
1.7.2. Bacteriophage receptors.....	20
1.7.3. Bacterial lysis and lysogenization.....	21
1.7.4. Bacterial phage defense mechanisms.....	22
<b>1.8. Influence of EcN on STEC strains .....</b>	<b>24</b>
<b>1.9. <i>stx</i>-phages in the microbiota .....</b>	<b>25</b>
<b>1.10. Aim of the thesis.....</b>	<b>26</b>
<b>2. Materials .....</b>	<b>27</b>
<b>2.1. Equipment .....</b>	<b>27</b>

<b>2.2. Chemicals</b> .....	28
<b>2.3. DNA ladders</b> .....	30
<b>2.4. Bacterial strains</b> .....	31
<b>2.5. Oligonucleotides</b> .....	33
<b>2.6. Bacterial Growth Media</b> .....	37
<b>2.7. Commercially available assay kits</b> .....	38
<b>3. Methods</b> .....	<b>39</b>
<b>3.1. Microbiological Methods</b> .....	39
3.1.1. Bacterial storage.....	39
3.1.2. Overnight cultures.....	39
3.1.3. <i>E. coli</i> strain identification .....	39
3.1.4. Bacterial growth.....	40
3.1.5. <i>stx</i> -phage isolation .....	40
3.1.6. Bacterial cultivation and sample collection .....	40
3.1.7. Phage-Plaque-Assay.....	41
3.1.8. Verotoxin ELISA .....	41
3.1.9. Killing of <i>E. coli</i> .....	42
3.1.10. Supernatant collection.....	42
3.1.11. Lysogeny detection .....	42
3.1.12. Transwell Assay.....	43
3.1.13. Biofilm Assay .....	44
<b>3.2. Molecular biological methods</b> .....	45
3.2.1. Polymerase Chain reaction.....	45
3.2.2. Gel electrophoresis.....	47
3.2.3. RNA isolation .....	47
3.2.4. RNA Library Preparation for the Transcriptome Analysis.....	48
3.2.5. Analysis of deep-sequencing data.....	48
3.2.6. Quantitative Real-Time PCR .....	49
<b>3.3. Microscopic studies</b> .....	50
3.3.1. Electron microscopy .....	50
3.3.2. Light microscopy .....	50



3.4. Computer-assisted analyses .....	51
3.5. Statistical analysis.....	51
<b>4. Results .....</b>	<b>52</b>
4.1. <i>E. coli</i> strain identification.....	52
4.1.2. Confirmation of the <i>E. coli</i> purity.....	52
4.1.3. Strain identification PCR .....	54
4.1.4. EcN mutant screening .....	57
4.1.5. EcN mutant PCR verification .....	60
<b>4.2. Molecular mechanism of the Shiga toxin downregulation by EcN .....</b>	<b>63</b>
4.2.1. Influence of SK22D on the EDL933 pathogenicity.....	63
4.2.2. Protection capacity of SK22D after MMC induction .....	66
4.2.3. SK22D's influence on the Stx and phage level of STEC strains.....	68
4.2.4. Influence of EcN on the pathogenic agents of STEC strains.....	72
4.2.4.1. <i>stx2</i> -phage DNA detection .....	72
4.2.4.2. Influence of EcN on isolated Stx and the <i>stx2</i> -phage DNA.....	74
4.2.5. Investigation of the Stx reduction with EcN supernatant or heat killed EcN .....	76
4.2.6. Influence of EcN on EDL933 in the Transwell system .....	77
4.2.6.1. Transwell kinetics .....	77
4.2.6.2. Secretion factor stability .....	79
<b>4.3. EcN phage infection studies .....</b>	<b>82</b>
4.3.1. Electron microscopic studies of <i>stx</i> -phage binding to the <i>E. coli</i> surface.....	82
4.3.2. Bacteriophage life cycles .....	84
4.3.2.1. Bacterial cell lysis .....	84
4.3.2.2. Bacterial screen for lysogens .....	85
4.3.3. Transcriptome analysis .....	87
<b>4.4. <i>stx</i>-phage studies .....</b>	<b>90</b>
4.4.1. <i>stx</i> -phage kinetics.....	90
4.4.2. <i>stx</i> -phage localization.....	91
4.4.3. Influence of commensals and heat killed <i>E. coli</i> on <i>stx</i> -phages.....	92
4.4.4. Investigation of the <i>stx</i> -phage inactivating factor(s) properties.....	94
4.4.5. Impact of EcN's mutants on the <i>stx</i> -phage stability .....	97
4.4.6. Influence of EcN's biofilm on <i>stx</i> -phages .....	99

<b>4.5. K-12 protection studies</b> .....	103
4.5.1. SK22D protects K-12 strains from <i>stx</i> -phage infection .....	103
4.5.2. Light microscope study .....	104
4.5.3. MG1655 phage infection and SK22D protection kinetics .....	106
4.5.4. Protection of MG1655 infection by diverse <i>E. coli</i> strains.....	109
4.5.5. Protection of MG1655 from <i>stx</i> -phages of the O104:H4 isolates.....	112
4.5.6. Protection of MG1655 in the Transwell system .....	114
<b>5. Discussion</b> .....	<b>116</b>
<b>5.1. Studies towards the influence of EcN on the pathogenicity of STEC strains</b> .....	116
<b>5.2. Investigation of the influence of <i>stx</i>-phages on EcN</b> .....	120
<b>5.3. Evaluation of EcN’s phage defense mechanism</b> .....	125
<b>5.4. EcN protects K-12 strains from <i>stx</i>-phage infection</b> .....	129
<b>6. Outlook and conclusion</b> .....	<b>132</b>
<b>7. Bibliography</b> .....	<b>134</b>
<b>8. Appendix</b> .....	<b>151</b>
<b>8.1. <i>stx2</i>-prophage genes</b> .....	151
<b>8.2. Prophages of EcN</b> .....	154
<b>8.3. YaeT protein sequence comparison</b> .....	155
<b>8.4. Prophages of EcN, CFT073, SE11, SE15, IAI1 and MG1655</b> .....	156
<b>8.5. <i>E. coli</i> investigation for the Type 3,4,6 Secretion Systems</b> .....	158
<b>8.6. List of abbreviations</b> .....	159
<b>8.7. List of figures</b> .....	163
<b>8.8. List of tables</b> .....	165
<b>8.9. Workshops</b> .....	166
<b>8.10. Additional Activities</b> .....	166
<b>8.11. Curriculum Vitae</b> .....	167

### Summary

Shiga toxin producing *E. coli* strains (STEC) are a great concern to human health. Upon an infection with as few as 100 bacteria, humans can develop disease symptoms ranging from watery to bloody diarrhea or even develop the hemolytic uremic syndrome (HUS). The major factor contributing to the disease symptoms is Shiga toxin (Stx) which can bind to the eukaryotic cells in the intestine of the human and induce cell death via apoptosis. Based, among other things, on the microbiota composition, the impact of STEC can vary. Some bacteria of the microbiota can interfere with the colonization of STEC strains in the first place. Others cannot impair the colonization but interfere with the toxin production and there are still others which are even infected by *stx* encoding phages, being released from STEC strains. Those previously harmless bacteria subsequently contribute to the toxin increase and worsen the disease progression. Since the genetic information of Stx is encoded on a prophage, antibiotic treatment of patients can lead to an increased toxin and *stx*-phage release and is therefore not recommended. Several STEC epidemics in different countries, which even resulted in the death of some patients, demonstrated that there is an urgent need for alternative treatment strategies.

The *E. coli* strain Nissle 1917 (EcN) has been used as a probiotic to treat gastrointestinal infections for more than 100 years. It harbors several fitness factors which contribute to the establishment of an intact intestinal barrier in the human gut. Moreover, studies with EcN unraveled that the probiotic *E. coli* can interfere with the colonization of STEC strains and their toxin production. This study aimed to investigate if EcN could be a possible alternative or supplementary treatment strategy for STEC infected patients, or a preventive treatment for the patient's close contact persons.

Therefore, EcN was firstly investigated for a possible *stx*-prophage integration into its's genome which would eliminate it from being a potential treatment due to the possibility of disease worsening. Despite the presence of the *stx*-phage surface receptor YaeT, EcN demonstrated a complete resistance towards the lysis and the lysogeny by *stx*-phages, which was proven by PCR, phage-plaque assays and phage enrichment approaches. Transcriptome data could unravel that a lambdoid prophage in the genome of EcN is involved in the resistance towards the phage infection. Other commensal *E. coli* tested presented a *stx*-phage resistance as well and in silico analysis revealed that all of them harbor a complete lambdoid prophage besides the *stx*-phage susceptible K-12 strain MG1655. We assume that the resistance of EcN towards a *stx*-phage

infection is connected to the presence of an intact lambdoid prophage which interferes with superinfection.

Further experiments regarding the impact of the microcin negative EcN mutant SK22D towards STEC strains depicted that SK22D did not only interfere with the toxin production but also negatively regulated the transcription of the entire *stx*-prophage in coculture with all STEC strains tested (O157:H7, O26:H11, O145:H25, O103:H2, O111:H- and two O104:H4 isolates from the 2011 outbreak in Germany). This influence on the pathogenic factor production was evinced to be cell contact independent as SK22D could even interfere with the pathogenic factor production when being separated from the STEC strain EDL933 by a Transwell membrane with the pore size of 0.4  $\mu\text{m}$ . From this data we concluded, that factor(s) released by SK22D interfere with the lysis of STEC strains by stabilizing the lysogenic state.

Another positive aspect of EcN towards the pathogenicity of STEC strains was encountered when EcN was incubated with isolated *stx*-phages. The probiotic strain could reduce the infectivity of the phages towards a MG1655 lysis from  $\sim 1\text{e}7$  pfus/ml to 0 after 44 h of incubation. Various approaches to determine the characteristics of the factor(s) of EcN which are involved in the phage inactivation depicted it to be a heat resistant stationary phase protein on the surface of EcN, which could be a component of its biofilm.

Regarding the protective role of EcN we could further evince that SK22D was capable of interfering with the lysogenic K-12 mediated increase of Stx and *stx*-phages. Lysogenic K-12 strains were characterized by a huge increase of Stx and *stx*-phage production. The presence of SK22D anyhow, could interfere with this K-12 mediated pathogenic factor increase. Transwell and *stx*-phage infection kinetics led to the proposal that SK22D interfered with the *stx*-phage infection of K-12 strains in the first place rather than disturbing the lysis of lysogenic K-12. The protection from the phage infection could be due to the growth of K-12 strains within the SK22D culture, whereby the phage susceptible strains are masked from phage detection.

Summarizing, this work could underline the beneficial attributes of EcN towards the STEC pathogenicity *in vitro*. These results should be considered as pioneers for future *in vivo* studies to enable EcN medication as a supportive STEC infection treatment strategy.

### **Zusammenfassung**

Shiga toxin produzierende *E. coli* (STEC) stellen mit einer Infektionsdosis von gerade einmal 100 Bakterien ein großes Risiko für unsere Gesundheit dar. Betroffene Patienten können milde Krankheitssymptome wie wässrigen Durchfall aufweisen, welcher sich allerdings zu blutigem Durchfall oder dem hämolytisch urämischem Syndrom (HUS) weiterentwickeln kann. Die Ursache für das Krankheitsbild ist das zytotoxische Protein Shiga-Toxin (Stx), welches von STEC Stämmen produziert wird, eukaryotischen Zellen angreift und den apoptotischen Zelltod induziert. Es konnte gezeigt werden, dass infizierte Patienten in ihrem Krankheitsverlauf stark variieren, was unter anderem auf die Zusammensetzung ihrer Mikrobiota zurückzuführen sein könnte. Diesbezüglich können zum Beispiel einige Bakterien bereits die Darmbesiedlung von STEC Stämmen unterbinden, wohingegen andere die Toxin Produktion der pathogenen Stämme beeinflussen und wieder andere von den *stx* tragenden Phagen infiziert werden können und daraufhin selbst zu Toxin produzierenden Stämmen werden. Da die genetischen Informationen für das Toxin auf einem Prophagen im Genom der STEC Stämme kodiert ist, führt eine Antibiotika Behandlung von infizierten Patienten zwar zum Tod der Bakterien, hat allerdings auch einen Wechsel vom lysogenen zum lytischen Phagen Zyklus und damit einen enormen Anstieg an freigesetztem Stx zur Folge. In den letzten Jahrzehnten kam es immer wieder zu Epidemien mit STEC Stämmen, welche auch einige Todesopfer forderten. Die Behandlung von Patienten erfolgt auf Grund von mangelnden Behandlungsmöglichkeiten meist nur symptomatisch, weswegen neue Strategien für die Behandlung einer STEC Infektion dringend benötigt werden.

Der probiotische *E. coli* Stamm Nissle 1917 (EcN) zählt bereits seit mehr als 100 Jahren als Medikament für Behandlungen von Darmentzündungen. *In vitro* und *in vivo* Studien mit dem probiotischen Stamm und STEC Stämmen konnten zeigen, dass EcN die Produktion von Stx unterdrückt und gleichzeitig die STEC Zellzahl reduziert. Diese Ergebnisse waren der Anlass für diese Studie in der die Auswirkungen von EcN auf STEC Stämme genauer untersucht wurden, um eine mögliche Behandlung von STEC Infektionen mit dem Probiotikum zu gewährleisten.

Eines der Hauptziele dieser Studie war es, herauszufinden, ob EcN von *stx*-Phagen infiziert werden kann und damit selbst zu einem Toxin Produzenten wird. In diesem Falle wäre eine Behandlung mit dem *E. coli* Stamm ausgeschlossen, da es den Krankheitsverlauf

verschlimmern könnte. Verschiedene experimentelle Ansätze in denen versucht wurde den YaeT *stx*-Phagen Rezeptor tragenden Stamm zu infizieren schlugen fehl. Weder mittels PCR Analysen, Phagen Plaque Assays oder der Phagen Anreicherung konnte eine Lyse oder eine Prophagen Integration nachgewiesen werden. Transkriptom Analysen konnten zeigen, dass Gene eines lambdoiden Prophagen in EcN in Anwesenheit von *stx*-Phagen stark reguliert sind. Auch andere *E. coli* Stämme, welche sich ebenfalls durch eine Resistenz gegenüber einer *stx*-Phagen Infektion auswiesen, wurden positiv auf lambdoide Prophagen untersucht. Einzig dem *stx*-Phagen sensitiven K-12 Stamm MG1655 fehlt ein kompletter lambdoider Prophage, weswegen die Vermutung nahe liegt, dass ein intakter lambdoider Prophage vor der Superinfektion mit *stx*-Phagen schützen kann.

In weiteren Experimenten wurde der Einfluss der Mikrozin-negativen EcN Mutante SK22D auf STEC Stämme untersucht. Es konnte gezeigt werden, dass SK22D nicht nur die Produktion des zytotoxischen Proteins unterdrückt, sondern auch mit der Produktion der *stx*-Phagen von allen getesteten STEC Stämmen interferiert (O157:H7, O26:H11, O145:H25, O103:H2, O111:H- und zwei O104:H4 Isolate vom STEC Ausbruch in Deutschland im Jahr 2011). Transwell Studien konnten zeigen, dass der Faktor, welcher die Transkription des Prophagen unterdrückt, von SK22D sekretiert wird. Die Ergebnisse lassen vermuten, dass die Präsenz von SK22D den lysogenen Zustand des Prophagen stützt und somit den lytischen Zyklus unterdrückt.

Da *stx*-Phagen eine große Gefahr darstellen andere *E. coli* Stämme zu infizieren, haben wir uns in weiteren Studien dem Einfluss von EcN auf isolierte Phagen gewidmet. Die Kultivierungsexperimente von EcN mit Phagen zeigten, dass der probiotische Stamm in der Lage war die *stx*-Phagen in ihrer Effizienz der Lyse des K-12 Stammes MG1655 von  $\sim 1e7$  pfus/ml auf 0 pfus/ml nach einer 44 stündigen Inkubation zu inaktivieren. Diese Inaktivierung konnte auf die Aktivität eines hitzestabilen Proteins, welches in der stationären Wachstumsphase synthetisiert wird, zurückgeführt werden. Studien welche einen Anstieg der Biofilmmasse zur Folge hatten zeigten eine gesteigerte Effizienz in der Phagen Inaktivierung, weswegen Komponenten des Biofilms möglicherweise die Phagen Inaktivierung herbeiführen.

Neben dem direkten Einfluss auf die Phagen wurde auch ein Schutzeffekt von SK22D gegenüber dem *stx*-Phagen empfänglichen K-12 Stämmen untersucht. Lysogene K-12 Stämme zeichneten sich durch eine enorme *Stx* und *stx*-Phagen Produktion aus. Die Präsenz von SK22D konnte den K-12 vermittelten Anstieg der pathogenen Faktoren unterbinden. Transwell Ergebnisse und Kinetik Studien lassen vermuten, dass SK22D eher die Phagen Infektion von K-12 Stämmen unterbindet als die Lyse von lysogenen K-12 Stämmen zu stören. Eine mögliche

Erklärung für den Schutz der K-12 Stämme vor einer *stx*-Phagen Infektion könnte darin liegen, dass die K-12 Stämme innerhalb der SK22D Kultur wachsen und dadurch von den infektiösen Phagen abgeschirmt werden.

Zusammenfassend konnte in dieser Studie gezeigt werden, dass der probiotische Stamm EcN sowohl die Lyse von STEC Stämmen unterdrückt als auch die infektiösen *stx*-Phagen inaktiviert und sensitive *E. coli* Stämme vor der Phagen Infektion schützen kann. Diese Ergebnisse sollten als Grundlage für *in vivo* Studien herangezogen werden, um eine mögliche Behandlung von STEC infizierten Patienten mit dem Probiotikum zu gewährleisten.

### **1. Introduction**

#### **1.1. The human gut microbiota**

The human body consists of about  $3 \times 10^{13}$  cells, of which every cell has its own role in its functional unit. Knowing this number, it is surprising that metagenomic sequencing analysis could demonstrate that unicellular microbes cultivate human surfaces like the gastrointestinal tract, the skin, the saliva, the oral mucosa and conjunctiva in a ratio of 1:1 to human cells with around  $3.8 \times 10^{13}$  individuals (Sender, Fuchs, & Milo, 2016). These individuals can be assigned to 2172 species of which 93.5 % belong to the phyla of Proteobacteria, Firmicutes, Actinobacteria or Bacteroidetes (Hugon et al., 2015). Among the external and internal microbial surface attachment regions, the human gastrointestinal tract (GI) represents the largest mucosal host-microbe interaction region and is due to its high colonization also termed as “superorganism” or “forgotten organ” (Gill et al., 2006; O'Hara & Shanahan, 2006). The GI tract was shown to be sterile in the fetal gut by Gronlund et al. (Gronlund, Lehtonen, Eerola, & Kero, 1999). Immediately after birth, the microbial colonization of the GI begins and is influenced in its composition by the mode of delivery, hygiene, medication and environmental factors like diets or host genetics (Li et al., 2014). The diversity of microbes has been detected to be rather low in the early development of the infant but reaches the complexity of an adult after already 2.5 years of age (Koenig et al., 2011). The microbiota and the host's GI tract have co-evolved for thousands of years and demonstrate a mutual benefit, which is termed as symbiosis (Eloe-Fadrosh & Rasko, 2013). In case of homeostasis, the microbiota supports the shaping of the host's intestinal epithelium, the regulation of the host immunity and the protection against pathogens whereas the species of the microbiota use the GI tract as natural habitat and nutrient supplier (Thursby & Juge, 2017). In case of a disturbance of the microbial homeostasis (dysbiosis) anyhow, the composition of the gut species alters and the benefit of the microbiota like the protection against pathogen colonization is temporarily reduced or lost. Dysbiosis can be caused by e. g. inappropriate diets, pathogenic infections or antibiotic treatment. In case of the antibiotic treatment of a bacterial pathogen infection both, the pathogenic bacteria but also many of the commensal bacteria of the microbiota are killed, and the ecological niche of the commensals can be cultivated by other antibiotic resistant microorganisms (Jernberg, Lofmark, Edlund, & Jansson, 2010). For this reason, antibiotics are in concern of leading to long term alterations of the healthy gut microbiota (Jandhyala et al., 2015).



### **1.2. Probiotics**

Alternative or supportive strategies to maintain the homeostasis of the gut can be found in the administration of probiotics. Probiotics are microorganisms which have been defined as “live microorganisms, which when administered in adequate amounts, confer a health benefit to the host” (WHO, 2001). Probiotics are organisms from a healthy human gut flora and have been firstly described in 1907 by the “grandfather of modern probiotics” Elie Metchnikoff (Anukam & Reid, 2007; Metchnikoff, 1908). He observed, that the administration of lactic acid bacteria and fermented products like yogurt resulted in an enhanced health of the consumer. In parallel to Metchnikoff’s findings, the physician Henry Tissier discovered that children suffering from diarrhea had a low number of Y shaped bacteria in their stool compared to healthy children which exhibited a high number of this Y phenotypic bacteria, he called as “bifid” bacteria (Tissier, 1906). He assumed that those bacteria contributed to the wellbeing of the healthy children and suggested the administration of the same for the treatment of diarrhea. Until now, probiotics were found in the genera of *Lactobacillus*, *Bifidobacterium*, *Saccharomyces*, *Enterococcus*, *Streptococcus*, *Pediococcus*, *Leuconostoc*, *Bacillus* and *Escherichia coli* (*E. coli*) (Fijan, 2014). *Lactobacilli*, for example, were discovered to convert hexose sugars to lactic acid. By this they create an acidic environment which results in an interference of growth for some pathogenic bacteria. These probiotics can be found as food additives in e. g. yogurts, cheese and other fermented products (Siragusa et al., 2014). The Y-shaped, gram-positive *Bifidobacteria*, which were discovered by H. Tissier, have been identified to improve the intestinal barrier function and to increase the regulatory immune response of their human host (Vlasova, Kandasamy, Chattha, Rajashekara, & Saif, 2016). *E. coli* probiotic strains have also been used to treat patients suffering from infectious diseases for around 100 years. Amongst other beneficial properties, they can outcompete pathogens due to their bacteriocins and growth advantages (Wassenaar, 2016).

### **1.3. Escherichia coli**

*E. coli* belong to the phylum of Proteobacteria and are ubiquitous present in the human gut (Hill & Drasar, 1975). They were firstly discovered by the pediatrician Theodor Escherich in the year 1885, who called them “bacterium coli commune”, which was later changed to *Escherichia coli* in his honor (Escherich, 1886). The bacteria exhibit a thin peptidoglycan layer (gram-negative) and a typical size of 1 x 3 µm (Reshes, Vanounou, Fishov, & Feingold, 2008).

### **1.3.1. Phases of *E. coli* culture growth**

The growth of *E. coli* can be categorized into 4 different phases: the lag-phase, the logarithmic phase, the stationary phase and the death phase. The lag phase is characterized by an absence of culture growth due to the adaption of the bacterial culture to new habitat conditions and the activation of the cellular metabolism (Pin & Baranyi, 2008). During the logarithmic phase, the *E. coli* culture grows exponentially with a doubling time of around 30 min at 37 °C. As soon as the nutrient sources are exhausted, the numbers of cells that divide and of cells that die are equal. This equilibrium is called stationary phase and ends in the death phase when the cells start to die due to the accumulation of toxic products (Pletnev, Osterman, Sergiev, Bogdanov, & Dontsova, 2015).

Each growth phase has its own characteristic gene expression pattern and depicts alterations in the *E. coli* phenotype. The switch from the logarithmic growth phase to the stationary growth phase for example, results in morphological and physiological changes like a decrease of the cell volume, a change of the cell shape, nucleoid compaction, accumulation of storage material, alterations in the cell wall composition and biofilm formation which serves the *E. coli* protection (Beloin, Roux, & Ghigo, 2008; Makinoshima et al., 2003).

### **1.3.2. *E. coli* categorization**

Owing to their great diversity, *E. coli* are classified according to their antigenic surface regions (serotypes): the lipopolysaccharide (LPS, O), the capsule (K) the flagellum (H) and more rarely used, the fimbriae (F) (figure 1).

The LPS is the lipopolysaccharide of the outer cell membrane of *E. coli*, which protects the prokaryote from chemical attacks and exhibits a thermostable character. It is composed of three parts: the lipid A (disaccharides of two  $\beta$ -1,6-bound D-glycosamines), which anchors the LPS to the outer membrane, a short oligosaccharide core and an O-side chain. *E. coli* lacking the O-chain are specified to have a rough (R) LPS, whereas the classical formation of the LPS is called smooth (S) LPS (Wilkinson, 1996). The serotype classification is based on its highly specific O polysaccharide repeating units (Kauffmann, 1944).

The second antigenic specification of *E. coli* is its capsule. It is comprised of polysaccharides and can be found outside of the cell envelope. The function of the capsule is to protect *E. coli* from unspecific immune responses of the host during early colonization and is therefore mostly connected to pathogenic *E. coli* (Kauffmann & Vahlne, 1945). Another serotype classification,

the flagella, is the motility apparatuses of the bacterium. *E. coli* can harbor flagella with a typical length of 10  $\mu\text{m}$  and a diameter of 20 nm either polar, which means only one or several flagella at a single location, or peritrichous, which means that the flagella are all over the bacterium (Haiko & Westerlund-Wikstrom, 2013). Next to enabling the bacterial movement and chemotaxis, the flagella exhibit additional functions like protein export, adhesion and involvement in the biofilm formation. Fimbriae are long, polymeric proteins dispersed on the entire surface of the *E. coli*. They are responsible for the adherence of the bacteria to various surfaces or to other bacteria and are involved in the colonization of a host (Klemm, 1985; Mol & Oudega, 1996). Until now 186 different O-groups, 80 K-groups and 53 H-groups are identified (Fratamico et al., 2016; Whitfield & Roberts, 1999).

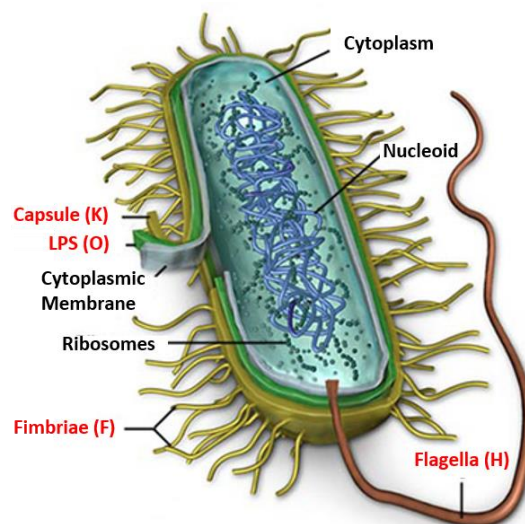


**Figure 1: Antigenic surface structures of *E. coli*.** LPS: lipopolysaccharide. Modified from (Laurel)

A further tool of *E. coli* differentiation is based on their evolutionary relationship. Due to their similarity or difference in the chromosomal level they are assigned to the major phylogenetic groups A, B1, B2, D1, D2 and E (figure 2). Most of the virulent extra-intestinal strains are part of the phylogenetic groups B2 and D, whereas most commensal strains are declared to be part of the group A (Clermont, Bonacorsi, & Bingen, 2000).

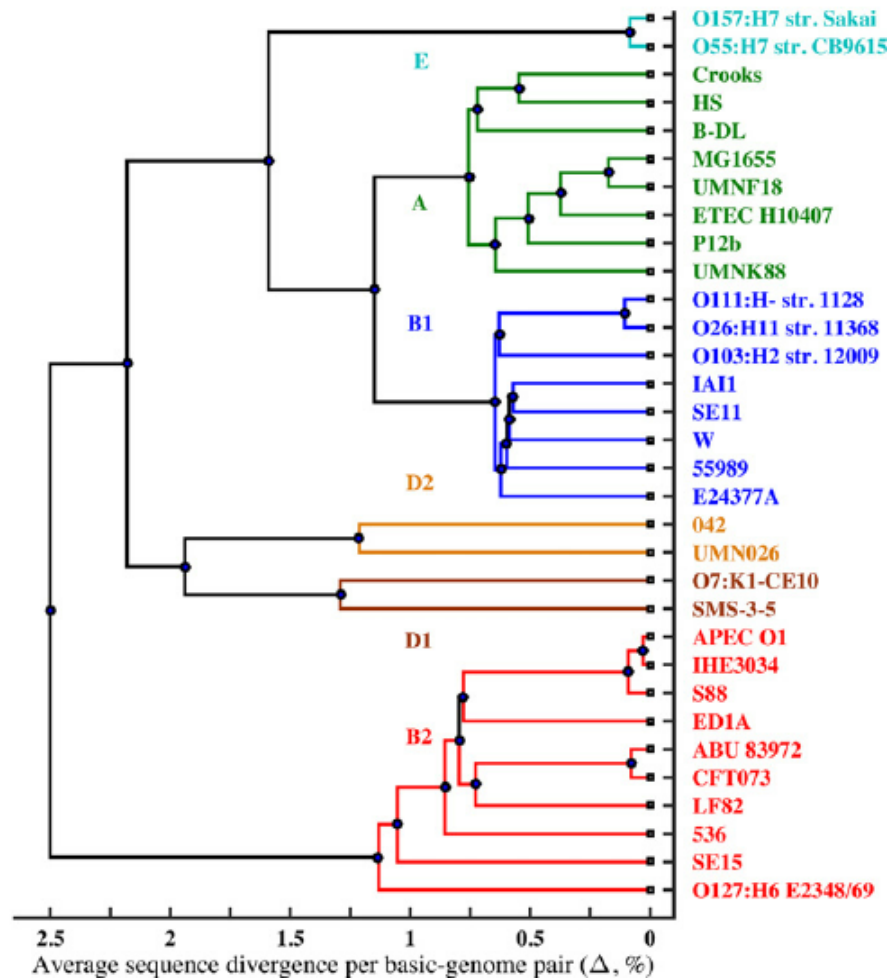


**Figure 2: Phylogenetic tree of *E. coli*.** Phylogenetic tree with the major *E. coli* phylogenetic groups A (green), B1 (dark blue), B2 (red), D1 (brown), D2 (yellow) and E (turquoise) (Dixit, Pang, Studier, & Maslov, 2015).

Based on their influence on the host, *E. coli* strains are attributed to a pathogenic, commensal or probiotic nature. Pathogenic *E. coli*, that cause infection in their host are classified according to their virulence factors: enteropathogenic *E. coli* (EPEC), enterotoxigenic *E. coli* (ETEC), enteroinvasive *E. coli* (EIEC), enteroaggregative *E. coli* (EAEC), enterohemorrhagic *E. coli* (EHEC), diffusely adherent *E. coli* (DEAC), adherent invasive *E. coli*, uropathogenic *E. coli* (UPEC), neonatal meningitis *E. coli* (NMEC), sepsis-associated *E. coli* (SEPEC) and Shiga toxin producing *E. coli* (STEC) (Fratamico et al., 2016). Commensal *E. coli* on the other hand are normal inhabitants of the human gut that result in no infection, rather contribute to the stabilization of the microbiota. Only a few *E. coli* strains were found to have a probiotic nature

according to the definition from the WHO in 2001 (WHO, 2001). Until now, there are three different *E. coli* probiotics commercially available: “Symbioflor”, a mix of 6 nonmotile *E. coli* strains, “Colifant”, a single *E. coli* strain and “Mutaflor”, a motile *E. coli* strain.

### **1.4. *E. coli* Nissle 1917**

At the time of the first identification of microorganisms with beneficial effects for their host in the early 20<sup>th</sup> century, the physician Alfred Nissle discovered a gram-negative probiotic *E. coli* strain. During his studies on stool samples from soldiers in the first World War in 1917, he isolated the probiotic *E. coli* strain, which was named *E. coli* Nissle 1917 (EcN), from a soldier who was the only one that did not develop diarrhea in a heavily *Shigella* contaminated environment (Nissle, 1918; Sonnenborn, 2016). After his discovery, Alfred Nissle started to cultivate EcN on agar-plates and launched the probiotic strain under the name Mutaflor®. Until today the probiotic is sold by the companies Ardeypharm GmbH and Pharma-Zentrale GmbH (Herdecke, Germany) and is used to treat intestinal inflammatory disorders like acute enteritis in children, ulcerative colitis and Crohn’s disease in adults (Malchow, 1997).

#### **1.4.1. Molecular characteristics of EcN**

The probiotic *E. coli* strain EcN was identified to have the serogroup O6:K5:H1:F1C (Blum, Marre, & Hacker, 1995). The O6 LPS can be found in both, pathogenic and apathogenic *E. coli*, is synthesized by the polymerization of O repeating units with the Wzy polymerase and is involved in the serum-resistance of the bacteria (Burns & Hull, 1998). EcN anyhow, has been detected to have a single nucleotide exchange in the *wzy* gene which results in a loss of function of the polymerase and thereby in a semi rough LPS that lacks serum-resistance and is free of immunotoxic effects for patients (Grozdanov et al., 2002). The K5 capsule of EcN is mostly found in *E. coli* colonizing the extraintestinal and urinal tract of the human host. The capsule of EcN was identified to be essentially important for its immunomodulatory effects on the epithelial cells of the host’s gut (Hafez et al., 2009). Both, the polar H1 flagella and the F1C fimbriae generate a bridge between EcN and the human gut cells and support thereby the probiotic nature of EcN as they demonstrate strong inhibitory effects on pathogen infection, adhesion and growth efficiencies (Kleta et al., 2014). Additionally, the flagella and the fimbriae are involved in the biofilm formation of EcN together with other factors such as cellulose and curli fibers.

EcN harbors several fitness factors like six iron uptake systems that increase the iron acquisition of the probiotic and cause a strong growth benefit (Grozdanov et al., 2004). It produces also two types of bactericides: microcin H47 and microcin M. Both microcins kill susceptible, pathogenic *E. coli* by mimicking siderophores which can enter the cytoplasm of the *E. coli* through their iron uptake receptors (Patzer, Baquero, Bravo, Moreno, & Hantke, 2003). Additionally, EcN harbors two cryptic plasmids (pMUT1 ~3.2 kbp, pMUT2 ~5.5 kbp) of unknown function, which might contribute to its genome stability (figure 3) (Blum-Oehler et al., 2003; Feldgarden, Golden, Wilson, & Riley, 1995).

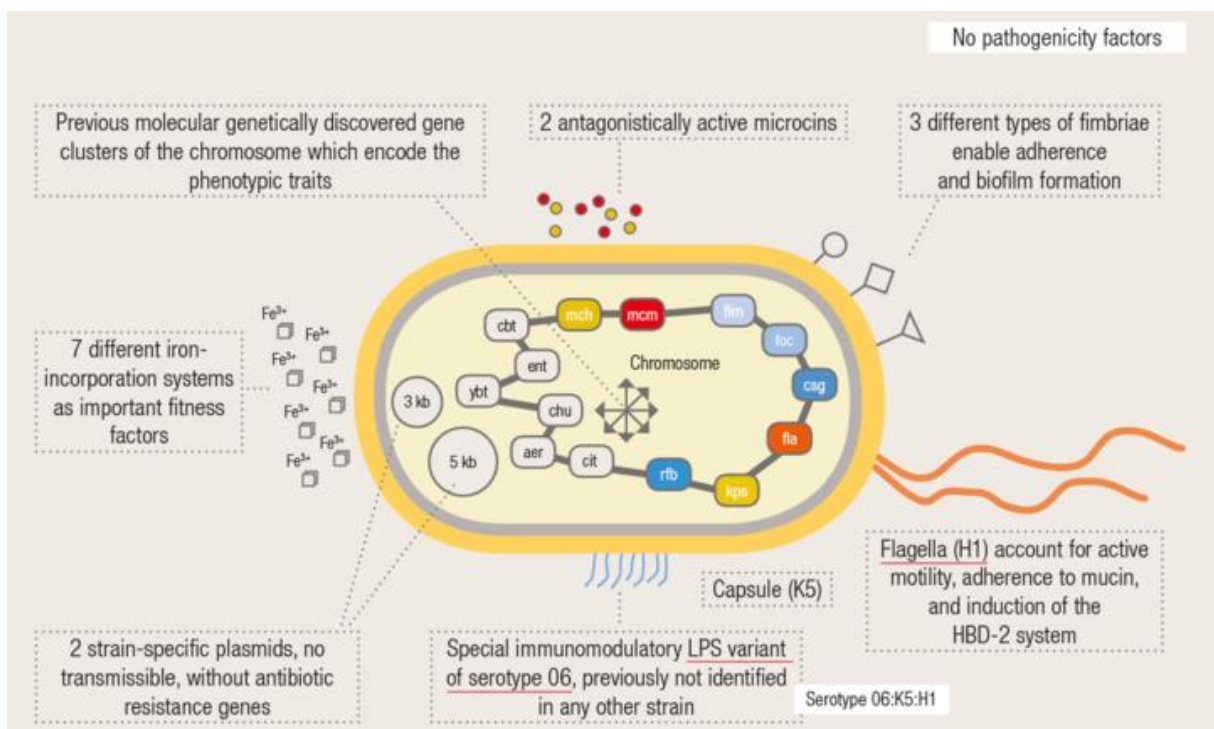


**Figure 3: EcN's fitness factors.** Schematic overview of EcN's phenotypic characteristics and their genomic location. Red underlined: Structural components that exhibit signal-mediated properties. (Pharmazentrale).

EcN belongs to the phylogenetic group B2 and is closely related to the virulent, uropathogenic strain CFT073 with only minor genetic variations. Despite this close relation, the single mutations in the genome of EcN contribute to its avirulent character. (Vejborg, Friis, Hancock, Schembri, & Klemm, 2010).

### **1.5. Shiga toxin producing *E. coli***

In contrast to probiotic *E. coli*, which contribute to the host's health, pathogenic *E. coli* induce an infectious response in their host. STEC strains are human pathogenic *E. coli*, whose natural, asymptomatic reservoir are cattle (Wray, McLaren, Randall, & Pearson, 2000). They harbor the genomic information to produce Shiga toxin (Stx). This toxin uses the Globotriaosylceramide (Gb3) receptor of eukaryotic cells for cell entry (Melton-Celsa, 2014). The Gb3 receptor however, is absent in the intestinal tract of cattle which is the source for their immunity (Pruimboom-Brees et al., 2000). Humans are getting infected by STEC strains due to the consumption of contaminated bovine products like undercooked meat, milk or dairy products (Armstrong, Hollingsworth, & Morris, 1996). Also contaminated water and vegetables that were fertilized with cow dung pose a risk for STEC infections (Hilborn et al., 1999; Olsen et al., 2002).

#### **1.5.1. Shiga toxin mode of action**

Konowalchuk discovered in 1977, that some *E. coli* strains were able to kill cultured African green monkey kidney cells (Vero cells). Those strains were therefore called Verotoxin producing *E. coli* (VTEC) (Konowalchuk, Speirs, & Stavric, 1977). In 1980, the verotoxin was identified to be identical to the Shiga toxin serotype 1 of *Shigella dysenteriae*, which resulted in a name change to Shiga toxin producing *E. coli* (Calderwood, Auclair, Donohue-Rolfe, Keusch, & Mekalanos, 1987; O'Brien et al., 1984). STEC can have the genetic information for two major Stx families: Stx1 (Stx1 and Stx1c) and the more heterogenous Stx2 group (Stx2, Stx2c, Stx2d, Stx2e, Stx2f). Contrary to Stx1, Stx2 is by 42 % distinct to Stx1 of *S. dysenteriae* at the amino acid (aa) sequence level, even though it shares the same receptor affinity and intercellular mode of action (Jackson, Newland, Holmes, & O'Brien, 1987).

Stx is an AB<sub>5</sub> holotoxin, with a single A subunit bound to an oligomerized pentamer of the B subunit (figure 4 a). The B pentamer of Stx recognizes the Gb3 (CD77) receptor of eukaryotic cells. Following the surface attachment, Stx is cleaved at its protease sensitive loop (242 - 261 aa) by the endoprotease furin (cleavage site: Arg251 - Met252), which is present on the surface of the eukaryotic cell (Garred, van Deurs, & Sandvig, 1995). The enzymatic action of furin results in the subunits StxA-A1 and A2-StxB which are only connected by a disulphide bond between Cys242 and Cys261 (Figure 4 b, c). Subsequent to binding to the receptor, the holotoxin is translocated through the trans-Golgi network and the Golgi apparatus by the host

cell machinery, before it reaches the endoplasmic reticulum (ER) (Torgersen, Lauvrak, & Sandvig, 2005). Once in the ER lumen, the disulphide bond which connects the A and B subunit of the toxin is reduced and the StxA-A1 subunit is translocated to the cytoplasm of the eukaryotic cell. In the cytoplasm, the released StxA subunit can attach to the 28S ribosomal RNA (rRNA) of the ribosomes and cleaves an adenine base of the  $\alpha$  sarcin-loop at the position 4,324 with its highly specific RNA N-glycosidase activity (Endo et al., 1988). As a result, the transfer RNA (tRNA) cannot bind any longer to the ribosome and the peptide chain elongation is blocked (Hale & Formal, 1980). The inhibition of protein synthesis leads to an initiated cell death by apoptosis.

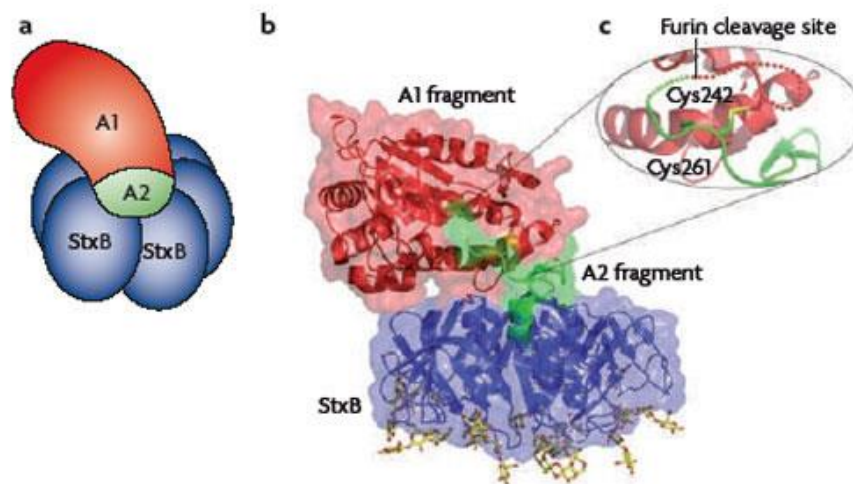


**Figure 4: Schematic figure of Shiga toxin.** (a) Schematic figure of Stx with its A subunit bound to the pentameric B subunit. (b) 3D structure of Stx. (c) Zoom into the furin cleavage site between StxA-A1 and StxA2-B between Arg251 - Met252 and the disulphide bound between Cys242 and Cys261. Modified from (Johannes & Romer, 2010).

### 1.5.2. Clinical outcome of STEC infections

A major risk of the infection with a STEC strain is due to its low infectivity dose. Less than 100 organisms are sufficient to result in an infection in human (Tilden et al., 1996). The symptoms of the infected patients can range from watery to bloody diarrhea up to the development of the hemolytic uremic syndrome (HUS). Watery diarrhea together with abdominal tenderness appears 3 to 4 days after the STEC infection and can last for 1 to 3 days (Bell et al., 1994). If the patient does not recover during this time the symptoms can worsen to a bloody diarrhea



which goes along with grossly bloody stool and abdominal tenderness (Karch, Tarr, & Bielaszewska, 2005). In the worst case, the infection progresses to a HUS, which is associated with hemolytic anemia, thrombocytopenia and acute renal failure, 5 to 13 days after the onset of diarrhea (Bell et al., 1997; Iijima, Kamioka, & Nozu, 2008). Disease symptoms that come along with the HUS can be as severe as lethargy, seizures, stupor, coma and strokes (Gerber, Karch, Allerberger, Verweyen, & Zimmerhackl, 2002). Most of the patients recover completely from a HUS but some of the patients suffer from long time consequences like chronic renal illness (Garg et al., 2003).

The treatment of patients suffering from a STEC infection is rather complicated as antibiotic administration is not recommended due to the possibility of documented disease worsening (Dundas et al., 2001; Wong, Jelacic, Habeeb, Watkins, & Tarr, 2000). In case of a STEC infection, patients are voluntarily hospitalized, get a symptomatic treatment and are observed for their disease progression. Most patients that develop a HUS need to furthermore receive erythrocyte transfusions (Tarr & Neill, 2001; Tarr et al., 1989).

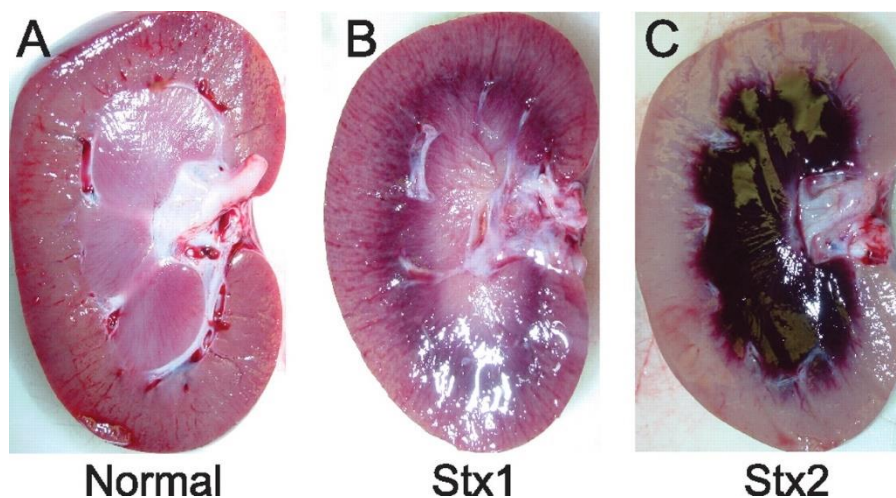


**Figure 5: Pathology of kidneys from baboons being challenged with shiga toxins.** The kidneys were challenged with Stx1 (B) or Stx2 (C) compared to an untreated control (A) (Stearns-Kurosawa, Collins, Freeman, Tesh, & Kurosawa, 2010).

The Stx of subtype 2 was detected to lead to a more severe disease progression in both animal and human (Eklund, Leino, & Siitonen, 2002; Stearns-Kurosawa et al., 2010). The influence of the different Stx types on a baboon kidney model confirms these results with an immense cell

death of kidney cells being exposed to Stx2 rather than to Stx1 (figure 5). Anyhow, the reason for the difference in the disease outcomes based on the Stx subtypes is not solved yet.

### **1.5.3. STEC outbreaks**

The first detected food-borne infection by a STEC strain goes back to the year 1982 when about 47 people were infected in Oregon, Michigan by an STEC strain of the serotype O157:H7 that produced both, Stx1 and Stx2 and resulted in abdominal pain and watery or bloody diarrhea for the patients (Riley et al., 1983). The infection of the patients was traced back to undercooked burger beef. Since that year, several STEC outbreaks were reported: In 1993, 501 costumers of burger restaurants were infected by O157:H7 STEC in the USA. This outbreak had a more severe outcome than the one before, as 151 patients had to be hospitalized and of those 45 developed a HUS, which resulted in the death of 3 patients (Bell et al., 1994). In 1996, even 12,680 school children were infected after eating O157:H7 contaminated radish sprouts. 1,000 of those children had to be treated in the hospital, 121 cases of HUS were diagnosed, and 3 children died from the consequences of the infection (Michino et al., 1999). Furthermore, an enormous number of deaths was the consequence of a O157:H7 STEC epidemic in 1999 in China when 195 HUS patients were hospitalized and 177 of those died. 95 % of all HUS developments can be traced back to the “big five” STEC strains: O157:H7, O26:H11, O145:H25, O103:H2 and O111:H- (Eichhorn et al., 2015). Anyhow, in the year 2011 Germany was hit by a STEC epidemic with the unusual serotype O104:H4. The STEC contamination was traced back to Fenugreek seeds from Egypt and infected 855 patients with HUS and 2,987 with gastroenteritis (Buchholz et al., 2011). In total 53 people died from this infection (RKI, 2011a).

### **1.5.4. O104:H4 outbreak strain**

The STEC epidemic in 2011 started at the first of May with the infection of a 45-year-old man from Aachen. The number of infected patients peaked at the 20<sup>th</sup> - 22<sup>th</sup> of Mai and was officially declared to be over at the 25<sup>th</sup> of July, after three weeks of no new infection. This outbreak was the biggest recorded STEC epidemic Germany ever faced with 855 HUS and 2,987 gastroenteritis patients. 35 of the HUS patients and 18 of the gastroenteritis patients died from the impact of the infection. The course of the disease progression was in several aspects different to other STEC infections recorded before. Next to a longer incubation time of 8 instead of 3 to 4 days until the appearance of first diarrheal symptoms, the time towards the possibility

of the development of HUS was reduced to a median of only 5 days (normal median: 9 days) after the onset of diarrhea. Additionally, the age of the patients was highly increased with a median of 46 years. Only 2 % of the patients were younger than 5 years, whereas the incidents of STEC infections from 2001 until 2010 were detected in children younger than 5 years for 69 % of the cases (RKI, 2011a).

Strain identification from isolates of infected patients revealed a STEC unusual serotype of O104:H4. The outbreak strain combined amongst others the virulence factors *stx2* (99 % sequence identity to *stx2* from previous O157:H7 outbreaks) from EHEC and the adhesins *iha*, *ipf*<sub>O26</sub>, *ipf*<sub>O113</sub>, the adherence fimbriae *aggA* and an iron uptake system from EAEC strains. The combination of the production of Stx2 together with an enhanced adherence to the epithelial cells and a high antibiotic resistance are possible reasons for the unusual high infectivity of the O104:H4 strain (Bielaszewska et al., 2011).

### **1.6. Regulation of the Shiga toxin expression**

The genetic information for Stx1 and 2 are encoded on coliphage  $\lambda$  resembling prophages in the chromosome of STEC strains (Tyler, Mills, & Friedman, 2004). Thereby, the prophage 933W encodes *stx2* genes and the prophage 933J harbors the genes *stx1A* and *stx1B* for the synthesis of Stx1 (O'Brien et al., 1984). Both prophages were found in the genome of O157:H7, which is most frequently associated to STEC infections. As the toxin genes are encoded by the lambdoid prophages, the Stx synthesis is linked to the *stx*-phage cycles.

#### **1.6.1. Lysogenic and lytic *stx*-phage cycle**

During the lysogenic or quiescent phage cycle, the *stx*-prophage genes are suppressed by the lytic phase repressor protein CI, which is induced in synthesis by the lambda lysogeny establishing protein CII (Rokney et al., 2008). CI blocks the transcription from the phage early promoters *p<sub>R</sub>* and *p<sub>L</sub>* of the prophage genes by binding to the right and the left operator sites *o<sub>R</sub>* and *o<sub>L</sub>* (Waldor & Friedman, 2005). Therefore, the transcription of the entire prophage and connected to this the synthesis of the late phage genes *stxA* and *B* is suppressed (figure 6).

The lytic phage cycle on the other hand, is induced by the DNA damage of *E. coli*, which can occur by e. g. UV light exposure or the addition DNA damaging chemicals, like Mitomycin C (MMC), and results in a SOS response of the organism to repair the mutated DNA (Walker,

1984; Witkin, 1976). In case of a DNA damage, RecA monomers, which are permanently present in the cell, bind to ATP compounds and single stranded DNA and obtain thereby an activated state with specific protease activity. Thereby, the activated RecA cleaves the SOS response repressor LexA, which results in a transcription of SOS genes and an increase of the SOS regulator RecA from around ~10,000 monomers to 100,000 monomers in the cell (Little, 1983; Sommer, Boudsocq, Devoret, & Bailone, 1998). Next to activating the SOS response, activated RecA can cleave of the phage repressor CI. By this, the operator sites of the *stx*-prophage are released, and the promoters  $p_L$  and  $p_R$  are de-repressed (Muhldorfer et al., 1996). The transcription initiation at the promoter sites results in the expression of the downstream located antiterminator  $q$ . The antitermination factor Q induces the transcription initiation from the late phage regulator  $p_{R'}$  which is blocked in the lysogenic cycle by the transcription terminator  $t_R$  (Tyler et al., 2004). Thereupon, late phage genes like *stxAB* and genes involved in phage lysis, packaging and phage assembly (head, tail) are transcribed (Pacheco & Sperandio, 2012).

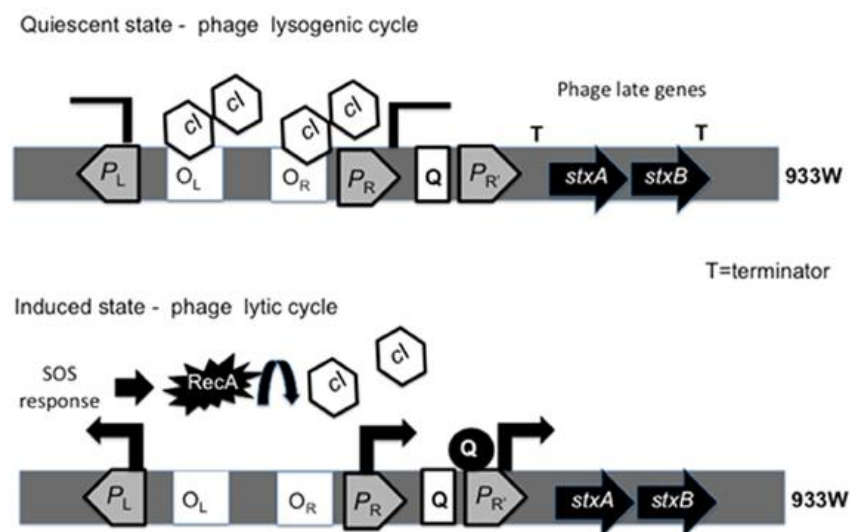


**Figure 6: 933W *stx2*-prophage regulation.** During the lysogenic cycle, the CI repressor binds to the left and right operator sites  $O_R$  and  $O_L$  which inhibits the prophage gene transcription from the transcription initiation promoter sites  $p_R$  and  $p_L$ . The lytic cycle is induced by the cleavage of CI by activated RecA. Upon CI release from the operator sites, the transcription from the left and right promoter is initiated and the antiterminators N and Q are expressed. Q in turn, binds to the promoter  $p_{R'}$  and induces the transcription of the late prophage genes like *stxAB* and genes for the phage assembly. Modified from (Pacheco & Sperandio, 2012)

The genes *s* and *r* are located downstream of *stxAB* and are involved in the bacterial cell lysis. *r* codes for an endolysin, which degrades the peptidoglycan layer of the bacterial cell wall. Due to a missing signal sequence, the transport of R across the cytoplasmatic membrane is enabled by the small holin protein S which degrades the bacterial cell membrane by pore formation (Blasi & Young, 1996). The release of Stx and *stx*-phages is achieved by the subsequent autolysis of the bacteria (O'Brien & Holmes, 1987). *stx*-phages inherit a genome size of 57,677 bp and exhibit a phenotypic icosahedral head of around 100 nm and have a short tail (~10 nm length) (Chatterjee & Rothenberg, 2012; Mondal et al., 2016).

### **1.7. Bacteriophages**

Bacteriophages are the most abundant member of virobiota in the human gut which has a density of virus like particles (VLPs) ranging from  $10^8$  to  $10^9$  VLPs/g in the stool of humans (Lusiak-Szelachowska, Weber-Dabrowska, Jonczyk-Matysiak, Wojciechowska, & Gorski, 2017). The genetic information they carry can be encoded on single stranded (ss) and double stranded (ds) RNA as well as on ss and dsDNA (Szekely & Breitbart, 2016). Some dsDNA bacteriophages have been reported to be the carriers for virulence factors like e. g. Stx1/2, Cholera toxin A/B, Cytotoxin and the Diphtheria toxin (Boyd, 2012). Therefore, these phages pose a high risk for the health of the human host.

#### **1.7.1. Phage assembly**

The bacteriophage assembly proceeds in its bacterial host, where the phage uses the machinery of the bacterial cell for the production of the phage components (Griffiths, Gelbart, Miller, & Lewontin, 1999). In a first step, the phage head, which is composed of the portal protein, the major head protein and scaffolding proteins are formed (Fokine & Rossmann, 2014). This preliminary head is called prohead or procapsid. In a next step, the dsDNA encoding the genetic information for the phage is transported into the prohead by the terminase complex and in parallel the scaffolding proteins are degraded to generate new space (Aksyuk & Rossmann, 2011). After the transport of the entire DNA into the head of the phage, the terminase complex is exchanged by head complementation proteins (Mondal et al., 2016). Finally, the now called capsid is closed by a connector which prevents DNA ejection and is joined to a contractile phage tail with its tailfibers that enable the infective phage to find its host receptor (figure 7) (Perucchetti, Parris, Becker, & Gold, 1988; Simpson, Sacher, & Szymanski, 2016).

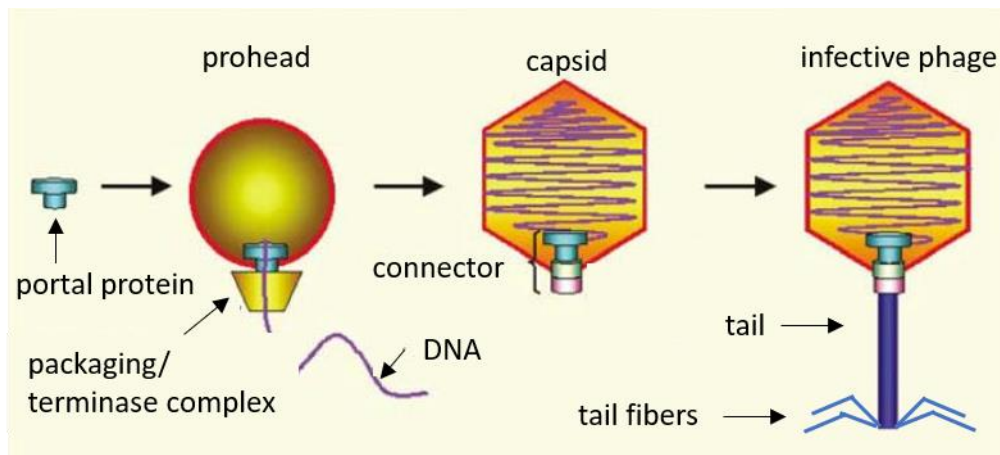


**Figure 7: Model of a DNA bacteriophage assembly.** Stepwise development of the infective phage. The dsDNA is packed into the prohead through the portal protein by the terminase complex. Prohead proteins are degraded and the capsid is formed. The connector prevents DNA ejection. The infective phage is connected to a tail with tail fibers for the host receptor identification. Modified from (Lebedev et al., 2007).

### **1.7.2. Bacteriophage receptors**

To inject their genetic information into the bacterial host, bacteriophages need to attach to receptors on the host's surface. Thereby, most of the phages exhibit a very narrow receptor range. Research on phage receptors uncovered that there is great diversity of possible phage receptors (Rakhuba, Kolomiets, Dey, & Novik, 2010). Among those, several proteins, localized in the host's membrane, have been identified to serve the phage adsorption to the cell. OmpA, a transmembrane protein, is for example recognized by T4- and T2-phages, likewise as the porins OmpC and OmpF (Schweizer & Henning, 1977). LamB, which facilitates the diffusion of maltodextrins across the outer membrane of Gram-negative bacteria, is the receptor of the lambda-phages, and another example for protein receptors is YaeT, a highly conserved protein on the outer membrane of *E. coli*, which has the function of protein insertion into the bacterial outer membrane, is recognized by *stx*-phages (Smith et al., 2007). Next to membrane associated protein receptors, also the rough and the smooth LPS are possible recognition regions for some T-like phages (Takeda & Uetake, 1973). Furthermore, surface structures like the capsule, the pili, the flagella and bacterial capsules can serve as host recognition structures (Rakhuba et al., 2010).

### **1.7.3. Bacterial lysis and lysogenization**

Once being attached to the phage specific receptor on the host's surface, the bacteriophage releases its genomic content into the bacterium. The presence of the phage dsDNA in the bacterial cytoplasm can result in a downregulation of the production of bacterial components and in the synthesis of the phage components by the bacterial machinery. After the phage assembly, the bacterial cell wall breaks open (bursts), and the newly established phages are released. This process is called bacterial lysis (figure 8) (De Paepe, Leclerc, Tinsley, & Petit, 2014). Bacteriophages can be categorized into two groups: virulent phages, that can exclusively use the bacterial host for the phage amplification and temperate phages, which can lyse the host but are also capable of integrating their phage DNA into the genome of the bacterium and turning it into a prophage carrying lysogen (Griffiths et al., 1999). The integrated DNA remains silent as prophage in the host until a signal shift induces the lysis cycle due to the SOS response of the host after bacterial DNA damage by UV light or antibiotics, temperature shifts or oxidative stress (Los, Los, Wegrzyn, & Wegrzyn, 2010; Matos et al., 2013; Monk & Kinross, 1975).

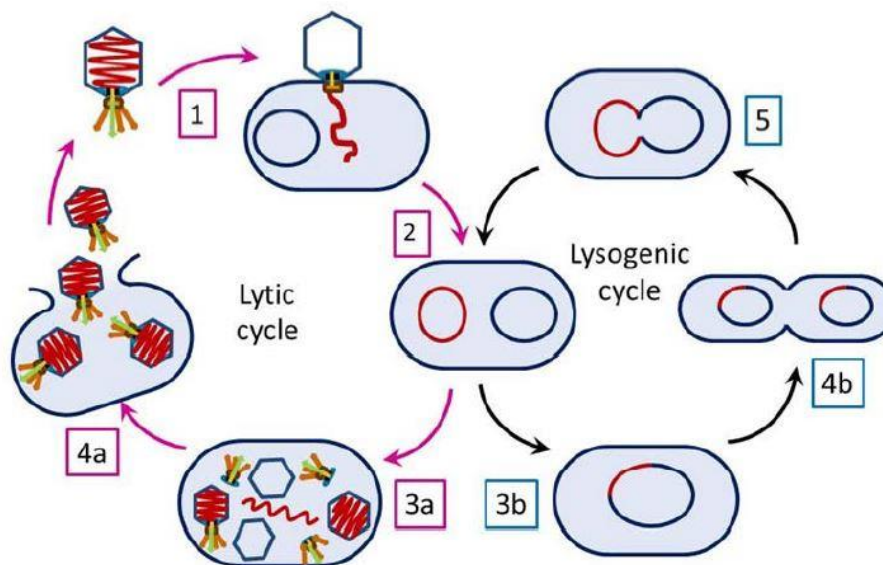


**Figure 8: Bacterial lysis, lysogenization by bacteriophages.** (1) Phage receptor binding to the surface of the host cell. (2) Phage DNA (red) inside of the host. (3a) Lytic cycle: Amplification of phage DNA and synthesis of new phages. (4a) Bacterial lysis and release of the phages. (3b) Lysogenic cycle: Integration of the phage DNA into the hosts genome (prophage). (4b) the prophage DNA is passed on the next host's generation. (5) SOS response can induce the entry into the lytic cycle (Orlova, 2012).

The integration of the lambdoid temperate *stx*-phage dsDNA into the genome of susceptible *E. coli* strains has been widely studied. It has been identified that the integration of the phage DNA within the *wrbA* tryptophan repressor gene is promoted by an integrase with a highly conserved C-terminal motif (Arg, His-X-X-Arg and Tyr) (Plunkett, Rose, Durfee, & Blattner, 1999). Unlike many other phages, *stx*-phages can infect a single *E. coli* cell more than once, which results in STEC strains that harbor multiple *stx*-prophages in their genome and are associated with an increased virulence (Allison et al., 2003)

### **1.7.4. Bacterial phage defense mechanisms**

Bacteriophages outnumber bacteria in the most environments by tenfold (Brussow & Hendrix, 2002). Anyhow, the co-evolution of phages and bacteria has not only led to a great diversity of possible phage receptors on the bacterial surface but also to the development of several strategies by which the bacteria protect themselves from phage infections.

One described phage defense mechanism is the prevention of phage binding to the phage receptors. This strategy can be subdivided into different categories like e. g. the mutation of the phage receptor masking of the phage receptors, assembly of an extracellular matrix and the production of competitive inhibitors (Labrie, Samson, & Moineau, 2010). The adsorption blockage strategy describes a method by which the bacteria mask the phage receptors from phage recognition by e. g. modification of the receptor structure or by lipoprotein binding to the receptor protein (figure 9 a, c) (Riede & Eschbach, 1986). The next category, the production of an extracellular matrix, depicts a technique by which the bacteria synthesize a physical barrier between the phages and their receptors (figure 9 b, c). This can be a capsule layer that shields the bacteriophage receptors and interferes thereby with the binding of the phages (Chakrabarty, Niblack, & Gunsalus, 1967). Also the biofilm extracellular matrix has been detected to be involved in the bacterial protection from phage infection by the group of Vidakovic et al., which unraveled that T7-phages bind to amyloid curli fibers of the biofilm network and thereby T7-phage susceptible *E. coli* are protected from infection (Vidakovic, Singh, Hartmann, Nadell, & Drescher, 2017). Another mechanism by which bacteria interfere with the phage binding to the receptor is by the production of competitive inhibitors. Thereby, molecules that are present in the environment of the bacteria are bound to the phage receptors and block thereby the phage recognition region (figure 9 a) (Labrie et al., 2010).



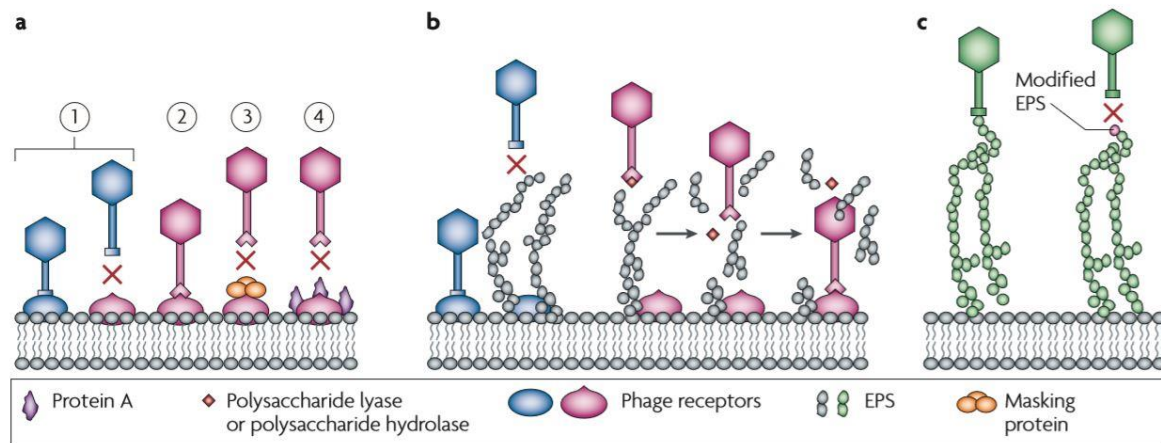


**Figure 9: Mechanisms to prevent phage adsorption.** (a) The bacterial host can block the phage adsorption by e. g the modification of the phage receptor (1). Phages can adapt to this modification and recognize the new receptor (2). Bacteria can synthesize proteins which bind to the phage receptor and mask it (3) or reduce the phage adsorption (4). (b) Phage binding can be blocked by the synthesis of an extracellular matrix (exopolysaccharides (EPS)). Some phages can detect this matrix and degrade it to reach the surface receptor. (c) Phages can use the O-side chains or the K-antigens as host recognition region which is prevented by a modification of the host's EPS. (Labrie et al., 2010)

Next to the development of strategies that prevent the phages from bacterial binding, other strategies evolved to protect the bacterium from the incoming phage DNA. Among those are the superinfection exclusion system (*sie*), the restriction modification system (R-M) and the Clustered Regularly Interspaced Short Palindromic Repeats (CRISPR-Cas) system. *sie* codes for a membrane anchored or membrane associated protein Sie, which was identified to block the entry of the incoming phage DNA and can mostly be found in prophages (Ranade & Poteete, 1993). Bacteria that encode the R-M system can recognize the unmethylated phage DNA in the cytoplasm and degrade it with its restriction enzyme (Pingoud, Fuxreiter, Pingoud, & Wende, 2005). CRISPR-Cas describes another technique that targets incoming DNA. This protection system has been identified to be present in about half of the sequenced bacteria (Stern & Sorek, 2011). It operates in three steps: first a repeating spacer unit which is part of the invading phage DNA is added to the CRISPR gene locus which is followed by the synthesis of the CRISPR transcript (Mojica, Diez-Villasenor, Garcia-Martinez, & Almendros, 2009). The produced transcript is cleaved within the repeats by Cas proteins which results in smaller RNAs (crRNA). In a final step, the mature crRNA is directed to the invading phage DNA, which is subsequently cleaved in a sequence specific manner (Barrangou et al., 2007).

A last protection system described, is the abortive infection (abi) system. This altruistic system results in the death of the infected cells. The best abi system studied is the Rex system of lambda-lysogenic *E. coli*. In case of the phage DNA entry into the bacterial cytoplasm, the initiation of the phage DNA amplification results in the activation of RexA which in turn activates the Ion channel RexB. Once activated, RexB reduces the membrane potential and the intercellular adenosine triphosphate (ATP) level decreases. The lack of ATP blocks the phage production but equally leads to the death of the host (Parma et al., 1992).

### **1.8. Influence of EcN on STEC strains**

The treatment of STEC infections with antibiotics results in the induction of the SOS response of the bacterium and thereby in a switch from the lysogenic cycle to the lytic phage cycle of their prophage. This in turn leads to an increased *stx*-phage and Stx release which can worsen the disease progression for the patient (Pacheco & Sperandio, 2012). Therefore, antibiotics are not the ideal treatment strategy for patients suffering from a STEC infection and alternative treatment strategies are strongly needed.

During routine Stx detection quality controls by the Robert Koch Institute (RKI) with stool specimens being spiked with known STEC strains, in some of the stool samples Stx could not be detected with the standard Stx enzyme-linked immunosorbent assay (ELISA). These stools specimens were closely analyzed, and the *E. coli* isolate 1307 was detected to show inhibitory effects on both, the growth of STEC strains and the Stx level. These results were equally observed when using the probiotic strain EcN but lacked in efficiency when other commensal *E. coli* or known probiotics of the genera of *Enterococci*, *Bacillus sp.* or *Lactobacillus acidophilus* were tested (Reissbrodt et al., 2009). Based on the observation, that the probiotic strain EcN reduces the Stx level when being cocultured with STEC strains, further *in vitro* studies were executed to closer investigate this finding. In the year 2013, Rund et al. demonstrated that STEC strains could less efficiently adhere to gut epithelial cells in the presence of EcN, which was assumed to result from the occupation of the adhesion sites by EcN. Moreover, he could show that EcN also reduces the Stx level from two isolates of the unusual O104:H4 serotype from the 2011 outbreak, when being cocultured (Rund, Rohde, Sonnenborn, & Oelschlaeger, 2013). In a study of 2015, it was furthermore unraveled that the reduction of the Stx level is based on a downregulation of the *stx* gene expression in the presence of EcN (Mohsin, Guenther, Schierack, Tedin, & Wieler, 2015).

*In vivo* studies in the mouse model with EcN and STEC strains could further illustrate, that commensal strains can provide a natural barrier for the intestine colonization by STEC strains (Leatham et al., 2009). EcN proved thereby to be an efficient antagonist for the STEC colonization, which is probably due to the competition for nutrients needed by STEC strains for a proper colonization of the gut (Mohsin et al., 2015).

These preliminary results suggest that EcN could be an alternative or supportive treatment strategy for patients suffering from a STEC infection.

### **1.9. *stx*-phages in the microbiota**

In 1999, Schmidt et al., detected that *stx*-phages whose *stx* gene was exchanged with a chloramphenicol cassette were able to integrate into the genome of a broad range of pathogenic *E. coli* (EPEC, EIEC, STEC, ETEC, EAEC) but also into the genome of commensal *E. coli* strains isolated from stool samples (Schmidt, Bielaszewska, & Karch, 1999). This phage integration was as well detected in the intestine of mice, where *stx1*-phages carrying an ampicillin resistance cassette were able to lysogenize susceptible *E. coli* (Acheson et al., 1998).

Based on these results, not only the Stx toxin but also the *stx*-phages pose a risk for the patient. As patients being infected by STEC strains exhibit a broad difference on the severity of the disease progression, it can be speculated that phage susceptible, commensal *E. coli* strains in the microflora of some patients are infected by *stx*-phages and are thereby turned into toxin producing pathogens.

### **1.10. Aim of the thesis**

The human gut is densely populated with over 2,000 different species. The entirety of these species is called microbiota and shows to strongly influence the hosts overall health (Jandhyala et al., 2015). The individuals of the microbiota can be assigned to have a commensal nature in case they are found in healthy individuals, a pathogenic nature if they contribute to the development of disease or a probiotic nature in case they confer a health benefit to the host (WHO, 2001). STEC strains are pathogenic *E. coli* that can cause the development of gastroenteritis or the HUS in their host due to the expression of the toxin Stx (Conway, 2015). As the patient treatment with antibiotics could result in an increase of toxin release, alternative treatment strategies are needed (Pacheco & Sperandio, 2012).

The probiotic strain EcN has been used to treat gastrointestinal diseases for more than 100 years. Furthermore, it was identified to interfere with the Stx production of STEC strains both *in vitro* and *in vivo*. The aim of this study was to closer investigate the anti Stx producing effects of EcN in the coculture with STEC strains. Next to the Stx toxin, also the *stx*-phages pose a risk for the human as the phages can convert harmless *E. coli* into pathogenic lysogens. Therefore, EcN was further examined for the possibility of a *stx*-prophage DNA genome integration. Moreover, the influence of EcN on isolated *stx*-phages and Stx was investigated in coculture and in triculture with *stx*-phage susceptible K-12 strains.

## 2. Materials

### 2.1. Equipment

**Table 1: Laboratory equipment and materials.**

<b>Equipment/ Material</b>	<b>Specification</b>	<b>Company</b>
<b>- 80 °C Freezer</b>	HFU 686 Basic	Thermo Fisher Scientific (Bremen)
<b>- 20 °C Freezer</b>	Premium NoFrost GN 3056	Liebherr (Ochsenhausen)
<b>4 °C Fridge</b>	Öko Energiesparer	Privileg (Fuerth)
<b>Analysis scale</b>	JL-180	Chyo Balance Corporation (Japan)
<b>Autoclave</b>	Systec DX-200	Systec (Linden)
<b>Centrifuge</b>	Alegra x-22 centrifuge	Beckman (Sinsheim)
<b>Copper grid</b>	Grid size 100 mesh × 250 µm pitch, copper	Sigma-Aldrich GmbH (Taufkirchen)
<b>Culture tubes</b>	13 ml	Sarstedt (Nuembrecht)
<b>Electrophoresis chamber</b>	Midi – large 460.000	Harnischmacher (Nottuln)
<b>ELISA Reader</b>	Multiscan FC Microplate Photometer	Thermo Scientific (Erlangen)
<b>Eppendorf tubes</b>	1.5 ml, 2 ml	Sarstedt (Nuembrecht)
<b>Falcon tubes</b>	15 ml, 50 ml	Sarstedt (Nuembrecht)
<b>Filtertips</b>	10 µl, 100 µl, 1 ml	A. Hartenstein (Wuerzburg)
<b>Gel documentation</b>	INTAS® GDS	Intas (Goettingen)
<b>Heating block</b>	TS-100	A. Hartenstein (Wuerzburg)
<b>Incubator</b>	AutoFlow NU-5510 Direct Heat CO <sub>2</sub> Incubator	Nuaire (Caerphilly, UK)
	Jouan EB1 Series INNOVENS™ Incubators	Thermo Scientific (Erlangen)
<b>Laminar hood</b>	HeraSafe® HS 12/2	Heraeus (Hanau)
<b>Light microscope</b>	Nikon Eclipse 50i	Nikon (Duesseldorf)

## Materials

<b>Microcentrifuge</b>	Heraeus Pico 21	Heraeus (Hanau)
<b>Microwave</b>	8017	Privileg (Stuttgart)
<b>NanoDrop</b>	NanoDrop 2000c spectrophotometer	Thermo Scientific (Erlangen)
<b>OD cuvette</b>	1.5 – 3 ml	Laborhaus Scheller (Euerbach)
<b>Petri dish</b>	92 x 16 mm	Nerbe Plus (Winsen)
<b>pHmeter</b>	Inolab pH 720	WTW (Weilheim)
<b>Pipetboy</b>	Accu – jet® pro	Brand (Wertheim)
<b>Serological pipettes</b>	5, 10, 25 ml	Greiner (Frickenhausen)
<b>Shaking incubator</b>	New Brunswick Scientific Innova 4000	New Brunswick Scientific (Nuertingen)
<b>Spectrophotometer</b>	Genesys 10 s uv-vis spectrophotometer	Thermo Scientific (Erlangen)
<b>Syringe filter</b>	Acrodisc PES 0.2 µm, 32 mm, sterile (Article No. 514-4131)	PALL (Dreieich)
<b>Thermocycler</b>	Flex Cycler	Analytik Jena AG (Jena)
<b>Transwell insert</b>	PET, 0.4 µm, 4.5 cm <sup>2</sup> , 24 mm (Article No. 657640)	Greiner (Frickenhausen)
<b>Transmission Electron Microscope</b>	JEOL JEM-2100	JEOL (Freising)
<b>Vivaspin</b>	Vivaspin®Turbo 15	Sartorius (Göttingen)
<b>Vortexer</b>	Labinco L46	A. Hartenstein (Wuerzburg)
<b>Well plates</b>	6, 24, 96 (F-form)	Laborhaus Scheller (Euerbach)

## 2.2. Chemicals

**Table 2: Chemicals used in this study.**

<b>Chemical (Abbreviation used)</b>	<b>Company</b>
<b>Acetic acid</b>	Carl Roth GmbH & Co. KG (Karlsruhe)
<b>Agar bacteriology grade</b>	AppliChem (Darmstadt)
<b>Agarose</b>	Peqlab Biotechnologie GmbH (Erlangen)

Materials

<b>Ampicillin</b>	Carl Roth GmbH & Co. KG (Karlsruhe)
<b>Chromogenic <i>E. coli</i> coliform agar (ECC)</b>	MedcoDiagnostica (Munich)
<b>Cellulase from <i>Trichoderma reesei</i></b>	Sigma-Aldrich GmbH (Taufkirchen)
<b>Disodium phosphate (Na<sub>2</sub>HPO<sub>4</sub>)</b>	Carl Roth GmbH & Co. KG (Karlsruhe)
<b>Dimethylsulfoxid (DMSO)</b>	Thermo Fisher Scientific (Erlangen)
<b>DNase I Rnasefree</b>	New England Biolabs (Frankfurt)
<b>DNA loading dye 6 x</b>	Thermo Fisher Scientific (Erlangen)
<b>DNA ladder 100 bp</b>	New England Biolabs (Frankfurt)
<b>DNA ladder 100 bp</b>	Thermo Fisher Scientific (Erlangen)
<b>DNA ladder 1 kbp</b>	Thermo Fisher Scientific (Erlangen)
<b>Calcium chloride (CaCl<sub>2</sub>)</b>	Carl Roth GmbH & Co. KG (Karlsruhe)
<b>Crystal Violet</b>	Sigma-Aldrich GmbH (Taufkirchen)
<b>Ethylenediaminetetraacetic acid (EDTA)</b>	Carl Roth GmbH & Co. KG (Karlsruhe)
<b>Ethanol (EtOH)</b>	Carl Roth GmbH & Co. KG (Karlsruhe)
<b>Ethidium bromide (EtBr)</b>	Carl Roth GmbH & Co. KG (Karlsruhe)
<b>Glutaraldehyde</b>	Sigma-Aldrich GmbH (Taufkirchen)
<b>Glycerol (86 %)</b>	Carl Roth GmbH & Co. KG (Karlsruhe)
<b>Glycol blue</b>	Thermo Fisher Scientific (Erlangen)
<b>Hydrogen chloride (HCl)</b>	Carl Roth GmbH & Co. KG (Karlsruhe)
<b>Isopropyl β-D-1-thiogalactopyranoside (IPTG)</b>	Carl Roth GmbH & Co. KG (Karlsruhe)
<b>Magnesium chloride(MgCl<sub>2</sub>)</b>	Carl Roth GmbH & Co. KG (Karlsruhe)
<b>Mitomycin C (MMC)</b>	AppliChem (Darmstadt)
<b>Monopotassium phosphate (KH<sub>2</sub>PO<sub>4</sub>)</b>	Carl Roth GmbH & Co. KG (Karlsruhe)
<b>Nucleoside triphosphate (dNTPs)</b>	Thermo Fisher Scientific (Erlangen)
<b>PCR Master Mix (2x)</b>	Thermo Fisher Scientific (Erlangen)
<b>Phusion High-Fidelity DNA Polymerase 2 U/μL</b>	Thermo Fisher Scientific (Erlangen)
<b>Phusion 5 x HF buffer</b>	Thermo Fisher Scientific (Erlangen)
<b>Potassium chloride (KCl)</b>	Carl Roth GmbH & Co. KG (Karlsruhe)
<b>Power SYBR® Green RNA-to-CT™ 1-Step Kit</b>	Thermo Fisher Scientific (Erlangen)
<b>Proteinase K</b>	Qiagen (Hilden)

## Materials

<b>RNAprotect Bacteria Reagent</b>	Qiagen (Hilden)
<b>RT enzyme mix</b>	Thermo Fisher Scientific (Erlangen)
<b>Sodium acetate</b>	Carl Roth GmbH & Co. KG (Karlsruhe)
<b>Sodium chloride (NaCl)</b>	Carl Roth GmbH & Co. KG (Karlsruhe)
<b>Sodium hydroxide (NaOH)</b>	Carl Roth GmbH & Co. KG (Karlsruhe)
<b>Tryptone</b>	MP Biomedicals GmbH (Eschwege)
<b>Tris(hydroxymethyl)aminomethane (Tris)</b>	Carl Roth GmbH & Co. KG (Karlsruhe)
<b>Uranyl acetate</b>	Science Services GmbH (Munich)
<b>Yeast extract</b>	MP Biomedicals GmbH (Eschwege)

### 2.3. DNA ladders

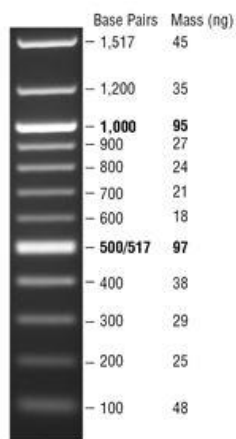


**Figure 10: 100 bp DNA Ladder.** New England Biolabs (Frankfurt)

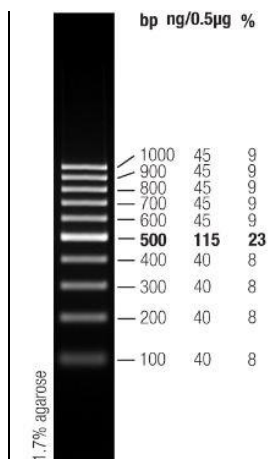


**Figure 11: GeneRuler 100 bp DNA Ladder.** Thermo Fisher Scientific (Erlangen)

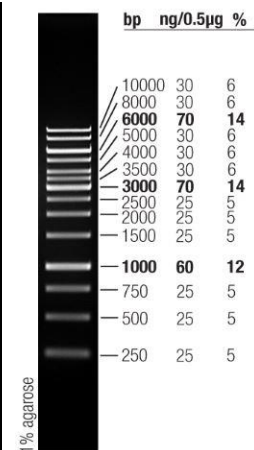


**Figure 12: GeneRuler 1 kb DNA Ladder.** Thermo Fisher Scientific (Erlangen)



**2.4. Bacterial strains****Table 3: *E. coli* strains used in this study.**

<i>E. coli</i> strain	Serotype	Description	Source	Nr. in the strain collection
<i>E. coli</i> Nissle 1917 (EcN)	O6:K5:H1	non-pathogenic probiotic strain	Ardeypharm, Herdecke	464
SK22D	O6:K5:H1	<i>mchCDEF</i> deletion mutant of EcN (no microzins)	Klaus Hantke, (Patzner et al., 2003)	498
EcN $\Delta$ <i>sat</i>	O6:K5:H1	<i>satS</i> deletion mutant of EcN (12.5 $\mu$ g/ml Cm)	Laura Baldomà (Tolosa et al., 2015)	509
EcN $\Delta$ <i>sat psat</i>	O6:K5:H1	Complementation of <i>satS</i> deletion mutant of EcN with pBR322_ <i>satS</i> (50 $\mu$ g/ml Amp)		510
EcN $\Delta$ <i>pks</i>	O6:K5:H1	<i>pks</i> island deletion mutant of EcN (no colibactin)	Ulrich Dobrindt, Muenster	515
EcN $\Delta$ <i>pks ppks</i>	O6:K5:H1	Complementation of <i>pks</i> deletion mutant of EcN with pBeloBAC_ <i>pks</i> (12.5 $\mu$ g/ml Cm)		370
EcN $\Delta$ <i>csg</i>	O6:K5:H1	<i>csg</i> deletion mutant of EcN (no curli adhesin)	Strain collection, IMIB Wuerzburg	96
EcN $\Delta$ <i>bcs</i>	O6:K5:H1	<i>bcs</i> deletion mutant of EcN (no cellulose)		97
EcN $\Delta$ <i>k5</i>	O6:K5:H1	<i>k5</i> deletion mutant of EcN (no K5 capsule)		94
EcN $\Delta$ <i>fliC</i>	O6:K5:H1	<i>fliC</i> deletion mutant of EcN (no flagella)		260
CFT073	O6:K2:H1	Uropathogenic <i>E. coli</i> strain. Close relative to EcN	Strain collection, IMIB Wuerzburg	212

Materials

<b>SE11</b>	O152:H28	Commensal strain	Japan Collection of Microorganisms (JCM)	528
<b>SE15</b>	O150:H5	Commensal strain	JCM	529
<b>IAI1</b>	O8	Commensal strain	Erick Denamur, University of Paris-Diderot	511
<b>DH5<math>\alpha</math></b>	OR:H48:K-	K-12 laboratory strain	Strain collection, IMIB Wuerzburg	278
<b>HB101</b>	OR:H48:K-	K-12 laboratory strain	Strain collection, IMIB Wuerzburg	502
<b>MG1655</b>	OR:H48:K-	K-12 laboratory strain	Strain collection, IMIB Wuerzburg	416
<b>MG1655R</b>	OR:H48:K-	MG1655 harboring the pUC19 plasmid (100 $\mu$ g/ml Amp)	Manonmani Soundararajan	566
<b>MG1655R<math>_{pr}</math></b>	OR:H48:K-	MG1655 harboring the pUC19 plasmid with the <i>phage repressor (pr)</i> (100 $\mu$ g/ml Amp)	Manonmani Soundararajan	550
<b>EHEC EDL933</b>	O157:H7	<i>stx1</i> , <i>stx2</i> harboring STEC strain	Ulrich Dobrindt, Muenster	3 (S3)
<b>EHEC 1530/99 (HUSEC018)</b>	O26:H11	<i>stx2</i> harboring STEC strain	Strain collection, IMIB Wuerzburg	5 (S3)

<b>EAHEC TY3730</b>	O104:H4	<i>stx2</i> harboring STEC strain, Clinical isolate from a gastroenteritis patient (2011)	Holger Rohde, Hamburg	15 (S3)
<b>EAHEC TY3456</b>	O104:H4	<i>stx2</i> harboring STEC strain, Clinical isolate from a HUS patient (2011)	Holger Rohde, Hamburg	28 (S3)
<b>EHEC 4392/97 (HUSEC033)</b>	O145:H25	<i>stx2</i> harboring STEC strain	Ulrich Dobrindt, Muenster	32 (S3)
<b>EHEC O111:H-</b>	O111:H-	<i>eae+</i> , <i>stx1+</i> harboring STEC strain	Strain collection, IMIB Wuerzburg	7 (S3)
<b>EHEC O103:H2</b>	O103:H2,	<i>eae+</i> , <i>stx1+</i> , <i>hly+</i> harboring STEC strain	Strain collection, IMIB Wuerzburg	6 (S3)
<b>EcN bacterial ghosts (BGs)</b>	O6:K5:H1	EcN bacterial envelope	Werner Lubitz, Wien (Langemann et al., 2010)	-

## 2.5. Oligonucleotides

**Table 4: Oligonucleotides used in this study.** Oligonucleotides used in this study were manufactured by Eurofins (Ebersberg).

Name	Sequence (5' – 3')	Amplicon size [bp]	Amplification region	Reference
<b>IL2</b>	AATGAACCAGATCCGTG TGA	EcN: 103	EcN specific chromosomal region	(Troge, 2012)
<b>IR2</b>	CAGGTCCAAACGTAACA GTGC			
<b>4L2</b>	GGGCGATCGGAT TTAATCAT	EcN: 186		

<b>4R2</b>	CGAGGACTCGGAGCTTA CTG			
<b>5L1</b>	GCCTCTCGCAACTTAAC GAC	EcN: 232		
<b>5R1</b>	AGTTATCCAGCGTTGCC ATC			
<b>mchC P8 fwd</b>	TGTCGAACACGTTTCCTG AG	EcN: 3,558 SK22D: 608	Control of <i>mchC-F</i> deletion	(Patzer et al., 2003)
<b>mchC P8 rev</b>	AAACGCGACTGGATATC ACC			
<b>SB67</b>	GGAATTACCCATCCACC TGTA	EcN: - SE11: 257	SE11 specific region ECSE_4549	(Oshima et al., 2008)
<b>SB68</b>	AAACCCCGTTTCACTAA C			
<b>SB69</b>	CCACTGATGTTGATAAT GC	EcN: - SE15: 540	SE15 specific fimbrial operon	(Toh et al., 2010)
<b>SB70</b>	TTAGTTCTTCTGGCATCG			
<b>SB111</b>	ACACGATGCCCTACCGA A	EcN: - IAI1: 478	O8 antigen ABC transporter of IAI1	this study
<b>SB112</b>	AGTTTGCTGAGATTGGG GAC			
<b>SB107</b>	AAGAAAAGAGCAGAGC GAT	EcN: - CFT073: 421	<i>hlyD</i> of CFT073	this study
<b>SB108</b>	TAACAACCCACCTTCA GTAT			
<b>K-12_fwd</b>	TTCCACGGACATGAAG ACTACA	EcN: - K-12: 969	K-12 specific genome region	(Kuhnert, Nicolet, & Frey, 1995)
<b>K-12_rev</b>	CGCGATGGAAGATGCTC TGTA			
<b>SB35</b>	GTATACGATGACGCCGG GAG	EcN: - STEC: 105	<i>stx2</i>	this study
<b>SB36</b>	ATTCTCCCCACTCTGACA CC			

Materials

<b>SB51</b>	CTGGGTTTTTCTTCGGTA TCCT	EcN: - STEC: 518	<i>stx2A</i>	this study
<b>SB52</b>	ACAGTGACAAAACGCAG AAC			
<b>SB37</b>	CCCTGTGCCACTATCAAT CATC	EcN: - EDL933: 156	<i>stx1</i>	this study
<b>SB38</b>	TCAGTTAATGTGGTTGC GAAGG			
<b>O104rfb O-fwd</b>	TGAACTGATTTTTAGGAT GG	TY3730/ TY3456: 356	O104 specific O antigen gene cluster	(Bielasze wska et al., 2011)
<b>O104rfb O-rev</b>	AGAACCTCACTCAAATT ATG			
<b>fl iCH4-a</b>	GGCGAAACTGACGGCTG CTG	TY3730/ TY3456: 201	H4 specific gene for the flagella	
<b>fl iCH4-b</b>	GCACCAACAGTTACCGC CGC			
<b>LP43</b>	ATCCTATTCCCGGGAGTT TACG	TY3730/ TY3456: 584	<i>stx2A</i>	(Bielasze wska, Zhang, Tarr, Sonntag, & Karch, 2005)
<b>LP44</b>	GCGTCATCGTATACACA GGAGC			
<b>TerD1</b>	AGTAAAGCAGCTCCGTC AAT	TY3730/ TY3456: 434	Tellurite resistance gene D	
<b>TerD2</b>	CCGAACAGCATGGCAGT CT			
<b>SB95</b>	GCGGAAAACGGAGATTT AAAAG	EcN: 1,322 EcN $\Delta$ <i>csg</i> : 345	<i>csg</i> of EcN	this study
<b>SB96</b>	CCCTTGCTGGGTCGTATT			
<b>SB97</b>	CCACCATTGCCATCTGCT	EcN: 10,681	<i>bcs</i> of EcN	this study
<b>SB98</b>	ACCGACGAAATGCTCAC AG	EcN $\Delta$ <i>bcs</i> : 1,412		
<b>K5_1 fwd</b>	AGTGAAGGAAGGCCCGG AAG	EcN: 17,523 EcN $\Delta$ <i>k5</i> : 1,126	<i>k5</i> of EcN	this study

Materials

<b>K5_2 rev</b>	ATCAATCGCGTGCGTTCT GG			
<b>SB43</b>	TCGGTAGAACGGCGGAC TGTTAAT	EcN:901 EcN $\Delta$ <i>pks</i> : -	<i>pks</i> of EcN	this study
<b>SB44</b>	TGGTGAGTTCCCGTCCTT GGT			
<b>SB43</b>	TCGGTAGAACGGCGGAC TGTTAAT	EcN: 55,017 EcN $\Delta$ <i>pks</i> :455	<i>pks</i> of EcN	this study
<b>SB46</b>	ATGGACACTGCTCTAAG CGAGGTT			
<b>SB109</b>	GACGATTAGTGGGTGAA ATGA	EcN: 2,184 EcN $\Delta$ <i>fliC</i> :475	<i>fliC</i> of EcN	this study
<b>SB110</b>	CGTCGACTAACAAAAA TGCC			
<b>SB10</b>	AGGCCCGGTACTCTGA ATGTTCA	EcN: 690 EcN $\Delta$ <i>sat</i> : 1,800	<i>satS</i> with or without the insertion of a cat cassette	this study
<b>SB11</b>	GCATTGTTCAAGGTGTAA TGTAT			
<b>SB71</b>	GGAAAAAATCACAACAG GTG	EcN: - <i>stx2</i> -phage: 185	z1468 of <i>stx2</i> - prophage	this study
<b>SB72</b>	TACGCCGGTCTTCTTTAA TC			
<b>SB73</b>	GGAAGCTGGAAAAAGCTGG A	EcN: - <i>stx2</i> -phage: 277	z1475 of <i>stx2</i> - prophage	this study
<b>SB74</b>	AATCCGTTTCGTTTCTGC			
<b>SB75</b>	GGTCCTAAAGGCGAAAC AG	EcN: - <i>stx2</i> -phage: 445	z1483 of <i>stx2</i> - prophage	this study
<b>SB76</b>	TTGCATCAGCCACATTTG			
<b>SB77</b>	CAGCAAATATCACAGC GA	EcN: - <i>stx2</i> -phage: 149	z1449 of <i>stx2</i> - prophage	this study
<b>SB78</b>	AGACCGAAGCTATAAAC CT			

<b>SB79</b>	ACATACTCCACCTTTGCT AC	EcN: - <i>stx2</i> -phage: 595	z1447 of <i>stx2</i> - prophage	this study
<b>SB80</b>	TAGCGCAAGCCTGTAAA G			
<b>SB81</b>	TATTTTCATCCTCCTGGTC AC	EcN: - <i>stx2</i> -phage: 307	z1424 of <i>stx2</i> - prophage	this study
<b>SB82</b>	TCACAAGGCGGGTATTA AC			
<b>SB83</b>	CAGACCTGCGACATATT CC	EcN: - EDL933: 484	z1423 of EDL933	this study
<b>SB84</b>	CGCTGAAGTTGTCGTTA AG			
<b>SB65</b> (200 nM)	ACAAACGCAGGCCAGAA AG	EcN: 127	Real-Time PCR: reference gene <i>hcaT</i> of EcN	(Zhou et al., 2011)
<b>SB66</b> (100 nM)	GCTGCTCGGCTTTCTCAT C			
<b>SB89</b> (150 nM)	TCCGATTAGCAGGGCTT T	EcN: 59	Real-Time PCR: <i>pr</i> of EcN	this study
<b>SB90</b> (150 nM)	CCGGGCGTTTTTTATTGG T			

## **2.6. Bacterial Growth Media**

All autoclavable media were sterilized for 20 min at 121 °C and a pressure of 1 bar. Non autoclavable ingredients were sterile filtered before being added to the media.

**Table 5: LB-medium composition.**

<b>Contents</b>	<b>Amount</b>
Yeast extract	5 g
NaCl	5 g
Trypton	10 g
dH <sub>2</sub> O	ad 1000 ml

**Table 6: 0.7 % LB-Agar composition.**

Contents	Amount
Yeast extract	5 g
NaCl	5 g
Trypton	10 g
Agar	7 g
dH <sub>2</sub> O	ad 1000 ml

**Table 7: 1.5 % LB-Agar composition.**

Contents	Amount
Yeast extract	5 g
NaCl	5 g
Trypton	10 g
Agar	15 g
dH <sub>2</sub> O	ad 1000 ml

## **2.7. Commercially available assay kits**

**Table 8: Kits used in this study.**

Assay kit	Company
RIDASCREEN® Verotoxin ELISA C2201 (Lot: 14166)	R-Biopharm AG (Darmstadt)
Rnaesy®Mini Kit	Qiagen (Hilden)
QIAquick PCR Purification Kit	Qiagen (Hilden)



### **3. Methods**

#### **3.1. Microbiological Methods**

##### **3.1.1. Bacterial storage**

All Bacterial strains were cultivated in Luria-Bertani broth (LB) medium (10 g/l tryptone, 5 g/l yeast, 5 g/l NaCl) medium. For long time storage the bacterial pellet of a 2 ml bacterial overnight culture (ONC) (3.1.2.) was collected by centrifugation for 5 min at 13,000 xg, room temperature (RT). The pellet was resuspended with 500 µl of 500 mM MgCl<sub>2</sub> before 1 ml 87 % glycerol were added. After a brief vortexing step the bacteria were stored at -20 °C or – 80 °C.

##### **3.1.2. Overnight cultures**

For the cultivation of bacteria an ONC was prepared by adding 20 µl of a glycerol stock to 2 ml LB medium in a 13 ml culture tube. The ONC was incubated in a shaking incubator for 14-16 h at 37 °C, 200 rpm.

##### **3.1.3. *E. coli* strain identification**

At the onset of the studies the used *E. coli* strains were investigated for their identity and purity by PCR (3.2.1.) and with the strain color selective Chromogenic *E. coli* coliform agar (ECC) plates. In case of the strain identification, selective genes of the individual strain were determined, and matching primers were designed. In a follow up PCR, the strains were investigated for the presence of the individual gene. Additionally, *E. coli* strains were tested for their purity with ECC plates. The plates enable the differentiation among *E. coli* strain harboring only the β-D-Galactosidase enzyme (pink colonies) or additionally the β-D-Glucuronidase enzyme, which results in a blue colony phenotype. For the EcN mutant determination, primers were designed outside of the deleted genomic region to confirm the deletion by PCR and a follow up sequencing. The amplified region of the EcN mutants was cleaned from PCR residuals with the QIAquick PCR Purification Kit according to the manufacturer's instructions and the DNA concentration was determined with the

NanoDrop 2000c spectrophotometer at an absorbance of 260/280 nm and 260/230 nm. The purified DNA amplicon was sent to LGC genomics for DNA sequencing.

### **3.1.4. Bacterial growth**

To determine the bacterial density at the onset or the ending of an experiment the optical density (OD) of the bacterial suspension was measured at a wavelength of  $\lambda = 600$  nm with the spectrophotometer. For a live bacterial number evaluation, the colony forming units (CFUs) were counted. Therefore, bacteria were diluted in 0.9 % saline. A final 100  $\mu$ l of the appropriate dilution (100-300 CFUs/100  $\mu$ l) was plated with glass beads on LB-Agar plates with or without 100  $\mu$ g/ml Ampicillin (Amp) or on ECC plates in case of co-cultures. The plates were incubated upside-down, overnight at 37 °C, static before the CFUs were counted.

### **3.1.5. stx-phage isolation**

*stx*-phages and Stx were isolated from the *E. coli* strain EDL933 to investigate the direct effect of EcN on the phages and the protein. For the phage and toxin enrichment in the supernatant of EDL933, the OD<sub>600</sub> of a EDL933 ONC was determined. X  $\mu$ l of the ONC were transferred to 10 ml LB medium in a 250 ml glass culture flask to get a final OD<sub>600</sub> of 0.02 (~ 1.6e7 CFUs/ml). The bacterial suspension was either incubated for 24 h without MMC or in case of the phage and toxin induction it was incubated for 2 h at 37 °C, 200 rpm in a shaking incubator, until the lysogenic *E. coli* culture reached its mid-log growing phase (OD<sub>600</sub> 0.3 - 0.5). Then, 1  $\mu$ g/ml MMC was added before the culture was incubated for another 22 h at 37 C, 200 rpm in the dark. Subsequently, suspensions (with or without MMC) were transferred to a 15 ml falcon tube and the bacteria were pelleted at 9,400 xg for 5 min at RT. The supernatant was sterile filtered (0.22  $\mu$ m, PALL), determined for the phage level with a Phage-Plaque-Assay (PPA) (3.1.7.) and immediately used for the mono-/co-/and triculture (3.1.6.) experiments.

### **3.1.6. Bacterial cultivation and sample collection**

The OD<sub>600</sub> of a bacterial ONC was determined with the spectrophotometer. 1 ml of the culture was transferred to a 15 ml falcon tube and centrifuged for 5 min at 9,400 xg, RT. The supernatant was discarded, and the pellet was resuspended in LB medium to get a final OD<sub>600</sub> of 1.0 (~8e8 CFUs/ml) for the commensal *E. coli* and 0.1 (~8e7 CFUs/ml) for the STEC strains.

For the mono-/co-/ and tri-culture experiments 100 µl of the commensal *E. coli* (~8e7 CFUs) were added to 100 µl of a STEC strain (~8e6 CFUs) or 100 µl of isolated phages (~1e7 plaque forming units (pfus) (3.1.5.) in a 24 well plate and adjusted to a volume of 1 ml with LB medium, to get a final relation of 10:1 (commensal *E. coli*: STEC/ *stx*-phages). The plates were sealed with parafilm and incubated for 24 h, or the indicated amount of time at 37 °C, static. Following the incubation time, the samples were collected by sterile filtration (0.22 µm, PALL) and diluted 1:10 with 0.9 % saline for the Stx level determination with the Verotoxin-ELISA (3.1.8.) and/or in 10-fold steps for the plaque forming units evaluation with a PPA (3.1.7.).

### **3.1.7. Phage-Plaque-Assay**

A MG1655 ONC was prepared to determine the number of plaque forming units. For the preparation of one plate, 200 µl of the ONC (OD<sub>600</sub> 2.0 - 3.0) were transferred to a 50 ml falcon tube. A maximum of 10 plates were prepared with one 50 ml falcon tube. 1.5 µg/ml MMC, 20 mM CaCl<sub>2</sub> were added and adjusted to 3 ml/plate with 0.7 % of hand warm LB agar. After a short homogenization of the mixture by inversion of the falcon tube, the 3 ml/plate were poured on top of a 1.5 % LB agar plate with a 25 ml serological pipette. The plates were incubated at 4 °C until use (at the maximum for one day). In case of the MG1655 recombinant strains (MG1655R) harboring a pUC19 plasmid with an Ampicillin (Amp) cassette, MG1655R were grown as ONC in a 100 µg/ml Amp supplemented LB medium with or without 1 mM IPTG. The MG1655R strains were used as indicator strains in a PPA containing 100 µg/ml Amp + 1 mM IPTG. To allow IPTG induction the plates were incubated for another 2 h at RT before the *stx*-phages were dropped on the bacterial lawn.

### **3.1.8. Verotoxin ELISA**

With the Ridascreen®Verotoxin ELISA the Stx level of a suspension can be determined in a 96-well microtiter plate, which is coated with a monoclonal antibody binding specifically to Stx1 and Stx2. To detect the Stx in the sterile filtered samples, the filtrates were 1:10 diluted in 0.9 % saline, mixed by vortexing and subsequently, 100 µl of the diluted samples were transferred to the provided 96-well microtiter plate of the Ridascreen®Verotoxin ELISA Kit. Following the protocol indicated by the manufacturer's instructions, the toxin concentrations in each well were measured with the Multiscan FC Microplate Photometer at the OD<sub>450</sub>. The

obtained values were multiplied by 10. A control provided by the Kit served as positive control. 0.9 % saline was used as negative control.

### **3.1.9. Killing of *E. coli***

*E. coli* strains were killed by heat to study the phage inactivation mechanism of EcN. Therefore, the OD<sub>600</sub> of an ONC was determined and x µl of the culture were transferred to 10 ml LB medium in a 250 ml glass culture flask to receive an OD<sub>600</sub> of 0.1 (~8e7 CFUs/ml). The flask was incubated for 24 h at 37 °C, static before the OD<sub>600</sub> was once more determined. The culture was transferred to a 15 ml falcon tube and pelleted for 5 min at 9,400 xg, RT. The supernatant was discarded, and the pellet was resuspended in x µl LB medium to have a final cell density of ~1.6e10 CFUs/ml (OD<sub>600</sub> = 20). A maximum of 500 µl was transferred to a 1.5 ml eppendorf tube. Finally, the bacteria were killed by heat in the heat block TS-100 for 1 h at 100 °C. To detect further characteristics of the *stx*-phage inactivating component, heat killed *E. coli* or a LB control were incubated for 1 h at 37 °C with 1 mg/ml Proteinase K (PK). The PK was inactivated at 100 °C for 8 min. 100 µl of the differently processed heat killed *E. coli* (~1.6e9 CFUs)/LB medium were used in a *E. coli* + *stx*-phage coculture experiment (3.1.6.).

### **3.1.10. Supernatant collection**

To examine the effect of EcN's secreted factors(s) on the Stx production of STEC strains, the supernatant containing the total secretome was collected. Therefore, EcN was grown for 24 h static at 37 °C in a volume of 10 ml LB medium in a 250 ml glass culture flask. The supernatant of the culture was collected by centrifugation for 15 min at 19,000 xg, 4 °C. Finally, the supernatant was concentrated 10-x with the Vivaspin®Turbo 15 (molecular weight cut off: 3 kDa) for 30 to 60 min in a swing bucket rotor at 4,000 xg, 4 °C. 100 µl of the 10-x concentrated supernatant were used instead of a EcN culture in the coculture experiment with STEC strains (3.1.6.).

### **3.1.11. Lysogeny detection**

Two approaches were used to detect *stx*-phage lysogenic *E. coli*. The first method was to identify a possible phage integration by PCR. Therefore, *E. coli* strains were incubated with *stx*-phages for 24 h (3.1.6.) and afterwards diluted and plated on LB agar plates. All colonies

(~100 - 300) were collected from the agar plates with a spatula, further 1:1000 diluted with 0.9 % saline and heat incubated for 10 min at 100 °C. 2 µl of the diluted bacteria were used as template for a *stx2A* specific PCR (SB51/SB52). Another approach to identify a possible phage genome integration, was to induce phage production accompanied by bacterial lysis. In this set up, *E. coli* strains were incubated with *stx*-phages (10:1) for 48 °h instead of 24 h, to allow possible lysogeny. Subsequently, the bacteria were washed three times with 0.9 % saline (13,000 xg, 5 min, RT) in a 1.5 ml eppendorf tube to dispose *stx*-phages that were bound to the bacterial surface. After the final washing step, the pellet was resuspended in 1 ml LB medium and transferred to a 24 well plate. To force phage production of lysogenic strains 1 µg/ml MMC was added and the bacteria were incubated for 8 h at 37 °C, static in the dark. To collect the phages from lysed bacteria, the suspensions were sterile filtered. In a following phage amplification step, 500 µl of the filtrate was adjusted to 1 ml with LB medium and 100 µl MG1655 (~8e7 CFUs) in a 24 well plate and incubated for 24 h, 37 °C, static. The supernatant was once more collected by sterile filtration and a dilution series of the filtrate was lastly used in PPA (3.1.7.) to investigate for the presence of *stx*-phages.

### **3.1.12. Transwell Assay**

With the Transwell Assay we aimed to identify whether direct cell to cell contact is necessary for EcN to interfere with the Stx and *stx*-phage production of the STEC strains. In this approach the bacterial strains were separated by a 0.4 µm ThinCert™ Cell Culture Insert, which allowed the diffusion of all secreted substrates but interfered with direct bacterial cell contact. As described in (3.1.6.), the bacterial strains were centrifuged and diluted to the mentioned OD<sub>600</sub> values. 250 µl of the *E. coli* strains were added to either the well or insert in a 6 well plate and each compartment was adjusted to a final volume of 2.5 ml LB medium (table 9). The plates were sealed with parafilm and incubated for the desired amount of time at 37 °C, static before the Stx-level and *stx*-phage titer of the filtered samples were evaluated. In the “insert transfer” approach, EDL933 was transferred to a new Transwell insert with LB medium in the lower compartment after the indicated amount of time and incubated for another 3 or 16 h at 37 °C, static (figure 13).

**Table 9: Transwell assay set up.**

Insert		Well
250 $\mu$ l EDL933 ( $\sim 8 \times 10^7$ CFUs/ml), 2.25 ml LB	Monoculture	2.5 ml LB medium
250 $\mu$ l EDL933 ( $\sim 8 \times 10^7$ CFUs/ml), 2.25 ml LB	Coculture	250 $\mu$ l SK22D or MG1655 ( $\sim 8 \times 10^8$ CFUs/ml), 2.25 ml LB medium
250 $\mu$ l EDL933 ( $\sim 8 \times 10^7$ CFUs/ml) +/- 250 $\mu$ l SK22D or MG1655 ( $\sim 8 \times 10^8$ CFUs/ml), add 2.5 ml LB	Triculture	250 $\mu$ l SK22D +/- MG1655 ( $\sim 8 \times 10^8$ CFUs/ml), add 2.5 ml LB medium

**Figure 13: Schematic figure of the EDL933 “insert transfer” from an insert with only LB medium or with SK22D in the well into a new insert with LB medium in the well.****3.1.13. Biofilm Assay**

With the biofilm assay we aimed to investigate if an increase in the biofilm had an influence on the *stx*-phages. *E. coli* ONCs were diluted to the desired  $OD_{600}$  in LB medium as mentioned in (3.1.6.). 24 or 96 well plates were prepared with a final volume of 1 ml in the 24 well plate set up (3.1.6.) and 200  $\mu$ l in the 96 well plate set up (20  $\mu$ l *stx*-phages ( $\sim 1 \times 10^8$  pfus/ml) + 20  $\mu$ l *E. coli* ( $\sim 8 \times 10^8$  CFUs/ml), add 200  $\mu$ l LB medium). For the biofilm induction a sub inhibitory concentration of cellulase (0.09 g Cellulase (0.7 U/mg)) was added to the set up at time point 0 h. The plates were incubated for 24 h at 37 °C, static. Subsequently, the growth was determined by measuring the  $OD_{600}$  values and samples for the phage titer and Stx level determination were collected from the 24 well plates. For the biofilm detection the liquid was carefully removed from all wells before they were washed twice with 1 ml (24 well) or 200  $\mu$ l

(96 well) of PBS (pH 7.4). In a next step the biofilm was fixed in the well plates by heat for 1 h at 60 °C without the cover. The biofilm was stained with 1.25 ml (24 well) or 250 µl (96 well) crystal violet (0.3 % w/v in dH<sub>2</sub>O) for 5 min at RT. Proximately, the crystal violet was removed, and the plates were washed three times with 1.25 ml (24 well) or 250 µl (96 well) dH<sub>2</sub>O to remove excessive stain. The plates were incubated for another 30 min at RT before the crystal violet was dissolved in 1.25 ml (24 well) or 250 µl (96 well) 95 % EtOH. The optical density of the resulting crystal violet solution was determined with the Multiscan FC Microplate Photometer at the OD<sub>570</sub>.

### **3.2. Molecular biological methods**

#### **3.2.1. Polymerase Chain reaction**

The polymerase chain reaction (PCR) is a basic tool in the molecular biology to amplify specific genomic regions. In a first step of the PCR program, the DNA is denaturated at 94 °C, to break the double stranded DNA to single strands. Following the DNA splitting, primers that amplify a desired genomic region can bind to the single stranded DNA at an annealing temperature that is adjusted to the optimal binding temperature of the designed primers. After the primer binding, a copy of the DNA template is synthesized by the elongation of the primers with a polymerase at 72 °C. The elongation time is depending on the amplicon size and the polymerase activity. The DNA splitting, primer binding and elongation cycle is repeated for at least 30 times to increase the DNA concentration. Finally, a last elongation phase terminates the DNA amplification.

In the case of the *E. coli* template preparation 100 µl of bacterial ONCs were transferred to a 1.5 ml eppendorf tube or a colony from a LB agar plate was picked and diluted in 100 µl 0.9 % saline. The bacterial templates were incubated for 10 min at 100 °C. For the *stx*-phage template preparation, 100 µl of the sterile filtrate were heat incubated for 10 min at 100 °C. Free DNA fragments were cleaved by incubating 10 µl phage suspension with 2 µl DNase (2 U/ml) for 10 min at 37 °C followed by a DNase inactivation for 10 min at 100 °C. 2 µl of the phage suspension or 2 µl of the heat boiled bacteria were used as template in a 25 µl PCR reaction using the Taq polymerase (table 10) for standard PCR or the Phusion polymerase (table 11) for subsequent sequencing of the amplicon. The PCR protocol was adapted to the optimal annealing temperature of the primers used.

All primers were designed with the CLC MainWorkbench 6 and synthesized by the company Eurofins MWG Operon (Ebersberg).

**Table 10: Taq Polymerase PCR reaction.**

Volume	Component	Final concentration
2 µl	template	0.5 – 125 ng/25 µl
12.5 µl	2 x PCR Master Mix	1 x
1.25 µl	Primer forward	0.5 µM
1.25 µl	Primer reverse	0.5 µM
add 25 µl	dH <sub>2</sub> O	

PCR protocol Taq polymerase:

94°C/5 min - [94°C/45 sec- x °C/30 sec- 72 °C/1 min/kb] 30 x – 72 °C/10 min- 4°C/∞.

Initial Denaturation - [Denaturation - Annealing - Elongation] - Final Elongation - Cooling

**Table 11: Phusion polymerase PCR reaction.**

Volume	Component	Final concentration
4 µl	template	0.5 – 125 ng/50 µl
10 µl	5 x Phusion HF buffer	1 x
1 µl	20 mM dNTP mix	0.2 mM of each
1.5 µl	DMSO	3 %
2.5 µl	Primer fwd	0.5 µM
2.5 µl	Primer rev	0.5 µM
0.5 µl	2 U/µl Phusion	1 U/50 µl
add 50 µl	dH <sub>2</sub> O	



PCR protocol Phusion polymerase:

94°C/5 min - [94°C/45 sec- x °C/30 sec- 72 °C/30 sec/kb] 30 x – 72 °C/10 min- 4°C/∞.

Initial Denaturation - [Denaturation - Annealing - Elongation] - Final Elongation - Cooling

### **3.2.2. Gel electrophoresis**

To visualize the PCR amplicons, 2 % DNA gels were prepared. Therefore, 3 g agarose were mixed with 150 ml TAE buffer (pH 8.0) in a 250 ml glass culture flask and incubated in the microwave until the agarose was completely dissolved. The solution was poured into a gel chamber with a comb and left until complete hardening. Meanwhile, the PCR mixture was mixed with a 6 x DNA loading dye. 13 µl of the PCR mixture containing the loading dye were pipetted into a gel pocket. As a DNA size control 8 µl of a marker with the appropriate DNA lengths was loaded on the gel. The DNA was electrophoretically separated by size in the DNA gel for 1 h at 150 v, 500 mA in a TAE bath (pH 8.0). Then the gel was incubated for 20 min with the DNA interchelator Ethidium bromide (EtBr) (1 % EtBr bath). Unbound EtBr was washed off with dH<sub>2</sub>O. The DNA, bound to EtBr, was visualized at the EtBr absorbance maxima of 300 nm at the Gel documentation device from INTAS.

### **3.2.3. RNA isolation**

To evaluate the defense mechanism of EcN towards *stx*-phage infection, total EcN bacterial RNA was isolated from EcN cultures incubated with or without *stx*-phages. Bacterial cultures were prepared as mentioned in (3.1.6.) and *stx*-phages were isolated from a MMC induced EDL993 culture (3.1.5.). 300 µl EcN (~8e8 CFUs/ml) were transferred to a 6 well plate with or without 300 µl *stx*-phages (~1e8 pfus/ml). The volume was adjusted to 3 ml with LB medium. The plate was sealed with parafilm and incubated for 3 h or 16 h at 37 °C, static. The cultures were subsequently transferred to 6 ml of RNeasy Protect® Bacteria Reagent (Qiagen, Hilden) in a 15 ml falcon tube. Total bacterial RNA was isolated with the RNeasy Mini Kit (Qiagen, Hilden) according to the manufacturer's instructions. Contaminating DNA was removed by DNase (2 U/ml) digestion for 10 min at 37 °C. The remaining RNA was further purified by ethanol precipitation. Therefore, the isolated RNA was pipetted to a 1.5 ml eppendorf tube and adjusted to a final volume of 180 µl with RNase free dH<sub>2</sub>O. 18 µl of 3 M sodium acetate and 1.33 µl of 15 mg/ml GlycoBlue were added and the sample was gently vortexed. 600 µl of ice cold

100 % EtOH were added and the solution was incubated at  $-20\text{ }^{\circ}\text{C}$  ON. In a next step, the RNA was collected during a 30 min, 13,000 x g at  $4\text{ }^{\circ}\text{C}$  centrifugation time. The resulting pellet was cleaned in a double washing step with 250  $\mu\text{l}$  70 % ice cold EtOH (13,000 x g, 5 min,  $4\text{ }^{\circ}\text{C}$ ). Finally, the RNA pellet was dissolved in 25  $\mu\text{l}$  of RNase free  $\text{dH}_2\text{O}$ . The RNA content was determined by measuring the absorbance at 260 nm and 230 nm at the NanoDrop 2000c spectrophotometer.

### **3.2.4. RNA Library Preparation for the Transcriptome Analysis**

Extracted RNA was depleted of ribosomal RNA using the Ribo-Zero rRNA Removal Kit for bacteria (Illumina) according to the manual. Depleted RNA was fragmented for 3 min at  $94\text{ }^{\circ}\text{C}$  using the NEBNext Magnesium RNA Fragmentation Module. The RNA ends were repaired with two consecutive T4 PNK incubations (-/+ ATP) and an RppH treatment. Library preparation was performed according to the NEBNext Multiplex Small RNA Library Preparation Guide for Illumina. All adapters and primers were diluted 1:4 and 15 and 16 cycles of PCR were used, respectively. No size selection was performed at the end of the protocol. 12 libraries were pooled and sequenced on a NextSeq 500 with a read length of 75 nt.

### **3.2.5. Analysis of deep-sequencing data**

The quality of raw reads (Phred scores, number of duplicates and adapter) were assessed using FastQC (version-0.11.31) (Andrews, 2010). In order to assure a high sequence quality, the Illumina reads in FASTQ format were trimmed with a cut-off phred score of 20 by cutadapt (version-1.15) (Martin, 2011) that was also used to remove the sequencing adapter sequences. The following steps were performed using the subcommand "create", "align" and "coverage" of the tool READemption (Forstner, Vogel, & Sharma, 2014) (version 0.4.3) with default parameters. Reads with a length below 20 nt were removed and the remaining reads were mapped to the reference genome sequences (In-house Genome [21.02.2017]) using segemehl (Hoffmann et al., 2009). Coverage plots in wiggle format representing the number of aligned reads per nucleotide were generated based on the aligned reads and visualized in the Integrated Genome Browser (Freese, Norris, & Loraine, 2016). Each graph was normalized to the total number of reads that could be aligned from the respective library. To restore the original data range and prevent rounding of small error to zero by genome browsers, each graph was then multiplied by the minimum number of mapped reads calculated over all libraries. The

differentially expressed genes were identified using DESeq2 version 1.16.1 (Love, Huber, & Anders, 2014). In all cases, only genes with maximum Benjamini-Hochberg corrected p-value ( $p_{adj}$ ) of 0.05, were classified as significantly differentially expressed. The data were represented as MA plots using R.

The RNA-Seq data presented in this work has been deposited at the NCBI Gene Expression Omnibus (Edgar, Domrachev, & Lash, 2002) and can be accessed through GEO series accession number GSE109932 (<https://www.ncbi.nlm.nih.gov/geo/query/acc.cgi?acc=GSE109932>).

### **3.2.6. Quantitative Real-Time PCR**

The quantitative Real-Time PCR (qRT-PCR) displays a method to analyze the transcription activity of an organism at a certain time point. In a first step, isolated RNA has to be reverse transcribed to cDNA with the reverse transcriptase enzyme (RT), which was first discovered in Retrovirus (Temin & Mizutani, 1970). The cDNA is thereafter used as template in the qRT-PCR, which monitors the DNA amplification by the detection of a fluorescent dye (in this study: SYBR) that binds single stranded DNA. The qRT-PCR method can be subdivided in three phases: (I) the starting phase, the so-called baseline phase (the DNA concentration and therefore, the level of bound fluorescent dye is too low to be detected); (II) the exponential phase (the amplification of the template proceeds and the fluorescence dye exceeds a certain threshold). From this time point the DNA amplification can be tracked at a wavelength of 510 nm. In the last plateau phase (III) the DNA amplification has reached its maximum as the number of free enzymes is too low to continue the amplification. In our study, the qRT-PCR method was used to reconfirm the upregulation of certain genes in EcN which was observed in the transcriptome analysis. Primers were designed which bind to the selected genes and were tested for their ideal concentration (table 4). The isolated RNA was diluted to 40 ng/ $\mu$ l with RNase free dH<sub>2</sub>O. 1  $\mu$ l of the RNA was used as template in the Power SYBR<sup>TM</sup> Green RNA-to-CT<sup>TM</sup> 1-Step Kit. Following thermal cycler conditions were applied:

48 °C/30 min - 95 °C/10 min - [95 °C/15 sec - 60 °C/1 min] 40 x

Reverse transcription - Activation of the polymerase - [Denaturation - Annealing/Elongation]

The constant expressed *E. coli* gene *hcaT* was used as reference gene (Zhou et al., 2011).

### **3.3. Microscopic studies**

#### **3.3.1. Electron microscopy**

For the electron microscopy (EM) studies of *stx*-phage binding to the surface of *E. coli* all vessels used were cleaned with sterile filtered dH<sub>2</sub>O beforehand and filtered tips were used. 900 µl of *stx*-phages (1e8 pfus/ml) from a MMC induced EDL933 culture (3.1.5.) were incubated with 100 µl of a EcN or MG1655 culture (3.1.6.) (~8e7 CFUs/ml) in a 24 well plate for 1 h at 37 °C, static. The bacteria + phage samples were concentrated at 9,400 xg, 5 min at RT and the pellet was resuspend in 100 µl dH<sub>2</sub>O with a 1 ml pipette tip. 100 µl of the concentrated phage +/- bacteria suspension was incubated with 10 µl of 5 % glutaraldehyde (final: 0.5 %) for 1 min to crosslink the proteins before 10 µl of the suspension was dropped on a copper grid and incubated for another 2 min at RT. The superfluous liquid was removed with a filter paper and the copper grid was washed twice with 10 µl dH<sub>2</sub>O. In a last step the sample was stained with 10 µl of 0.5 % uranyl acetate for 1 min and superfluous liquid was removed with a filter paper in a 30 ° angle towards the copper grid. The dried copper grid was stored in a grid box at RT until it was analyzed with the JEOL JEM-2100 Transmission Electron Microscope.

#### **3.3.2. Light microscopy**

To analyze the phenotypic formation of various *E. coli* strains, they were visualized with the light microscope. Mono- and cocultures of *E. coli* strains with or without the K-12 strain MG1655 were prepared in a 24 well plate as mentioned in (3.1.6.) and incubated for 24 h at 37 °C. The samples were mixed carefully by pipetting them up and down and afterwards 10 µl were dropped on 1.5 % agarose slabs (figure 14). The bacteria were visualized at the Nikon Eclipse 50i microscope at a 500-x magnification.

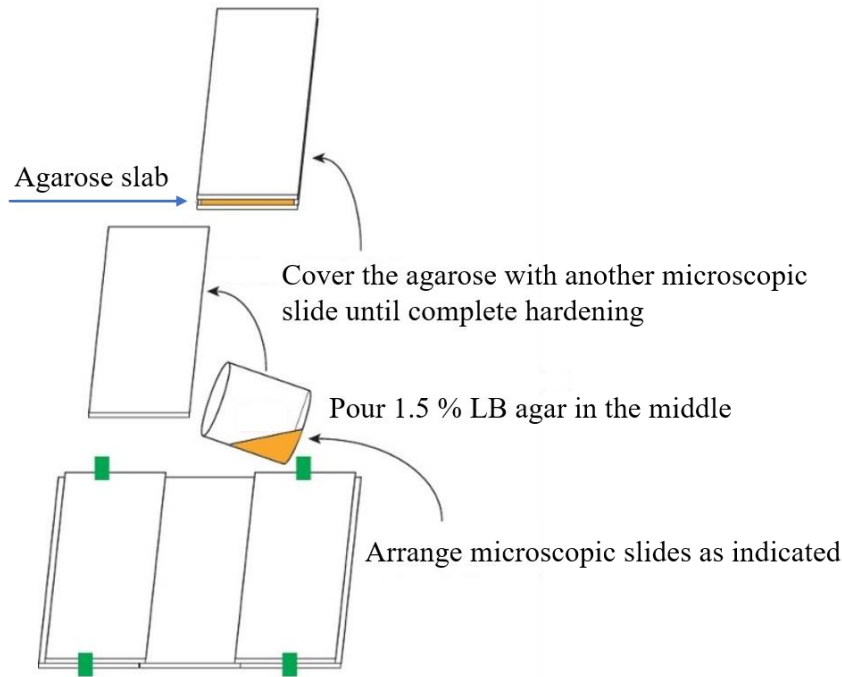


**Figure 14: Schematic instruction of agarose slab preparation (modified from (Zeng & Golding, 2011)).**

### **3.4. Computer-assisted analyses**

For the comparison and analysis of nucleotide sequences, the basic local alignment search tool (BLAST) was used (Altschul, Gish, Miller, Myers, & Lipman, 1990) from the webpage: [https://blast.ncbi.nlm.nih.gov/Blast.cgi?PAGE\\_TYPE=BlastSearch&BLAST\\_SPEC=blast2seq&LINK\\_LOC=align2seq](https://blast.ncbi.nlm.nih.gov/Blast.cgi?PAGE_TYPE=BlastSearch&BLAST_SPEC=blast2seq&LINK_LOC=align2seq). The comparison of protein sequences was performed with the multiple sequence alignment (MUSCLE) program from the webpage: <https://www.ebi.ac.uk/Tools/msa/muscle/>. The search for prophages in the genome of several *E. coli* strains was performed with the PHAge Search Tool (PHAST) on the webpage: <http://phast.wishartlab.com/>. The presence of secretion systems was screened with the T346Hunter on the webpage: <http://bacterial-virulence-factors.cbgp.upm.es/T346Hunter> (Martinez-Garcia, Ramos, & Rodriguez-Palenzuela, 2015).

### **3.5. Statistical analysis**

The experiments were performed independently for at least 3 times in duplicates. Data are shown as mean +/- standard deviation (SD). For the statistical analysis of the experimental data GraphPad Prism® version 7 was used. For the significance determination the t-test was used.

## **4. Results**

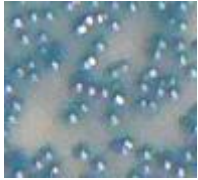











### **4.1. *E. coli* strain identification**

At the start of the studies, the *E. coli* strains used were analyzed for their identity and purity. The strain purity was confirmed by plating the strains on color selective ECC plates. The identity of the strains was further verified with a PCR for strain specific genes.

#### **4.1.2. Confirmation of the *E. coli* purity**

The purity examination of the used *E. coli* strains was carried out with ECC plates containing the chromophore-substrate complexes X-GLUC and Salmon-GAL (de Sioniz, Valderrama, & Peinado, 2000). ONCs of *E. coli* strains were diluted to 1000 - 3000 CFUs/ml and 100  $\mu$ l were plated on ECC plates (3.1.3.). During the ON incubation at 37 °C, bacteria harboring the  $\beta$ -D-Glucuronidase enzyme hydrolyzed X-GLUC to glucuronic acid and X-gal. The dimerized X-gal, was proximately oxidized to 5,5'-dibromo-4,4'-dichloro-indigo and stained thereby the bacterial colonies blue. Bacteria harboring the  $\beta$ -D-Galactosidase enzyme cleaved Salmon-GAL by hydrolysis, which resulted in a pink colony formation. In case of *E. coli* harboring both enzymes, bacteria reflected a violet phenotype on the ECC plates. Due to this differences in the bacterial metabolic activity the ECC plates provided a first tool for the strain purity identification.

EcN *wildtype* (*wt*) and the EcN microcin negative mutant SK22D (figure 15) formed blue colonies on the ECC plates. All EcN mutants used in this study showed the same phenotype (data not shown). The MG1655 strain formed pink colonies which slowly turned into a blue color in case of a longer incubation time. The ECC plates unraveled that there was no contamination of the tested *E. coli* strains on a single colony level (figure 15).

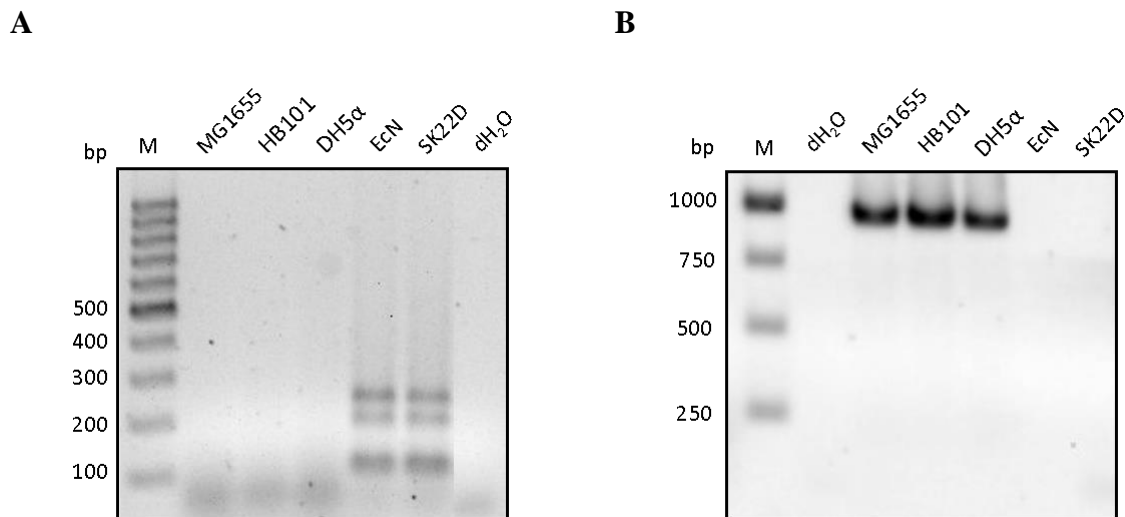
			
<b>EcN (+ relative)</b>	<b>EcN: dark-blue</b>	<b>SK22D: dark-blue</b>	<b>CFT073: violet</b>
			
<b>K-12 strains</b>	<b>MG1655: pink*</b>	<b>HB101: pink</b>	<b>DH5α: light-blue</b>
			
<b>Commensals</b>	<b>SE11: dark-blue</b>	<b>SE15: dark-blue</b>	<b>IAI1: dark-blue</b>
			
<b>STEC strains</b>	<b>EDL933: pink</b>	<b>TY3730: dark-blue</b>	<b>TY3456: dark-blue</b>

**Figure 15: *E. coli* colonies on ECC plates.** The *E. coli* strains EcN, SK22D, CFT073, MG1655, DH5 $\alpha$ , HB101, SE11, SE15, IAI1, EDL933, TY3730, TY3456 were serially diluted and plated on ECC plates for the strain purity identification.

### 4.1.3. Strain identification PCR

In the next step the *E. coli* strains were verified for their identity with a strain specific PCR using an aliquot of an ONC. Primers were designed that amplify specific genes from the investigated *E. coli* strain. The PCR reactions for the strain identification were performed with the 2 x PCR Master-Mix (3.2.1.).

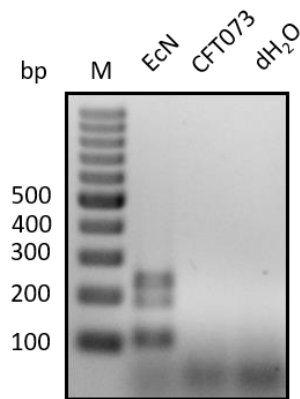
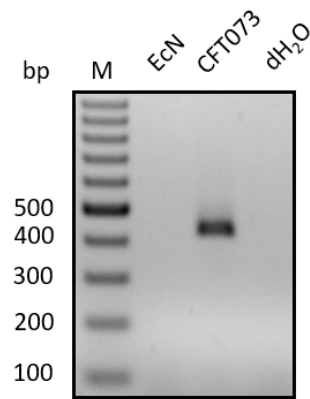
The EcN identity for EcN and SK22D was confirmed on the chromosome level with the primer pairs IL2/IR2 (amplicon: 103 bp), IL4/IR4 (amplicon: 186 bp) and IL5/IR5 (amplicon:232 bp) (figure 16 A). The K-12 strains MG1655, HB101 and DH5 $\alpha$  were screened for a K-12 specific genomic region with the K-12\_fwd and K-12\_rev primers (amplicon: 969 bp) (Kuhnert et al., 1995). All strains showed the expected DNA amplicon size (figure 16 B).



**Figure 16: PCR screen to identify specific chromosomal regions of EcN and the K-12 strains.** (A) For the EcN strain identification a multiplex PCR was performed with the primer pairs IL2/IR2 (103 bp), IL4/IR4 (186 bp) and IL5/IR5 (232 bp). (B) The K-12 MG1655, HB101 and DH5 $\alpha$  strains were identified with the primer pair K-12\_fwd/rev (969 bp). M: Marker, dH<sub>2</sub>O: negative control.

The EcN close relative, uropathogenic strain CFT073 was identified with a PCR for the *hemolysin D* (*hlyD*) gene, which is only present in CFT073 but not in EcN. The PCR (figure 17 B) proofed the presence of the *hlyD* (amplicon: 421 bp) in the CFT073 but not in the EcN template, by which the strain purity of 4.1.2. was reconfirmed.



**A****B**

**Figure 17: PCR screen to identify specific chromosomal regions of EcN and CFT073.**

(A) For the EcN strain identification a multiplex PCR was performed with the primer pairs IL2/IR2 (103 bp), IL4/IR4 (186 bp) and IL5/IR5 (232 bp). (B) CFT073 was screened for *hlyD* with the primer pair SB107/108 (421 bp). M: Marker, dH<sub>2</sub>O: negative control.

The commensal *E. coli* strains SE11, SE15 and IAI1 were all isolated from healthy individuals and served as commensal control strains. SE11 was screened for the presence of the SE11 specific region ECSE\_4549 with the primers SB67/SB68 (amplicon: 257 bp) (Oshima et al., 2008) (figure 18 B). The SE15 strain identity was confirmed by a PCR for the SE15 fimbrial operon with the primer pair SB69/SB70 (amplicon: 540 bp) (Toh et al., 2010) (figure 18 C). The commensal strain IAI1 was investigated for the O8 antigen ABC transporter with the primers SB111/SB112 (amplicon: 478 bp) (figure 18 E). All strains were successfully identified and showed no EcN contamination (figure 18 A, D).

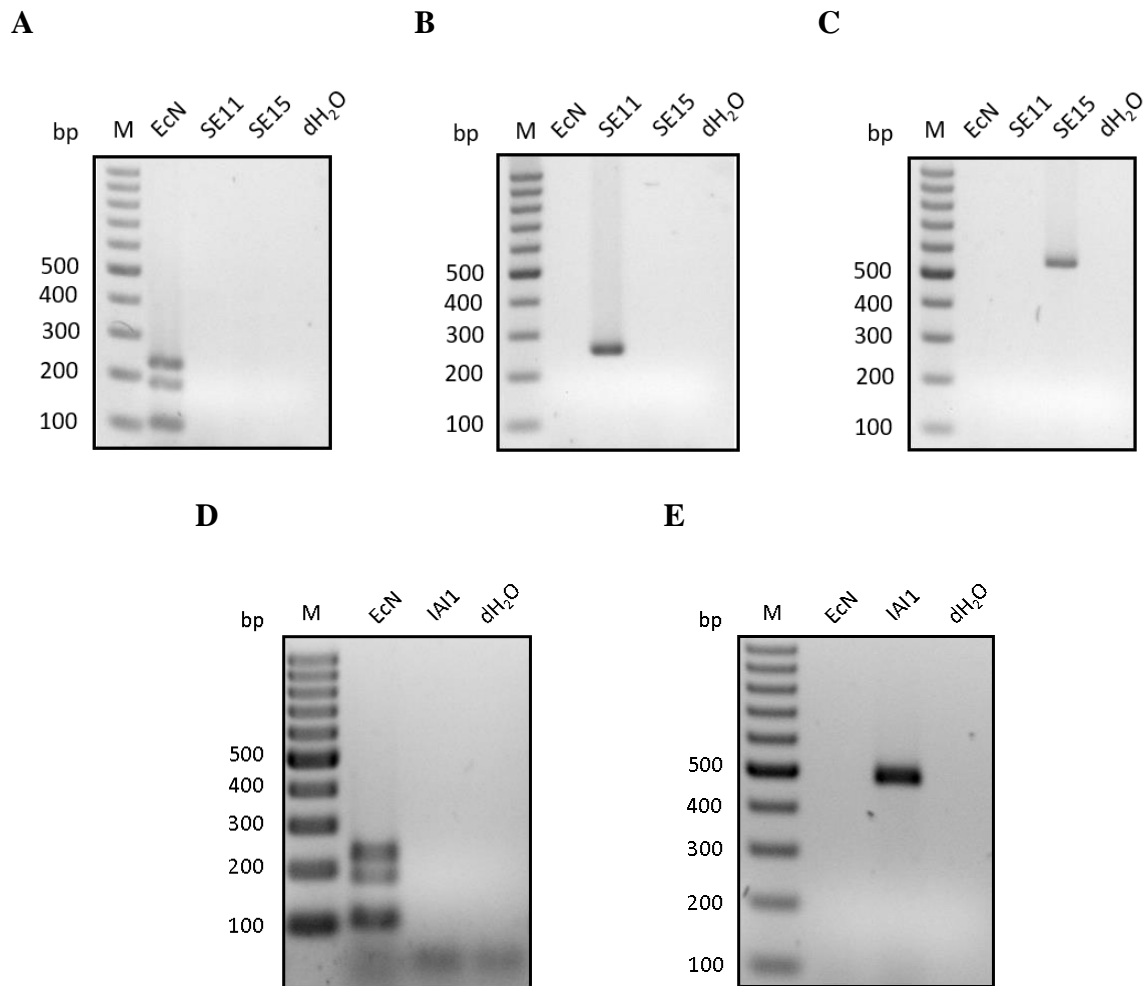


**Figure 18: PCR screen to identify specific chromosomal regions of EcN and the commensal control strains SE11, SE15 and IAI1.** (A), (D) For the EcN strain identification a multiplex PCR was performed with the primer pairs IL2/IR2 (103 bp), IL4/IR4 (186 bp) and IL5/IR5 (232 bp). (B) SE11 was screened for ECSE\_4549 with the primer pair SB67/68 (257 bp), (C) SE15 was identified for fimbrial operon with the primers SB69/70 (540 bp) and (E) IAI1 O8 was screened for the O8 antigen ABC transporter with the primers SB111/112 (478 bp). M: Marker, dH<sub>2</sub>O: negative control.

The STEC strains EDL933 and two O104:H4 isolates (TY3730, TY3456) from the EHEC epidemic in the year 2011, were investigated for the presence of strain specific genes. EDL933 was analyzed with primers that amplify *stx1* and *stx2*: SB37/SB38 (amplicon: 156 bp) and SB35/SB36 (amplicon: 105 bp) (figure 19 A, B). The TY strains were screened in a multiplex PCR for the *rfb* O104 gene cluster with O104rfbO-fwd/rev (amplicon: 351 bp), the flagellar serotype H4 with fliCH4-a/b (amplicon: 201 bp), *stx2* with LP43/44 (amplicon: 584 bp) and the tellurite resistance domain (*terD*) with TerD1/2 (434 bp) (Bielaszewska et al., 2011). The

rfb O104 amplicon for the TY3456 strain was only weak visible. Besides, all expected DNA amplicons could be detected in the strain specific PCR (figure 19 C).

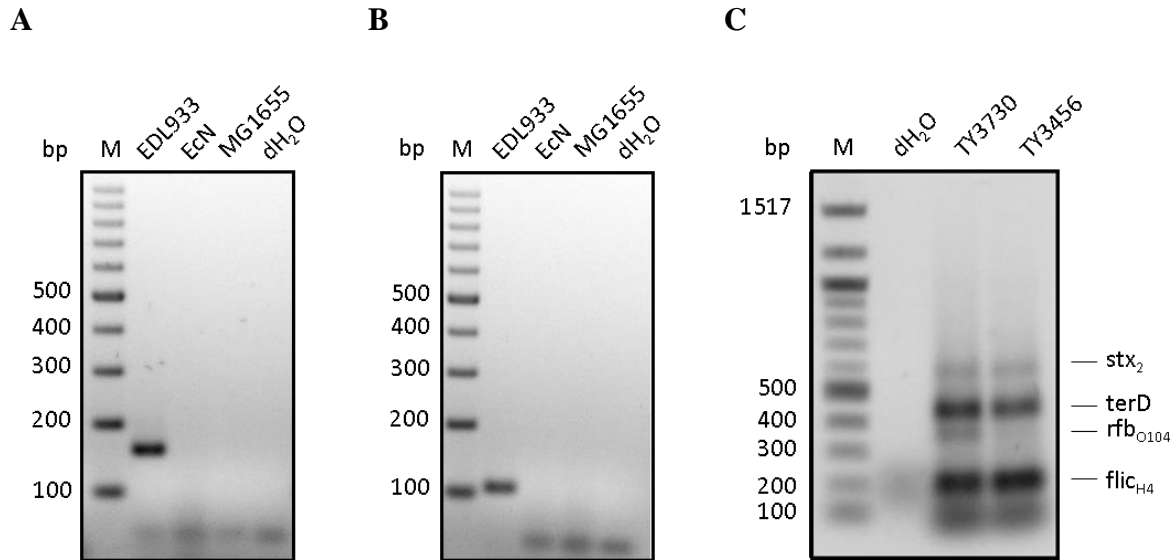


**Figure 19: PCR screen to identify specific chromosomal regions of the STEC strains EDL933 the 2011 outbreak strains TY3730 and TY3456 (O104:H4).** (A) EDL933 *stx1* screen with the primers SB37/SB38 (156 bp). (B) EDL933 *stx2* screen with the primers SB35/SB36 (105 bp). (C) TY strain identification with the primer pairs O104rfbO-fwd/rev (351 bp), fl iCH4-a/b (201 bp), LP43/44 (*stx2*) (584 bp) and TerD1/2 (434 bp). M: Marker, dH<sub>2</sub>O: negative control.

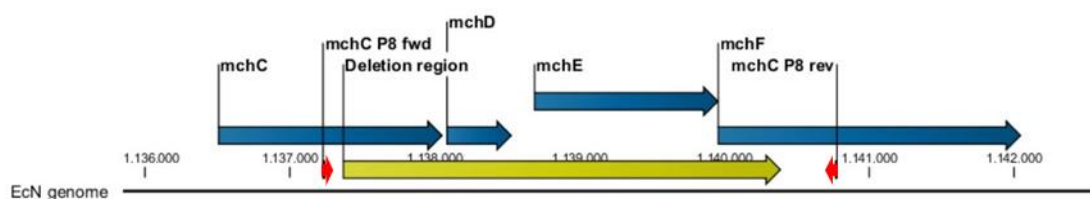
#### 4.1.4. EcN mutant screening

The EcN mutants used in this study were firstly screened for a positive gene deletion. Primers were designed to bind up- and downstream of the deleted genomic regions. The deletions were investigated by an amplicon sequencing. Table 12 shows the exact deletion regions of the EcN mutants and the primer binding sites. The microcin mutant SK22D was identified to have a deletion of 3,026 bp in the *mchC-F* gene cluster. In the EcN cellulose mutant EcN $\Delta$ *bcs* the region *yhjQ*, *bcsA/B/Z/C* is deleted by 9,269 bp. The curli mutant EcN $\Delta$ *csg* has a 977 bp deletion in *csgA/B*. For the EcN K5 capsule mutant EcN $\Delta$ *k5* a 17,523 bp deletion was determined in the *kpsF/E/D/U/C/S/T/M* and *kfiA/B/C/D* gene cluster. The flagellin mutant EcN $\Delta$ *fliC* has a complete deletion of the *fliC* gene with an 1,800 bp genomic shortening and the colibactin mutant EcN $\Delta$ *pks* demonstrated a deletion of the *clbA-R* gene cluster (54,562 bp). EcN $\Delta$ *sat*, the serine protease mutant of EcN, was kindly donated from the group of Laura

Baldoma in Spain. For the mutant preparation, a chloramphenicol acetyl transferase (*cat*) cassette from the pCAT19 plasmid was inserted at the indicated *Swa*I restriction side (Tolosa et al., 2015).

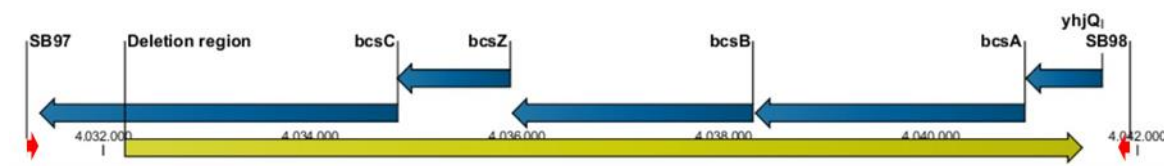
**Table 12: Deletion or insertion regions of EcN mutants.** The mutants *EcNΔmchC-F* (SK22D), *EcNΔbcs*, *EcNΔcsg*, *EcNΔk5*, *EcNΔfliC*, *EcNΔpks*, *EcNΔsat* were screened. Deletions are indicated as yellow arrows. Genes are indicated as blue arrows. Primers are indicated as red arrows.

A



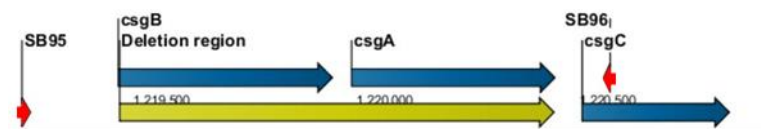
EcN mutant	Microcin genomic region	Deletion region
<i>EcNΔmchC-F</i> (SK22D)	1,136,505 - 1,142,049	1,137,366 - 1,140,391

B



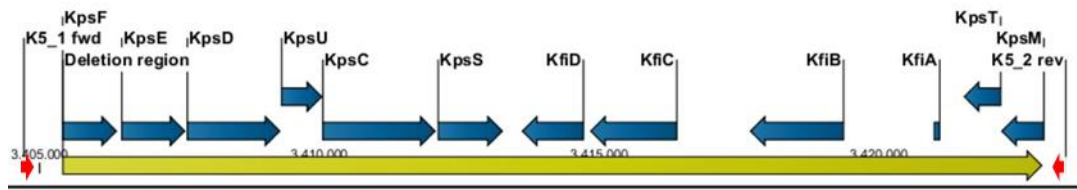
EcN mutant	Cellulose genomic region	Deletion region
<i>EcNΔbcs</i>	4,031,381 - 4,041,666	4,032,204 - 4,041,472

C



EcN mutant	Curli genomic region	Deletion region
<i>EcNΔcsg</i>	1,219,402 - 1,220,774	1,219,405 - 1,220,381

D



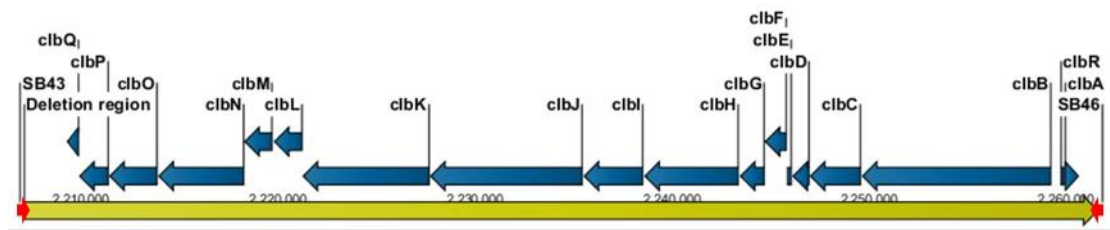
EcN mutant	Capsule genomic region	Deletion region
EcN $\Delta$ k5	3,405,403 - 3,422,968	3,405,406 - 3,422,928

E



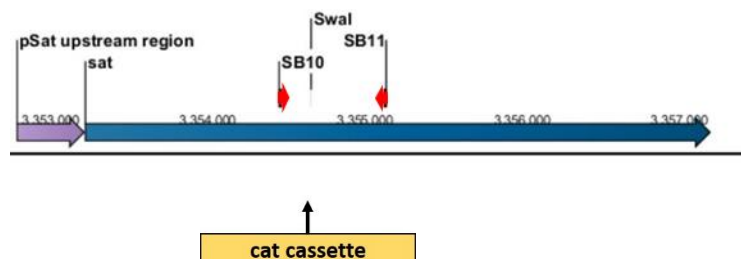
EcN mutant	Flagellin genomic region	Deletion region
EcN $\Delta$ fliC	2,099,443 - 2,101,230	2,099,435 - 2,101,234

F



EcN mutant	Colibactin genomic region	Deletion region
EcN $\Delta$ pks	2,209,289 - 2,260,669	2,207,101 - 2,261,662

G



EcN mutant	Serine protease genomic region	Insertion region
EcN $\Delta$ sat	3,353,219 - 3,357,200	SwaI: 3,354,661 - 3,354,662

#### **4.1.5. EcN mutant PCR verification**

The results from the mutant screening (4.1.4.) were regularly reconfirmed by PCR. All EcN mutants were positively identified for being EcN in the EcN chromosome multiplex PCR (figure 20-23 A). The deletion of the *mchC-F* gene cluster from SK22D was confirmed with the primer pair mch P8 fwd/rev (amplicon EcN: 3,558 bp, SK22D: 608 bp). The PCR in figure 20 B captured the microcin cluster deletion in SK22D. The additional amplicon of a size smaller than 500 bp is probable due to an unspecific binding of the primers.

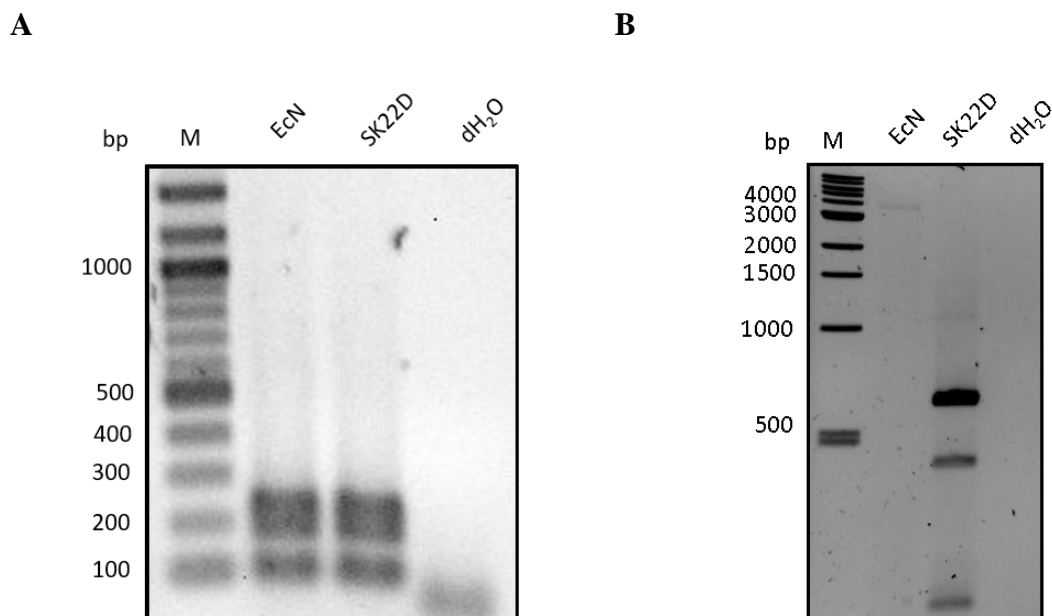


**Figure 20: PCR screen to identify the microcin mutant SK22D.** (A) For the EcN strain identification a multiplex PCR was performed with the primer pairs IL2/IR2 (103 bp), IL4/IR4 (186 bp) and IL5/IR5 (232 bp). (B) The *mchC-F* gene cluster deletion was confirmed with the primer pair mch P8 fwd/rev (EcN: 3,558 bp, SK22D: 608 bp). M: Marker, dH<sub>2</sub>O: negative control.

To verify the deletion of the cellulose gene cluster in EcN $\Delta$ *bc*s, the primer pair SB97/98 which annealed outside of the deleted region amplified a 1,412 bp DNA fragment for the mutant. The 10,681 bp amplicon of the EcN *wt* was not amplified (figure 21 B). The mutation in the curli genome was reconfirmed with the primers SB95 and SB96. The deletion mutant template resulted in an amplicon size of 345 bp, whereas the EcN *wt* amplicon had a size of 1,322 bp (figure 21 C). For the EcN K5 capsule mutant EcN $\Delta$ *k5*, the primers K5\_1\_fwd and K5\_2\_rev

amplified a 1,126 bp region. The amplification region of the *EcN wt*, with a size of 17,523 bp, was too long to be amplified in the PCR reaction (figure 21 D).

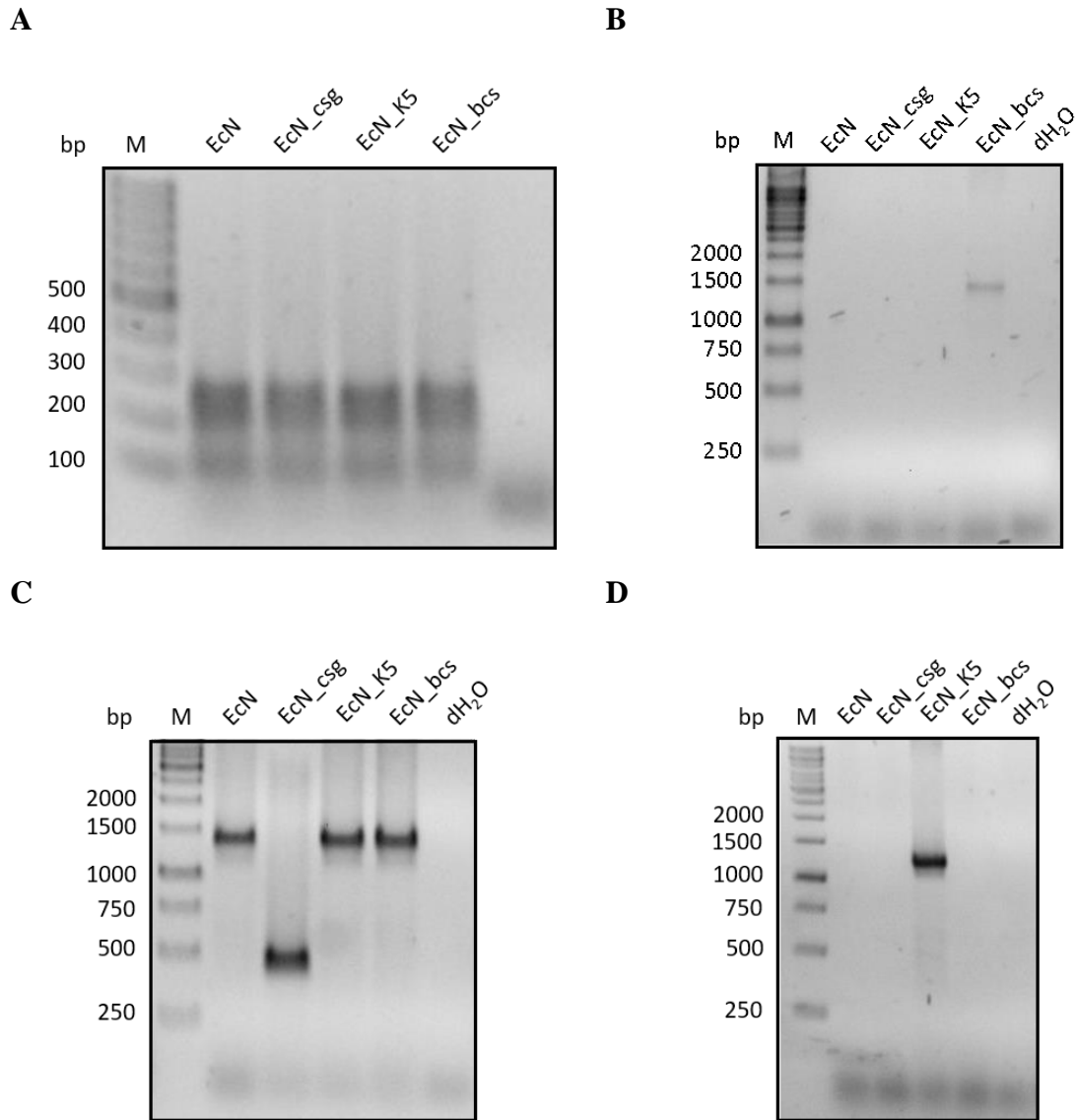


**Figure 21: PCR screen to identify the *EcN* mutants *EcN*Δ*bcs*, *EcN*Δ*csg*, *EcN*Δ*k5*.** (A) For the *EcN* strain identification a multiplex PCR was performed with the primer pairs IL2/IR2 (103 bp), IL4/IR4 (186 bp) and IL5/IR5 (232 bp). (B) The *bcs* gene cluster deletion was confirmed with the primer pair SB97/98 (*EcN*: 10,681 bp, *EcN*Δ*bcs*: 1,412 bp). (C) The curli deletion was confirmed with the primer pair SB95/96 (*EcN*: 1,322 bp, *EcN*Δ*csg*: 345 bp). (D) The K5 capsule deletion was confirmed with the primer pair K5\_1 fwd/rev (*EcN*: 17,523 bp, *EcN*Δ*k5*: 1,126 bp). M: Marker, dH<sub>2</sub>O: negative control.

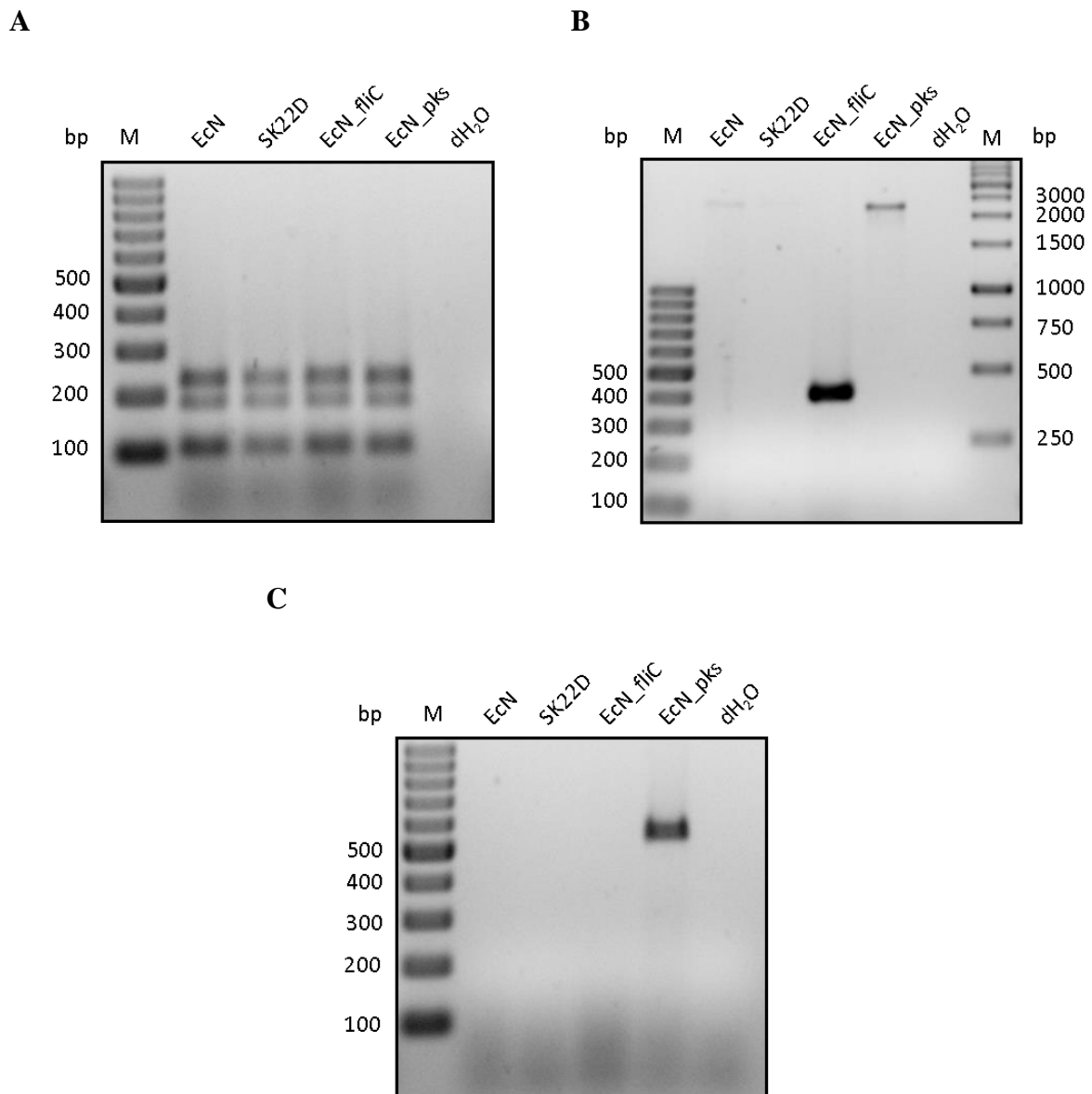


**Figure 22: PCR screen to identify the EcN mutants  $EcN\Delta fliC$ ,  $EcN\Delta pks$ .** (A) For the EcN strain identification a multiplex PCR was performed with the primer pairs IL2/IR2 (103 bp), IL4/IR4 (186 bp) and IL5/IR5 (232 bp). (B) The flagellin deletion was confirmed with the primer pair SB109/110 (EcN: 2,184 bp,  $EcN\Delta fliC$ : 475 bp). (C) The colibactin cluster deletion was verified with the primer pair SB43/46 (EcN: 55,017 bp,  $EcN\Delta pks$ : 455 bp). M: Marker, dH<sub>2</sub>O: negative control.

To identify the *fliC* mutant the primer pair SB109 and SB110 annealed up- and downstream of *fliC*. The amplicon of  $EcN\Delta fliC$  had a size of 475 bp compared to 2,184 bp of in the EcN *wt* (figure 22 B). For the EcN mutant SK22D, the *fliC* amplicon was very weak visible in the PCR gel picture. In case of the colibactin deletion mutant  $EcN\Delta pks$  a large region of the gene



cluster was deleted. Therefore, only the mutant showed a PCR amplicon of 455 bp after the PCR with the primer pair SB43 and SB46 (EcN *wt*: 55,017 bp) (figure 22 C).

The EcN $\Delta$ *sat* mutant from Spain was investigated for the cat cassette insertion. The primer pair SB10/SB11 resulted in a PCR amplicon of 690 bp for the EcN *wt* and the *sat* complementation plasmid (pSat) and of 1,800 bp in case of the cat insertion (figure 23 B).

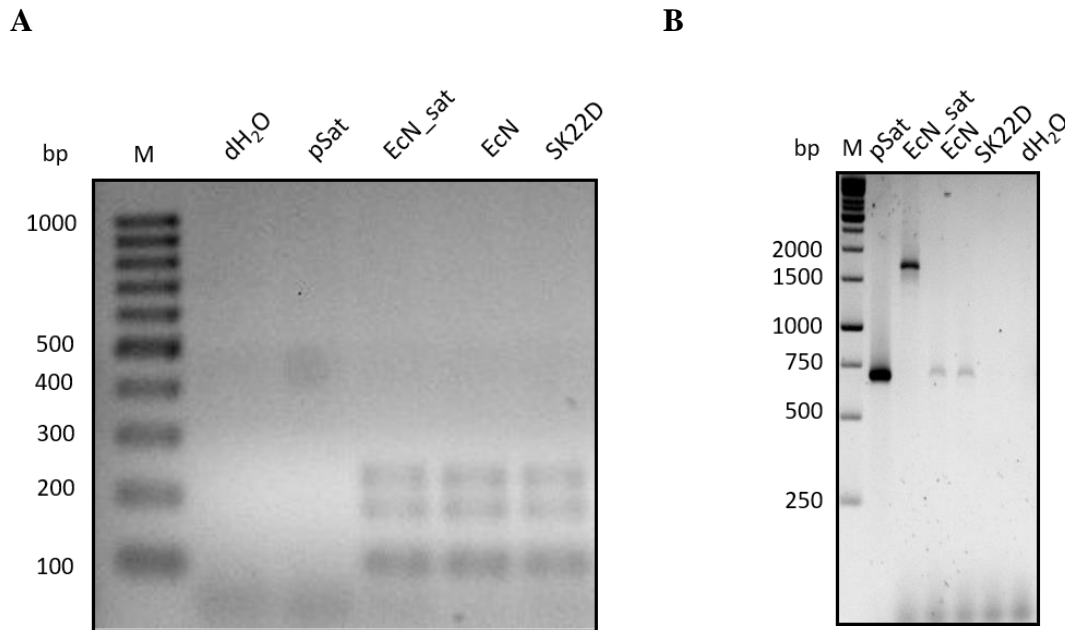


**Figure 23: PCR screen to identify the EcN mutant EcN $\Delta$ *sat*.** (A) For the EcN strain identification a multiplex PCR was performed with the primer pairs IL2/IR2 (103 bp), IL4/IR4 (186 bp) and IL5/IR5 (232 bp). (B) EcN $\Delta$ *sat* verification PCR with the primer pair SB10/11 (EcN/ pSat: 690 bp, EcN $\Delta$ *sat*: 1,800 bp). M: Marker, dH<sub>2</sub>O: negative control.

## **4.2. Molecular mechanism of the Shiga toxin downregulation by EcN**

The interference with the Stx production of STEC strains by EcN was shown by Rund et al., 2013, and was aimed to be investigated closer during this study.

### **4.2.1. Influence of SK22D on the EDL933 pathogenicity**

The pathogenic *E. coli* 0157:H7 strain EDL933 is associated to the development of gastroenteritis in human and serves as a STEC laboratory strain since it was isolated in the first

reported STEC outbreak of 1982 (Perna et al., 2001). A specific feature of EDL933 is that it harbors both a *stx1* and a *stx2* prophage.

At the onset of the experiments, the kinetics of the *stx*-phage and Stx production from the statically incubated pathogenic *E. coli* strain EDL933 were determined. Moreover, the effect of the microcin negative EcN mutant SK22D and the laboratory K-12 strain MG1655 on the pathogenic factor production was analyzed in co- and triculture studies (3.1.6.). The Stx and *stx*-phage level of EDL933 were determined in the sterile filtered supernatants after 2 h, 6 h and 24 h of static incubation in LB medium. The CFUs of EDL933 were counted on LB Agar plates in case of the monoculture or with ECC plates for the co- and tricultures at the equivalent time points. The EHEC monoculture results reflected a continuous increase of the toxin level detection at the OD<sub>450</sub> of 0.56 at 2 h, 1.89 at 6 h and 6.23 at 24 h with the Stx-ELISA (3.1.8.). Moreover, 6.5e5 pfus/ml *stx*-phages were detected in the supernatant of the 24 h static culture of EDL933 with the PPA (3.1.7.) (figure 24 A).

When SK22D was added at time point 0 h at a ratio of 1:10 (EDL933:SK22D) the toxin level did not significantly increase (0 h: OD<sub>450</sub>= 0.62, 6 h: OD<sub>450</sub>= 0.74, 24 h: OD<sub>450</sub>= 0.93) and a phage decrease of over 1,000 pfus/ml was detected at the 24 h time point (2e2 pfus/ml) (figure 24 B). Anyhow, the CFUs of EDL933 were about 10 -fold reduced compared to the monoculture. On the opposite, the CFUs of EDL933 were comparable to the monoculture if the K-12 strain MG1655 was added with a starting ratio of 1:10 (EDL933: MG1655). After 6 h incubation the Stx level was comparable to that of the EDL933 and SK22D coculture (OD<sub>450</sub>: 0.78) but increased around 23-fold after 24 h incubation (OD<sub>450</sub>: 17.7). Likewise, the phage plaque increased 1,000-fold at the 24 h time point, compared to the monoculture set up (figure 24 C). During the triculture kinetics experiment, the Stx level (OD<sub>450</sub>: ~0.8) was comparable to the Stx level from the EDL933 and SK22D coculture, the pfus/ml decreased 10-fold from 6e5 to 1e4 pfus/ml compared to the EDL933 monoculture and the CFUs of EDL933 decreased by 10-fold (figure 24 D).

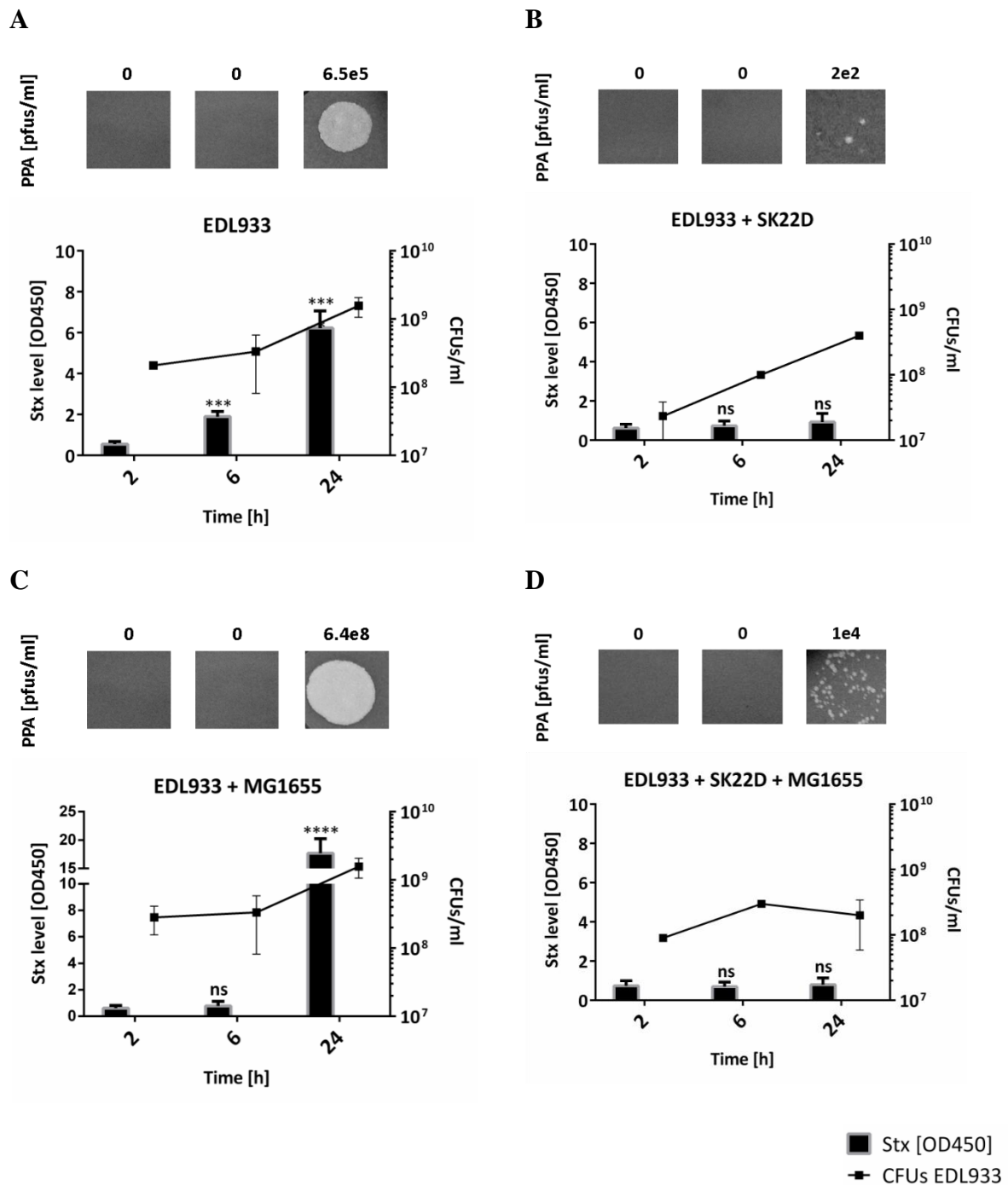


**Figure 24: Stx level, *stx*-phage titer and CFU kinetics of the EHEC strain EDL933 in mono-/co- and triculture. (A) EDL933 monoculture. (B) Coculture of EDL933 and SK22D (1:10). (C) Coculture of EDL933 and MG1655 (1:10). (D) Triculture kinetics of EDL933 and SK22D and MG1655 (1:10:10). PPA: Phage Plaque Assay, CFUs: Colony forming units, ns: not significant, \*\*\* $p < 0.001$  and \*\*\*\* $p < 0.0001$ .**

The kinetic studies showed that the presence of SK22D resulted in a toxin and phage reduction whereas the presence of MG1655 led to a pathogenic factor increase in coculture.

#### **4.2.2. Protection capacity of SK22D after MMC induction**

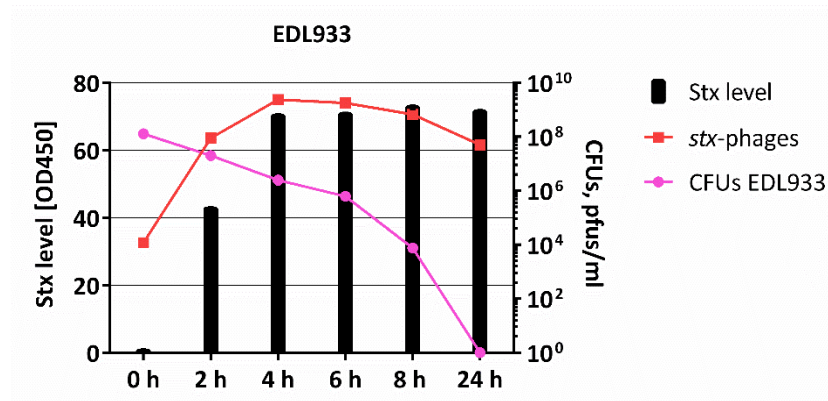
MMC is a DNA damaging agent which triggers the SOS response in *E. coli* and it is therefore used *in vitro* to induce the Stx and *stx*-phage production and release of STEC strains.

We aimed to identify the capabilities of SK22D towards the reduction of Stx and *stx*-phage production by EDL933 after the addition of 1 µg/ml MMC to a 2 h shaking culture. EDL933 was incubated in mono- or in coculture with SK22D (1:10) for 24 h at 200 rpm in the dark. At the time points 0 h, 2 h, 4 h, 8 h and 24 h (after MMC addition), samples were collected to determine the CFUs, the pfus and the Stx level at the individual time points. Figure 25 A illustrates the results gained from the MMC induced EDL933 monoculture. It could be observed that the Stx level (black bars) raised from the OD<sub>450</sub> of 0.6 at the time point 0 h to 42.7 after only 2 h of incubation and reached a plateau of 72 +/- 1.7 after 4 h - 24 h of MMC addition. This equals an increase of the toxin level by 1,000 % towards the Stx level after 24 h incubation without the addition of MMC (OD<sub>450</sub> = 6.23) in the previous kinetic studies in 4.2.1.. The *stx*-phage titer evaluation (red line) depicted a phage titer of 1.2e4 pfus/ml at the time point of MMC addition which increased to 9e7 pfus/ml after 2 h, 2.4 pfus/ml after 4 h and reached a maximum of 1.6e9 pfus/ml after 6 h of incubation with MMC. Afterwards, the phage titer decreased by 2.6-fold at the 8 h time point (6.8e8 pfus/ml) and was even reduced by 35-fold after 24 h incubation (5.1e7 pfus/ml). Looking at the CFUs of EDL933 (figure 25 A, pink line) we observed a continuous CFUs reduction over the time which resulted in no colony detection after 24 h of incubation.

For the investigation of the SK22D protection capability, SK22D was incubated along with EDL933 at a ratio of 1:10 (EDL933: SK22D) and as in the monoculture experiment, 1 µg/ml MMC was added to a 2 h shaking culture (figure 25 B). As in the EDL933 monoculture a Stx level increase was detected 2 h after MMC addition. The Stx level of OD<sub>450</sub> = 12.8 nevertheless, is 70 % reduced compared to the Stx level of the monoculture. Also, the coculture reached a toxin plateau of 48.9 +/- 1.2 after 4 h to 24 h incubation, thus a 32 % reduction towards the monoculture toxin level. The phage titer in the 2 h shaking culture (= 0 h time point) equaled the one in the monoculture with 1.1e4 pfus/ml and increased to a maximum of 5.4e7 pfus/ml after 6 h incubation. Compared to the EDL933 monoculture the presence of SK22D resulted in a ~33-fold phage reduction. Likewise, the phage titer decreased after the 6 h incubation time point. The CFUs of EDL933 decreased over time until no EDL933 colonies could be detected 24 h after MMC induction. Also, SK22D demonstrated a CFUs reduction triggered by the DNA damaging agent. The CFUs dropped from 1.6e8 CFUs/ml before the

addition of MMC (0 h) to a minimum of  $5.8 \times 10^6$  CFUs/ml after 4 h. Unlike EDL933, SK22D recovered again and grew to a CFUs/ml of  $2 \times 10^9$  after 24 h of incubation.

A



B

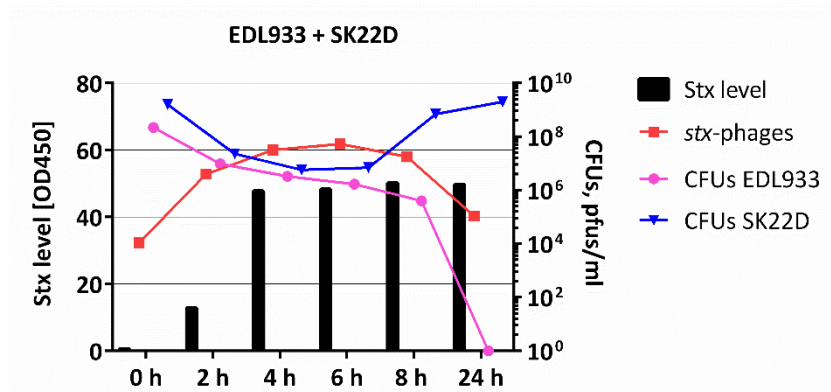


**Figure 25: Stx and *stx*-phage kinetics after MMC induction.** The kinetics of the Stx level (black bars), the *stx*-phage plaques (red line) and the CFUs of EDL933 (pink line) and SK22D (blue line) were determined after the induction of the SOS response in 2 h cultures with 1 mg/ml Mitomycin C (MMC) at 0 h, 4 h, 6 h, 8 h and 24 h in (A) the EDL933 monoculture and in (B) the coculture with SK22D (1:10).

The MMC experiment unraveled an influence of SK22D towards the Stx and *stx*-phage production by EDL933 even after the addition of MMC. Anyhow, the protecting effects were reduced compared to its potency without the addition of MMC which could be due to an influence on the growth of SK22D by MMC.

#### **4.2.3. SK22D's influence on the Stx and phage level of STEC strains**

Since the STEC outbreak in 1982, a high number of STEC epidemics have been reported all over the world (Byrne, Jenkins, Launder, Elson, & Adak, 2015; Karch, Bielaszewska, Bitzan, & Schmidt, 1999; Vally et al., 2012). The *E. coli* strains involved in the disease outbreaks were found to be also non-O157 STEC (Bettelheim, 2007). In the year 2011, even Germany was hit by an unusual O104:H4 STEC epidemic (Bielaszewska et al., 2011; RKI, 2011b). Therefore, we investigated the effect of SK22D on other *stx1* and *stx2* STEC strains in coculture (STEC: SK22D, 1:10) and triculture (STEC: SK22D: MG1655, 1:10:10).

The *stx2* STEC strains TY3730 and TY3456, isolated from patients in the 2011 outbreak and the *stx2* prophage harboring strains EDL933 (*stx2* and *stx1*), O26:H11 and H145:H25 as well as the *stx1* strains O103:H2 and O111:H- were incubated with SK22D and/ or MG1655 for 24 h, static. The Stx level and the plaque forming units were subsequently determined in the sterile filtered supernatants. For the *stx2* STEC strains EDL933, TY3730 and TY3456 a 91 - 92 % reduction of the Stx level was observed in the coculture with SK22D (figure 26 A). In coculture with the *stx2* strain O26:H11, the toxin was reduced by 84 %. Only when being cultured with the weak Stx producer O145:H25 (Stx level: 0.49) no Stx reduction was observed. Comparably to the results in 4.2.1., the toxin level increased by ~ 118 % when MG1655 was added in the coculture incubation with EDL933 or the TY strains. For the O26:H11 strain no toxin increase was detected as well as for O145:H25. The toxin level of the *stx2* STEC + SK22D + MG1655 triculture experiment was comparable the toxin detected in the SK22D coculture (~ 90 % reduction compared to the monoculture). O145:H25 was not influenced in the low Stx production by MG1655. The further performed *stx*-phage plaque forming unit determination on a MG1655 bacterial lawn unraveled a ~5,900-fold ( $5.7 \times 10^9$  pfus/ml) increase of *stx2*-phage plaques if MG1655 was used in the coculture experiment with EDL933 (EDL933 monoculture:  $9.7 \times 10^5$  pfus/ml). When MG1655 was cultured with the TY strains the pfus raised 16 x for TY3730 ( $1.3 \times 10^5$  pfus/ml to  $2.1 \times 10^6$  pfus/ml) and 114 x for the TY3456 strain ( $1.1 \times 10^5$  pfus/ml to  $1.3 \times 10^7$  pfus/ml) compared to the STEC monoculture. In the coculture of MG1655 with O26:H11 the pfus/ml increased from  $9.5 \times 10^3$  pfus/ml to  $1.6 \times 10^4$ . This was contrasted by the results from the phage plaques in the presence of SK22D. The *stx2*-phage plaques were decreased by ~4,800-fold in the coculture of EDL933 with SK22D ( $2 \times 10^2$  pfus/ml) and 93-fold ( $1 \times 10^4$  pfus/ml) in the triculture of EDL933 with SK22D and MG1655.

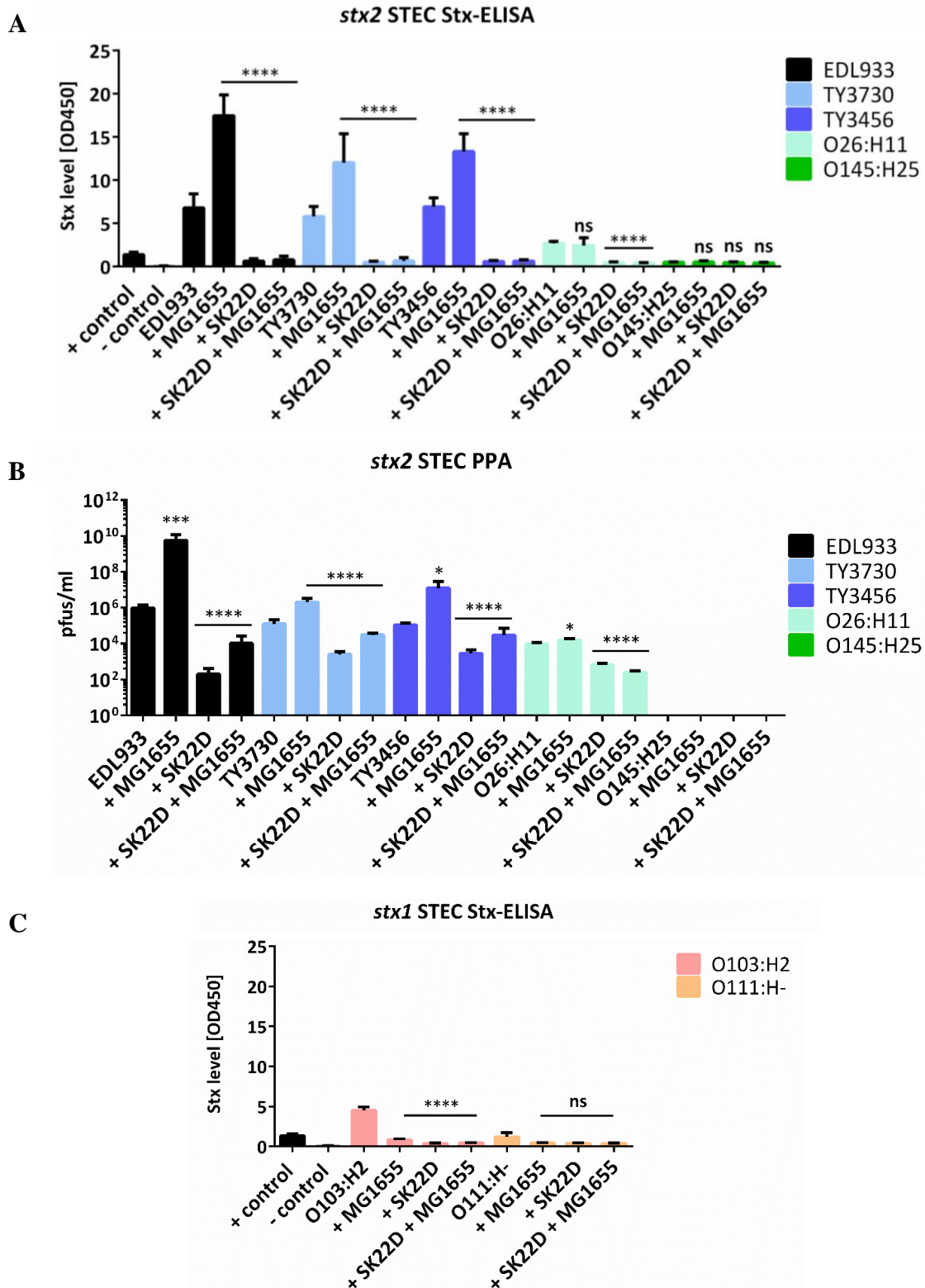


**Figure 26: Stx level and *stx*-phage titer of *stx2* and *stx1* STEC strains in mono-/co-(1:10)/ and triculture (1:10:10) with SK22D and/or MG1655. (A) Stx ELISA of *stx2* STEC strains. (B) Phage Plaques of *stx2* STEC strains. (C) Stx ELISA of *stx1* STEC strains. PPA: Phage Plaque Assay, ns: not significant, \* $p < 0.05$ , \*\*\* $p < 0.001$  and \*\*\*\* $p < 0.0001$ . (Images modified from Bury et al., 2018, under review).**

For both TY strains the plaque units decreased by 40 -50-fold ( $2.7e3 \pm 1.5e2$  pfus/ml) in the coculture with SK22D and by 4-fold in the triculture with TY3730, SK22D and MG1655 ( $3.1 e4$  pfus/ml) and 37-fold in the triculture of TY3456, SK22D and MG1655 ( $3.0 e4$  pfus/ml). The pfus were also decreased by around 20-fold in the co- and tricultures with O26:H11 (monoculture:  $9.5e3$  pfus/ml, coculture:  $6.5e2$  pfus/ml, triculture:  $2.5e2$  pfus/ml). The *stx2* strain O145:H25 produced no phages that could be detected with the PPA in any experimental set up (figure 26 B).

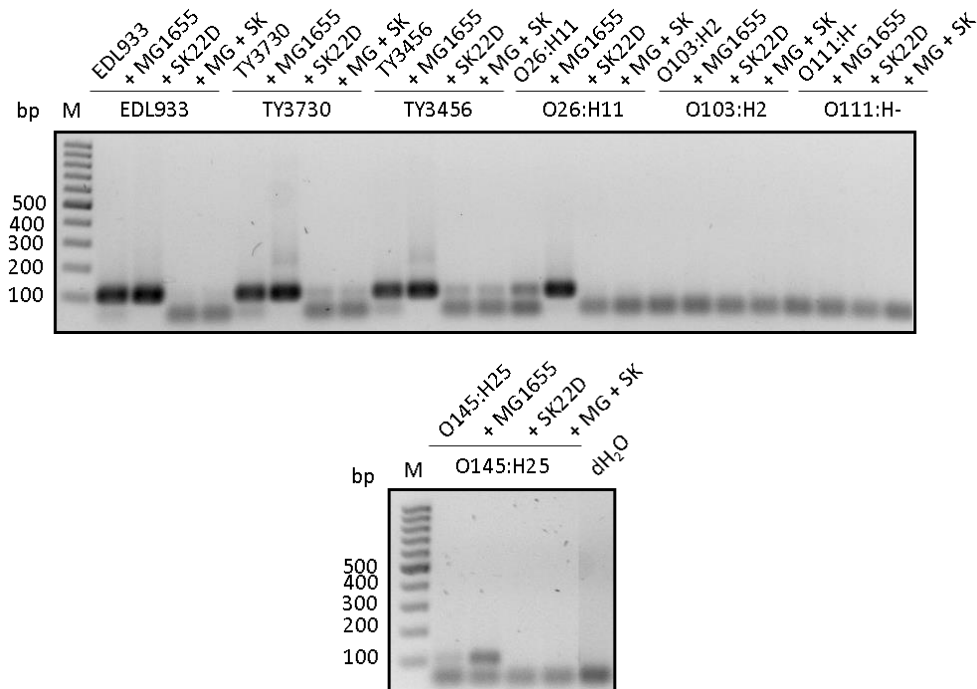
Contrary to the Stx2 results, the *stx1* prophage harboring STEC strains O103:H2 and O111:H- showed to be negatively influenced in their toxin level by both, SK22D and MG1655. The Stx1 level of O103:H3 was decreased by 80 - 90 % in all co- and triculture set ups. The O111:H- strain exposed a weak Stx1 level of OD<sub>450</sub>: 1.21 in monoculture and a ~33 % reduction of Stx1 in the co- and triculture with both *E. coli* strains (figure 26 C). No phage plaques could be detected with the PPA for both tested *stx1* STEC strains.

Because not all *stx*-phages could be detected with the MG1655 indicator PPA, the sterile filtered supernatants of the mono-/co-/and tricultures were further analyzed for the presence of *stx*-phage DNA. For this, the supernatant was heat incubated for 10 min at 100 °C and was subsequently used as template in a *stx2* or *stx1* specific PCR with the primer pairs SB35, SB36 (*stx2*) and SB37, SB38 (*stx1*). The expected *stx2* amplicon had a size of 105 bp and the *stx1* amplicon had a size of 156 bp. Figure 27 A represents the results of the *stx2* specific PCR. The PCR gel confirmed that the presence of SK22D lead to a reduction of *stx2*-phage numbers and connected to this to a reduction of *stx2* DNA in the filtered supernatant. The coculture with the K-12 strain MG1655 resulted in a *stx2*-phage increase and was proved by an increase in the *stx2* amplicon intensity. The DNA band intensity in the triculture experiments equaled the *stx2* amplicon intensity from the STEC and SK22D coculture. The *stx1* PCR enabled the detection of *stx1*-phage DNA in the supernatant of the cultures EDL933, O103:H2 and O111:H-, for which phage plaques were not detected with the PPA. In the figure 27 B, the reduction of the *stx1* DNA amplicon intensity in the presence of MG1655 and to no DNA amplicon recognition in the presence of SK22D reconfirmed the Stx1 level reduction by both *E. coli* strains that was observed in figure 27 C. The supernatants of all STEC strain monocultures showed only PCR amplicons for the *stx*-prophage type present in their genome.

With the *stx* specific PCR the results from the Stx ELISAs and the PPA were reconfirmed (figure 26). The presence of SK22D resulted in a reduction of the toxin level and the phage plaque formation for all tested STEC strains.



A



B

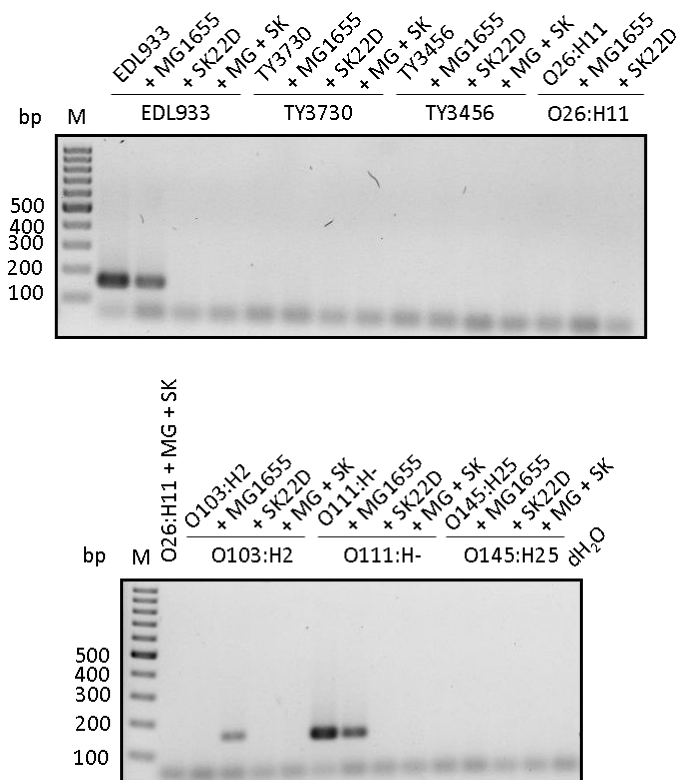


**Figure 27: *stx*-phage detection by PCR in the supernatant of the mono-/co- and tricultures.** The sterile filtered supernatants of the *stx2* and *stx1* STEC strains were used as a PCR template after mono-/co-/and triculture incubation. (A) *stx2* PCR with the primer pair SB35/36 (105 bp). (B) *stx1* PCR with the primer pair SB37/38 (156 bp). M: Marker, dH<sub>2</sub>O: negative control.

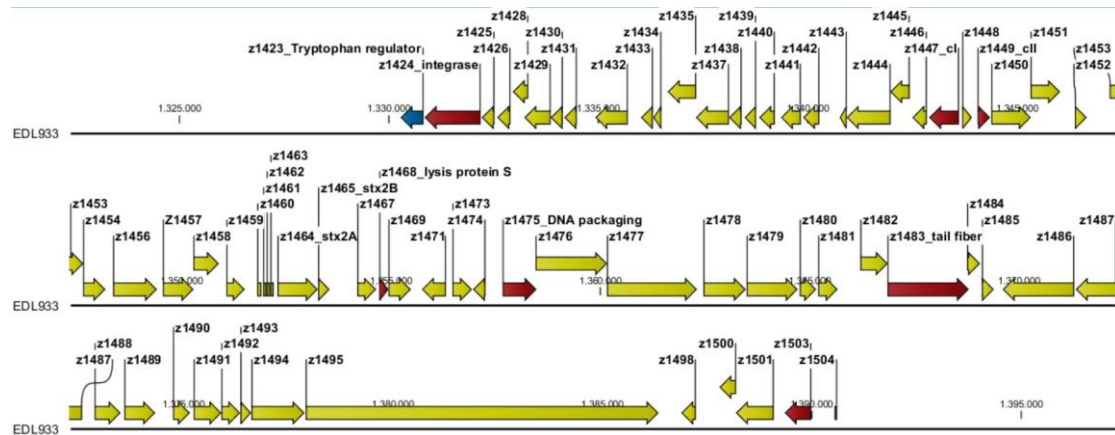
#### **4.2.4. Influence of EcN on the pathogenic agents of STEC strains**

It is known that the incubation of EcN with EHEC strains results in a toxin decrease (Rund et al., 2013). This reduction was traced back to a significant downregulation of the *stx2a* transcription (Mohsin et al., 2015). In our experiment we aimed to reconfirm these findings by detecting the *stx*-phage DNA from STEC and EcN cocultures, as the Stx production is known to be connected to the *stx*-phage synthesis (Pacheco & Sperandio, 2012). Moreover, we wanted to identify the impact of EcN on isolated Stx and *stx2*-phages themselves.

##### **4.2.4.1. *stx2*-phage DNA detection**

The PCR results of the experiment in 4.2.3. were expanded in a next approach, in which several genes spanning the *stx2*-prophage genome (figure 28 A) were investigated for their presence in the supernatant of mono- or cocultures of EDL933 with SK22D or MG1655 to confirm the absence or presence of the entire phage DNA (*stx2*-prophage genes: table 15). The bacterium EDL933 served thereby as a positive *stx2*-prophage control. *z1423*, which codes for the tryptophan (TRP) repressor binding protein is located upstream of the *stx2*-prophage and was used as negative control for the presence of free EDL933 DNA in the filtered supernatants. The gene was amplified with the primer pair SB83 and SB84 (amplicon: 484 bp). All other genes tested (figure 28 A, marked as red arrows) were part of the *stx2*-prophage genome. *z1424*, the integrase of the prophage, was amplified with the primers SB81, SB82 and resulted in the expected DNA amplicon of 307 bp. The amplification of the *cI* phage transcriptional repressor (*z1447*) created an amplicon of 595 bp with the primers SB79, SB80. *cII*, the transcriptional regulator of the phage (*z1449*) was investigated for its presence with SB77 and SB78, which amplified a 149 bp DNA region. Another more downstream located gene *z1468*, coding for the phage lysis protein S, was detected with SB71/SB72 (amplicon: 185 bp). The gene *z1475*, which codes for the small subunit of the terminase was investigated for being present with the primer pair SB73 and SB74 (amplicon 277 bp), the gene *z1483*, coding for the tail fiber protein, was amplified with the primers SB75 and SB76 (amplicon: 455 bp) and the last prophage gene *z1503* of unknown function was amplified with the primer pair SB115/SB116 (amplicon: 260 bp).

A



B

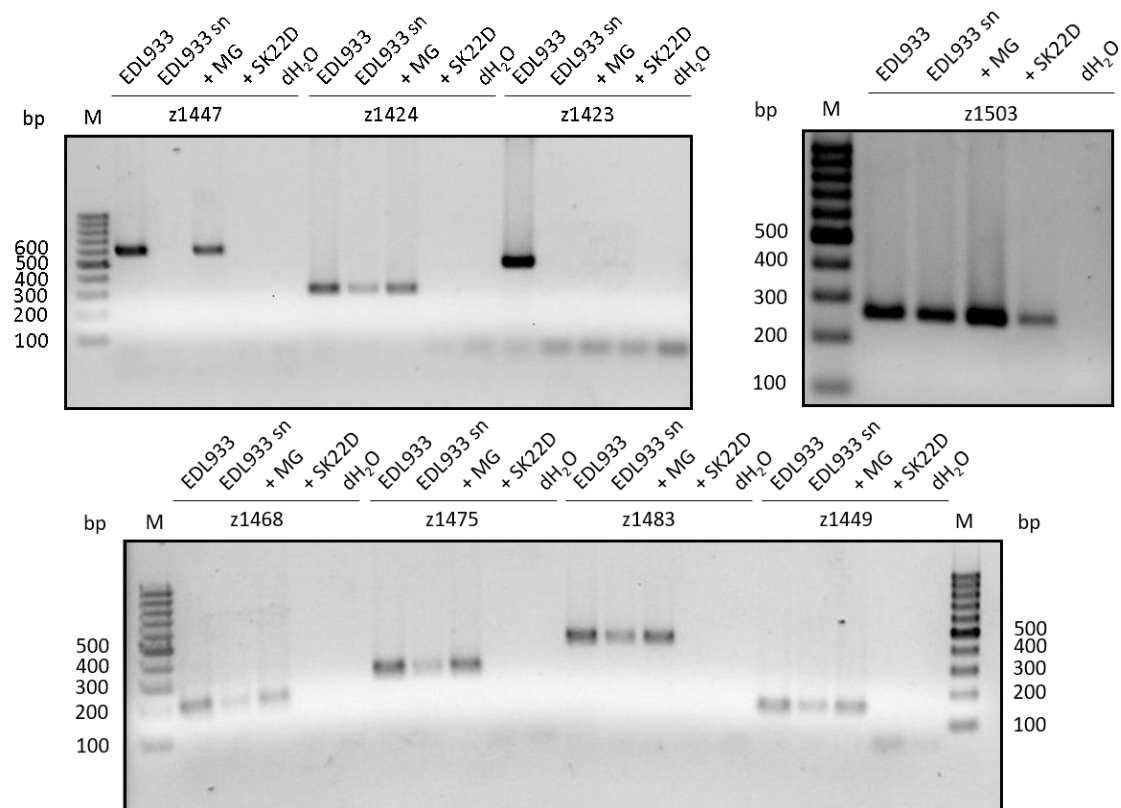


**Figure 28: PCR screen to detect genes spanning the entire *stx2*-phage genome in the supernatant of the mono- and cocultures. (A) *stx2*-prophage gene cluster. Yellow arrows symbolize *stx2*-prophage genes, red arrows symbolize *stx2*-prophage genes that were amplified by PCR, the blue arrow shows a gene outside of the *stx2*-prophage being amplified by PCR. (B) PCR with EDL933 or the sterile filtered supernatants (sn) of 24 h cultures as template. Amplification of *z1447* (repressor protein CI) with SB79/80 (595 bp), *z1424* (Integrase) with SB81/82 (307 bp), *z1423* (trp repressor binding protein) with SB83/84 (484 bp), *z1503* (last prophage gene) with SB115/116 (260 bp), *z1468* (lysis protein S) with SB71/72 (185 bp), *z1475* (terminase small subunit) with SB73/74 (277 bp), *z1483* (tail fiber protein) with SB75/76 (455 bp) and *z1449* (regulatory protein CII) with SB77/78 (149 bp). M: Marker, dH<sub>2</sub>O: negative control.**

The PCR results in figure 28 B displayed the presence of all prophage genes in the supernatant of EDL933 cultures but the EDL933 non-prophage gene *z1423*, which was only detected in the EDL933 bacteria control. All *stx2*-prophage genes were amplified with the designed primers in the EDL933 monoculture supernatant. The amplicon of the phage repressor *cI* (*z1447*) was only very weak visible. In the supernatant of the EDL933 and MG1655 (1:10) coculture, the DNA amplicons for all tested genes but *z1423* were identified in a higher concentration than in the EDL933 monoculture supernatant. Contrary, if SK22D was incubated with EDL933, the *stx2*-prophage genes could not be detected by PCR in any of the supernatants of the 24 h coculture but in the *z1503* gene PCR control, which depicts a higher sensitivity.

#### **4.2.4.2. Influence of EcN on isolated Stx and the *stx2*-phage DNA**

The toxin and *stx*-phages were isolated from a 24 h EDL933 culture with or without the addition of 1 µg/ml MMC (3.1.5.) by sterile filtration of the supernatant. The filtrate containing both, the phages and the toxin, was incubated for 24 h with EcN, MG1655 or LB medium as a control. After the 24 h incubation period the samples were sterile filtered and the Stx level of time point 0 h (Start) and after the 24 h incubation period with or without *E. coli* was determined with the Stx-ELISA (figure 29).

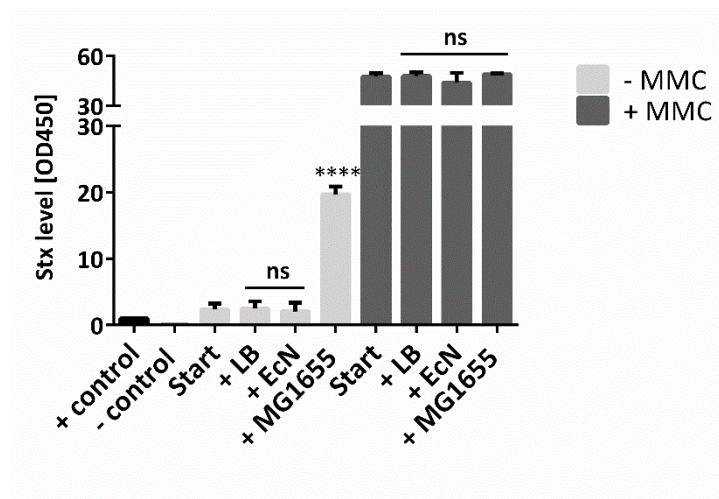


**Figure 29: Stx-ELISA of isolated Stx.** Stx was isolated from a 24 h EDL933 culture with (dark grey bars) or without (light grey bars) 1 µg/ml Mitomycin C (MMC) induction. The isolated toxin was incubated with LB medium or the *E. coli* strains EcN and MG1655 for 24 h, static. Start: Stx at time point 0 h, ns: not significant, \*\*\*\*p<0.0001.

## Results

The ELISA results demonstrated a consistent Stx level of  $OD_{450} 2.31 \pm 0.16$  between the start time point and after a 24 h incubation time with LB medium or EcN. In the presence of MG1655 the toxin level was significantly increased by ~830 % to that of the LB control (LB: 2.37, MG1655: 19.67). The Stx level in the MMC induced filtrate was as high as 47.44, which corresponds to a ~2,000 % increase compared to the no MMC sample. In the MMC induced filtrate, neither the 24 h LB incubation nor the incubation with EcN or MG1655 influenced the toxin level significantly.

In a next approach the MMC induced filtrate was investigated for the presence of *stx2*-phages with a *stx2a* specific PCR. Therefore, the phages were incubated with EcN or LB medium for 24 h, static. The filtrate was subsequently diluted in tenfold steps with 0.9 % saline and digested with DNase (2 U/ml) for 10 min at 37 °C to get rid of DNA outside of the bacteriophage heads. Following the DNase inactivation for 10 min at 100 °C the filtrate was used as template for a *stx2a* specific PCR with the primer pair SB51/SB52 (amplicon: 518 bp). The PCR in figure 30 depicted a *stx2a* DNA band decrease in accordance to the dilution series. The *stx2a* amplicon intensity of phages being incubated with LB medium or with the probiotic EcN was equivalent.

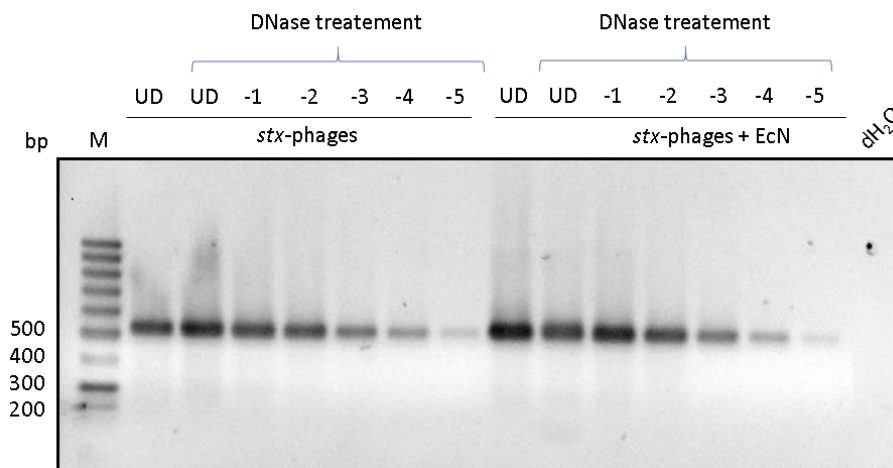


**Figure 30: Determination of the *stx2a* stability in the absence and presence of EcN.** The sterile filtered supernatants of the isolated *stx*-phages incubated with LB medium or EcN were used as PCR template. The template was undiluted (UD) or diluted in tenfold steps (-1 to -5) with or without a previous DNase digestion (2 U/ $\mu$ l) of the template. For the *stx2a* PCR the primer pair SB35/36 (105 bp) was used. M: Marker, dH<sub>2</sub>O: negative control.

Summarizing, these experiments showed that EcN had no influence on isolated Stx and the *stx2*-phage DNA but reduced the toxin level and the *stx*-phage DNA when being cocultured with the STEC strains.

#### **4.2.5. Investigation of the Stx reduction with EcN supernatant or heat killed EcN**

Bacterial supernatant (sn) contains proteins, peptides and everything else secreted by the bacterial culture. To identify the factor(s) of EcN, that resulted in the Stx decrease in the coculture with STEC strains, the microcin free sn of SK22D was tested. Therefore, a SK22D culture with a starting CFUs of  $\sim 8 \times 10^7$  CFUs/ml was incubated for 24 h, static. The sn of the culture with or without being supplemented with a Proteinase Inhibitor Cocktail (P.I.), was collected and 10 x concentrated. 100  $\mu$ l of the sn or 100  $\mu$ l of a SK22D control culture were used in the 24 h coculture experiment with EDL933. Proximately, the Stx level was determined (figure 31 A). The experiment showed that the concentrated sn had a  $\sim 60$  % reduced effect on the Stx decrease of EDL933 compared to the SK22D bacteria control.

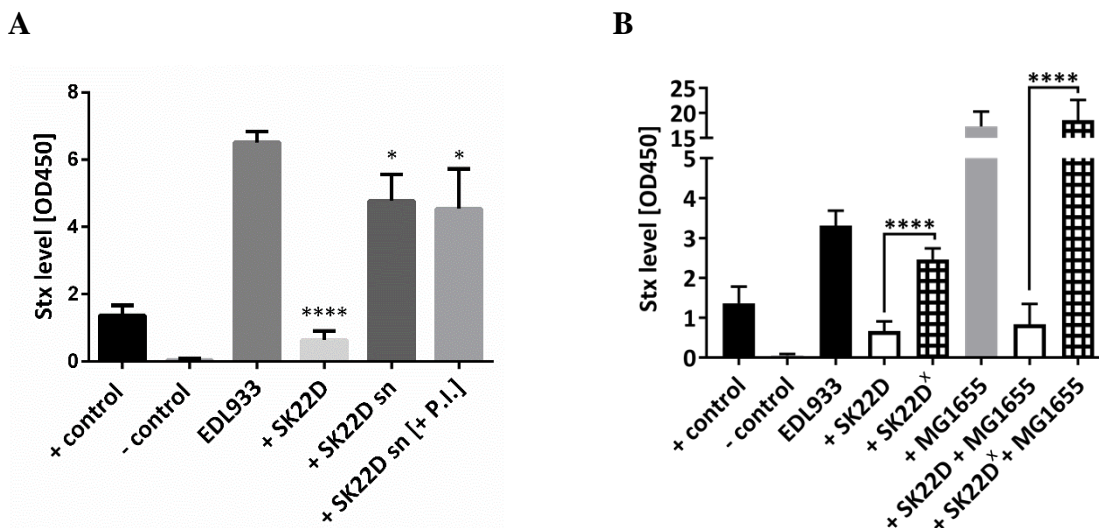


**Figure 31: Investigation of the Stx reduction by SK22D's supernatant or heat killed SK22D.** Analysis of the Stx level of EDL933 after a 24 h incubation period. (A) EDL933 was incubated with SK22D (1:10) or 100  $\mu$ l of a 10-x concentrated supernatant (sn) of a 24 h SK22D culture with or without a Proteinase Inhibitor (P.I.) cocktail. (B) Mono-/co-/ or triculture incubation of EDL933 with a living SK22D or a heat killed SK22D<sup>x</sup> culture with or without MG1655. \* $p < 0.05$ , \*\*\* $p < 0.001$  and \*\*\*\* $p < 0.0001$ .

Besides testing the sn of EcN for anti Stx producing factors, also the bacterial surface was investigated for influencing the Stx level. For this, a 24 h static SK22D culture was concentrated and in a next step killed by heat for 1 h at 100 °C. 100 µl of the heat killed culture (SK22D<sup>x</sup>), with a CFU of ~ 1.6e9 were incubated with EDL933 in co- or triculture for 24 h, static. The living SK22D culture was used as a positive control for the Stx reduction. Evaluation of the Stx results depicted that the heat killed SK22D<sup>x</sup> were 55 % less efficient in interfering with the Stx production in coculture than living SK22D (SK22D<sup>x</sup>: OD<sub>450</sub>: 2.46, SK22D: OD<sub>450</sub>: 0.67) and moreover, it could not interfere with the Stx increase of over 400 % (17.94 +/- 0.62) in the presence of MG1655 compared to a Stx level of OD<sub>450</sub>: 0.83 for the living triculture control (figure 31 B).

The experiments revealed, that neither the supernatant of SK22D nor heat killed SK22D were able to interfere with the Stx production of the STEC strain EDL933 like the living SK22D control. However, the concentrated SK22D supernatant as well as the heat killed SK22D reduced the amount of Stx produced by EDL933 to some extent.

### **4.2.6. Influence of EcN on EDL933 in the Transwell system**

The Transwell system facilitates a prevention of direct bacterial cell to cell contact with a membrane as physical barrier (in our study: 0.4 µm pore size). Anyhow, the membrane allows the diffusion of the bacterial secretome. By this, bacteria can sense factors being secreted by bacteria in the other Transwell compartment without having direct cell contact. We wanted to investigate if SK22D could interfere with the Stx production of EDL933 when being separated by a Transwell membrane.

#### **4.2.6.1. Transwell kinetics**

Bacterial cultures for the Transwell assay were prepared as mentioned in 3.1.12.. For the evaluation of the impact of SK22D on the toxin and phage production / release, the kinetics of the toxic agents were determined at 3 h, 5 h, 8 h and 24 h of static incubation in both, the insert and the well. During the experiment, EDL933 was incubated in the Transwell insert, whereas SK22D or the LB control were incubated in the well. The kinetics of the Stx level of EDL933 (figure 32 A) indicated a lower Stx concentration of -55 % after 5 h incubation, when SK22D

was incubated in the well instead of LB. This difference in the toxin concentration was further observed at 8 h (76 % reduction) and 24 h (60 % reduction).

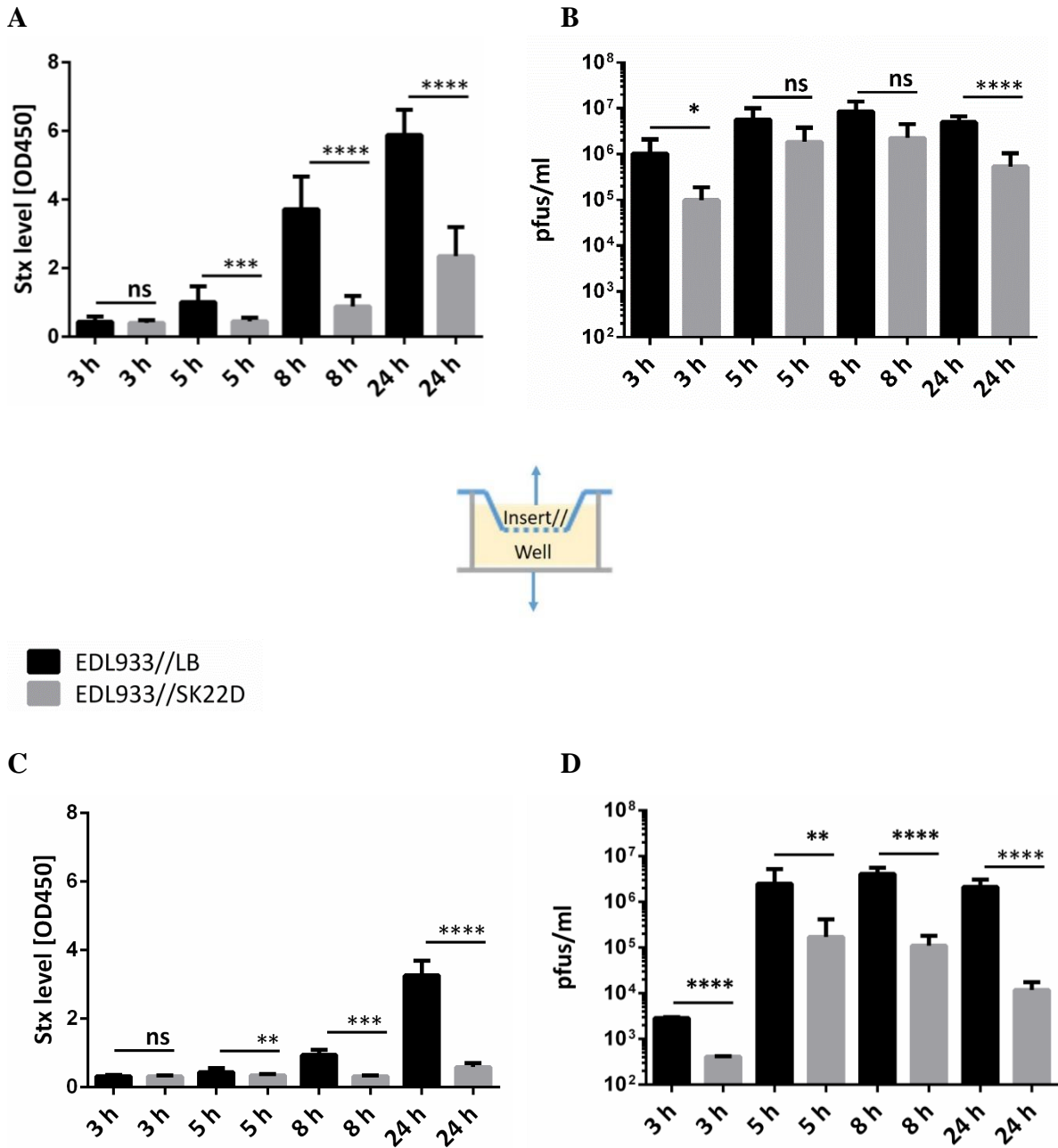


**Figure 32: Stx and *stx*-phage kinetics of EDL933 in the Transwell system.** EDL933 was incubated for the indicated amount of time in the insert of a Transwell system with LB medium (black bars) or SK22D (grey bars) in the well. The Stx level (A) and the pfus (B) of the insert, as well as the Stx level (C) and the pfus (D) of the well were determined. ns: not significant, \* $p < 0.05$ , \*\* $p < 0.01$ , \*\*\* $p < 0.001$  and \*\*\*\* $p < 0.0001$ .



The phage plaque forming units detection, showed a phage difference of -91 % as early as 3 h which decreased to a pfus difference of 68 % after 5 h and to a 74 % reduction after 8 h incubation. After a 24 h incubation period with SK22D, a detectable phage decrease of 89 % compared to the LB control was investigated (figure 32 B).

The analysis of the well for Stx and plaque forming units, demonstrated a similar distinction between SK22D and the LB control. As observed for the Stx level in the insert also the toxin level in the well was strongly reduced by 82 % in the presence of SK22D after 24 h (figure 32 C). The phage plaque forming units detected in the sterile filtered supernatant showed a reduction of 86 % after 3 h incubation and stayed significantly reduced (> 90 %) compared to the LB control in the follow up time points (figure 32 D).

Both, Stx and the phage plaques showed a reduced concentration in the sterile filtered well sample compared to the insert filtrate. In the EDL933 plus LB experimental set up, the values gradually converged over the amount of time with a toxin difference of 75 % at 8 h to a difference of 45 % at 24 h and a pfus difference of around 99 % at the first detection time point towards a ~ 50 % variance of the pfus in the well and the insert at the later time points.

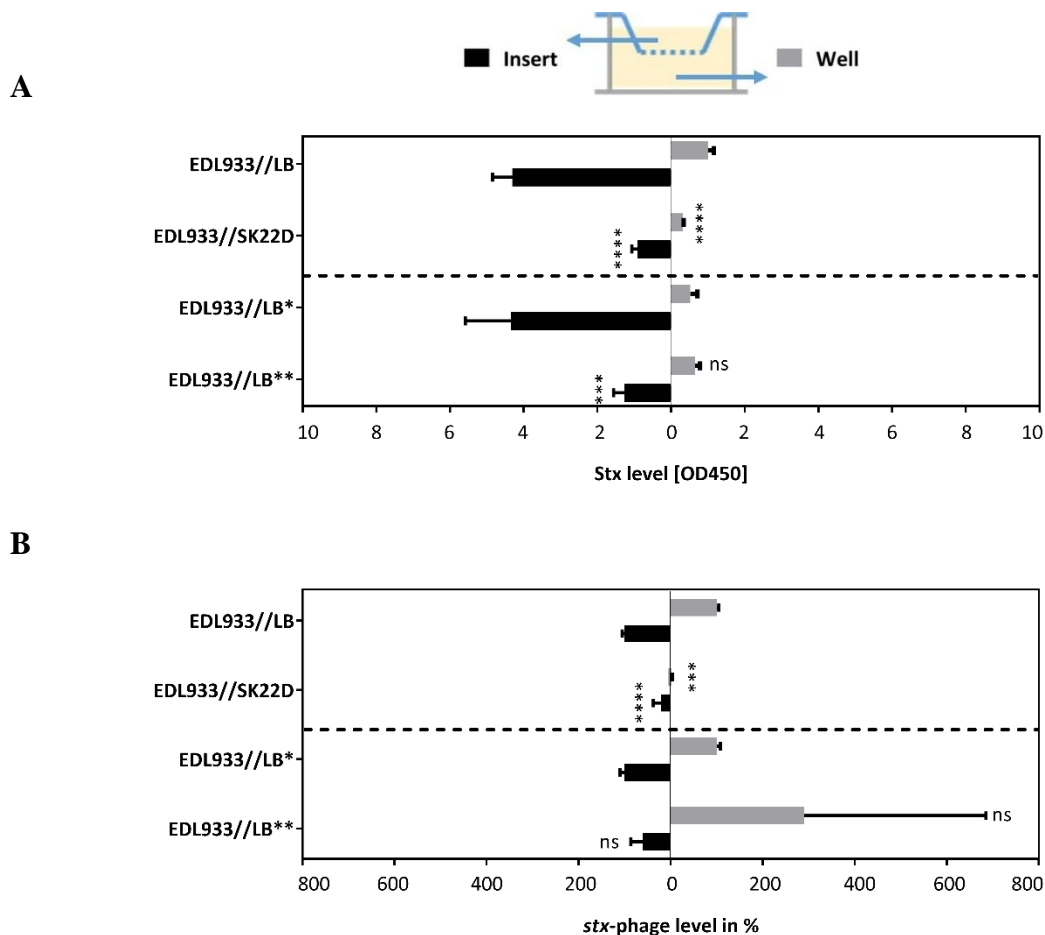
It can therefore be concluded, that SK22D influenced the Stx and *stx*-phage production of EDL933 without having direct cell to cell contact. The toxin and the *stx*-phages depicted a gradual migration from the insert to the well.

### **4.2.6.2. Secretion factor stability**

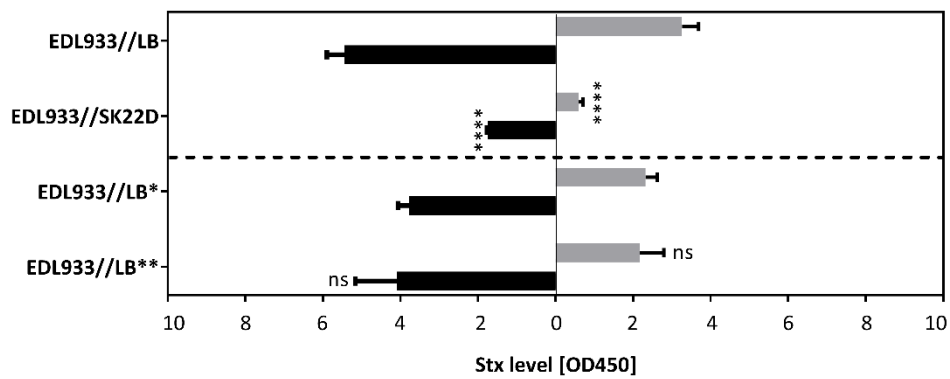
From the Transwell results in 4.2.6.1., the discrepancy in the toxin and phage level between the presence of SK22D or LB medium in the well remained to be investigated. We intended to find out more about the stability and the long-term effects of the secreted factor(s) from SK22D that resulted in this toxic agent reduction. Therefore, we incubated EDL933 with only LB medium or SK22D in the well as described before. Anyhow, after an incubation period of 3 h (figure 33 A/B) or 8 h (figure 33 C/D) the EDL933 insert was transferred to a new insert with LB medium in the well. It was investigated if the transfer of EDL933 with LB in the well to a new insert with LB in the well (EDL//LB\*), or the transfer from EDL933 with SK22D in the well to a new insert with LB in the well (EDL//LB\*\*) resulted in a renewed toxic agent increase or if the factor(s) secreted by SK22D had a long term effect on the toxin and phage production of EDL933. In case of the early transfer after 3 h, EDL933 was further incubated in the new

## Results

insert for 5 h. As a control EDL933 was incubated for a complete period of 8 h with LB or SK22D in the well (EDL//LB or EDL//SK22D). In the transferred insert sample, a significant difference of the toxin level between EDL//LB\* (OD<sub>450</sub>: 4.35) and EDL//LB\*\* (OD<sub>450</sub>:1.27) was observed in the insert but not in the well (OD<sub>450</sub>: 0.52 (LB\*), 0.65 (LB\*\*) (figure 33 A). It should be noted, that the toxin reduction by SK22D in the insert controls was 79 % (EDL//LB (OD<sub>450</sub>:4.31) and EDL//SK22D (OD<sub>450</sub>:0.91) whereas, the toxin reduction in the transferred inserts decreased to 71 %. The phage detection showed a non-significant difference between EDL//LB\* and EDL//LB\*\* of 39 % in the insert which was detected to be significant with a 79 % reduction by SK22D in the control insert (figure 33 B).



C



D

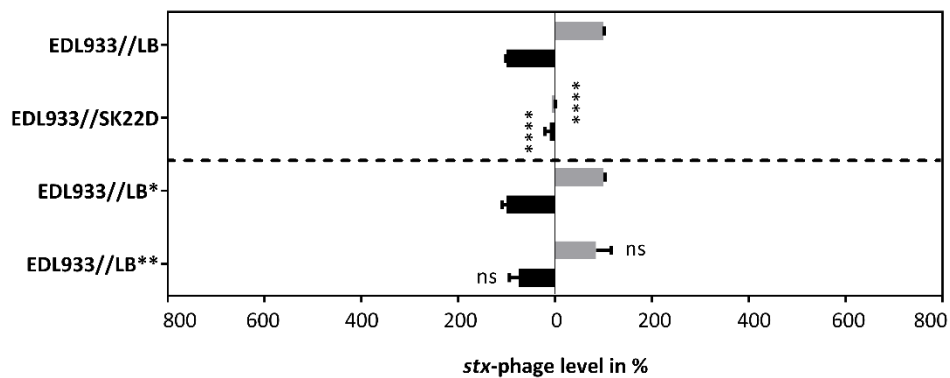


**Figure 33: Stx and *stx*-phage reduction efficiency of SK22D in the Transwell system.**

EDL933 was incubated in the insert of a Transwell system with LB medium (black bars) or SK22D (grey bars) in the well and subsequently transferred to a new insert with LB medium in the well (LB\*: transfer from EDL//LB, LB\*\*: transfer from EDL//SK22D). EDL933 cultures not being transferred (EDL//LB, EDL//SK22D) were used as controls. The Stx level (A) and the *stx*-phage level (B) were determined from a EDL933 culture being incubated for 3 h before and 5 h after the transfer (8 h for the controls). The Stx level (C) and the *stx*-phage level (D) were determined from a EDL933 culture being incubated for 8 h before and 16 h after the transfer (24 h for the controls). ns: not significant, \*\*\* $p < 0.001$  and \*\*\*\* $p < 0.0001$ .

In a next step the pre and after “insert transfer” time was increased. EDL933 was incubated for 8 h with LB medium or SK22D in the well and was proximately incubated for another 16 h in the new insert with LB medium in the well. The controls were incubated for total 24 h with LB medium or SK22D in the well. In this next experiment the toxin level of EDL933 with an  $OD_{450}$ : 3.78 in the EDL//LB\* sample was comparable to the one of an  $OD_{450}$ : 4.08 in the EDL//LB\*\* insert sample (8 % difference). Also, the toxin values in the well with  $OD_{450}$ : 2.32 (LB\*) and  $OD_{450}$ : 2.16 (LB\*\*) were comparable (0.05 % difference).

The controls anyhow had a variance in the toxin level of 68 % in the insert and 82 % in the well (figure 33 C). The phage detection equaled the toxin detection results with a *stx2*-phage reduction of 39 % in the insert of the transferred samples to a significant discrepancy of ~ 80 % in the 24 h insert controls (figure 33 D).

The Transwell results could showed that a constant presence of SK22D was necessary to permanently interfere with the toxic factor production by EDL933. Anyhow, the influence of SK22D on the toxin production was still detectable after being transferred from SK22D for 5 h.

### **4.3. EcN phage infection studies**

EcN is a probiotic strain, which is used to treat gastrointestinal infections in human, registered under the name “Mutaflor”. To use EcN as an additive during an EHEC infection, it is of high importance to rule out the possibility of turning EcN into a *stx*-prophage carrying lysogen (Schmidt, 2001).

#### **4.3.1. Electron microscopic studies of *stx*-phage binding to the *E. coli* surface**

The transmission electron microscope (TEM) displays a technique to visualize an object by beaming electrons through a specimen and observing the interaction between the electrons and atoms. This microscopic technique makes it possible to visualize objects as small as 0.2 nm compared to standard light microscopes, which are limited in their resolution by the wavelength of the light (maximal resolution: 200 nm).

The *stx*-phages have a head diameter of around ~ 100 nm and possess a short tail of around ~ 10 nm (Mondal et al., 2016). Therefore, the TEM instead of the light microscope had to be used to visualize the *stx*-phages. In this study approach we wanted to monitor if there is a binding of the *stx*-phages to the surface of EcN and we used MG1655 as an *E. coli* control strain.

The *stx*-phages in figure 34 A had the expected icosahedral head size of ~ 100 nm and depicted a short phage tail. As a control the *E. coli* phenotypes were captured without the *stx*-phages for EcN in figure 34 B and for MG1655 in figure 34 C. The *E. coli* strains did not show any particles bound to the surface and in the case of EcN the pili, framing the gram-negative bacterium, were well recognizable. Both *E. coli* strains exhibited a typical size of 1 x 3  $\mu$ m (Reshes et al., 2008).

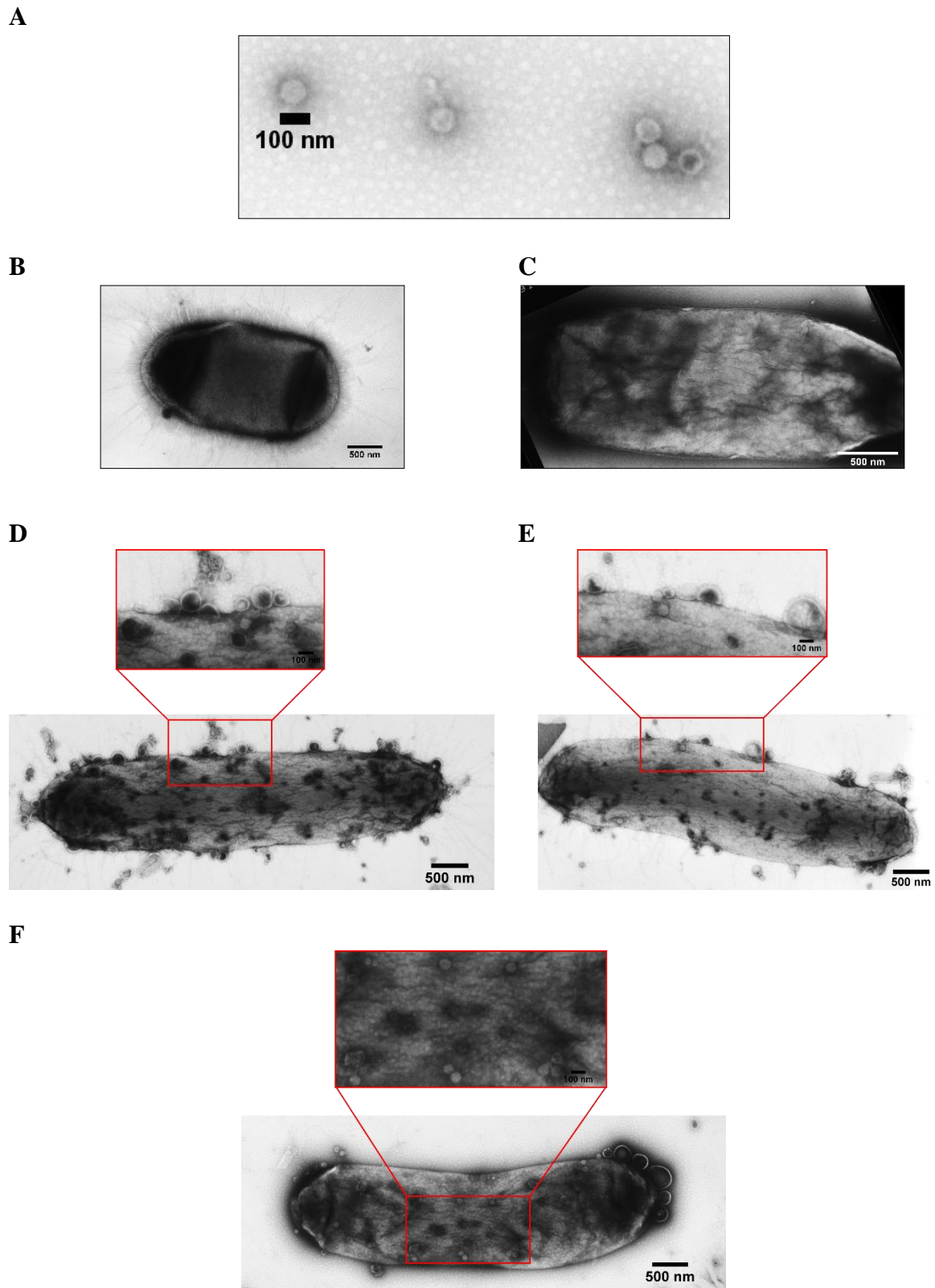


**Figure 34: Electron microscopy images of *stx*-phages and the *E. coli* strains EcN and MG1655. (A) Isolated *stx*-phages. (B) EcN and (C) MG1655 without *stx*-phages. (D, E) EcN with the *stx*-phage filtrate. (F) MG1655 with the *stx*-phage filtrate. Red boxes frame zoomed in areas. Scale bar in *E. coli* images: 500 nm, Scale bar zoomed images: 100 nm.**

The *stx*-phage surface binding was further investigated by incubating EcN or MG1655 (1e8 CFUs) for 1 h with a 1 µg/ml MMC induced phage filtrate (1e8 pfus) (1:1). After fixation of the bacteria-phage complex with glutaraldehyde, they were stained with 0.5 % uranyl acetate. Figure 34 D and figure 34 E displayed the EcN and *stx*-phage coculture and the incubation of phages with MG1655 was detected in figure 34 F. In the red framed, zoomed in figures, a binding of particles to the surface of both *E. coli* types was detected. The size of the particles varied a lot as outer membrane vesicles (OMVs) were isolated along with the *stx*-phages from the MMC induced EDL933 strain. OMVs exhibit a varying size of 20 - 250 nm (Schwechheimer & Kuehn, 2015).

Therefore, the TEM results could not evidence whether the observed EcN surface binding particles were *stx*-phages or OMVs of EDL933.

### **4.3.2. Bacteriophage life cycles**

*Stx*-phages are temperate bacteriophages, which means that they can lyse or lysogenize a bacterial host. During the lytic phage cycle, the phages use the host to replicate their DNA and amplify therewith the phage particles before they lyse their host to set the phages free. In the lysogenic cycle on the other hand, phages integrate their DNA into the genome of the host and remain there as a prophage (De Paepe et al., 2014).

#### **4.3.2.1. Bacterial cell lysis**

We wanted to find out whether the temperate *stx*-phages were able to lyse the probiotic EcN and amplify therewith the phage particles.

For the investigation of the lysis efficiency of *stx*-phages on EcN, PPA plates were prepared with 200 µl of an EcN ONC. MG1655 PPA plates were used as a positive control for bacterial lysis. To investigate possible lysis, *stx*-phages were isolated from a 1 µg/ml MMC induced EDL933 culture and immediately diluted in tenfold steps in 0.9 % saline before 10 µl drops of the dilution series were dropped on top of the PPA plates. The plates were incubated ON at 37 °C, to allow bacterial growth and cell lysis by the *stx*-phages. Proximately, the plates were investigated for lysis plaques. In figure 35 the detected phage plaques dilution series was captured. In case of the probiotic *E. coli* strain EcN, no lysis plaques were detected at any dilution nor in the undiluted (UD) phage drop. The *stx*-phage sensitive K-12 strain MG1655

anyhow, showed a complete bacterial lysis plaque in the UD and in the 10-fold (-1) diluted phage drop. Starting from the second dilution, single plaques became gradually visible. In the 5<sup>th</sup> (-5) dilution a total of 9 phage plaques could be detected. Counting back 9e5 pfus were dropped on the bacterial lawn in the undiluted sample.

With this experiment we could show, that the *stx*-phages were unable to use EcN as a host for phage particle amplification, but they could lyse the K-12 strain MG1655.

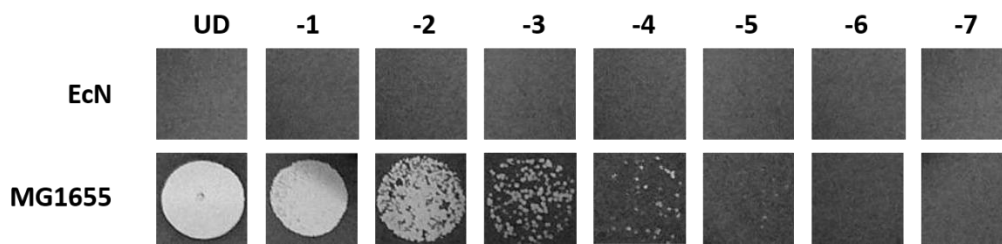


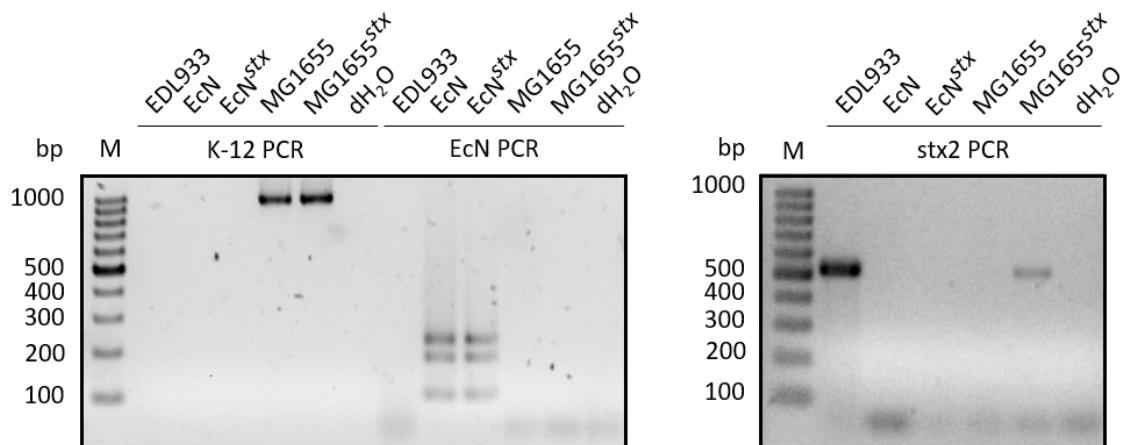
**Figure 35: Bacterial lysis by *stx*-phages.** Phage Plaque Assay (PPA) plates were prepared with ONCs of EcN or MG1655 as indicator strains. *stx*-phages from a 1 µg/ml Mitomycin C (MMC) induced EDL933 culture were serially tenfold diluted in 0.9 % saline (UD to -7). 10 µl of each dilution were dropped in the PPA plates. UD: undiluted.

#### 4.3.2.2. Bacterial screen for lysogens

Subsequently, to testing the bacterial lysis by the *stx*-phages we analyzed the possibility of *stx*-phage DNA integration into the genome of EcN.

One approach was to incubate EcN or the MG1655 control strain with isolated phages from a non MMC induced EDL933 culture for 24 h, as the addition of MMC interfered with the Stx increase by MG1655 in the Stx stability experiment (figure 29). The *E. coli* strains were incubated with the isolated phages (EcN<sup>stx</sup>/MG1655<sup>stx</sup>) or LB medium (EcN/MG1655) before the bacteria were washed 3 times with 0.9 % saline, to wash off phages binding to the bacterial surface. Proximately, the bacteria were diluted to 100-300 CFUs/100 µl and plated on LB Agar plates. The grown colonies were scratched from the plates and used as template in a *stx2a* specific PCR with the primer pair SB51 and SB52 (amplicon: 512 bp) (figure 36 A). Additionally, the *E. coli* strain identity was confirmed with the multiplex EcN chromosomal PCR for EcN (EcN PCR) and the K-12 specific PCR (K-12). With the amplification of the *stx2a* DNA fragment a positive *stx*-prophage integration was detected for MG1655<sup>stx</sup> but no *stx2a* amplicon could be detected for EcN<sup>stx</sup>.

A



B

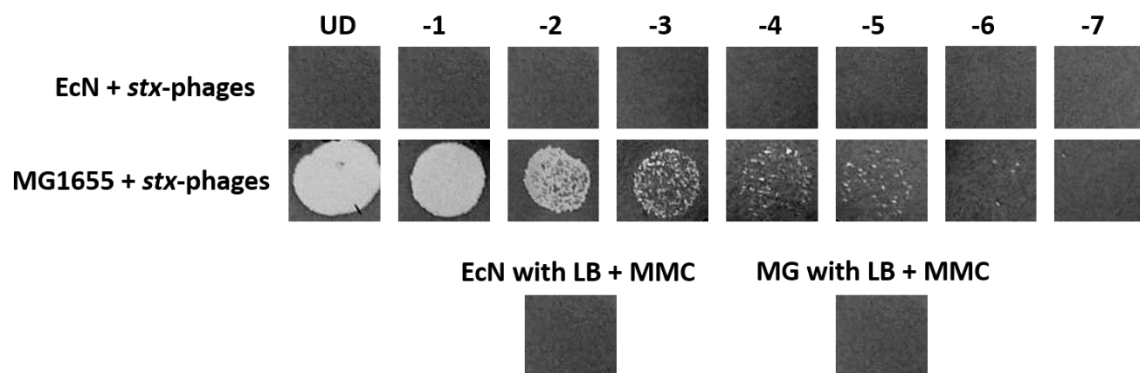


**Figure 36: Identification of EcN and MG1655 *stx*-prophage lysogens.** *E. coli* cultures were incubated for 44 h with *stx*-phages (EcN/MG1655<sup>stx</sup>) or with LB medium (EcN/MG1655). (A) The 2 x washed cultures were plated on LB agar plates, collected and screened for the *stx2a* gene of the *stx2*-prophage with the primer pair SB51/SB52 (512 bp) (*stx2* PCR). The strain identity was determined in a multiplex PCR with the primer pairs IL2/IR2 (103 bp), IL4/IR4 (186 bp) and IL5/IR5 (232 bp) (EcN PCR). The K-12 strain identity was confirmed with the primer pair K-12\_fwd/rev (969 bp) (K-12 PCR). (B) The washed *E. coli* strains were incubated with 1 µg/ml Mitomycin C (MMC) for 8 h and sterile filtered. Phages in the filtrate were amplified with MG1655 in a liquid culture. The final pfus were determined with a Phage Plaques Assay, M: Marker, dH<sub>2</sub>O: negative control, UD: undiluted, -1 to -7: tenfold dilutions of the phages in 0.9 % saline. (Images modified from Bury et al., 2018, under review).

Another approach was to incubate the non MMC induced phages with the *E. coli* strains for 48 h, to offer a longer phage genome integration period. As described above, the bacteria were washed 3 times to lose surface bound phages. In a next step, the hypothetical lysogens were induced to lyse by the addition of 1 µg/ml MMC and incubated for 8 h in the dark. Following,



the supernatant was collected by sterile filtration and 500  $\mu$ l of the filtrate were incubated with a MG1655 culture ( $8 \times 10^7$  CFUs/ml) for another 24 h to allow a phage amplification by MG1655. Finally, the filtered supernatant was screened for pfus with a PPA.

Despite a phage coculture incubation time of 48 h, EcN showed no pfus in the lysis induced and phage amplified supernatant, likewise to the control EcN incubated with LB medium (figure 36 B). MG1655 cultures with *stx*-phages however, showed a high phage titer in the supernatant of  $1 \times 10^9$  pfus/ml. The control of MG1655 cultured with LB medium for 48 h depicted that there were no lysing prophages present the MG1655 *wt* genome.

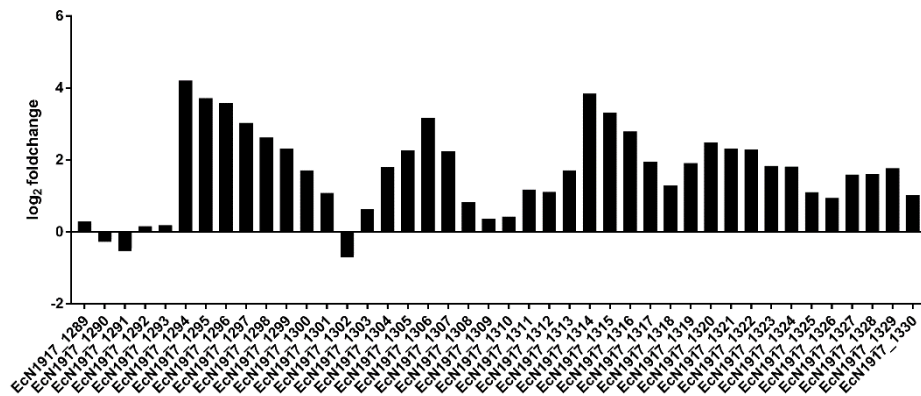
The PCR detection of *stx2*-prophage DNA in the *E. coli* genome and the lysis inducing experiment demonstrated that the *stx*-phages were incapable of integrating their prophage DNA into the genome of EcN but the K-12 strain could serve as *stx*-phage amplification and prophage integration source.

### **4.3.3. Transcriptome analysis**

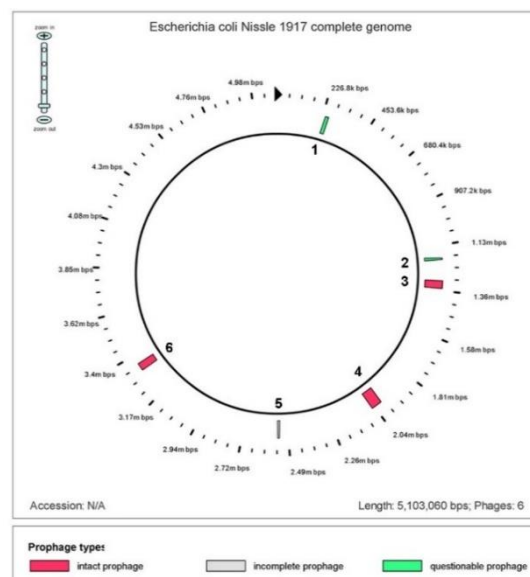
The transcriptome of an organism is defined as the total of all RNA transcribed from its DNA at a certain time point (Tjaden et al., 2002). With the transcriptome analysis it is possible to monitor the transcriptomic reaction of an investigated organism towards a substrate added. In our case, we aimed to identify the transcriptomic reaction of EcN towards the isolated *stx*-phages of the EDL933 strain to examine the defense mechanism of the probiotic strain towards a *stx*-phage infection.

In a first step EcN was incubated with isolated *stx*-phages or only LB medium as a control for 16 h. The total RNA of EcN was isolated with the RNase Mini Kit and further processed as described in 3.2.3.. A RNA library was prepared, and the transcriptome was subsequently analyzed by next generation sequencing. From the research results on the transcriptome, a strong upregulation of genes of a prophage of EcN appeared in the presence of the *stx*-phages (figure 37 A). A follow up PHAST prediction for prophages in EcN (performed by Manonmani Soundararajan) identified the upregulated phage as a lambdoid prophage (prophage 3) of completely 6 prophages detected in EcN. Only the prophages 3,4 and 6 were predicted to be complete, prophages 1 and 2 were determined as questionable prophages and prophage 5 was detected to be an incomplete prophage (figure 37 B).

A



B



C

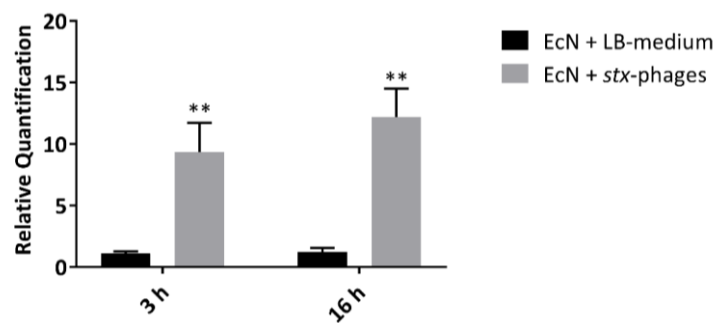


**Figure 37: Analysis of the transcriptome of EcN cocultured with *stx*-phages.** (A)  $\log_2$  fold transcriptome regulation changes of the prophage 3 of EcN. (B) PPHAST prediction of EcN's prophages (from Manonmani Soundararajan). (C) Verification of the phage repressor (*pr*) upregulation in EcN being cocultured with *stx*-phages at the time points 3 h and 16 h.  $**p < 0.01$ . (Images A, B and C (modified) from Bury et al., 2018, under review).

None of the prophages of EcN were inducible, which was tested with heat and antibiotic treatments of EcN beforehand. The upregulated lambdoid prophage 3 of EcN, depicted a  $\log_2$  fold change upregulation of above 2 for a large set of the genes (prophage gene regulations: table 15). The gene EcN\_1294, coding for the phage repressor gene (*pr*), was  $\log_2$  4.21-fold upregulated in the presence of *stx*-phages (gene list: table 13). The gene was found to be involved in the protection from phage infection in other bacteria and was therefore investigated further (Alvarez, Rodriguez, & Suarez, 1999). The strong regulation of the *pr* in the presence of *stx*-phages was reconfirm by qRT-PCR (3.2.6.).

With this technique, the transcriptomic activity of single genes can be perused at selected time points. In our case the 16 h transcriptomic results and additionally a time point as early as 3 h of coculture was screened for the *pr* regulation. *hcat*, a constantly expressed gene of *E. coli* served as qRT-PCR control gene (Zhou et al., 2011). Figure 37 C, representing the qRT-PCR results, confirmed the transcriptomic results with an upregulation of the *pr* of 12.2-fold in the presence of *stx*-phages after 16 h of incubation and detected a gene upregulation of 9.3-fold after already 3 h compared to the EcN plus LB medium control.

The *pr* of EcN's lambdoid prophage, showed a strong upregulation in the presence of *stx*-phages. Nevertheless, it remained to be tested if the *pr* was involved in the protection of EcN towards the phage infection. Therefore, *pr* was cloned into a pUC19 plasmid harboring an Ampicillin resistance cassette and next the phage lysis susceptible strain MG1655 was transformed with the plasmid containing the *pr* or with an empty pUC19 plasmid (work by Manonmani Soundararajan). The recombinant MG1655 clones, harboring the empty plasmid (MG1655R) or the *pr* containing plasmid (MG1655R*pr*) were thereupon tested for phage lysis by using them as indicator strains in a PPA, supplemented with 100  $\mu\text{g/ml}$  Amp and 1 mM IPTG to induce the gene expression. EcN, which showed to be not lysed by the phages, and MG1655 as positive for bacterial lysis were used as control indicator strains. As in the lysis experiment in 4.3.2.1., a phage dilution series was dropped on top of the bacterial lawn and the plates were incubated ON to allow bacterial growth and lysis by the phages. Figure 38 summarized the results from the MG1655 lysis protection experiment. The plaque detection evaluated that the recombinant MG1655R empty plasmid control was not significantly influenced in the bacteriophage lysis with  $2.3 \times 10^7$  pfus/ml counted, when compared to the MG1655 control with  $4.2 \times 10^7$  pfus/ml. When analyzing the pfus/ml on MG1655R*pr* anyhow, the lysis of MG1655 was reduced by 294-fold ( $1.5 \times 10^5$  pfus/ml).

Concluding these experiments, the *pr* of EcN's lambdoid prophage seemed to be involved in the protection of EcN from the lysis by *stx*-phages.

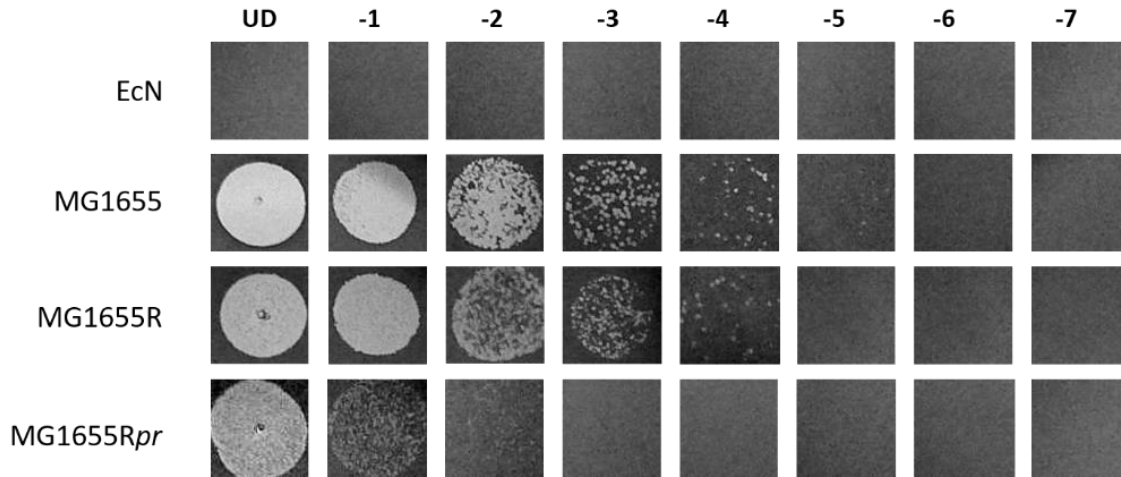


**Figure 38: Phage Plaque Assay with MG1655 recombinant strains.** The MG1655 recombinant strains harboring the pUC19 plasmid (MG1655R) or the plasmid with the phage repressor gene (*pr*) (MG1655R*pr*) from EcN's prophage were used as indicator strains in a Phage Plaque Assay. EcN and MG1655 served as control strains. UD: undiluted, -1 to -7: tenfold dilutions of the phages in 0.9 % saline. (Image from Bury et al., 2018, under review).

#### **4.4. *stx*-phage studies**

*stx*-phages are known to survive several inactivation conditions as they can be found in water, food and fecal samples (Allue-Guardia, Martinez-Castillo, & Muniesa, 2014). Therefore, the risk of infecting harmless *E. coli* strains and turning them thereby into pathogenic strains is highly increased (Schmidt, 2001). Based on this, it is of great interest to identify factors that inactivate the toxin carrying phages.

##### **4.4.1. *stx*-phage kinetics**

During *stx*-phage kinetic studies, the phage plaques of a MMC induced phage filtrate were monitored. The isolated phages, with a starting titer of  $\sim 1e7$  pfus/ml, were incubated with only LB medium or with an EcN culture with a starting OD<sub>600</sub> of 0.1 ( $\sim 8e7$  CFUs/ml). The phage plaques formed on a MG1655 PPA indicator plate were detected every 2 h from 0 h until 24 h. For long time incubation, samples were collected by sterile filtration after 44 h and 72 h.

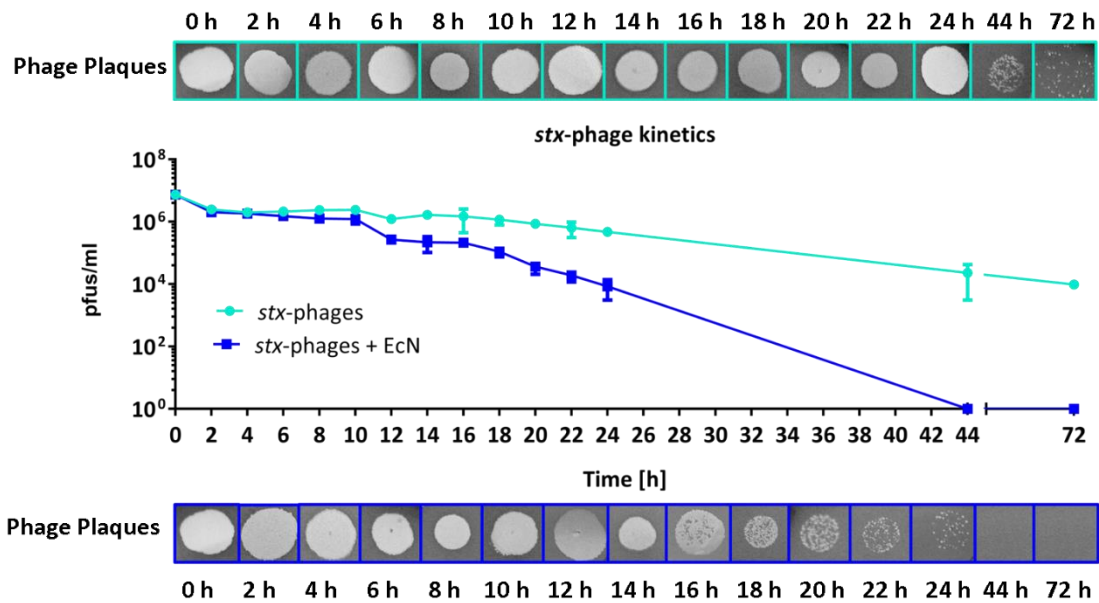


**Figure 39: *stx*-phage reduction kinetics.** Kinetics of the pfus/ml of *stx*-phages being incubated with LB medium (turquoise) or EcN (blue). The phage titer was detected on Phage Plaque Assay plates every 2 h from 0 h until 24 h and after 44 h and 72 h. (Image from Bury et al., 2018, under review).

The kinetics in figure 39 depicted a slow decrease of the *stx*-phages in LB medium, resulting in  $9.8 \times 10^3$  pfus/ml after 72 h of incubation. If EcN was added to the phage filtrate on the other hand, a  $9.6 \times 10^5$  pfus decrease was observed after 12 h of coculture, which escalated to a difference of 98 % after 24 h of incubation (LB:  $4.73 \times 10^5$  pfus/ml, + EcN:  $8.46 \times 10^3$  pfus/ml). After an incubation period of 44 h no plaque forming phages could be observed in the filtered supernatant with EcN any longer (LB:  $2.3 \times 10^5$  pfus/ml).

The kinetic studies could thereby depict a strong phage inactivating influence of EcN when being cocultured with *stx*-phages.

#### 4.4.2. *stx*-phage localization

Next, we examined whether the reduction of the *stx*-phages detectable in the supernatant of a coculture of phages and EcN, could be traced back to a binding of the phages to the surface structures of EcN, like the *stx*-phage receptor YaeT (Smith et al., 2007). EcN and MG1655 were identified to share a homologous YaeT aa sequence (table 16). To screen whether the phages bind to the surface of EcN or MG1655, the *E. coli* strains were incubated with isolated

phages for 24 h and the pellet and the filtered supernatant were heat incubated to use them as template in a *stx2a* specific PCR. The PCR gel in figure 40 located a more intense *stx2a* amplicon (518 bp) in the supernatant of the EcN coculture than in the pellet. The determination of the phage DNA in the MG1655 control showed for both, the pellet and the supernatant, DNA amplicons of comparable intensity.

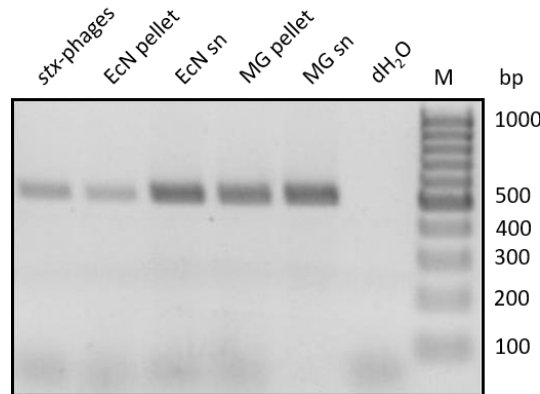


**Figure 40: PCR screen for the *stx*-phage localization.** The pellet and the supernatant (sn) of an EcN and a MG1655 (MG) 24 h culture with *stx*-phages, was used as template in a *stx2a* PCR with the primer pair SB51/SB51 (518 bp). M: Marker, dH<sub>2</sub>O: negative control. (Image from Bury et al., 2018, under review).

Taken together, this experiment and the phage dilution PCR in figure 30, the reduction of the plaque forming units in the supernatant of an EcN and phage coculture could not be assigned to a binding of the phages to the surface of EcN.

#### **4.4.3. Influence of commensals and heat killed *E. coli* on *stx*-phages**

As we could observe an intense reduction of phage plaque forming units in the presence of EcN it was of interest to find out whether this is an *E. coli* common or an EcN specific attribute. To address this issue, the EcN close relative uropathogenic strain CFT073, as well as the commensal strains SE11, SE15 and IAI1, all isolated from feces of healthy human, were screened for phage inactivation activities (Oshima et al., 2008; Toh et al., 2010; Touchon et al., 2009). Additionally, MG1655 was tested for its influence on the phage infectivity.

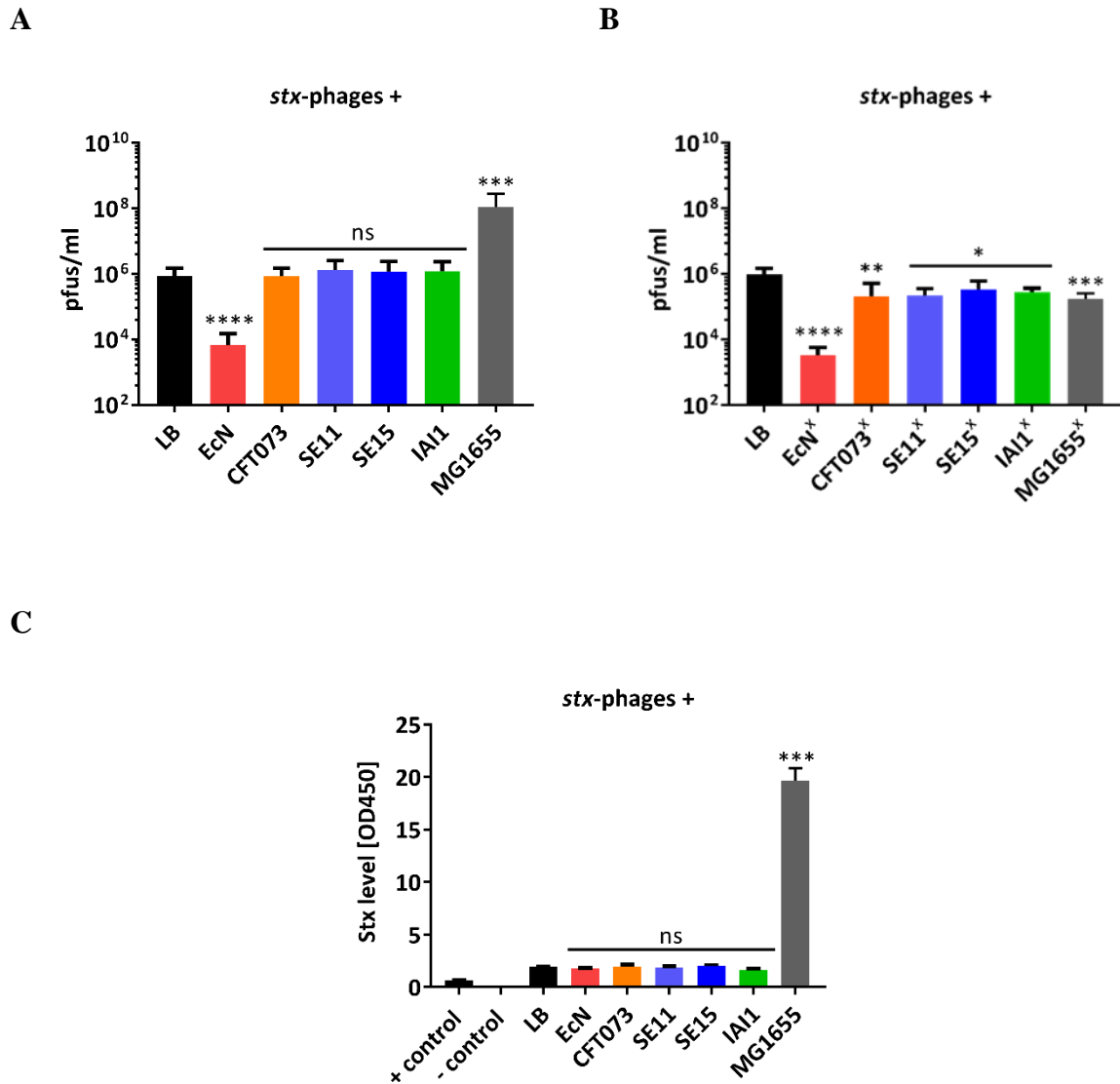


**Figure 41: Identification of the *stx*-phage inactivation by various *E. coli* strains.** *stx*-phages were incubated for 24 h static, with the living (A) or 1 h, 100 °C heat killed (B) *E. coli* (*E. coli*<sup>x</sup>) strains EcN, its uropathogenic relative CFT073, the commensals SE11, SE15, IAI1 and the K-12 strain MG1655. The sterile filtered supernatants were examined for the phage plaque forming units (pfus) with a Phage Plaque Assay and additionally for (C) the toxin level with the Stx ELISA. ns: not significant, \*p<0.05, \*\*p<0.01, \*\*\*p<0.001 and \*\*\*\*p<0.0001.

The *E. coli* strains named, were incubated with non MMC induced *stx*-phages at a starting ratio of 10:1 (*E. coli*: phages) for a period of 24 h. Afterwards, the pfus and the Stx level were detected in the filtered supernatants. The phage plaques on the PPAs were enumerated and displayed in figure 41 A. As observed in the experiment 4.4.1., the coculture of EcN and *stx*-phages resulted in a phage decrease from 8.6e5 pfus/ml to 6.7e3 pfus/ml (99 % reduction). In

contrast to this reduction, the EcN relative CFT073, as well as the commensal controls could not significantly reduce the phage plaque forming activity ( $1.2e6 \pm 3e5$  pfus/ml). At the same time, the coculture of *stx*-phages with MG1655 resulted in a 116-fold phage increase ( $1e8$  pfus/ml).

From the same filtrates, the Stx level was determined to identify possible effects of the tested *E. coli* strains on the toxin stability. Regarding the toxin interaction, all *E. coli* strains depicted an EcN similar result as none of the strains could degrade the toxin and reduce thereby the toxin level detected with the Stx-ELISA. In coculture with MG1655, the toxin level increased however dramatically from the OD<sub>450</sub>: 1.95 in the LB control to 19.67 (+ 1,000 %) in the coculture (figure 41 C).

It was inspected, whether the *stx*-phage reducing factor(s) of EcN were phage induced and if they were heat sensitive. Therefore, all *E. coli* strains were grown without phages in a volume of 10 ml LB medium for 24 h, static. The bacteria were harvested by centrifugation, concentrated to a CFUs/ml of  $1.6e10$  and heat killed for 1 h at 100 °C (*E. coli*<sup>x</sup>). 100 µl of the heat killed *E. coli*, that had never been in contact with *stx*-phages, were incubated with the isolated phages likewise in the living control for 24 h, static. The phage plaque forming units were once more detected with PPA plates.

The pfus/ml determined are represented in the figure 41 B. It could be detected, that heat killed EcN led to a phage decrease from  $1e6$  pfus/ml in the control to  $3.4e3$  pfus/ml, which equaled a reduction of 98 % (living control: 99 %). The killed *E. coli* strain CFT073, with a 4.7-fold phage reduction ( $2.13e5$  pfus/ml), and the commensal strains with a reduction of 4.5-fold for SE11 ( $2.24e5$  pfus/ml), 2.9-fold for SE15 ( $3.5e5$  pfus/ml) and 3.5-fold for IAI1 ( $2.9e5$  pfus/ml) proved a less efficient phage reduction effect. The phage amplifying strain MG1655, reduced the phages 5.6-fold when being heat killed compared to the LB control ( $1.8e5$  pfus/ml).

The experiments with the commensal and heat killed *E. coli* strains could unravel the special characteristic of a *stx*-phage inactivation by EcN which was not phage induced. Moreover, the phage inactivating factor(s) demonstrated heat stability.

#### **4.4.4. Investigation of the *stx*-phage inactivating factor(s) properties**

For a closer investigation of the *stx*-phage inactivating factor(s) we examined whether the factor(s) could be found in the supernatant of a SK22D culture or rather within the bacterial

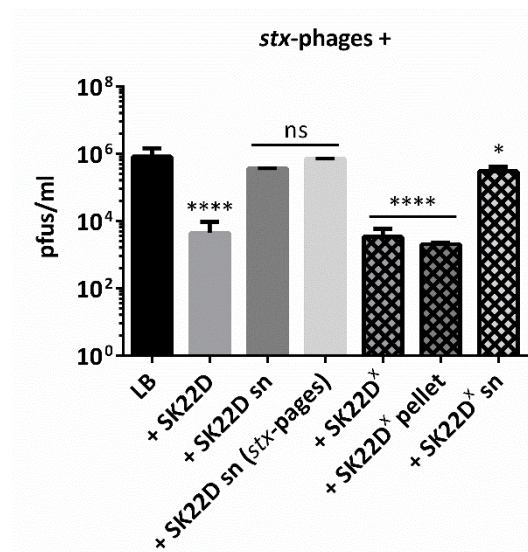


pellet. To answer this question, the sn of a 24 h culture of SK22D with or without *stx*-phages (*stx*-phages: SK22D: 1:10) was sterile filtered and 900  $\mu$ l of the sn were immediately incubated with 100  $\mu$ l of isolated *stx*-phages (start pfus/ml:  $\sim 1e7$ ). Figure 42 A illustrates, that the supernatant of the SK22D culture was not able to significantly reduce the phage titer compared to the LB control ( $8.2e5$  pfus/ml) neither when SK22D was cultured without phages ( $3.7e5$  pfus/ml) nor when SK22D was incubated along with *stx*-phages before the sn was collected ( $7e5$  pfus/ml). Additionally, the heat killed SK22D<sup>x</sup> was tested for the location of the phage inactivation factor(s). Therefore, the 1 h at 100 °C heat killed 500  $\mu$ l culture was centrifuged to collect the supernatant (SK22D<sup>x</sup> sn) and the pellet was washed 3 x with 0.9 % saline before it was again diluted in 500  $\mu$ l LB and tested for its phage inactivation capability. The results unravel that the SK22D<sup>x</sup> pellet ( $2.1e3$  pfus/ml) inactivated the phages >200-fold like the heat killed SK22D<sup>x</sup> ( $3.4e3$  pfus/ml) which was not deprived of substances passed to the supernatant during the heat incubation period. The supernatant of the heat killed SK22D<sup>x</sup> culture on the other hand, depicted only a very low influence on the phage titer ( $3e5$  pfus/ml), with a 2.7-fold reduction.

To compare the phage inactivation mechanism of living and heat killed SK22D, the location of the phages was detected with a *stx2a* PCR. Therefore, a 1 h, 100 °C heat killed SK22D 24 h culture and a SK22D ONC were incubated with 100  $\mu$ l of MMC induced *stx*-phages (start pfus/ml:  $\sim 1e7$ ) with a starting MOI of 1:100 for the heat killed SK22D and 1:10 for the living control. After a 24 h incubation period, the samples were centrifuged at 13,000 xg for 5 min and the supernatant was collected. The pellet was 2 x washed by carefully pipetting up and down and finally resuspended in 1 ml of LB medium. 10  $\mu$ l of the samples were DNase digested for 10 min at 37 °C and incubated for 10 min at 100 °C before 4  $\mu$ l of each sample was used as template in a *stx2a* specific PCR with the primer pair SB51/SB52 (amplicon: 518 bp). As an undigested control, 2  $\mu$ l of 10 min at 100 °C incubated samples were used as template in the *stx2a* PCR (figure 42).

The *stx2a* PCR could depict the *stx*-phages for both the living and the heat killed SK22D rather in the supernatant than in the pellet. After the DNase digestion the DNA band intensity was strongly reduced which implies, that a huge amount of free DNA was released by EDL933 upon MMC treatment.

A



B

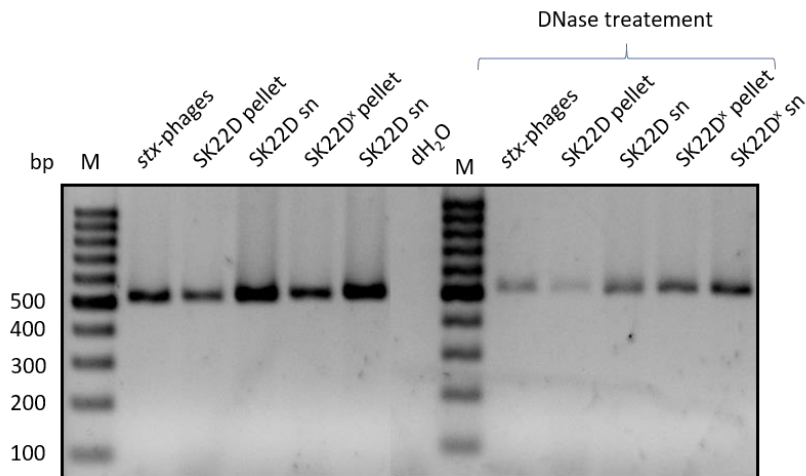


**Figure 42: Investigation of the *stx*-phage inactivation agent.** (A) *stx*-phages were incubated for 24 h static, with the living SK22D (1:10) or 900  $\mu$ l filtered supernatant (sn) of a 24 h static culture (+/- *stx*-phages). 1 h, 100  $^{\circ}$ C heat killed SK22D (SK22D<sup>x</sup>) (1:100, *stx*-phages: SK22D<sup>x</sup>), the washed heat killed pellet (SK22D<sup>x</sup> pellet) and the sn of the heat killed SK22D (SK22D<sup>x</sup> sn) were tested. Subsequently, the sterile filtered supernatants were examined for the phage plaque forming units (pfus) with a Phage Plaque Assay. (B) The location of the *stx*-phages was furthermore determined for the living and the heat killed SK22D with a *stx2a*-PCR with the primer pair SB51/SB52 (amplicon: 518 bp) before and after the DNase (2 U/ml) digestion for 10 min at 37  $^{\circ}$ C. ns: not significant, \* $p$ <0.05, \*\*\*\* $p$ <0.0001.

#### **4.4.5. Impact of EcN's mutants on the *stx*-phage stability**

As it was shown, that the phage inactivation was EcN specific and moreover, could be achieved with heat killed pellet of SK22D, various EcN mutants were tested for their phage inactivation ability. Additionally, EcN bacterial ghosts (BG) were tested. BGs are bacterial envelopes, which were induced to lyse by the lysis gene *e*. Thereby, the cytoplasmic content is released through a transmembrane tunnel formed by the lysis protein E whereas the periplasmic components remain at the empty bacterial envelope (Langemann et al., 2010). The prospective BGs were grown at 35 °C in LB medium (shaking) until they reached the mid-logarithmic growth phase. Subsequently, the lysis was induced with a temperature switch to 42 °C (Paton et al., 2015).

The capsule mutant (EcN $\Delta k5$ ), the cellulose mutant (EcN $\Delta bcs$ ), the curli mutant (EcN $\Delta csg$ ) and the flagellin mutant (EcN $\DeltafliC$ ) of EcN were screened for their phage inactivation capacity along with the EcN *wt* and the EcN BGs. As in the experiment with the commensal *E. coli* (4.4.3.), the EcN strains were tested alive and heat killed (24 h, static cultures). Figure 43 A summarizes the results from the phage inactivation by living EcN mutants. None of the mutants showed a loss of the phage inactivation function (> 90 % reduction). Anyhow, they depicted ranging efficiency in the phage inactivation of - 125-fold for EcN (6.6e3 pfus/ml), - 230-fold for EcN $\Delta k5$  (3.6e3 pfus/ml), - 52-fold for EcN $\Delta bcs$  (1.6e4 pfus/ml), - 32-fold for EcN $\Delta csg$  (2.6e4 pfus/ml), - 11-fold for EcN $\DeltafliC$  (7.8e4 pfus/ml) (figure 43 A). Contrary, the BGs (2.2e6 pfus/ml) could not reduce the plaque titer compared to the LB control (8.3e5 pfus/ml). The same could be observed for the heat killed mutants in figure 43 B. All EcN<sup>x</sup> mutants could reduce the phage titer by > 99 % but with ranging efficiency. Once more, the BGs lacked this functionality (LB: 1.7e6 pfus/ml, + BGs: 6.4e6 pfus/ml). Besides, it was tested if the digestion of the heat killed pellet with 1 mg/ml Proteinase K (PK) influenced the phage inactivation function. PK cleaves between amino acids (X-↓-Y; X = aliphatic, aromatic or hydrophobic amino acid, Y = any amino acid) and is thereby very efficient in protein degradation. The digested EcN<sup>x</sup> was detected to be inefficient in the phage reduction, as the phage titer in the filtrate 8.65e5 pfus/ml was comparable to the 1.14e6 pfus/ml in the PK treated LB control. The Stx level was not significantly influenced neither by any mutant nor by the BGs (OD<sub>450</sub>: 2.66 +/- 0.2) (figure 43 C).

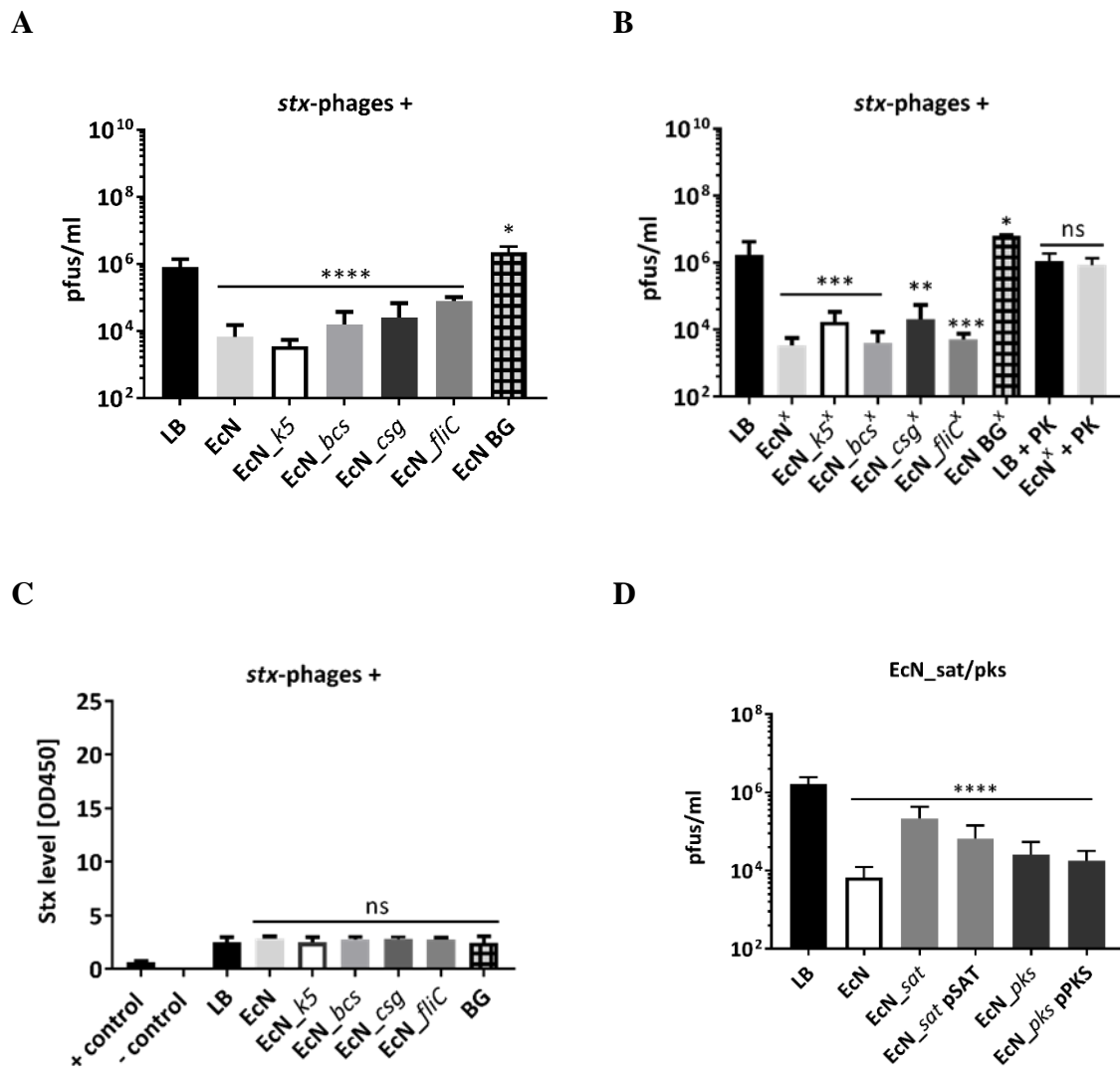


**Figure 43: *stx*-phage inactivation by *EcN* surface mutants.** *stx*-phages were incubated for 24 h static, with (A) the living or (B) the 1 h, 100 °C heat killed *EcN* surface mutants (*EcN*<sup>x</sup>) *EcN*Δ*k5*, *EcN*Δ*bcs*, *EcN*Δ*csg* and *EcN*Δ*fliC* or the bacterial ghosts (BG) of *EcN*. The heat killed *EcN* *wt* and a LB control were digested with 1 mg/ml Proteinase K (PK). The sterile filtered supernatants were examined for the phage plaque forming units (pfus) with a Phage Plaque Assay and additionally for (C) the toxin level with the Stx-ELISA. (D) The *EcN* *sat* protease (*EcN*Δ*sat*) and the colibactin mutants (*EcN*Δ*pks*) as well as the complemented mutants (pSAT, pPKS) were tested for their phage inactivation activities. ns: not significant, \**p*<0.05, \*\**p*<0.01, \*\*\**p*<0.001 and \*\*\*\**p*<0.0001.

Next to the surface mutants of *EcN* we tested if virulence associated genes in *EcN* could have an impact on the phage viability as the function of these genes in *EcN* are not solved yet. The serine protease autotransporter (*sat*) codes for a protease that has been shown to have cytotoxic effects on undifferentiated epithelial cells (Tolozza et al., 2015). The other virulence associated

genomic region investigated was the *pks* island. The island codes for colibactin, which induces DNA double strand breaks in eukaryotic cells when being in cell to cell contact (Nougayrede et al., 2006). An intact mucus layer however, counteracts with this outcome (Reuter, Alzheimer, Walles, & Oelschlaeger, 2018).

The effect of EcN lacking the *sat* or the *pks* genomic information (EcN $\Delta$ *sat*, EcN $\Delta$ *pks*) and the complemented strains were tested for their impact on *stx*-phages. The results in figure 43 D revealed a 230-fold less efficient phage reduction by the EcN $\Delta$ *sat* mutant (2.2e5 pfus/ml) compared to the EcN *wt* (6.7e3 pfus/ml). Anyhow, the complemented mutant EcN $\Delta$ *sat* pSAT could not retrieve the *wt* inactivation level (220-fold less efficient than the *wt*, 6.6e4 pfus/ml). The EcN $\Delta$ *pks* mutant and the complemented EcN $\Delta$ *pks* pPKS strain were with 2.6e4 pfus/ml and 1.8e4 pfus/ml a bit less efficient in the phage reduction that the EcN *wt*.

The experiments could reveal, that all EcN mutants tested, were able to inactivate the *stx*-phages with variable efficiency. The BGs and the PK digested EcN on the other hand, lacked this function.

#### **4.4.6. Influence of EcN's biofilm on *stx*-phages**

*E. coli* strains form communities to increase their tolerance to stress and host defense mechanisms (Beloin et al., 2008). These communities are called biofilm and are complex matrix structures composed of polysaccharides, proteins and nucleic acids (Wood, 2009). We aimed to identify whether the biofilm of EcN was involved in the observed *stx*-phage inactivation. Therefore, the biofilm of EcN was induced with a low concentration of cellulase (0.09 mg), which we identified to increase the biofilm formation beforehand.

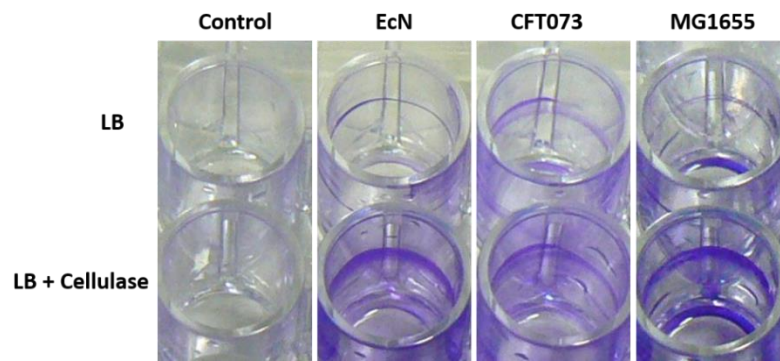
In a first experiment, the effect of an increased biofilm of EcN was compared to the effect of the increased biofilms of CFT073 and MG1655. The *E. coli* strains were incubated with *stx*-phages (isolated from a 6 h 1  $\mu$ g/ml MMC induced EDL933 culture) for 24 h with or without the addition of cellulase (*E. coli*<sup>+C</sup>). Figure 44 A captured the biofilms of *E. coli* grown in LB medium and LB medium supplemented with cellulase. A clear increase of the crystal violet stained biofilms could be observed by the addition of cellulase. The detection of the in EtOH dissolved crystal violet stained biofilm supported the optical evaluation with an increase of 118 % for EcN, 46 % for CFT073 and 87 % for MG1655 (figure 44 B). Additionally, the bacterial growth was determined at the OD<sub>600</sub>. Likewise, to the biofilm increase also the bacterial mass (planktonic cells + biofilm) increased by 41 % for EcN, 87 % for CFT073 and

40 % for MG1655 (figure 44 C). The final determination of the plaque forming units of the filtered samples disclosed a massive phage reduction increase of 99 % for EcN, 99 % for CFT073 and 95 % for MG1655 in the samples complemented with cellulase compared to the strains grown in LB medium (figure 44 D).

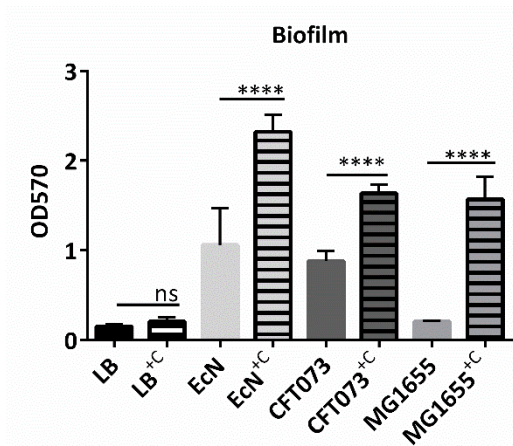
Besides testing the effect of the EcN *wt*, the biofilm matrix mutants lacking the curli gene cluster EcN $\Delta$ *csg* (table 8 C) and EcN $\Delta$ *bcs* (table 8 B), deprived of the cellulose gene cluster were investigated. Cellulose and curli are involved in the formation of the three-dimensional biofilm matrix (Beloin et al., 2008). Despite the lack of these gene clusters, both mutants formed a biofilm, which was ~40 % reduced compared to the biofilm of the *wt*. The biofilm of the mutants increased to a comparable OD<sub>570</sub> level of ~2.4 +/-0.14 like the EcN<sup>+C</sup> control (OD<sub>570</sub>: 2.32) when cellulase was added to the growth medium (figure 45 A, B). Likewise, to the EcN *wt* the mutants were increased in the planktonic cells and biofilm mass (OD<sub>600</sub>) by 18 % for EcN $\Delta$ *csg* and 33 % for EcN $\Delta$ *bcs* (figure 45 C). Both mutants were more potent in the *stx*-phage inactivation (in LB: 7.5e4 +/- 2.5e4 pfus/ml, LB<sup>+C</sup>: 2.5e3 +/-3e2 pfus/ml) when cellulase was added to the medium.

The increase of biofilm did lead to an intense *stx*-phage inactivation for all *E. coli* strains tested. The accompanying rise in the OD<sub>600</sub> values, did not allow a clear assignment to the phage reducing component.

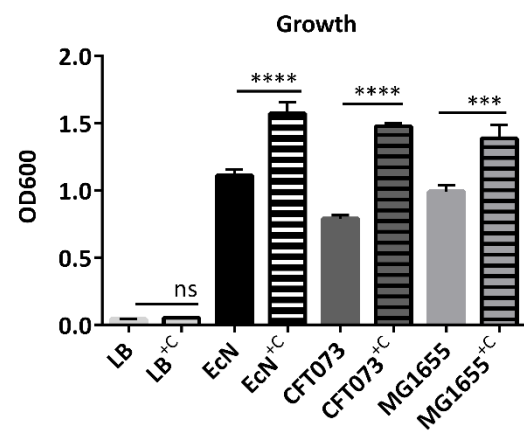
A



B



C



D

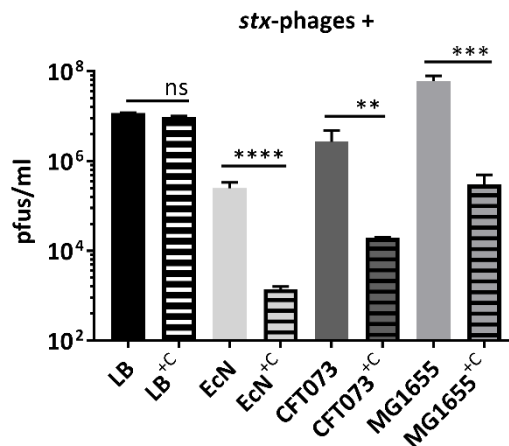
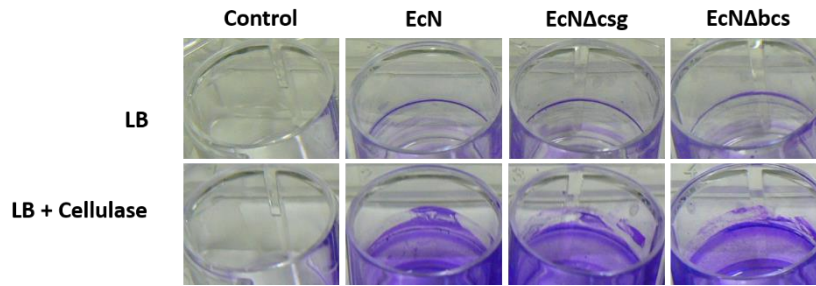
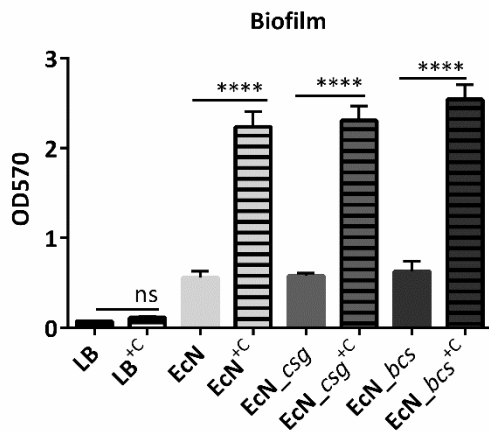


**Figure 44: Investigation of the biofilm of EcN, CFT073 and MG1655 for *stx*-phage inactivating activities.** The influence of biofilm on *stx*-phages by EcN, CFT073 and MG1655 was investigated after a 24 h incubation period in LB medium with or without 0.09 g Cellulase (*E. coli*<sup>+C</sup>). (A) Crystal violet stained biofilms in a 96 well plate. (B) Biofilm detection of the in EtOH dissolved biofilm at an OD<sub>570</sub>. (C) OD<sub>600</sub> values of the 24 h cultures. (D) Phage plaque forming units (pfus/ml) of the sterile filtered supernatant from 24 h cultures in a 24 well plate. ns: not significant, \*\*p<0.01, \*\*\*p<0.001 and \*\*\*\*p<0.0001.

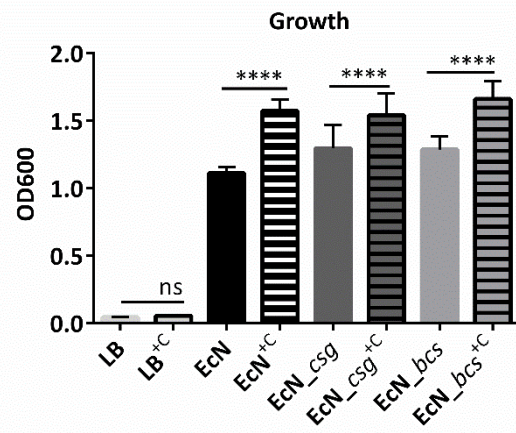
A



B



C



D

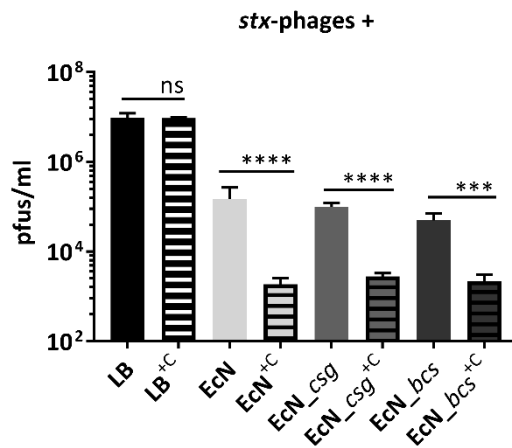


**Figure 45: Investigation of the biofilm of EcN, and the biofilm mutants EcNΔbcs and EcNΔcsg for stx-phage inactivating activities.** The influence of biofilm on stx-phages by EcN, and the curli mutant EcNΔcsg and the cellulose mutant EcNΔbcs was investigated after a 24 h incubation period in LB medium with or without 0.09 g Cellulase (*E. coli*<sup>+C</sup>). (A) Crystal violet stained biofilms in a 96 well plate. (B) Biofilm detection of the in EtOH dissolved biofilm at an OD<sub>570</sub>. (C) OD<sub>600</sub> values of the 24 h cultures. (D) Phage plaque forming units (pfus/ml) of the sterile filtered supernatant from 24 h cultures in a 24 well plate. ns: not significant, \*\*\*p<0.001 and \*\*\*\*p<0.0001.



### **4.5. K-12 protection studies**

(Schmidt et al., 1999) could prove that *stx*-phages can turn harmless *E. coli* strains into toxin carrying pathogens. In their study, *stx*-phages carrying a chloramphenicol cassette were positively integrated as prophages into the genome of about 30 % of the tested pathogenic and nonpathogenic *E. coli* strains. This turn of harmless bacteria into pathogens can be responsible for the different outcome of patients with a STEC infection, based on their microbiota composition. Concerning this matter, it is of great interest to combat the lysogeny formation of bacteria.

#### **4.5.1. SK22D protects K-12 strains from *stx*-phage infection**

During the Stx studies, it was observed that SK22D interfered in triculture with the toxin increase that was observed in the cocultures of *stx2* STEC strains with MG1655 (figure 26 A). In a next study, we wanted to investigate this observation further by testing the effect of isolated *stx*-phages (without MMC) on three different K-12 strains: MG1655, HB101 and DH5 $\alpha$  and examine the protection capability of SK22D. The mono-, co- or tricultures (phages: SK22D: MG1655 = 1:10:10) were incubated for 24 h, static before the Stx level and the phages plaques were analyzed. The Stx level evaluation in figure 46 A detected a Stx increase (OD<sub>450</sub>: 1.19) for MG1655 of ~ 1,600 % (OD<sub>450</sub>: 19.18), for HB101 of ~ 1,800 % (OD<sub>450</sub>: 21.99) and for DH5 $\alpha$  of ~ 1,600 % (OD<sub>450</sub>: 19.30). However, if SK22D was cultured along with the K-12, phage mix, the toxin level stayed as low as 2.99 +/- 0.5, which equals a reduction of ~ 85 %. A similar result was observed in the phage enumeration. The K-12 strains increased the phage titer from 3.8e5 pfus/ml to 8.7e8+/-3.7e8 pfus/ml, whereas the presence of SK22D resulted in a 2.7e4-fold reduction towards the monoculture in the case of MG1655 (2.2e4 pfus/ml) and to no phage plaques detectable with the PPA in case of the K-12 strains HB101 and DH5 $\alpha$  (figure 46 B).

This experimental outcome confirmed the results from the STEC co- and triculture study in 4.2.3.. The *stx*-phages could turn all K-12 strains into strong Stx and *stx*-phage producers. Anyhow, in the presence of SK22D both, the toxin level and the phage titer stayed low.

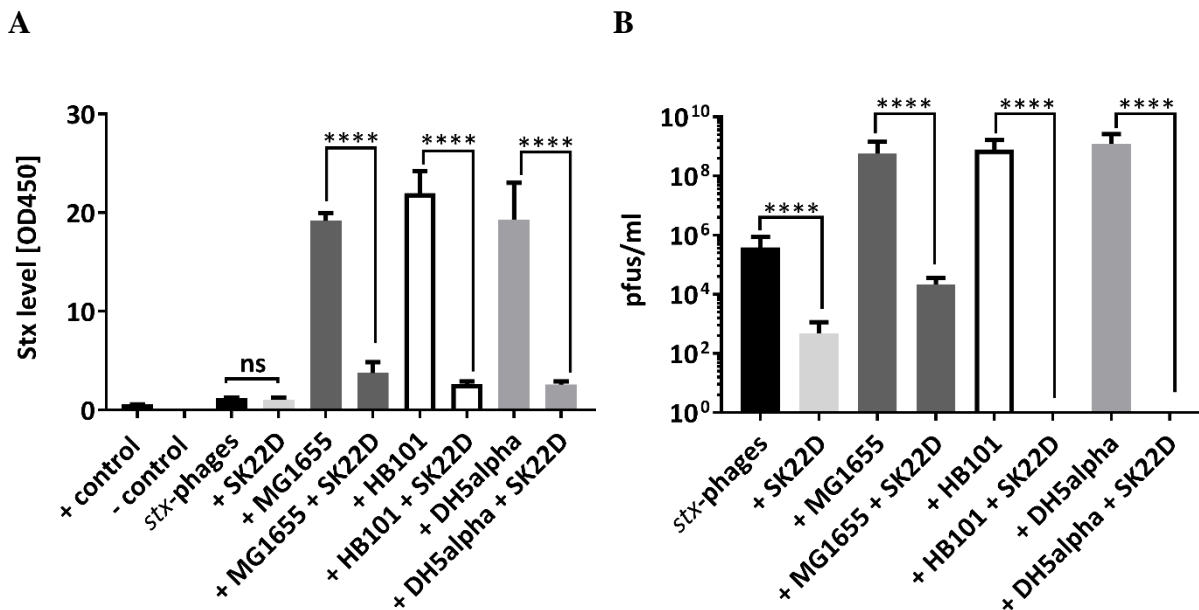


**Figure 46: SK22D protects K-12 strains from *stx*-phage infection.** Isolated *stx*-phages (no MMC) were incubated with SK22D and/or the K-12 strains MG1655, HB101 and DH5 $\alpha$  for 24 h, static. The (A) Stx level and the (B) phage plaque forming units (pfus) were determined in the filtered supernatant. ns: not significant, \*\*\*\* $p < 0.0001$ . (Images from Bury et al., 2018, under review).

#### 4.5.2. Light microscope study

In the presence of SK22D the toxin increase by MG1655 was observed to be strongly reduced. In a next step, we tried to identify possible SK22D and MG1655 interactions or bacterial aggregate formation by which SK22D protected MG1655. As *E. coli* exhibit a size of 1 - 3  $\mu\text{m}$  the light microscope Nikon Eclipse 50i microscope with at a 500-x magnification was used to examine the bacterial growth structures.

The *E. coli* strains SK22D, MG1655 and CFT073 were watched in mono- and in coculture with MG1655. Figure 47 A and B showed single SK22D bacteria in monoculture after a 24 h incubation period in LB medium. Different growth formations were found like single colonies in figure 47 A, but also bacterial cluster regions as seen in figure 47 B. A similar observation was made for the MG1655 monoculture. A wide distribution of MG1655 bacteria could be seen in figure 47 C and a bacterial clumping formation in figure 47 D. The MG1655 bacteria exhibited a rod-shaped phenotype of around 1  $\mu\text{m}$  length, whereas the SK22D bacteria were found to have about only have of this size.

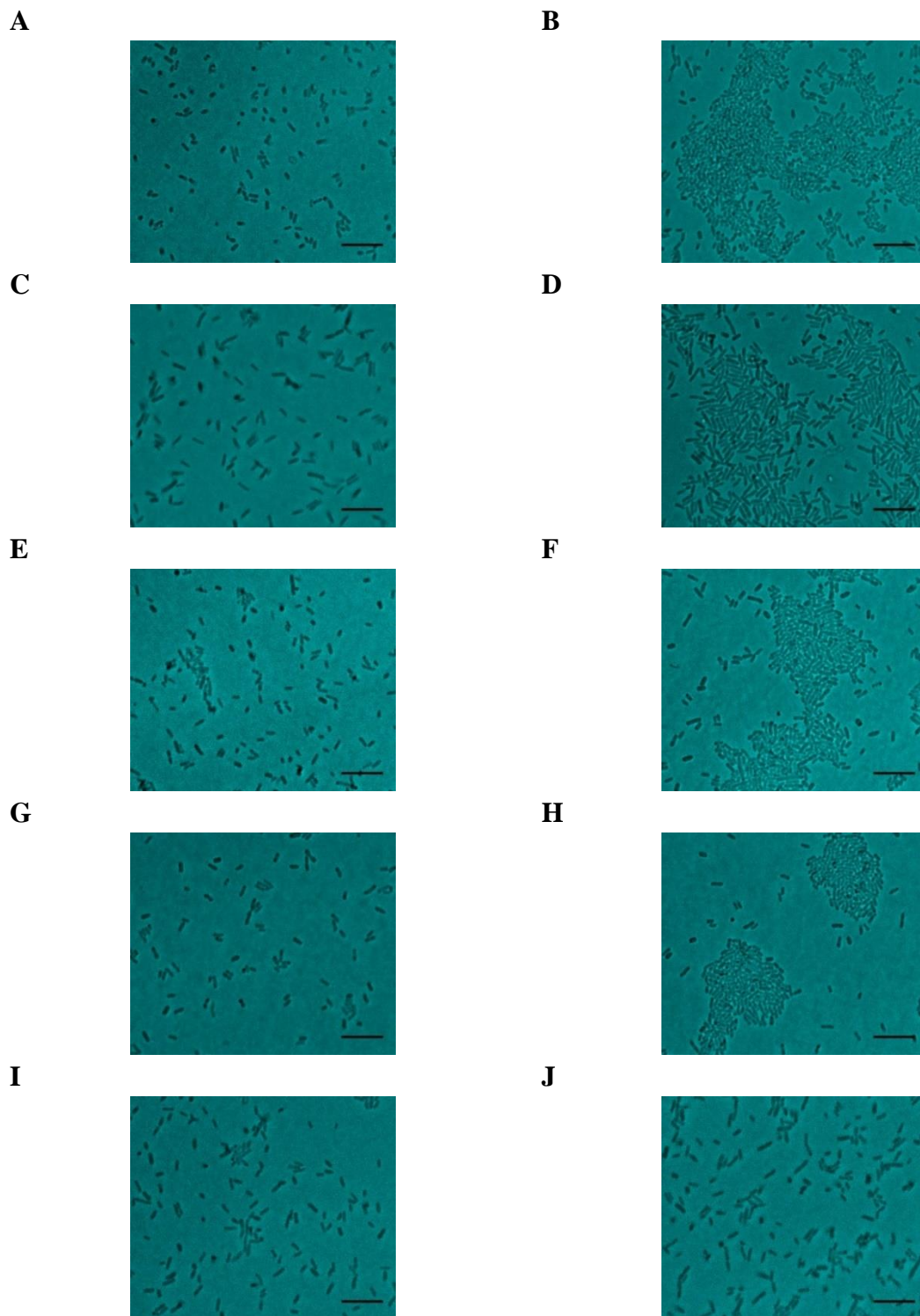


**Figure 47: Light microscope study of the *E. coli* growth formations.** *E. coli* strains were grown in mono- or cocultures for 24 h static at 37 °C. The colonies were observed on a microscopic slab and visualized at the Nikon Eclipse 50i microscope at a 500-x magnification. (A, B) SK22D, (C, D) MG1655, (E, F) SK22D + MG1655 (1:1), (G, H) CFT073, (I, J) CFT073 + MG1655 (1:1). Scale bar: 5  $\mu$ m, Color change to cyan with ImageJ 64.

When being cocultured, the single bacteria (figure 47 E) and the clumped regions (figure 47 F) were once more observed. It was not possible to distinguish the bacteria according to their size. Figure 44 G and H showed the single bacteria and the clumping regions depicted for the EcN relative strain CFT073. In the coculture with MG1655 anyhow (figure 47 I/J), no bacterial clumping regions were detected.

The microscopic analysis of the phenotypic bacterial growth formation did reveal two different growth structures for all investigated strains in monoculture. Only SK22D was detected to form bacterial clusters in the presence of MG1655. If the K-12 bacteria were integrated in this cluster could not be identified with this microscopy study.

### **4.5.3. MG1655 phage infection and SK22D protection kinetics**

The kinetics of the MG1655 infection by the *stx*-phages were examined in a next approach. Moreover, the protection effect of SK22D was closely monitored in a period of 24 h at every 4<sup>th</sup> hour. The *stx*-phages were cultured with a starting a ratio of 1:100:100 with SK22D and / or MG1655 in a static environment at 37 °C. The kinetics of the Stx level in figure 48 A showed that the existing toxin level of the phage/toxin filtrate was not influenced by SK22D, nor did it decrease in monoculture at any time point. Contrary, the K-12 strain MG1655 increased the toxin by 600 % after already 8 h of incubation with the isolated *stx*-phages, which extended to a toxin increase of 1,700 % after 12 h incubation. The Stx level stayed constant after 16 h of incubation at an OD<sub>450</sub> of 19.35 +/- 0.17, which equaled an increase of 1,900 % towards the isolated *stx*-phage monoculture control. Impressively, in the presence of SK22D the toxin level increased to a maximum OD<sub>450</sub> of 3.76 in the 20 h culture and was 80 % reduced compared to the K-12 and phage coculture after 24 h of incubation.

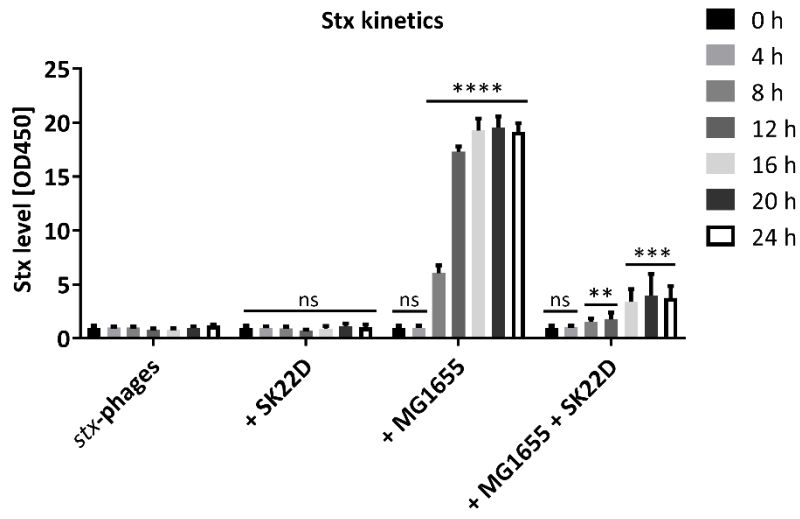
A similar observation was made for the *stx*-phage plaque units detection in the filtered supernatants (figure 48 B). In the coculture of MG1655 with the isolated phages, the phage titer raised from 2.3e5 pfus/ml to 8.5e7 pfus/ml after 8 h of incubation, peaked at 12 h - 20 h incubation time with an ~3.5e5 pfus/ml increase towards the phage control (3.3e4 +/- .3e4 pfus/ml), and dropped after 24 h of incubation to a 3.5e3 pfus/ml difference to the control (1.5e4 pfus/ml). SK22D could even interfere with this immense phage increase during triculture incubation. The highest phage titer of 2.4e6 pfus/ml was detected in the 8 h culture. All samples collected at later time points revealed a continuous phage decrease of 1.9e6 pfus/ml to 4.42e5 pfus/ml after 12 - 20 h and 2.1e3 pfus/ml reduced towards the phage

titer in the MG1655 culture at the final sample collection time point. The results for the SK22D and phage coculture and the phage monoculture matched the phage reduction kinetics with the EcN *wt* in figure 39. The *stx*-phage plaque units decreased 10-fold in monoculture after 24 h incubation and were firstly decreased by 75 % after 12 h of incubation with SK22D and by 96 % after 24 h incubation.

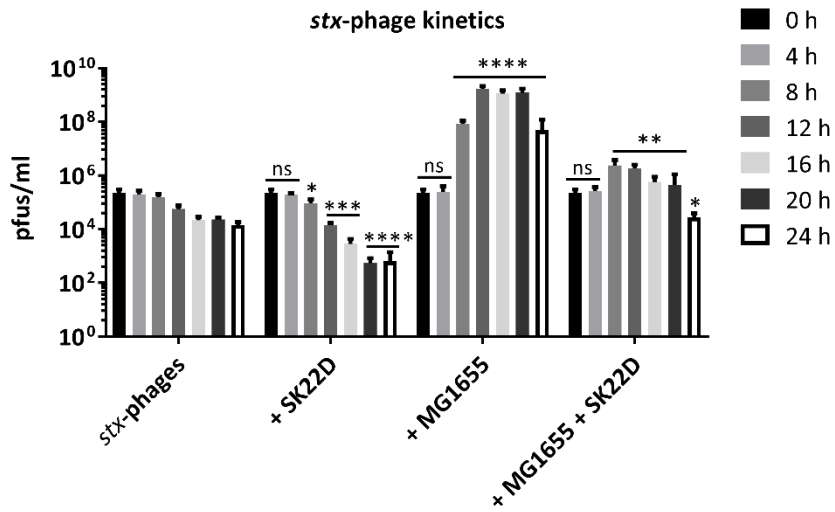
In addition to the toxin and phage kinetic investigation, the *E. coli* CFUs response towards the different culture conditions was examined. In monoculture with only LB medium (black line), in coculture the opposite *E. coli* strain (red line) or phages (green line) or in triculture with phages and SK22D/MG1655 (blue line). The *E. coli* strain enumeration showed that the probiotic strain SK22D was not influenced in its growth at any time point by the addition of MG1655, *stx*-phages or both (figure 48 C). The CFUs detection depicted a homogenous growth curve of a starting  $8.4 \times 10^7$  CFUs/ml at time point 0 h, a logarithmic growth phase from 4 h to 12 h ( $2.9 \times 10^8 \pm 4 \times 10^7$  CFUs/ml to  $7.6 \times 10^9 \pm 7 \times 10^8$  CFUs/ml) and the stationary growth phase after 16 h of incubation with  $3.8 \times 10^9 \pm 7.6 \times 10^8$  CFUs/ml. The growth curve of MG1655 was comparable to that of SK22D when being cultured in LB medium (figure 48 D). The exponential growth phase was monitored from 4 h to 12 h of incubation ( $9.13 \times 10^8$  CFUs/ml -  $1.6 \times 10^9$  CFUs/ml) and resulted in a stationary bacterial culture of  $3.3 \times 10^9 \pm 2 \times 10^8$  CFUs/ml after 16 h of static incubation. Already the presence of the probiotic strain SK22D itself could strongly interfere with the growth of MG1655. A first growth was observed between 0 h and 4 h ( $8.4 \times 10^7$  CFUs/ml to  $5.7 \times 10^8$  CFUs/ml) after which the K-12 strain depicted stationary phase growth behavior with a constant CFUs/ml of  $5.9 \times 10^8 \pm 1.1 \times 10^8$  CFUs/ml at all later time points. An even greater growth influence was observed in presence of *stx*-phages. The CFUs counted after 4 h demonstrated a growth to only  $2.2 \times 10^8$  CFUs/ml. The CFUs stayed constant until 20 h of incubation at around  $3.1 \times 10^8 \pm 4 \times 10^7$  CFUs/ml and dropped to  $2.2 \times 10^8$  CFUs/ml after 24 h. In the triculture set up the CFUs of MG1655 were comparable to those of the phage and MG1655 coculture.

Summarized, a phage and toxin increase by the lysogenic MG1655 could be observed after an 8 h incubation time. The microcin negative EcN mutant SK22D showed a strong interference with this toxin increase by protecting MG1655 from the *stx*-phages. Connected to this, the presence of SK22D unbalanced the growth curve of MG1655 and pushed the strain into an early stationary phase with a ~10-fold CFUs/ ml reduction.

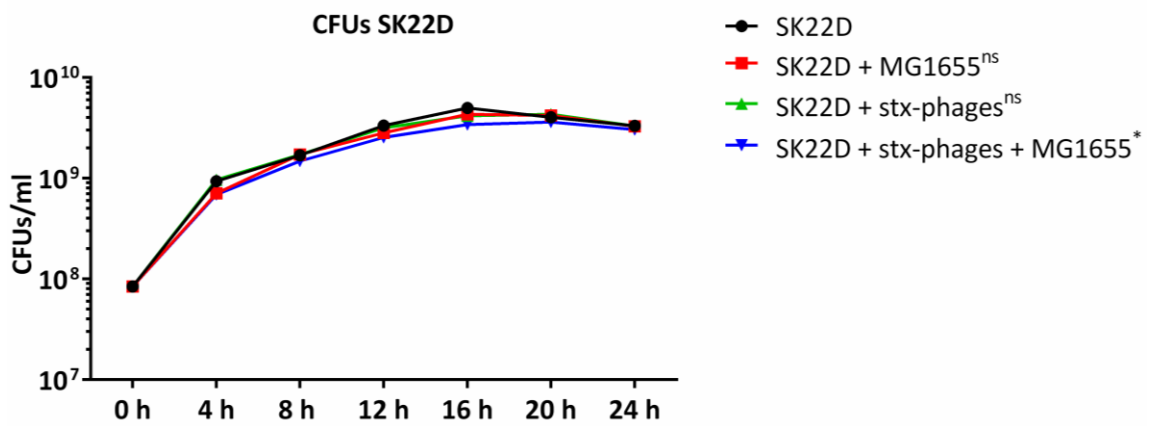
A



B



C



D

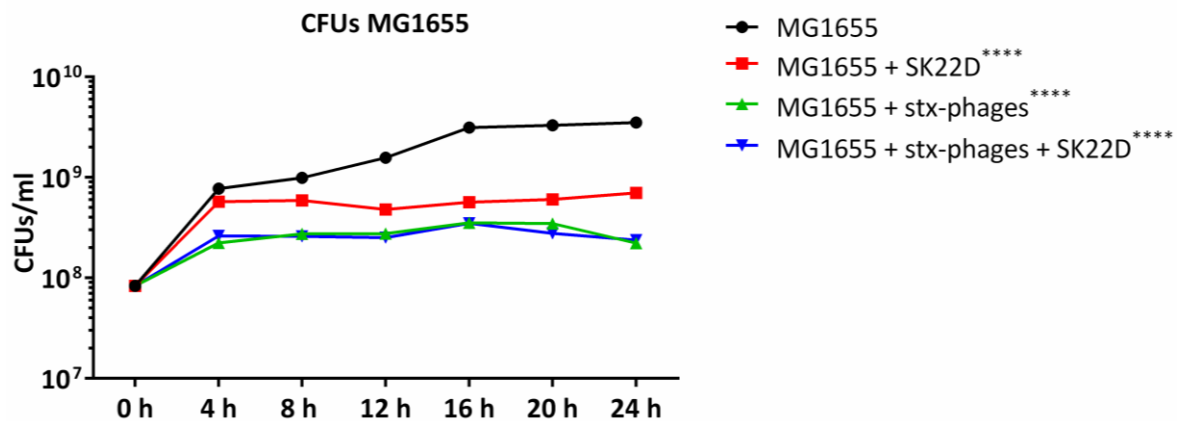


**Figure 48: Kinetics of MG1655 phage infection or protection by SK22D.** Isolated *stx*-phages were incubated with SK22D and or MG1655, static. Samples for the (A) *Stx* level and (B) *stx*-phage titer evaluation were collected every 4 h until 24 h. The CFUs kinetics of (C) SK22D and (D) MG1655 were determined at the same time points in the monocultures (black bars), the cocultures (+ *E. coli*: red bars, + *stx*-phages: green bars) and in tricultures (blue bars) (*stx*-phages: SK22D: MG1655 = 1:100:100). ns: not significant, \* $p < 0.05$ , \*\* $p < 0.01$ , \*\*\* $p < 0.001$  and \*\*\*\* $p < 0.0001$ . (Images A and B from Bury et al., 2018, under review).

#### 4.5.4. Protection of MG1655 infection by diverse *E. coli* strains

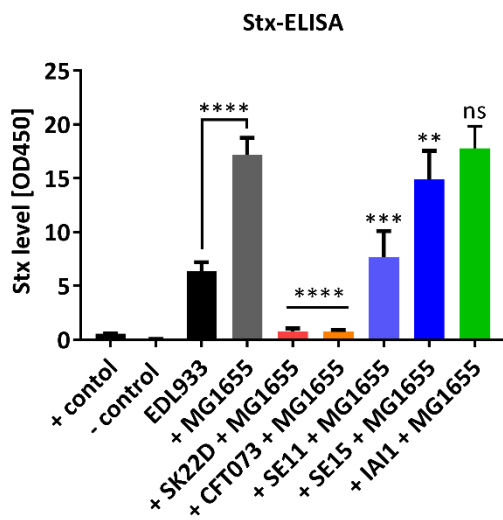
The experiment in 4.4.3. identified the *stx*-phage inactivation as an EcN specific characteristic compared to the other *E. coli* strains tested. The same *E. coli* control strains were used in a next study to screen them for their MG1655 protection capacity.

The commensal *E. coli* strains SE11, SE15 and IAI1 as well as the EcN relative CFT073 and SK22D as a positive control for MG1655 protection were tested after a 24 h, static incubation period. In a first experimental phase, the pathogenicity background for the tricultures was the O157:H7 strain EDL933. The coculture of this strain with a MG1655 culture (1:10) resulted in an increase of the toxin level of ~170 % (figure 49 A). Both, SK22D and CFT073 could interfere with this increase in triculture and showed an even 88 % reduced *Stx* level (OD<sub>450</sub>: 0.75) compared to the EDL933 monoculture (OD<sub>450</sub>: 6.38). The commensal strains however, varied in their protection capacity of MG1655 with an *Stx* level of OD<sub>450</sub> 7.66 for SE11, 14.92 for SE15 and 17.78 for IAI1. As expected, also the phage plaque forming units were increased in the coculture of EDL933 and MG1655 by ~ 190-fold (EDL933 monoculture:

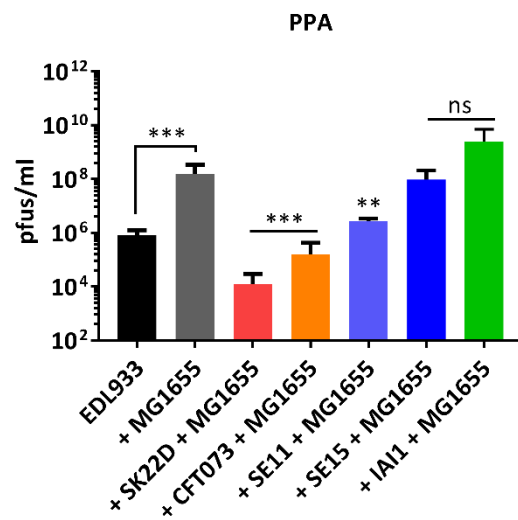
## Results

7.9e5 pfus/ml, coculture with MG1655: 1.5e8 pfus/ml) (figure 49 B). The presence of SK22D resulted in a detectable phage titer of 1.2e4 pfus/ml and a 10-fold higher phage titer of 1.6e5 pfus/ml for CFT073. The triculture with the commensal strain SE11 revealed a ~3-fold a phage increase (2.7e6 pfus/ml) compared to the EDL933 monoculture and SE15 and IAI1 could not interfere with the MG1655 induced increase of phages (SE15: 9.6e7 pfus/ml, IAI1: 2.5e9 pfus/ml).

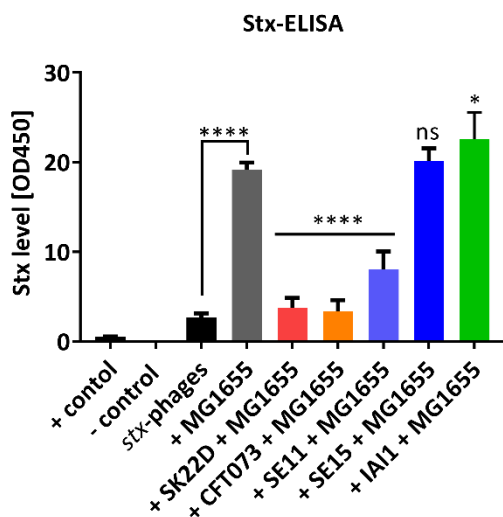
A



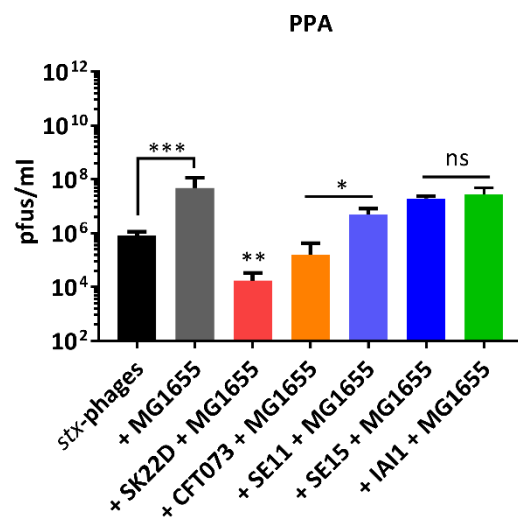
B



C



D





## E

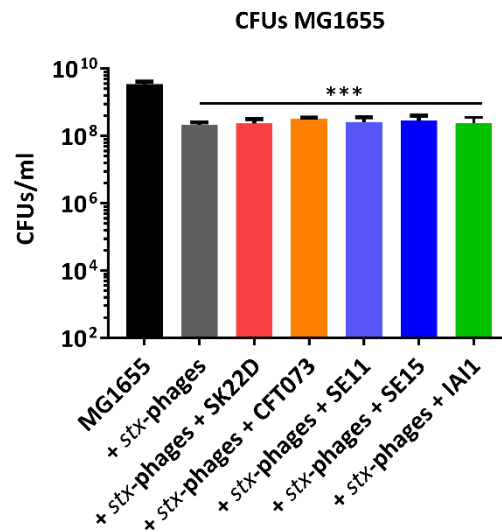


**Figure 49: Protection of MG1655 against *stx*-phage infection by various *E. coli* strains.** The K-12 strain MG1655 was incubated with EDL933 or isolated *stx*-phages (no MMC) for 24 h, static. SK22D, the uropathogenic strain CFT073 and the commensals SE11, SE15 and IAI1 were screened for the protection of MG1655 in tricultures (EDL933/*stx*-phages: MG1655: “protector strain” = 1:10:10). The (A) Stx level and the (B) phage titer were determined in the presence of EDL933 or isolated *stx*-phages (C (Stx), D (phage plaques)). (E) The CFUs of MG1655 were determined in the tricultures with isolated phages. ns: not significant, \* $p < 0.05$ , \*\* $p < 0.01$ , \*\*\* $p < 0.001$  and \*\*\*\* $p < 0.0001$ .

In a next experiment, isolated *stx*-phages were used as pathogenicity source. Just as in the first approach, the toxin and phage level increased in the presence of MG1655. The isolated phages however, induced the toxin production by MG1655 drastically by ~ 600 % (*stx*-phages: OD<sub>450</sub>: 2.7, coculture with MG1655: OD<sub>450</sub>: 19.2) and the phage plaques 58-fold (*stx*-phages: 8.4e5 pfus/ml, coculture with MG1655: 4.9e7 pfus/ml) (figure 49 C). SK22D, CFT073 and the commensal strain SE11 could significantly interfere with this toxin increase. However, a toxin difference of 2.7-fold in the presence of SE11 (OD<sub>450</sub>: 8.05) compared to SK22D and CFT073 (OD<sub>450</sub>: 3.76, 3.37) was determined. The commensal isolates SE15 and IAI1 could not significantly interfere with the toxin increase compared to the MG1655 coculture results (OD<sub>450</sub>: MG1655: 19.2, + SE15:20.17, + IAI1: 22.57). The phage plaque evaluation with the PPA presented SK22D as most potent in phage reduction with a decrease of ~2,900-fold (1.7e4 pfus/ml) compared to the coculture of MG1655 and phages (figure 49 D). CFT073 reduced the pfus/ml by ~300-fold (1.6e5 pfus/ml) and the commensal strain SE11 10-fold

(4.9e6 pfus/ml). As observed for the toxin level, SE15 and IAI1 did not reduce the MG1655 mediated phage increase (SE15: 2e7 pfus/ml, IAI1: 2.8 pfus/ml).

The CFUs of MG1655 were 10-fold decreased in the tricultures with *stx*-phages and all “protective” *E. coli* (figure 49 E).

Only the EcN close relative strain CFT073 could protect the MG1655 strain from phage infection likewise the SK22D control. The other commensals tested depicted variable, less potent protection efficiency.

### **4.5.5. Protection of MG1655 from *stx*-phages of the O104:H4 isolates**

The EHEC epidemic in Germany in 2011, was caused by the EHEC unusual serotype O104:H4 and resulted in a high human infection rate which was never observed before. Usually around 1,000 cases of EHEC infections are detected every year in patients of a median age of 5 years (Frank, Faber, et al., 2011). During the epidemic in 2011 however, about 3,000 patients were diagnosed with the O104:H4 infection. The infected patients had a median age of 46 years. 866 of the patients developed HUS and 53 people died (Frank, Werber, et al., 2011). According to this dramatic outcome, the newly evolved *stx2*-prophage carrying O104:H4 strains are by far more dangerous to human health than the until this point detected EHEC outbreak strains. Two isolates of patients in 2011 were consulted in our K-12 protection studies. TY3730, isolated from a patient suffering from gastroenteritis and TY3456, isolated from a patient who developed the HUS. We aimed to identify if these highly pathogenic *E. coli* strains will show similar results in the triculture studies with the commensal *E. coli* as the EDL933 strain.

The TY strains were cultured with MG1655 and, or the “protecting” *E. coli* strains in a starting ratio of 1:10:10 for 24 h. The Stx level (black bars) and the phage plaques (blue boxes) were determined in the mono- co- and tricultures for TY3730 (figure 50 A) and TY3456 (figure 50 B). Interestingly, we could observe a toxin decrease in the coculture with all tested “protecting” *E. coli* compared to the TY monocultures. SK22D and CFT073 could reduce the toxin level by~ 90 %, SE11 and SE15 by around 70 % and IAI1 was least efficient with a toxin reduction of ~32 %. The *stx*-phage susceptible strain MG1655 increased the toxin level by ~160 %, which was already detected in 4.2.3.. In the tricultures, SK22D, CFT073 and SE11 could most strongly interfere with the toxin increase mediated by the K-12 strain with a reduction of ~83 % in the presence of SK22D, CFT073 and ~73 % reduction for SE11 compared to the monocultures. The commensal strains SE15 and IAI1 on the other hand, failed

in the toxin reduction with an increase of ~40 % in the presence of SE15 and ~100 % for IAI1. The phage plaques enumeration depicted, that the phage titer was increased by ~130-fold in the cocultures with MG1655 (TY strains: ~ 1.5e5 pfus/ml, + MG1655: ~1.9 e7pfus/ml). All other *E. coli* strains investigated in the coculture studies reduced the phage titer to some extent compared to the monoculture (SK22D: 41-fold, CFT073: 125-fold, SE11: 8.3-fold, SE15: 3.7-fold, IAI1: 2.7-fold). In the tricultures, SK22D stabilized the phage titer to ~1.2e4 pfus/ml. The CFT073 and SE11 depicted a similar phage titer of ~6.3e5 pfus/ml which means a reduction of 30-fold compared to the MG1655 and TY strain cocultures. The commensal strains SE15 and IAI1 were least efficient in the phage reduction with an increase of 16-fold when SE15 was added (~2.35e6 pfus/ml) and a 44-fold increase in the presence of IAI1 (~6.4e6 pfus/ml) compared to the TY monocultures.

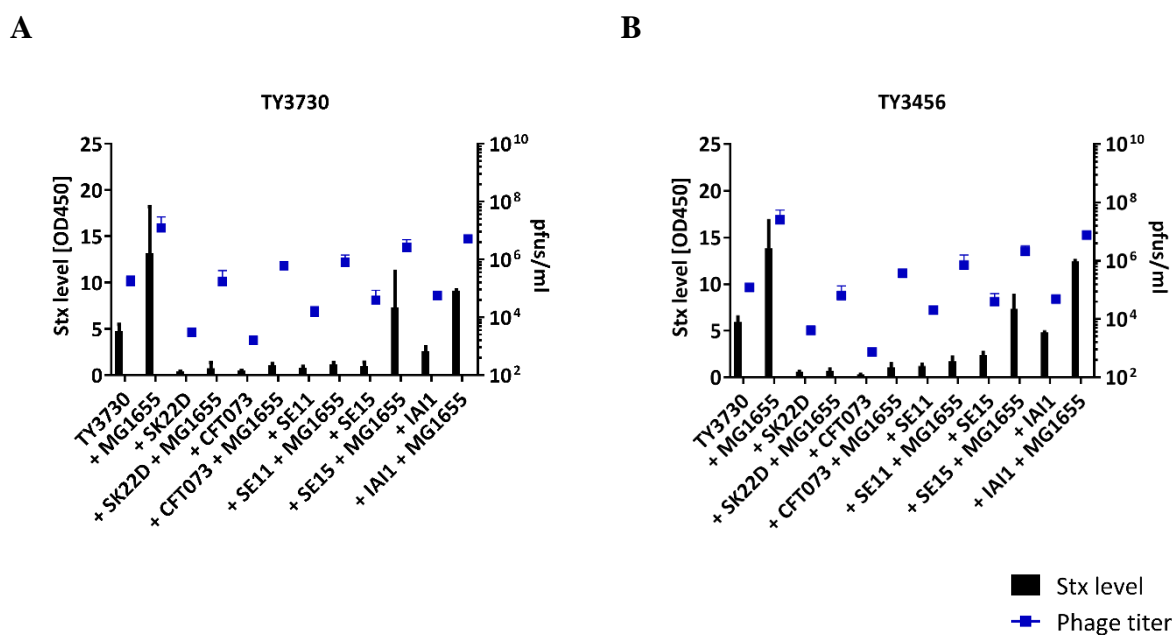


**Figure 50: Protection of MG1655 infection by *stx*-phages from the 2011 O104:H4 outbreak strains.** The K-12 strain MG1655 was incubated with the O104:H4 strains (A) TY3730 and (B) TY3456 for 24 h, static. SK22D, the uropathogenic strain CFT073 and the commensals SE11, SE15 and IAI1 were screened for the protection of MG1655 in tricultures (TY strains: MG1655: “protector strain” = 1:10:10). The Stx level (black bars) and the phage titer (blue boxes) were determined in the sterile filtered supernatants.

Summarizing the results from the experiments with the TY strains we could show that all “protecting” *E. coli* strains interfered with the pathogenic factor production like SK22D but

with variable efficiency. CFT073 and SE11 were comparable efficient in protecting the MG1655 mediated toxin increase as SK22D but unraveled a 10-fold reduced efficiency in the *stx*-phage reduction. SE15 and IAI1 showed only weak MG1655 protection facilities.

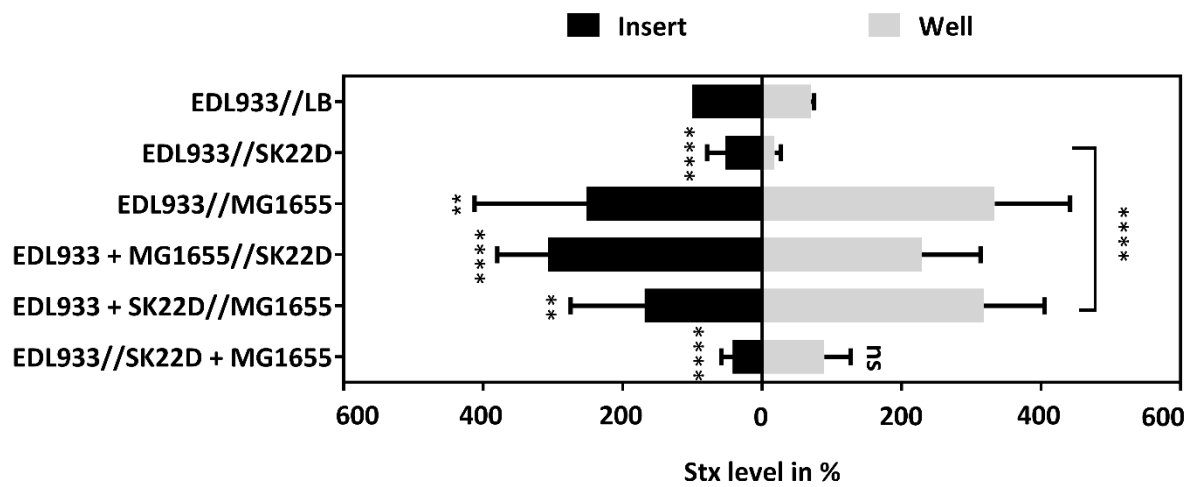
### **4.5.6. Protection of MG1655 in the Transwell system**

With the Transwell System the mechanism of MG1655 protection towards the *stx*-phage lysogeny was closer investigated. The *stx2*-phage producing strain EDL933, the phage susceptible strain MG1655 and the protective strain SK22D were incubated in the Transwell system in various combinations to investigate the protection ability of SK22D. As in the previous Transwell experiments (4.2.6.) EDL933 was cultured in a ratio of 1:10:10 to SK22D and MG1655. After an incubation period of 24 h the toxin level (figure 51 A) and the pfus (figure 51 B) were evaluated.

The Stx analysis unraveled the expected toxin decrease in the insert (-47 %) and the well (-82 %) in the presence of SK22D. The K-12 strain was infected by the *stx*-phages, despite being separated from EDL933 by the Transwell membrane. The infection led to a toxin increase of ~250 % in the insert and ~230 % in the well. The pfus were also influenced by SK22D and showed a reduction of 90 % (5.2e6 pfus/ml to 5.6e5 pfus/ml) in the insert and 99 % (1.9e6 pfus/ml to 1.1e4 pfus/ml) in the well. The MG1655 mediated phage increase of 230-fold could only be detected in the well (1.2e9 pfus/ml), whereas the *stx*-phages in the insert were decreased by 2-fold (2.6e6 pfus/ml). In case of the MG1655 protection evaluation, it was observed that SK22D was only able to interfere with the toxin increase (-11 % compared to the EDL//LB control) when being cultured in the same Transwell compartment as MG1655 (EDL933//SK22D + MG1655). In the remaining Transwell approaches with the three *E. coli* strains, a toxin increase of 240 % (insert) and ~290 % (well) was observed. The pfus detection depicted, that SK22D could reduce the phage titer from 3.6e6 +/- 1.6e6 pfus/ml to 4e5 +/- 3.9e4 pfus/ml (8-fold reduced) in the compartments it was cultured. Nevertheless, it could only interfere with the MG1655 mediated phage increase of 9.5e8 +/- 2.5e8 pfus/ml to 1.7e6 pfus/ml (559-fold reduced) when being cultured in the same compartment and therewith direct cell to cell contact was given (EDL933//SK22D + MG1655).

This experimental approach disclosed, that direct cell to cell contact was necessary for the MG1655 protection by SK22D.

A



B

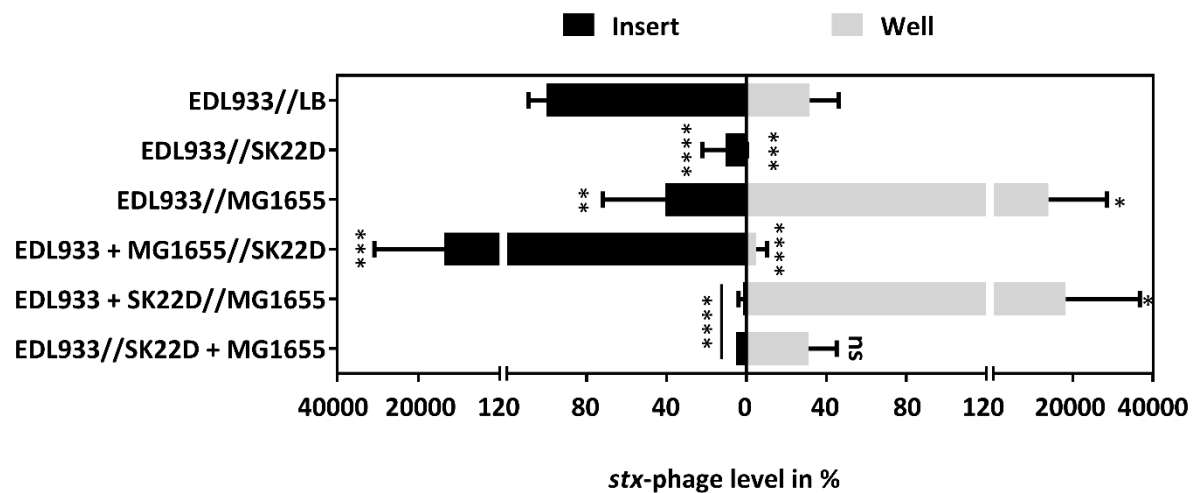


**Figure 51: Protection of MG1655 in the Transwell system.** EDL933 was incubated for 24 h in the insert of a Transwell system. Various combinations of the *E. coli* strains EDL933, SK22D and MG1655 (1:10:10) in the insert and the well were investigated. The Stx level (A) and the pfus (B) of the insert (black bars) and the well (grey bars) were determined and presented in percentage compared to the EDL933//LB control. ns: not significant, \* $p < 0.05$ , \*\* $p < 0.01$ , \*\*\* $p < 0.001$  and \*\*\*\* $p < 0.0001$ . (Images from Bury et al., 2018, under review).

## **5. Discussion**

Humans being infected by pathogenic STEC strains can develop mild disease symptoms like watery diarrhea up to more severe symptoms like bloody diarrhea and, or the HUS (Karch et al., 2005). The major cause for the disease is Stx, a toxin which is produced by STEC strains, that enters the eukaryotic cells of the host through the Gb3 receptor where it induces cell death by apoptosis (Johannes & Romer, 2010). *stx* is encoded on a prophage, hence the synthesis of Stx is connected to the production of dsDNA *stx*-phages, which can lysogenize commensal *E. coli* and turn them into toxin producing pathogens (Schmidt, 2001). So far there is no ideal patient treatment strategy available, as antibiotics lead to bacterial death but simultaneously induce the SOS response of the *stx*-prophage carrying STEC strains which results in an increased Stx and *stx*-phage release that can worsen the disease progression (Pacheco & Sperandio, 2012). Research for alternative treatment strategies revealed, that the probiotic *E. coli* strain EcN can reduce the CFUs of STEC strains and additionally interfere with the toxin production when being cocultured (Reissbrodt et al., 2009; Rund et al., 2013).

### **5.1. Studies towards the influence of EcN on the pathogenicity of STEC strains**

In this first part of the study we aimed to study the inhibitory effects of EcN towards the pathogenicity factor production of STEC strains in closer detail. Therefore, EcN was cultivated along with the “big five” STEC strains and two isolates from the 2011 outbreak in coculture. To investigate the influence of EcN towards the production of Stx and the *stx*-phages by STEC strains, the bacteria were cultivated *in vitro*, in rich medium (LB medium) for 24 h at 37 °C, static.

As it was already illustrated by other studies, we could demonstrate that EcN interfered with the Stx production by STEC strains. To exclude bacterial killing effects, the coculture experiments were performed with the microcin negative EcN mutant SK22D. SK22D being cultured with the “big five” STEC or the two O104:H4 isolates TY3730 and TY3456 (10:1) resulted in a reduction of the Stx level of about 90 % for all of them but the weak Stx producer O145:H25. The decrease of the toxin in the cocultures compared to the STEC monocultures can be assigned to a reduction of the *stx* transcription, which was previously evinced by the group of Mohsin et al. (Mohsin et al., 2015). Further to the investigation of the Stx level, also the presence of *stx*-phages was analyzed with a PPA and a *stx1* or *stx2* specific PCR to detect

the dsDNA in the capsid of the phages. The PPA studies with MG1655 as indicator strain enabled the detection of phage plaques from the *stx2* cultures EDL933, TY3730, TY3456 and O26:H11. For the *stx2* strain O145:H25 anyhow, no phage plaques could be detected which is most likely based on a low phage production, as also the Stx level was significantly lower compared to the other *stx2* STEC strains. Just as it was observed for the Stx level in the presence of SK22D, also the *stx*-phage plaques were strongly decreased for all STEC strains by 10 up to 1,000-fold and furthermore, the *stx2* PCR confirmed the strong reduction of the *stx2* phage DNA in the supernatants. The absence of a *stx2* DNA amplicon in the PCR of the cocultures of EDL933, O26:H11 and O145:H25 with SK22D in contrast to the detected phage plaques can be assigned to a PCR detection limit, as the phage density in the 1  $\mu$ l PCR template was below 0. For the cocultures with both TY strains however, a weak DNA amplicon was detected in the *stx2* PCR which had a calculated phage density of  $\sim 2.7$  phages in 1  $\mu$ l PCR template. In contrast to the *stx2*-phages, the *stx1*-phages from the STEC strains O103:H2 and O111:H- could not be detected with the standard PPA. As *stx1*-phage DNA was detected in the monoculture supernatants with *stx1* specific primers, it can be assumed that the standard PPA technique is not suitable for *stx1*-phages as it was confirmed that *stx1*-phages depict a low MG1655 infection efficiency (Asadulghani et al., 2009). For both strains, the *stx1*-phage DNA was below the detection limit in the presence of SK22D. The transcription of the late phage *stx* genes is linked to the transcription of the entire prophage DNA (Pacheco & Sperandio, 2012). As the reduction of the Stx production in the presence of SK22D is caused by a transcriptional downregulation of the late phage genes, it is likely that the lower *stx*-page titer is as well linked to a reduction of the phage transcription rather than to a degradation of the produced phages.

To proof this hypothesis, and to detect possible effects of EcN on already synthesized Stx, EcN was further analyzed for its effect on isolated Stx and *stx*-phages. Therefore, the Stx and *stx*-phage enriched supernatant of an EDL933 culture was collected by sterile filtration and subsequently incubated with EcN (MOI EcN: *stx*-phages= 10:1). The isolated toxin demonstrated a long-time stability in terms of the detection with the Ridascreen® ELISA Kit. The OD<sub>450</sub> values of the fresh isolate equaled the ones being incubated for 24 h at 37 °C (figure 29). Based on this Stx evaluation technique, EcN had no significant effect on the Stx stability. These results support the findings that EcN negatively influences the transcription of the *stx* genes and unravel that the strong toxin reduction which was detected by the Ridascreen® ELISA is not additionally linked to a degradation of Stx.

Studies on the mechanism of the phage reduction could unravel that EcN cannot degrade the *stx2* DNA in the capsid of synthesized *stx*-phages (figure 30), which supports the theory that both, the Stx and *stx*-phage production in the presence of SK22D are suppressed by a transcriptional downregulation. Multiple PCRs with primers that anneal to several genes spanning the 933W *stx2*-prophage could further substantiate a downregulation of the entire prophage transcription as the supernatant of the EDL933 and SK22D coculture (1:10) contained far less *stx*-phage DNA template compared to the monoculture control. Only in the more sensitive PCR for the last 933W prophage gene *z1503* (unknown function), a DNA amplicon was detected in the coculture which was fainter compared to the monoculture supernatant control (figure 28). A PCR which amplified *trp*, which is located outside of the *stx*-prophage in the typical *wrbA* *stx*-phage integration region, was only amplified in the EDL933 bacterial control and confirmed the absence of free EDL933 DNA in the filtered supernatants besides the DNA in the *stx*-phage capsids (Plunkett et al., 1999).

Based on the observations gathered from the STEC and SK22D cocultures we could reconfirm the results from previous studies of Rund and Reissbrodt et al., who observed that EcN reduces the Stx production of STEC strains (Reissbrodt et al., 2009; Rund et al., 2013). The results of the *stx*-phage PCRs suggest a similar effect of EcN towards a transcriptional downregulation for the entire *stx*-prophage as it is documented for *stx2* (Mohsin et al., 2015).

The previous described experiments were performed without the addition of any SOS response inducing agents. The kinetics of an EDL933 monoculture represented a continuous increase of the toxin with a 3,3-fold rise after already 6 h of static incubation (figure 24 A). Based on the CFUs determination, the EDL933 culture was in its logarithmic growth phase which is characterized by an exponential cell growth, the abundance of nutrients and the absence of toxic products (Pletnev et al., 2015). The nonetheless determined toxin accumulated could be either due to a small percentage of dying *E. coli* or a leaky prophage repression by the CI repressor.

To answer the question if EcN can be used as an additive during the antibiotic treatment of STEC infected patients, the kinetics of an EDL933 monoculture were compared to the coculture with SK22D (1:10) in the presence of the DNA damaging agent MMC (Walker, 1984). An alarmingly > 1,000 % increase of the Stx level compared to the untreated monoculture was detected after the addition of MMC which explains the possibility of the development of HUS in case of an antibiotic treatment of the patient (Pacheco & Sperandio, 2012). The addition of the probiotic strain SK22D, could reduce the toxin accumulation by around 32 %. Anyhow the toxin values were still critically high. The lack of the previous observed intense interference of



SK22D with the toxin production by EDL933 (>90 %) in the absence of MMC were probably due to SK22D bacterial harming effects by MMC, which was reflected by a SK22D CFUs decrease until 8 h of incubation before the culture could overcome the MMC influence. To enable an efficient EcN supplementary treatment of patients, alternative antibiotics should be investigated that can both, kill STEC strains but do not harm the probiotic *E. coli*.

EcN's antigenic surface structures are fitness factors that contribute to the well-being of the host. To investigate if thermostable surface structures like the LPS or the capsule are recognized by STEC strains and induce the observed transcriptional repression of the entire *stx*-prophage, a 24 h static SK22D culture was heat killed and incubated along with EDL933 for another 24 h (Start ratio: 100:1) (Vasanthakumari, 2007). The heat killed culture resulted in a far less reduced Stx reduction than the living SK22D control. As the CFUs of the heat killed SK22D resemble the CFUs of the 24 h SK22D in coculture a similar toxin decrease was expected in case of the involvement of a heat stable surface structure of SK22D (figure 31 B).

In accordance to testing surface structures of SK22D for their inhibitory effects on the Stx production also the secretome containing supernatant was investigated. In this regard it could be shown that SK22D interfered with the production of the toxin and the *stx*-phages even when being separated from the STEC strain EDL933 by a Transwell membrane with a pore size of 0.4  $\mu\text{m}$ . The first inhibitory effects on the pathogenic factor production by SK22D were observed as early as 3 h after static incubation and were continuously present at all follow up time points. These results indicate that no direct cell-to-cell contact, rather secreted factor(s) from SK22D are sensed by EDL933 and result in the downregulation of the *stx*-prophage transcription. Further investigations on the EDL933 influencing factor(s) revealed, that the toxin synthesis of EDL933 was still influenced by an initial 3 h presence of SK22D in the Transwell system, even after subsequent 5 h of separation (figure 33 A). Contrary, after an initial 8 h coincubation in the Transwell system, and a follow up separation for 16 h resulted in a regain of the Stx level comparable to an EDL933 monoculture. One possible explanation for rise of the toxin production could be that the pathogenicity interfering factor(s) of SK22D are continuously reduced in the medium by bacterial inclusion. Bacteria produce chemical, hormone-like molecules, the so-called autoinducers, which are recognized by other bacteria and influence their gene expression (Camilli & Bassler, 2006). The mainly produced autoinducers of gram-negative *E. coli* are acyl homoserine lactones (AHLs) which can freely cross bacterial membranes and activate the transcription of quorum-sensing controlled genes (Fuqua, Parsek, & Greenberg, 2001). The presence of AHLs from SK22D might influence the *stx*-prophage

transcription in STEC, as a study could demonstrate that the Stx expression is also controlled by quorum-sensing signals (Sperandio, Torres, Giron, & Kaper, 2001). It might be that AHLs or other factor(s) secreted by SK22D lead to a stabilization of the SOS response repressor LexA, induce the LexA transcription or interfere with the activation of the RecA protease activity by ATP and ssDNA binding due to an occupation of the RecA attachment sites and block thereby the cleavage of the CI repressor of the *stx*-prophage.

Another indication for the involvement of a quorum-sensing regulation of the *stx*-prophage transcription, is that also other commensal *E. coli* tested were able to interfere with the toxin synthesis of STEC strains with varying potency (figure 50). Since the commensal strains tested do belong to different phylogenetic groups, it is presumable that the secreted factor(s) involved in the pathogenic factor reduction are *E. coli* common. If the factor(s) from SK22D and the other commensals are synthesized due to sensing molecule mixtures secreted from EDL933 or if they are EDL933 independent, supernatants of SK22D (and commensal *E. coli*) with or without ED933 should be incubated for a reasonable amount of time with EDL933 before the pathogenic factor concentration is determined.

Overall, SK22D demonstrated a strong interference with the pathogenic factor production of all STEC strains tested, which can be associated to secreted factor(s) of SK22D.

### **5.2. Investigation of the influence of *stx*-phages on EcN**

Studies with *stx*-phages disclosed, that the phages can lysogenize *E. coli* and create thereby new pathogenic strains both *in vitro* and *in vivo* (Acheson et al., 1998; Muniesa et al., 2004; Schmidt et al., 1999). To use EcN as treatment during a STEC infection, it is of major importance to verify that EcN is not infected by *stx*-phages and thereby turned into a *stx*-prophage carrying lysogen.

In an initial approach, it was investigated if the *stx*-phages can adhere to the surface of EcN in the first place. Therefore, *stx*-phages were induced with 1 µg/ml MMC from an EDL933 culture and isolated by sterile filtration. The filtered supernatant was further incubated with EcN and investigated for phage adherence to the bacterial surface by the electron microscope. The electron microscopic figures depicted a broad range of particles bound to the surface of EcN incubated with the phage filtrate in comparison to the EcN control (figure 34 B/D/E). However, an evaluation of these data according to a *stx*-phage adherence was unfeasible as literature research revealed, that the addition of MMC to O157:H7 does not only induce the synthesis of

*stx*-phages but also increases the OMVs production by 470-fold (Bauwens, Kunsmann, Karch, Mellmann, & Bielaszewska, 2017). As OMVs exhibit a size of 20 - 200 nm and the icosahedral head of the short-tailed *stx*-phages has a diameter of ~ 100 nm it was not possible to distinguish the surface bound particles (Mondal et al., 2016; Schwechheimer & Kuehn, 2015).

In a next step of the study, EcN was tested for possible lysis or lysogeny by *stx*-phages as a sequence analysis revealed that EcN encodes the *stx*-phage binding receptor *yaeT* (Smith et al., 2007). Various approaches to force EcN to lyse or to lysogenize failed. In case of the phage lysis, EcN was used as indicator strain in a PPA which works efficiently for the YaeT carrying K-12 strain MG1655 (Islam et al., 2012). A comparison with the MG1655 indicator plate revealed, that even though  $9 \times 10^5$  pfus were dropped in a volume of 10  $\mu$ l on the EcN lawn, no phage induced bacterial lysis plaque was formed. Temperate phages, like *stx*-phages are not only able to lyse bacteria for the phage amplification but can also integrate their DNA into the host and remain there as a prophage (Griffiths et al., 1999). To exclude this possibility, EcN and the MG1655 control were incubated with *stx*-phages (*E. coli*: *stx*-phages = 10:1) for 24 h or 48 h to allow phage genome integration. The search for lysogens from 24 h cultures took place by collecting 100-300 CFUs, which were washed, diluted and plated on LB agar plates. The collected colonies were subsequently screened for the presence of the *stx2a* gene of the *stx*-prophage. For EcN, which was incubated with the *stx*-phages, no *stx2a* amplicon was obtained which indicates that the phages could not integrate into the genome of the probiotic strain. The MG1655 control anyhow, was positively determined for the prophage integration (figure 36). To ensure, that the absence of the *stx2a* amplicon was not based on a detection limit by the *stx2a* PCR, 48 h cultures of EcN and *stx*-phages were washed and forced to lyse by the addition of 1  $\mu$ g/ml MMC. Subsequently, possible *stx*-phages from the supernatant of the induced EcN culture were amplified by MG1655 lysis. Like for the *stx2a* lysogeny PCR control, also this attempt lacked the detection of EcN as a *stx*-prophage lysogen for which reason we are confident to assume that the *stx*-phages are not able to integrate into the genome of the probiotic strain nor to use it as a host for the phage amplification.

Bacteria evolve strategies to circumvent the infection by phages like e. g. the extracellular capsule which can mask phage receptors (Chakrabarty et al., 1967). The K5 capsule of EcN anyhow was determined not to be the reason for the resistance of EcN towards a *stx*-phage infection, as also the capsule mutant EcN $\Delta$ k5 was not turned into a Stx producer after being incubated with isolated *stx*-phages (figure 43 C).

To examine the cause of EcN's *stx*-phage resistance, the transcriptome of EcN incubated with *stx*-phages was analyzed in comparison to EcN cultured without the presence of *stx*-phages. The evaluation of the data revealed that some genes of a lambdoid prophage of totally three complete and three incomplete prophages in the genome of EcN (figure 52) were highly regulated in the presence of *stx*-phages. The early phage repressor gene of the lambdoid prophage was  $\log_2$  4.21-fold upregulated. An impact of the phage repressor towards the immunity of bacterial lysis was identified for *Lactobacillus casei* beforehand and was therefore chosen as a candidate for further phage resistance studies (Alvarez et al., 1999). MG1655 recombinant strains carrying the genetic information of the *pr* gene of EcN's lambdoid prophage were less accessible for phage lysis which was reflected by an around 300-fold reduced lysis efficiency (figure 38). As the phage repressor of phages is involved in the lysogeny maintenance, it is possible that the reduction of bacterial lysis is based on an increase of lysogeny formation (Griffiths et al., 1999). However, the 1.5  $\mu\text{g/ml}$  MMC that are contained in the PPA soft agar should force the lysis of those lysogens. As there was no complete protection of the recombinant MG1655R*pr* from *stx*-phage lysis, EcN must use an additional mechanism for its complete phage resistance. It is possible that only the entire lambdoid prophage of EcN in MG1655 recombinant strains would result in a complete resistance towards phage infection, as the presence of a prophage can result in a prophage mediated protection from phage superinfection (Ranade & Poteete, 1993).

None of the commensal *E. coli* nor the EcN close relative uropathogenic strain CFT073 depicted any sign of a *stx*-phage infection like an increase in the toxin or phage level after an incubation with isolated *stx*-phages in contrast to the K-12 strain MG1655 (figure 49). Sequence analysis revealed that all tested *E. coli* strains share the same aa sequence for the *stx*-phage receptor YaeT (table 16). Therefore, it is of interest to identify the resistance mechanism(s) towards a *stx*-phage infection of the investigated *E. coli* strains in contrast to the phage susceptible strain MG1655. A PFAST prediction revealed, that all strains harbor lambdoid prophages in their genome (figure 53). CFT073 was positively identified to harbor all genes of the lambdoid prophage of EcN (CFT073's prophage 4), whereas the commensal *E. coli* inherit lambdoid prophages with slight discrepancies, like different phage repressor *cI* and *cII* sequences and the lack of certain EcN's prophage genes. It is striking that the *stx*-phage susceptible strain MG1655 is the only strain that lacks the presence of most of the lambdoid prophage genes (table 13) and the PFAST prediction annotates the lambdoid phage with only 17 coding sequences (CDS) in comparison to at least 50 CDS in the lambdoid prophages of the other strains. Moreover, MG1655 was identified to lack a lambdoid phage repressor CDS

(EcN\_1294) which was identified to be present in all commensals and was proven to confer a protection benefit towards the lysis of MG1655 by *stx*-phages. Summarizing the in-silico research, a plausible reason for the *stx*-phage resistance is the presence of an entire lambdoid prophage. To verify this, MG1655 should be infected with a lambdoid phage and subsequently be tested for the possibility of a *stx*-phage infection.

**Table 13: Presence of EcN's lambdoid prophage genes in CFT073, the commensal strains SE11, SE15 and IAI1 and the K-12 strain MG1655.** +: gene present in the genome; -: gene not present; P1, P2, P3, P4: gene present in prophages 1, 2, 3, 4; \*: Sequence not identical to EcN; green marked: genes present in all strains but MG1655; red marked: genes present in all strains

EcN	Description	CFT073	SE11	SE15	IAI1	MG
1289	Mobile element protein	+	+	-	-	+
1290	putative superinfection exclusion protein	P4	-	-	-	-
1291	hypothetical protein	P4	-	-	-	-
1292	hypothetical protein	P4	-	-	-	-
1293	cI repressor protein	P4	P1*	P1*	P1*	-
1294	Phage repressor	P3, P4	P1*, P3*	P1*	P1*	-
1295	Origin specific replication initiation factor	P4	P1	P1	P1	-
1296	Replication protein P	P4	P1	P1	P1	-
1297	Phage NinB DNA recombination	P4	P1	P1	P1	-
1298	Phage DNA N-6-adenine methyltransferase	P4	-	-	-	-
1299	Phage NinX	P4	P1	P1	P1	P1
1300	Crossover junction endodeoxyribonuclease rusA	P4	P1	P1	P1	P1
1301	hypothetical protein	P4	P1	P1	P1	P1
1302	Phage antitermination protein Q	P4, P3	P1	P1	P1	P1
1303	Outer membrane porin protein NmpC	P4	P1	P1	P1	P1
1304	Phage holin	P4	P1	P1	P1	P1
1305	Phage tail fiber protein	P4	P1	P1	P1	P1

<b>1306</b>	<b>Phage outer membrane lytic protein Rz3B Endopeptidase</b>	P4	P1	P1	P1	P1
<b>1307</b>	<b>Lipoprotein Bor</b>	P4	P1	P1	P1	P1
<b>1308</b>	<b>hypothetical protein</b>	P4	-	-	-	-
<b>1309</b>	<b>hypothetical protein</b>	P4	-	P1	-	-
<b>1310</b>	<b>Terminase small subunit</b>	P4	-	P1	-	-
<b>1311</b>	<b>Phage terminase 2C large subunit</b>	P4, P3	P3	P1	-	-
<b>1312</b>	<b>Phage head-to-tail joining protein</b>	P4, P3	P3	P1	-	-
<b>1313</b>	<b>Phage portal protein</b>	P4, P3	P3	P1	-	-
<b>1314</b>	<b>Phage capsid and scaffold</b>	P4, P3	P3	P1	-	-
<b>1315</b>	<b>Head decoration protein</b>	P4, P3	P3	P1	-	-
<b>1316</b>	<b>Phage major capsid protein</b>	P4, P3	P3	P1	-	-
<b>1317</b>	<b>Phage DNA-packaging protein</b>	P4	-	P1	-	-
<b>1318</b>	<b>Phage capsid and scaffold</b>	P4	P1	P1	P1, P2	-
<b>1319</b>	<b>Phage tail completion protein</b>	P4	P1, P3	P1	P1, P2	-
<b>1320</b>	<b>Phage minor tail protein</b>	P4	P1, P3	P1	P1, P2	-
<b>1321</b>	<b>Phage tail assembly</b>	P4	P1, P3	P1	P1, P2	-
<b>1322</b>	<b>Phage minor tail protein</b>	P4	P1, P3	P1	P1, P2	-
<b>1323</b>	<b>Phage minor tail protein</b>	P4	P1, P3	P1	P1, P2	-
<b>1324</b>	<b>Phage tail length tape-measure protein 1</b>	P4	P1, P3	P1	P1, P2	-
<b>1325</b>	<b>Phage minor tail protein</b>	P4	P1, P3	P1	P1, P2	-
<b>1326</b>	<b>Phage minor tail protein</b>	P4	P1, P3	P1	P1, P2	-
<b>1327</b>	<b>Phage tail assembly protein</b>	P4	P1, P3	P1	P1, P2	-
<b>1328</b>	<b>Phage tail assembly protein I</b>	P4	P1, P3	P1	P1, P2	-
<b>1329</b>	<b>Phage tail fiber protein</b>	P4	P1, P3	P1	P1, P2	-
<b>1330</b>	<b>Phage tail fiber protein</b>	P4	P1	P1	P2	-

Based on these results, it is likely that the lambdoid prophage of EcN contributes to its genomic stability by protecting it against lambdoid bacteriophage attacks. Another, additional strategy

of EcN's defense against the *stx*-phages infection could be an active fight against the phages which disables them from bacterial attack.

### **5.3. Evaluation of EcN's phage defense mechanism**

Based on a co-evolution of bacteria and bacteriophages, bacteria have evolved various bacteriophage defense strategies, intracellular as well as extracellular. To study if EcN cannot only interfere with a *stx*-phage infection but even influences the phage activity, the probiotic strain was incubated with isolated *stx*-phages (EcN: *stx*-phages = 10:1) and the phages were afterwards investigated for their infectivity towards MG1655.

In a first attempt the kinetics of the plaque forming efficiency of isolated *stx*-phages were investigated when being incubated with only LB medium or with the addition of EcN. In the presence of EcN a strong decrease of the phage infectivity towards MG1655 on a PPA was firstly observed after 12 h of incubation, which led to a ~100-fold pfus reduction after 24 h incubation with EcN and resulted in no pfus detection after 44 h in comparison to 2.3e5 pfus/ml in the LB control. As the *stx2a* PCR in figure 30 evinced that the DNA concentration in the 24 h EcN + *stx*-phages DNase digested supernatant was equal to the LB control and that the phage DNA containing capsid was in the supernatant rather than bound to the bacterial pellet (figure 40), the reduction of the phage infectivity seems to be not based on a degradation of the phage capsid or an irreversible binding of the phages rather an impact on the receptor recognizing phage tail is imaginable.

As it has been performed in the previous experiment, the factor(s) that influence the phage infectivity were screened for being cell detached in the secretome of EcN or if they are bound to the surface of EcN. To investigate the secretome of the microcin lacking mutant SK22D, the supernatants of 24 h cultures (with or without *stx*-phages) were investigated for their influence on the pfus formation in comparison to a SK22D culture (figure 42). Neither the supernatant of SK22D that was cultured along with *stx*-phages (starting MOI of SK22D: *stx*-phages = 10:1) nor the supernatant of a SK22D culture had a significant influence on the pfus. Contrary, the SK22D bacterial culture reduced the pfus likewise as the EcN *wt* and demonstrated thereby that the microcins are not involved in the pfus decrease. Mutants lacking the genes for the autotransporter serine protease (EcN $\Delta$ *sat*) or the genotoxin colibactin (EcN $\Delta$ *pks*) were less capable in inactivating the *stx*-phages than the *wt* but complementation did not result in a regain of the *wt* capacity for which reason it is impossible to draw any conclusion on their impact.

In a next step, heat stable surface structures of EcN were examined for their involvement in the *stx*-phage inactivation. Even after being incubated for 1 h at 100 °C, EcN<sup>x</sup> could reduce the pfus after a 24 h incubation with the *stx*-phages (MOI: 100:1) to the same extend as the living control. As the heat killed EcN culture was grown for 24 h without the presence of *stx*-phages beforehand, the phage inactivating factor can be assigned to be expressed in a *stx*-phage independent manner. Surface structure mutants like EcN $\Delta$ *k5* (capsule mutant), EcN $\Delta$ *bcs* (cellulose mutant), EcN $\Delta$ *csg* (curli mutant) and EcN $\Delta$ *fliC* (flagella mutant) could also inactivate *stx*-phages both living, and heat killed with varying capacity. Living EcN $\Delta$ *k5* was identified to stronger inactivate the *stx*-phages compared to the EcN *wt*. It is presumable, that *stx*-phages can bind to EcN's YaeT receptor only in the absence of the capsule which might otherwise mask the receptor (Labrie et al., 2010). Therefore, the capsule mutant could bind the phages, which anyhow showed to be unable to infect the strain, and reduced thereby the infective phages in the supernatant stronger than the *wt*. This assumption is further supported by the fact that heat killing of the mutant resulted in a decreased potency in the phage inactivation due to a probable receptor denaturation. The remaining ability of the capsule mutant to inactivate the phages excludes the capsule as the major phage inactivation factor. Closer investigations on the phage inactivating factor(s) depicted it to be still bound to the surface of the heat killed SK22D and not being released to the supernatant during the heat incubation (figure 42). As it was depicted for the living EcN, also the heat killed pellet resulted in a pfus reduction in the filtered supernatant although the phage DNA concentration was found to be higher in the supernatant than in the pellet. Based on this, we assume the same phage inactivation mechanism for both the living and the heat killed EcN.

In another approach to investigate the characteristics of the pfus reducing factor(s), the digestion of the heat killed pellet with proteinase K resulted in a loss of the phage inactivation function. Proteinase K is a serine protease from the saprophytic fungus *Tritirachium album* which cleaves peptide bonds preferably after hydrophobic aa whereby protein polypeptide chains are cleaved into smaller polypeptide fragments (Kraus & Femfert, 1976). The heat stable LPS can be isolated by Proteinase K treatment and can therefore be excluded from being the phage inactivation factor (Rezania et al., 2011). Incidence, that the factor(s) needs to be expressed by EcN during stationary growth are given by multiple results. Firstly, EcN was identified to exhibit the phage inactivation characteristics only after a 12 h incubation period, when it was in the stationary growth phase (figure 48 C). Secondly, the BG's of EcN lacked the phage inactivating capacity. The BG's of EcN are bacterial envelopes which harbor all EcN's surface structures produced until the logarithmic growth phase, at which time point the lysis gene *e* was



induced and resulted in a release of the cytoplasmic content (Langemann et al., 2010; Paton et al., 2015). The bacterial number of the BGs equaled the bacterial number of the heat killed EcN (~1e9 bacteria/ml) and were therefore expected to result in a similar phage inactivation in case of the involvement of surface structures present on BGs in the phage inactivation. Neither before nor after heat treatment the BG's exhibited any phage inactivation capacity.

The group of Vidakovic demonstrated that T7-phages bind to the curli fibers of the biofilm and are therefore blocked from bacterial infection (Vidakovic et al., 2017). The biofilm formation of *E. coli* is dependent on the expression of stationary phase genes and is therefore a possible candidate for being involved in the *stx*-phage inactivation (Beloin et al., 2008). Both biofilm component mutants EcN $\Delta$ *bcs* and EcN $\Delta$ *csg* did form a biofilm comparable to the one of the EcN *wt* and illustrated a similar efficiency in the phage inactivation. Therefore, these elements of the biofilm are unlikely to be involved in the phage inactivation. During the biofilm experiments, an immense increase in the biofilm mass was observed after the addition of cellulase from *Trichoderma reesei*. The cellulase has an exonuclease activity and degrades cellulose oligosaccharides into glucose monosaccharides. The increase in the glucose nutrient supply could be a possible explanation for the increase of the biofilm formation. Determinations of the pfus revealed that the pfus were by over 90 % reduced by the EcN strains compared to the controls without the addition of cellulase. As LB plus cellulase controls confirmed that the cellulase itself had no influence on the isolated *stx*-phages, the biofilm was getting increased attention in being involved in the *stx*-phage inactivation.

CFT073, the commensal controls and MG1655 were all unable to inactivate the *stx*-phages alive and after being heat killed. Anyhow, both CFT073 and MG1655 formed a strong biofilm upon cellulase addition which resulted in the gain of a *stx*-phage pfus reduction function. The phase-variable surface-located adhesin antigen 43 (Ag43) protein is associated with early steps of the biofilm formation, has been identified to facilitate bacteria to bacteria adhesions and supports the development of the three dimensional formation of the biofilm (Danese, Pratt, Dove, & Kolter, 2000; Ulett et al., 2007). Studies revealed, that Ag43 is not necessary for the biofilm formation in LB medium but in glucose supplemented minimal medium (Danese et al., 2000). It is assumable that the expression of Ag43 is depending on the presence of glucose and therefore, the addition of cellulase and the connected glucose enrichment in the medium could have resulted in an increased expression of the biofilm agent Ag43. Genome analysis unraveled that EcN harbors three copies of the *flu* gene which encodes Ag43 (EcN1917\_1112, EcN1917\_3240/3241, EcN1917\_4739/4740) in contrast to CFT073 (c1273, c3655) and SE15

(ECSF\_4202, ECSF\_4205/4206) which harbor 2 copies. MG1655 (EO53\_07915) encodes only one copy and SE11 as well as IAI1 were determined to encode no *flu* sequence. As EcN harbors an additional copy of the *flu* gene, and the cellulose and curli mutants could still express a biofilm it is assumable that EcN can express Ag43 even in LB medium which is not supplemented with glucose. The presence of glucose in the medium anyhow, might lead to an increased Ag43 expression. Other components of EcN's biofilm that differ from the biofilm genes of CFT073 are the capsule, which was excluded to be responsible for the pfus reduction and the Type 1 fimbriae which has an 86 % query cover to the sequence of EcN. It remains to be investigated if Ag43 or eventually the sequence difference in the type 1 fimbriae are possible factors that contribute to the phage inactivation (table 14).

Summarizing the results, the phage inactivation factor(s) was depicted to be expressed in a *stx*-phage independent manner during the stationary growth phase of EcN. The factor(s) is a heat stable protein or peptide which is bound to the surface structure of EcN, attacks the *stx*-phage tail and seems to be part of the *E. coli* biofilm.

**Table 14: Biofilm components of the *E. coli* strains EcN, CFT073, SE11, SE15, IAI1 and MG1655.** +: genes equal in all strains; -: genes not present; \*: Sequence not identical to EcN; x: number of flu genes; yellow marked: differences between EcN and CFT073;  $\beta$ -1,6-N-acetyl-D-glucosamine polymer (PGA), OR: rough LPS, ND: not determined

	EcN	CFT073	SE11	SE15	IAI1	MG1655
<b>PGA</b>	+	+	+	+	+	+
<b>Colanic Acid</b>	+	+	+	+	+	+
<b>Cellulose</b>	+	+	+	+	+	+
<b>Curli fimbriae</b>	+	+	+	+	+	+
<b>Antigen 43</b>	3 x	2 x	-	2 x	2 x	1 x
<b>LPS (O)</b>	O6	O6	O152	O150	O8	OR
<b>Capsule (K)</b>	K5	K2	-	K1	-	-
<b>Flagella (H)</b>	H1	H1	H28	H5	H <sup>ND</sup>	H48
<b>Conjugative Pili Type IV</b>	+	+	+*	+*	+*	+*
<b>Type 1 Fimbriae (F1)</b>	F1C	+*	+*	+*	+*	+*

#### **5.4. EcN protects K-12 strains from *stx*-phage infection**

*E. coli* K-12 strains have been proven to be susceptible for the *stx*-phage integration into their *wrbA* locus, which is followed by the Stx production of those lysogens (Asadulghani et al., 2009; Beutin & Martin, 2012). Our research could reconfirm these results and illustrated a MG1655 mediated Stx increase in the cocultures with all tested *stx2* STEC strains but the low *stx*-phage producer O145:H25. In coculture with *stx1* STEC strains on the other hand the presence of MG1655 resulted in a Stx decrease. This experimental outcome can be explained by a low *stx1*-phage transfer efficiency which was postulated by the group of Asadulghani et al., who demonstrated that *stx1*-phages isolated from a O157 strain had a transfer efficiency of as low as 8 colonies in comparison to a transfer efficiency of 746 infected MG1655 colonies after the incubation with isolated *stx2*-phages (Asadulghani et al., 2009). As the K-12 infection by *stx1*-phages is very low, the MG1655 strain was not turned into a toxin and phage producer itself and merely the pathogenic factors produced by the *stx1* STEC strains were determined. It is possible, that MG1655 can produce similar quorum-sensing signals like EcN or the commensals *E. coli* tested, which might be involved in a stabilization of the lysogenic state of the STEC *stx*-prophages.

For the investigation of the Stx and *stx*-phage production by infected K-12 strains, the K-12 strains MG1655, HB101 and DH5 $\alpha$  were incubated with isolated phages from a non MMC induced EDL933 culture (*stx*-phages: K-12 = 1:100), as the results in figure 29 depicted, that MMC induced phages cannot turn MG1655 into a Stx producer. This is probable due to the presence of remaining MMC in the phage filtrate, which induces the lysis of MG1655 and counteracts the lysogenization (Islam et al., 2012). All K-12 strains tested depicted a *stx*-phage increase of around 1,000-fold and a drastic Stx rise from OD<sub>450</sub> 1.19 to OD<sub>450</sub> ~ 20.

During our experiments we examined the impact of SK22D on the MG1655 induced pathogenic factor increase in triculture with *stx2* STEC strains. The determination of both the toxin and the pfus illustrated that the presence of SK22D resulted in a decrease of the toxin level comparable to the toxin level in the *stx2* STEC and SK22D cocultures and a reduction of infective phages below the *stx2* STEC monocultures. Possible explanations for this outcome are an interference with the MG1655 infection or that due to the reduction of the phage expression MG1655 is less likely to be infected.

To address this issue and to exclude the influence of the STEC strains, isolated *stx*-phages (without MMC) were incubated in triculture with the K-12 strains and SK22D (1:100:100). The experiment revealed, that SK22D strongly interfered with the infection of the K-12 strains by

*stx*-phages which had a starting phage density of around  $1e6$  pfus/ml. The presence of SK22D resulted in a decrease of the Stx level from the phage + K-12 coculture of  $OD_{450} \sim 20$  to  $OD_{450} 2.99$ . Moreover, the pfus were 10-fold reduced in the triculture with MG1655 in comparison to the phage + LB control and even no pfus could be detected in the tricultures with the K-12 strains HB101 and DH5 $\alpha$ .

As it has been demonstrated in the previous experiments, EcN did not only interfere with the production of the *stx*-phages in coculture with STEC strains but also inactivated *stx*-phages which was determined by a reduced efficiency of MG1655 lysis in PPAs. Therefore, another possible explanation for the strong interference with the pathogenic factor increase by K-12 strains could be that the phages are inactivated by SK22D before they can infect the K-12 strains. However, triculture experiments with heat killed SK22D, which can inactivate the *stx*-phages, lacked the protective ability of living SK22D (figure 31). Moreover, Transwell experiments with various position combinations of the *stx*-phage producer EDL933, MG1655 and SK22D showed that SK22D was only able to interfere with the MG1655 mediated pathogenic factor increase when being cultured in the same Transwell compartment. Even when SK22D was incubated along with EDL933 in the same compartment and induced thereby an intense phage reduction, MG1655 was turned into a strong Stx and *stx*-phage producer in the other Transwell compartment. Hence, the K-12 protection from *stx*-phage infection by SK22D demonstrated contact dependent characteristics.

The kinetics of the *stx*-phage infection of MG1655 as well as the interference of this by SK22D were additionally investigated. After an 8 h incubation period with isolated phages and MG1655, the Stx level was firstly increased which can be traced back to a Stx production by lysogenic MG1655. It can therefore be assumed that the *stx*-phages integrated into the genome of MG1655 before this time point. The toxin as well as the phage level reached a maximum after 12 h of incubation from which time point on the Stx level stayed constant and the *stx*-phage titer decreased after 20 h of incubation. The Stx in the LB control demonstrated a stability towards the detection by the Stx-ELISA at all time points. The *stx*-phages on the other hand, were decreased in their infection stability by 10-fold after 24 h of incubation. This corresponds to research results that demonstrated a weak stability of isolated *stx*-phage which is anyhow contrasted by a long time stability of *stx*-phages in foods (Plunkett et al., 1999; Rode et al., 2011). It is therefore assumable, that the lytic cycle of lysogenic MG1655 was depressed after the onset of the stationary growth phase at 12 h which resulted in the absence of newly produced Stx and *stx*-phages. In the presence of SK22D the toxin produced by MG1655 lysogens was by

80 % reduced at the 24 h time point compared to the coculture. Also, the phage titer illustrated only a weak rise at the 8 h time point before it was reduced by SK22D. Based on the fact that the pathogenic factors slightly increased after 8 h of incubation in the triculture, the interference with the toxin and phage increase can be either due to an interference with the lysogeny formation of MG1655 or due to a suppression of the lytic cycle of lysogenic MG1655. In case of the latter, the mechanism of the lysis suppression by SK22D would differ from the one in STEC as SK22D could interfere with the pathogenic factor production of EDL933 but not MG1655 when being separated in the Transwell system. Additionally, the commensal *E. coli* SE15 and IA11 were able to interfere with the pathogenic factor production by STEC strains but could barely interfere with the phage and toxin production by MG1655 lysogens. Since however the *stx2*-phage integrates into the same genomic *wrbA* locus in K-12 strains as they are localized in STEC strains a similar mechanism would be expected (Asadulghani et al., 2009). The close EcN relative strain CFT073 was the only *E. coli* identified to exhibited similar effects on the interference with the MG1655 mediated toxin and phage increase, both in triculture with isolated phages as in triculture with STEC strains (figure 49, 50). As CFT073 was incapable of inactivating isolated *stx*-phages, a protection mechanism via a phage inactivation seems to be rather unlikely. The MG1655 CFUs determination depicted a 10-fold CFUs decrease compared to the MG1655 monoculture in the presence of all tested *E. coli*. As all investigated *E. coli* strains but MG1655 were positively determined for the presence of the T3SS and the T6SS (table 23), these protein structures themselves seem to be not involved in the K-12 protection from *stx*-phage infection. However, a possible protection mechanism might be that EcN and CFT073, which depict sequence homology for many biofilm related genes like e. g. the flagella, the LPS and the type IV pili, grow around MG1655, shield it from the *stx*-phages and counteract thereby the MG1655 lysogenization (table 10). Light microscopy studies however did not enable a specific allocation of MG1655 in the cocultures, therefore a bacterial staining would be necessary to make a more precise statement on the way of action.

The *in vitro* experiments with the phage susceptible K-12 strains confirmed that harmless *E. coli* can be turned into strong pathogen producers. The presence of SK22D anyhow, resulted in a strong reduction of the K-12 mediated pathogenic factor increase, which was identified to be contact dependent, common for both EcN and CFT073 and probably due to an interference with the infection of *stx*-phages by shielding the K-12 strains.

## **6. Outlook and conclusion**

STEC strains are human pathogens of the gastrointestinal tract. So far there is no ideal treatment strategy available, as the administration of antibiotics can result in a disease worsening (Pacheco & Sperandio, 2012). The disease progression for individuals being infected with the same STEC strain can strongly vary. The observed variability in the disease outcome might be attributed to the microbiota composition. Humans can harbor bacteria in their microbiota that interfere with the colonization of STEC strains and are not susceptible to *stx*-phages or can be host to *stx*-phage susceptible *E. coli* strains that are turned into pathogenic lysogens and strong toxin producers themselves (Gamage, Strasser, Chalk, & Weiss, 2003; Schmidt et al., 1999).

This study aimed to identify if the probiotic *E. coli* strain EcN, which is used to treat gastrointestinal disorders for more than 100 years, could be an alternative or supplementary treatment strategy for patients being infected with STEC strains to support their individual microbiota in the STEC defense.

In the first part of the study, it could be demonstrated that the microcin negative EcN mutant SK22D did not only interfere with the production of the eukaryotic cells harming Stx but could also interfere with the production of the *stx*-phages. It was found that the factor(s) of SK22D which is responsible for the interference of the pathogenic factor production was secreted and had an impact on the STEC mediated pathogenic factor production even when being separated from SK22D by a Transwell membrane. For a more accurate determination of the factor(s) characteristics, the supernatant of SK22D cultures should be investigated closer for possible STEC influencing abilities in the future.

Besides the impact of EcN on STEC strains, we further investigated if there is a possibility of a *stx*-phage infection of EcN. This analysis was of major importance as patient treatment with EcN could result in a disease worsening if EcN would turn out to be *stx*-phage susceptible. The experiments could elucidate that EcN was not infected by *stx*-phages in any experimental set-up. Additionally, none of the commensal control strain nor the uropathogenic *E. coli* strain CFT073 were infected by the phages in contrast to the K-12 strain MG1655. A PFAST prediction could uncover, that all investigated strains but MG1655 harbor complete lambdoid prophages in their genome which are consistent in most of their CDS. Therefore, an involvement of the lambdoid prophages in the resistance towards the *stx*-phage infection is

imaginable and further studies should concentrate on creating a *stx*-phage resistant MG1655 strain by e. g. a complete lambdoid prophage integration.

EcN additionally illustrated capacities in inactivating released *stx*-phages against the MG1655 lysis on a PPA. Experiments that aimed to elucidate the mechanism behind, could uncover that the phage inactivation protein(s) was phage independently produced in the stationary growth phase of EcN, is heat stable and attached to EcN's cell surface. Future experiments should yield a closer investigation of EcN's biofilm components for phage inactivation capabilities.

Next to the mentioned supportive characteristics of EcN, we could furthermore demonstrate that EcN is capable of interfering with the immense toxin increase by lysogenized K-12 strains. Presumably, EcN protects the K-12 strains from getting infected in the first place by enclosing it in its biofilm structure.

All our *in vitro* results indicate that the administration of EcN would be an ideal alternative or supportive treatment strategy for STEC infected patients, as it does not only interfere with the toxin production but also inactivates *stx*-phages and interferes with the infection of *stx*-phage susceptible *E. coli*. These results should be pursued further in *in vivo* studies to investigate the capacity of EcN's protective effects against STEC strains in the complex community of the gastrointestinal microbiota.

## **7. Bibliography**

- Acheson, D. W., Reidl, J., Zhang, X., Keusch, G. T., Mekalanos, J. J., & Waldor, M. K. (1998). In vivo transduction with *shiga toxin 1*-encoding phage. *Infect Immun*, 66(9), 4496-4498.
- Aksyuk, A. A., & Rossmann, M. G. (2011). Bacteriophage assembly. *Viruses*, 3(3), 172-203. doi:10.3390/v3030172
- Allison, H. E., Sergeant, M. J., James, C. E., Saunders, J. R., Smith, D. L., Sharp, R. J., . . . McCarthy, A. J. (2003). Immunity profiles of wild-type and recombinant shiga-like toxin-encoding bacteriophages and characterization of novel double lysogens. *Infect Immun*, 71(6), 3409-3418.
- Allue-Guardia, A., Martinez-Castillo, A., & Muniesa, M. (2014). Persistence of infectious Shiga toxin-encoding bacteriophages after disinfection treatments. *Appl Environ Microbiol*, 80(7), 2142-2149. doi:10.1128/AEM.04006-13
- Altschul, S. F., Gish, W., Miller, W., Myers, E. W., & Lipman, D. J. (1990). Basic local alignment search tool. *J Mol Biol*, 215(3), 403-410. doi:10.1016/S0022-2836(05)80360-2
- Alvarez, M. A., Rodriguez, A., & Suarez, J. E. (1999). Stable expression of the *Lactobacillus casei* bacteriophage A2 repressor blocks phage propagation during milk fermentation. *J Appl Microbiol*, 86(5), 812-816.
- Andrews, S. (2010). FastQC: a quality control tool for high throughput sequence data. . Retrieved from <http://www.bioinformatics.babraham.ac.uk/projects/fastqc/>
- Anukam, K. C., & Reid, G. (2007). Probiotics: 100 years (1907-2007) after Elie Metchnikoff's Observation *FORMATEX*.
- Armstrong, G. L., Hollingsworth, J., & Morris, J. G., Jr. (1996). Emerging foodborne pathogens: *Escherichia coli* O157:H7 as a model of entry of a new pathogen into the food supply of the developed world. *Epidemiol Rev*, 18(1), 29-51.
- Asadulghani, M., Ogura, Y., Ooka, T., Itoh, T., Sawaguchi, A., Iguchi, A., . . . Hayashi, T. (2009). The defective prophage pool of *Escherichia coli* O157: prophage-prophage interactions potentiate horizontal transfer of virulence determinants. *PLoS Pathog*, 5(5), e1000408. doi:10.1371/journal.ppat.1000408



- Barrangou, R., Fremaux, C., Deveau, H., Richards, M., Boyaval, P., Moineau, S., . . . Horvath, P. (2007). CRISPR provides acquired resistance against viruses in prokaryotes. *Science*, *315*(5819), 1709-1712. doi:10.1126/science.1138140
- Bauwens, A., Kunsmann, L., Karch, H., Mellmann, A., & Bielaszewska, M. (2017). Antibiotic-Mediated Modulations of Outer Membrane Vesicles in Enterohemorrhagic *Escherichia coli* O104:H4 and O157:H7. *Antimicrob Agents Chemother*, *61*(9). doi:10.1128/AAC.00937-17
- Bell, B. P., Goldoft, M., Griffin, P. M., Davis, M. A., Gordon, D. C., Tarr, P. I., . . . et al. (1994). A multistate outbreak of *Escherichia coli* O157:H7-associated bloody diarrhea and hemolytic uremic syndrome from hamburgers. The Washington experience. *JAMA*, *272*(17), 1349-1353.
- Bell, B. P., Griffin, P. M., Lozano, P., Christie, D. L., Kobayashi, J. M., & Tarr, P. I. (1997). Predictors of hemolytic uremic syndrome in children during a large outbreak of *Escherichia coli* O157:H7 infections. *Pediatrics*, *100*(1), E12.
- Beloin, C., Roux, A., & Ghigo, J. M. (2008). *Escherichia coli* biofilms. *Curr Top Microbiol Immunol*, *322*, 249-289.
- Bettelheim, K. A. (2007). The non-O157 shiga-toxigenic (verocytotoxigenic) *Escherichia coli*; under-rated pathogens. *Crit Rev Microbiol*, *33*(1), 67-87. doi:10.1080/10408410601172172
- Beutin, L., & Martin, A. (2012). Outbreak of Shiga toxin-producing *Escherichia coli* (STEC) O104:H4 infection in Germany causes a paradigm shift with regard to human pathogenicity of STEC strains. *J Food Prot*, *75*(2), 408-418. doi:10.4315/0362-028X.JFP-11-452
- Bielaszewska, M., Mellmann, A., Zhang, W., Kock, R., Fruth, A., Bauwens, A., . . . Karch, H. (2011). Characterisation of the *Escherichia coli* strain associated with an outbreak of haemolytic uraemic syndrome in Germany, 2011: a microbiological study. *Lancet Infect Dis*, *11*(9), 671-676. doi:10.1016/S1473-3099(11)70165-7
- Bielaszewska, M., Zhang, W., Tarr, P. I., Sonntag, A. K., & Karch, H. (2005). Molecular profiling and phenotype analysis of *Escherichia coli* O26:H11 and O26:NM: secular and geographic consistency of enterohemorrhagic and enteropathogenic isolates. *J Clin Microbiol*, *43*(8), 4225-4228. doi:10.1128/JCM.43.8.4225-4228.2005
- Blasi, U., & Young, R. (1996). Two beginnings for a single purpose: the dual-start holins in the regulation of phage lysis. *Mol Microbiol*, *21*(4), 675-682.

- Blum-Oehler, G., Oswald, S., Eiteljorge, K., Sonnenborn, U., Schulze, J., Kruis, W., & Hacker, J. (2003). Development of strain-specific PCR reactions for the detection of the probiotic *Escherichia coli* strain Nissle 1917 in fecal samples. *Res Microbiol*, *154*(1), 59-66.
- Blum, G., Marre, R., & Hacker, J. (1995). Properties of *Escherichia coli* strains of serotype O6. *Infection*, *23*(4), 234-236.
- Boyd, E. F. (2012). Bacteriophage-encoded bacterial virulence factors and phage-pathogenicity island interactions. *Adv Virus Res*, *82*, 91-118. doi:10.1016/B978-0-12-394621-8.00014-5
- Brussow, H., & Hendrix, R. W. (2002). Phage genomics: small is beautiful. *Cell*, *108*(1), 13-16.
- Buchholz, U., Bernard, H., Werber, D., Bohmer, M. M., Renschmidt, C., Wilking, H., . . . Kuhne, M. (2011). German outbreak of *Escherichia coli* O104:H4 associated with sprouts. *N Engl J Med*, *365*(19), 1763-1770. doi:10.1056/NEJMoal106482
- Burns, S. M., & Hull, S. I. (1998). Comparison of loss of serum resistance by defined lipopolysaccharide mutants and an acapsular mutant of uropathogenic *Escherichia coli* O75:K5. *Infect Immun*, *66*(9), 4244-4253.
- Bury, S., Soundararajan, M., Bharti, R., von Buenau, R., Foerrstner, K., Oelschlaeger, T. (submitted 15.03.2018, under review). The probiotic *Escherichia coli* strain Nissle 1917 combats lambdoid bacteriophages *stx* and  $\lambda$ . *Frontiers in Microbiology*
- Byrne, L., Jenkins, C., Launders, N., Elson, R., & Adak, G. K. (2015). The epidemiology, microbiology and clinical impact of Shiga toxin-producing *Escherichia coli* in England, 2009-2012. *Epidemiol Infect*, *143*(16), 3475-3487. doi:10.1017/S0950268815000746
- Calderwood, S. B., Auclair, F., Donohue-Rolfe, A., Keusch, G. T., & Mekalanos, J. J. (1987). Nucleotide sequence of the Shiga-like toxin genes of *Escherichia coli*. *Proc Natl Acad Sci U S A*, *84*(13), 4364-4368.
- Camilli, A., & Bassler, B. L. (2006). Bacterial small-molecule signaling pathways. *Science*, *311*(5764), 1113-1116. doi:10.1126/science.1121357
- Chakrabarty, A. M., Niblack, J. F., & Gunsalus, I. C. (1967). A phage-initiated polysaccharide depolymerase in *Pseudomonas putida*. *Virology*, *32*(3), 532-534.
- Chatterjee, S., & Rothenberg, E. (2012). Interaction of bacteriophage  $\lambda$  with its *E. coli* receptor, LamB. *Viruses*, *4*(11), 3162-3178. doi:10.3390/v4113162
- Clermont, O., Bonacorsi, S., & Bingen, E. (2000). Rapid and simple determination of the *Escherichia coli* phylogenetic group. *Appl Environ Microbiol*, *66*(10), 4555-4558.

- Conway, E. M. (2015). HUS and the case for complement. *Blood*, *126*(18), 2085-2090. doi:10.1182/blood-2015-03-569277
- Danese, P. N., Pratt, L. A., Dove, S. L., & Kolter, R. (2000). The outer membrane protein, antigen 43, mediates cell-to-cell interactions within *Escherichia coli* biofilms. *Mol Microbiol*, *37*(2), 424-432.
- De Paepe, M., Leclerc, M., Tinsley, C. R., & Petit, M. A. (2014). Bacteriophages: an underestimated role in human and animal health? *Front Cell Infect Microbiol*, *4*, 39. doi:10.3389/fcimb.2014.00039
- de Sioniz, M. I., Valderrama, M. J., & Peinado, J. M. (2000). A chromogenic medium for the detection of yeasts with beta-galactosidase and beta-glucosidase activities from intermediate moisture foods. *J Food Prot*, *63*(5), 651-654.
- Dixit, P. D., Pang, T. Y., Studier, F. W., & Maslov, S. (2015). Recombinant transfer in the basic genome of *Escherichia coli*. *Proc Natl Acad Sci U S A*, *112*(29), 9070-9075. doi:10.1073/pnas.1510839112
- Dundas, S., Todd, W. T., Stewart, A. I., Murdoch, P. S., Chaudhuri, A. K., & Hutchinson, S. J. (2001). The central Scotland *Escherichia coli* O157:H7 outbreak: risk factors for the hemolytic uremic syndrome and death among hospitalized patients. *Clin Infect Dis*, *33*(7), 923-931. doi:10.1086/322598
- Edgar, R., Domrachev, M., & Lash, A. E. (2002). Gene Expression Omnibus: NCBI gene expression and hybridization array data repository. *Nucleic Acids Res*, *30*(1), 207-210.
- Eichhorn, I., Heidemanns, K., Semmler, T., Kinnemann, B., Mellmann, A., Harmsen, D., . . . Wieler, L. H. (2015). Highly Virulent Non-O157 Enterohemorrhagic *Escherichia coli* (EHEC) Serotypes Reflect Similar Phylogenetic Lineages, Providing New Insights into the Evolution of EHEC. *Appl Environ Microbiol*, *81*(20), 7041-7047. doi:10.1128/AEM.01921-15
- Eklund, M., Leino, K., & Siitonen, A. (2002). Clinical *Escherichia coli* strains carrying stx genes: stx variants and stx-positive virulence profiles. *J Clin Microbiol*, *40*(12), 4585-4593.
- Eloe-Fadrosh, E. A., & Rasko, D. A. (2013). The human microbiome: from symbiosis to pathogenesis. *Annu Rev Med*, *64*, 145-163. doi:10.1146/annurev-med-010312-133513
- Endo, Y., Tsurugi, K., Yutsudo, T., Takeda, Y., Ogasawara, T., & Igarashi, K. (1988). Site of action of a Vero toxin (VT2) from *Escherichia coli* O157:H7 and of Shiga toxin on eukaryotic ribosomes. RNA N-glycosidase activity of the toxins. *Eur J Biochem*, *171*(1-2), 45-50.

- Escherich, T. (1886). Die Darmbakterien des Säuglings und ihre Beziehungen zur Physiologie der Verdauung. Stuttgart: Ferdinand Enke.
- Feldgarden, M., Golden, S., Wilson, H., & Riley, M. A. (1995). Can phage defence maintain colicin plasmids in *Escherichia coli*? *Microbiology*, *141* ( Pt 11), 2977-2984. doi:10.1099/13500872-141-11-2977
- Fijan, S. (2014). Microorganisms with claimed probiotic properties: an overview of recent literature. *Int J Environ Res Public Health*, *11*(5), 4745-4767. doi:10.3390/ijerph110504745
- Fokine, A., & Rossmann, M. G. (2014). Molecular architecture of tailed double-stranded DNA phages. *Bacteriophage*, *4*(1), e28281. doi:10.4161/bact.28281
- Forstner, K. U., Vogel, J., & Sharma, C. M. (2014). READemption-a tool for the computational analysis of deep-sequencing-based transcriptome data. *Bioinformatics*, *30*(23), 3421-3423. doi:10.1093/bioinformatics/btu533
- Frank, C., Faber, M. S., Askar, M., Bernard, H., Fruth, A., Gilsdorf, A., . . . team, H. U. S. i. (2011). Large and ongoing outbreak of haemolytic uraemic syndrome, Germany, May 2011. *Euro Surveill*, *16*(21).
- Frank, C., Werber, D., Cramer, J. P., Askar, M., Faber, M., an der Heiden, M., . . . Team, H. U. S. I. (2011). Epidemic profile of Shiga-toxin-producing *Escherichia coli* O104:H4 outbreak in Germany. *N Engl J Med*, *365*(19), 1771-1780. doi:10.1056/NEJMoa1106483
- Fratamico, P. M., DebRoy, C., Liu, Y., Needleman, D. S., Baranzoni, G. M., & Feng, P. (2016). Advances in Molecular Serotyping and Subtyping of *Escherichia coli*. *Front Microbiol*, *7*, 644. doi:10.3389/fmicb.2016.00644
- Freese, N. H., Norris, D. C., & Loraine, A. E. (2016). Integrated genome browser: visual analytics platform for genomics. *Bioinformatics*, *32*(14), 2089-2095. doi:10.1093/bioinformatics/btw069
- Fuqua, C., Parsek, M. R., & Greenberg, E. P. (2001). Regulation of gene expression by cell-to-cell communication: acyl-homoserine lactone quorum sensing. *Annu Rev Genet*, *35*, 439-468. doi:10.1146/annurev.genet.35.102401.090913
- Gamage, S. D., Strasser, J. E., Chalk, C. L., & Weiss, A. A. (2003). Nonpathogenic *Escherichia coli* can contribute to the production of Shiga toxin. *Infect Immun*, *71*(6), 3107-3115.
- Garg, A. X., Suri, R. S., Barrowman, N., Rehman, F., Matsell, D., Rosas-Arellano, M. P., . . . Clark, W. F. (2003). Long-term renal prognosis of diarrhea-associated hemolytic uremic

- syndrome: a systematic review, meta-analysis, and meta-regression. *JAMA*, 290(10), 1360-1370. doi:10.1001/jama.290.10.1360
- Garred, O., van Deurs, B., & Sandvig, K. (1995). Furin-induced cleavage and activation of Shiga toxin. *Journal of Biological Chemistry*, 270(18), 10817-10821.
- Gerber, A., Karch, H., Allerberger, F., Verweyen, H. M., & Zimmerhackl, L. B. (2002). Clinical course and the role of shiga toxin-producing *Escherichia coli* infection in the hemolytic-uremic syndrome in pediatric patients, 1997-2000, in Germany and Austria: a prospective study. *J Infect Dis*, 186(4), 493-500. doi:10.1086/341940
- Gill, S. R., Pop, M., Deboy, R. T., Eckburg, P. B., Turnbaugh, P. J., Samuel, B. S., . . . Nelson, K. E. (2006). Metagenomic analysis of the human distal gut microbiome. *Science*, 312(5778), 1355-1359. doi:10.1126/science.1124234
- Griffiths, A. J., Gelbart, W. M., Miller, J. H., & Lewontin, R. C. (1999). *Modern Genetic Analysis*. In *Lambda phage: a complex of operons*.
- Gronlund, M. M., Lehtonen, O. P., Eerola, E., & Kero, P. (1999). Fecal microflora in healthy infants born by different methods of delivery: permanent changes in intestinal flora after cesarean delivery. *J Pediatr Gastroenterol Nutr*, 28(1), 19-25.
- Grozdanov, L., Raasch, C., Schulze, J., Sonnenborn, U., Gottschalk, G., Hacker, J., & Dobrindt, U. (2004). Analysis of the genome structure of the nonpathogenic probiotic *Escherichia coli* strain Nissle 1917. *J Bacteriol*, 186(16), 5432-5441. doi:10.1128/JB.186.16.5432-5441.2004
- Grozdanov, L., Zahringer, U., Blum-Oehler, G., Brade, L., Henne, A., Knirel, Y. A., . . . Dobrindt, U. (2002). A single nucleotide exchange in the *wzy* gene is responsible for the semirough O6 lipopolysaccharide phenotype and serum sensitivity of *Escherichia coli* strain Nissle 1917. *J Bacteriol*, 184(21), 5912-5925.
- Hafez, M., Hayes, K., Goldrick, M., Warhurst, G., Grecis, R., & Roberts, I. S. (2009). The K5 capsule of *Escherichia coli* strain Nissle 1917 is important in mediating interactions with intestinal epithelial cells and chemokine induction. *Infect Immun*, 77(7), 2995-3003. doi:10.1128/IAI.00040-09
- Haiko, J., & Westerlund-Wikstrom, B. (2013). The role of the bacterial flagellum in adhesion and virulence. *Biology (Basel)*, 2(4), 1242-1267. doi:10.3390/biology2041242
- Hale, T. L., & Formal, S. B. (1980). Cytotoxicity of *Shigella dysenteriae* 1 for cultured mammalian cells. *Am J Clin Nutr*, 33(11 Suppl), 2485-2490.

- Hilborn, E. D., Mermin, J. H., Mshar, P. A., Hadler, J. L., Voetsch, A., Wojtkunski, C., . . . Slutsker, L. (1999). A multistate outbreak of *Escherichia coli* O157:H7 infections associated with consumption of mesclun lettuce. *Arch Intern Med*, *159*(15), 1758-1764.
- Hill, M. J., & Drasar, B. S. (1975). The normal colonic bacterial flora. *Gut*, *16*(4), 318-323.
- Hoffmann, S., Otto, C., Kurtz, S., Sharma, C. M., Khaitovich, P., Vogel, J., . . . Hackermuller, J. (2009). Fast mapping of short sequences with mismatches, insertions and deletions using index structures. *PLoS Comput Biol*, *5*(9), e1000502. doi:10.1371/journal.pcbi.1000502
- Hugon, P., Dufour, J. C., Colson, P., Fournier, P. E., Sallah, K., & Raoult, D. (2015). A comprehensive repertoire of prokaryotic species identified in human beings. *Lancet Infect Dis*, *15*(10), 1211-1219. doi:10.1016/S1473-3099(15)00293-5
- Iijima, K., Kamioka, I., & Nozu, K. (2008). Management of diarrhea-associated hemolytic uremic syndrome in children. *Clin Exp Nephrol*, *12*(1), 16-19. doi:10.1007/s10157-007-0007-4
- Islam, M. R., Ogura, Y., Asadulghani, M., Ooka, T., Murase, K., Gotoh, Y., & Hayashi, T. (2012). A sensitive and simple plaque formation method for the Stx2 phage of *Escherichia coli* O157:H7, which does not form plaques in the standard plating procedure. *Plasmid*, *67*(3), 227-235. doi:10.1016/j.plasmid.2011.12.001
- Jackson, M. P., Newland, J. W., Holmes, R. K., & O'Brien, A. D. (1987). Nucleotide sequence analysis of the structural genes for Shiga-like toxin I encoded by bacteriophage 933J from *Escherichia coli*. *Microb Pathog*, *2*(2), 147-153.
- Jandhyala, S. M., Talukdar, R., Subramanyam, C., Vuyyuru, H., Sasikala, M., & Nageshwar Reddy, D. (2015). Role of the normal gut microbiota. *World J Gastroenterol*, *21*(29), 8787-8803. doi:10.3748/wjg.v21.i29.8787
- Jernberg, C., Lofmark, S., Edlund, C., & Jansson, J. K. (2010). Long-term impacts of antibiotic exposure on the human intestinal microbiota. *Microbiology*, *156*(Pt 11), 3216-3223. doi:10.1099/mic.0.040618-0
- Johannes, L., & Romer, W. (2010). Shiga toxins--from cell biology to biomedical applications. *Nat Rev Microbiol*, *8*(2), 105-116. doi:10.1038/nrmicro2279
- Karch, H., Bielaszewska, M., Bitzan, M., & Schmidt, H. (1999). Epidemiology and diagnosis of Shiga toxin-producing *Escherichia coli* infections. *Diagn Microbiol Infect Dis*, *34*(3), 229-243.

- Karch, H., Tarr, P. I., & Bielaszewska, M. (2005). Enterohaemorrhagic *Escherichia coli* in human medicine. *International Journal of Medical Microbiology*, 295(6-7), 405-418. doi:10.1016/j.ijmm.2005.06.009
- Kauffmann, F. (1944). *Zur Serologie der Coli-Gruppe*. (Vol. 21): Acta Pathol. Microbiol. Scand.
- Kauffmann, F., & Vahlne, G. (1945). Ueber die Bedeutung des serologischen Formenwechsels fMr die Bakteriophagenwirkung in der Coli-Gruppe. (Vol. 22).
- Klemm, P. (1985). Fimbrial adhesions of *Escherichia coli*. *Rev Infect Dis*, 7(3), 321-340.
- Kleta, S., Nordhoff, M., Tedin, K., Wieler, L. H., Kolenda, R., Oswald, S., . . . Schierack, P. (2014). Role of F1C fimbriae, flagella, and secreted bacterial components in the inhibitory effect of probiotic *Escherichia coli* Nissle 1917 on atypical enteropathogenic *E. coli* infection. *Infect Immun*, 82(5), 1801-1812. doi:10.1128/IAI.01431-13
- Koenig, J. E., Spor, A., Scalfone, N., Fricker, A. D., Stombaugh, J., Knight, R., . . . Ley, R. E. (2011). Succession of microbial consortia in the developing infant gut microbiome. *Proc Natl Acad Sci U S A*, 108 Suppl 1, 4578-4585. doi:10.1073/pnas.1000081107
- Konowalchuk, J., Speirs, J. I., & Stavric, S. (1977). Vero response to a cytotoxin of *Escherichia coli*. *Infect Immun*, 18(3), 775-779.
- Kraus, E., & Femfert, U. (1976). Proteinase K from the mold *Tritirachium album* Limber. Specificity and mode of action. *Hoppe Seylers Z Physiol Chem*, 357(7), 937-947.
- Kuhnert, P., Nicolet, J., & Frey, J. (1995). Rapid and accurate identification of *Escherichia coli* K-12 strains. *Appl Environ Microbiol*, 61(11), 4135-4139.
- Labrie, S. J., Samson, J. E., & Moineau, S. (2010). Bacteriophage resistance mechanisms. *Nat Rev Microbiol*, 8(5), 317-327. doi:10.1038/nrmicro2315
- Langemann, T., Koller, V. J., Muhammad, A., Kudela, P., Mayr, U. B., & Lubitz, W. (2010). The Bacterial Ghost platform system: production and applications. *Bioeng Bugs*, 1(5), 326-336. doi:10.4161/bbug.1.5.12540
- Laurel, J. Prokaryotes vs Eukaryotes. Retrieved from <https://sites.google.com/site/laurelbiology/cells/prokaryotes-vs-eukaryotes>
- Leatham, M. P., Banerjee, S., Autieri, S. M., Mercado-Lubo, R., Conway, T., & Cohen, P. S. (2009). Precolonized human commensal *Escherichia coli* strains serve as a barrier to *E. coli* O157:H7 growth in the streptomycin-treated mouse intestine. *Infect Immun*, 77(7), 2876-2886. doi:10.1128/IAI.00059-09

- Lebedev, A. A., Krause, M. H., Isidro, A. L., Vagin, A. A., Orlova, E. V., Turner, J., . . . Antson, A. A. (2007). Structural framework for DNA translocation via the viral portal protein. *EMBO J*, 26(7), 1984-1994. doi:10.1038/sj.emboj.7601643
- Li, J., Jia, H., Cai, X., Zhong, H., Feng, Q., Sunagawa, S., . . . Meta, H. I. T. C. (2014). An integrated catalog of reference genes in the human gut microbiome. *Nat Biotechnol*, 32(8), 834-841. doi:10.1038/nbt.2942
- Little, J. W. (1983). The SOS regulatory system: control of its state by the level of RecA protease. *J Mol Biol*, 167(4), 791-808.
- Los, J. M., Los, M., Wegrzyn, A., & Wegrzyn, G. (2010). Hydrogen peroxide-mediated induction of the Shiga toxin-converting lambdoid prophage ST2-8624 in *Escherichia coli* O157:H7. *Fems Immunology and Medical Microbiology*, 58(3), 322-329. doi:DOI 10.1111/j.1574-695X.2009.00644.x
- Love, M. I., Huber, W., & Anders, S. (2014). Moderated estimation of fold change and dispersion for RNA-seq data with DESeq2. *Genome Biol*, 15(12), 550. doi:10.1186/s13059-014-0550-8
- Lusiac-Szelachowska, M., Weber-Dabrowska, B., Jonczyk-Matysiak, E., Wojciechowska, R., & Gorski, A. (2017). Bacteriophages in the gastrointestinal tract and their implications. *Gut Pathog*, 9, 44. doi:10.1186/s13099-017-0196-7
- Makinoshima, H., Aizawa, S., Hayashi, H., Miki, T., Nishimura, A., & Ishihama, A. (2003). Growth phase-coupled alterations in cell structure and function of *Escherichia coli*. *J Bacteriol*, 185(4), 1338-1345.
- Malchow, H. A. (1997). Crohn's disease and *Escherichia coli*. A new approach in therapy to maintain remission of colonic Crohn's disease? *J Clin Gastroenterol*, 25(4), 653-658.
- Martin, M. (2011). Cutadapt removes adapter sequences from high-throughput sequencing reads. 2011, 17(1). doi:10.14806/ej.17.1.200, pp. 10-12
- Martinez-Garcia, P. M., Ramos, C., & Rodriguez-Palenzuela, P. (2015). T346Hunter: a novel web-based tool for the prediction of type III, type IV and type VI secretion systems in bacterial genomes. *PLoS One*, 10(4), e0119317. doi:10.1371/journal.pone.0119317
- Matos, R. C., Lapaque, N., Rigottier-Gois, L., Debarbieux, L., Meylheuc, T., Gonzalez-Zorn, B., . . . Serror, P. (2013). Enterococcus faecalis prophage dynamics and contributions to pathogenic traits. *PLoS Genet*, 9(6), e1003539. doi:10.1371/journal.pgen.1003539
- Melton-Celsa, A. R. (2014). Shiga Toxin (Stx) Classification, Structure, and Function. *Microbiol Spectr*, 2(4), EHEC-0024-2013.
- Metchnikoff, E. (1908). *Optimistic studies New York*: Putman's Sons.



- Michino, H., Araki, K., Minami, S., Takaya, S., Sakai, N., Miyazaki, M., . . . Yanagawa, H. (1999). Massive outbreak of *Escherichia coli* O157:H7 infection in schoolchildren in Sakai City, Japan, associated with consumption of white radish sprouts. *Am J Epidemiol*, *150*(8), 787-796.
- Mohsin, M., Guenther, S., Schierack, P., Tedin, K., & Wieler, L. H. (2015). Probiotic *Escherichia coli* Nissle 1917 reduces growth, Shiga toxin expression, release and thus cytotoxicity of enterohemorrhagic *Escherichia coli*. *International Journal of Medical Microbiology*, *305*(1), 20-26. doi:10.1016/j.ijmm.2014.10.003
- Mojica, F. J., Diez-Villasenor, C., Garcia-Martinez, J., & Almendros, C. (2009). Short motif sequences determine the targets of the prokaryotic CRISPR defence system. *Microbiology*, *155*(Pt 3), 733-740. doi:10.1099/mic.0.023960-0
- Mol, O., & Oudega, B. (1996). Molecular and structural aspects of fimbriae biosynthesis and assembly in *Escherichia coli*. *FEMS Microbiol Rev*, *19*(1), 25-52.
- Mondal, S. I., Islam, M. R., Sawaguchi, A., Asadulghani, M., Ooka, T., Gotoh, Y., . . . Hayashi, T. (2016). Genes essential for the morphogenesis of the Shiga toxin 2-transducing phage from *Escherichia coli* O157:H7. *Sci Rep*, *6*, 39036. doi:10.1038/srep39036
- Monk, M., & Kinross, J. (1975). The kinetics of derepression of prophage lambda following ultraviolet irradiation of lysogenic cells. *Mol Gen Genet*, *137*(3), 263-268.
- Muhldorfer, I., Hacker, J., Keusch, G. T., Acheson, D. W., Tschape, H., Kane, A. V., . . . Donohue-Rolfe, A. (1996). Regulation of the Shiga-like toxin II operon in *Escherichia coli*. *Infect Immun*, *64*(2), 495-502.
- Muniesa, M., Blanco, J. E., De Simon, M., Serra-Moreno, R., Blanch, A. R., & Jofre, J. (2004). Diversity of *stx2* converting bacteriophages induced from Shiga-toxin-producing *Escherichia coli* strains isolated from cattle. *Microbiology*, *150*(Pt 9), 2959-2971. doi:10.1099/mic.0.27188-0
- Nissle, A. (1918). Die antagonistische Behandlung chronischer Darmstörungen mit Kolibakterien. (Vol. 2).
- Nougayrede, J. P., Homburg, S., Taieb, F., Boury, M., Brzuszkiewicz, E., Gottschalk, G., . . . Oswald, E. (2006). *Escherichia coli* induces DNA double-strand breaks in eukaryotic cells. *Science*, *313*(5788), 848-851. doi:10.1126/science.1127059
- O'Brien, A. D., & Holmes, R. K. (1987). Shiga and Shiga-like toxins. *Microbiol Rev*, *51*(2), 206-220.

- O'Brien, A. D., Newland, J. W., Miller, S. F., Holmes, R. K., Smith, H. W., & Formal, S. B. (1984). Shiga-like toxin-converting phages from *Escherichia coli* strains that cause hemorrhagic colitis or infantile diarrhea. *Science*, 226(4675), 694-696.
- O'Hara, A. M., & Shanahan, F. (2006). The gut flora as a forgotten organ. *EMBO Rep*, 7(7), 688-693. doi:10.1038/sj.embor.7400731
- Olsen, S. J., Miller, G., Breuer, T., Kennedy, M., Higgins, C., Walford, J., . . . Mead, P. (2002). A waterborne outbreak of *Escherichia coli* O157:H7 infections and hemolytic uremic syndrome: implications for rural water systems. *Emerg Infect Dis*, 8(4), 370-375. doi:10.3201/eid0804.000218
- Orlova, E. V. (2012). *Bacteriophages*. In I. Kurtboke (Ed.), *Bacteriophages and their structural organisation*. Retrieved from <http://www.intechopen.com/books/bacteriophages/bacteriophages-and-their-structural-organisation->
- Oshima, K., Toh, H., Ogura, Y., Sasamoto, H., Morita, H., Park, S. H., . . . Hattori, M. (2008). Complete genome sequence and comparative analysis of the wild-type commensal *Escherichia coli* strain SE11 isolated from a healthy adult. *DNA Res*, 15(6), 375-386. doi:10.1093/dnares/dsn026
- Pacheco, A. R., & Sperandio, V. (2012). Shiga toxin in enterohemorrhagic E.coli: regulation and novel anti-virulence strategies. *Front Cell Infect Microbiol*, 2, 81. doi:10.3389/fcimb.2012.00081
- Parma, D. H., Snyder, M., Sobolevski, S., Nawroz, M., Brody, E., & Gold, L. (1992). The Rex system of bacteriophage lambda: tolerance and altruistic cell death. *Genes Dev*, 6(3), 497-510.
- Paton, A. W., Chen, A. Y., Wang, H., McAllister, L. J., Hoggerl, F., Mayr, U. B., . . . Paton, J. C. (2015). Protection against Shiga-Toxigenic *Escherichia coli* by Non-Genetically Modified Organism Receptor Mimic Bacterial Ghosts. *Infect Immun*, 83(9), 3526-3533. doi:10.1128/IAI.00669-15
- Patzer, S. I., Baquero, M. R., Bravo, D., Moreno, F., & Hantke, K. (2003). The colicin G, H and X determinants encode microcins M and H47, which might utilize the catechol siderophore receptors FepA, Cir, Fiu and IroN. *Microbiology*, 149(Pt 9), 2557-2570.
- Perna, N. T., Plunkett, G., 3rd, Burland, V., Mau, B., Glasner, J. D., Rose, D. J., . . . Blattner, F. R. (2001). Genome sequence of enterohaemorrhagic *Escherichia coli* O157:H7. *Nature*, 409(6819), 529-533. doi:10.1038/35054089

- Perucchetti, R., Parris, W., Becker, A., & Gold, M. (1988). Late stages in bacteriophage lambda head morphogenesis: in vitro studies on the action of the bacteriophage lambda D-gene and W-gene products. *Virology*, *165*(1), 103-114.
- Pharmazentrale. (26.02.2018). The molecular mechanisms of action and its relevance to clinical practice. Retrieved from <http://www.mutaflor.com/studies-subline-3-z-b-zu-den-studienergebnissen-studies-using-doloteffin/molecular-mechanisms-of-action.html>
- Pin, C., & Baranyi, J. (2008). Single-cell and population lag times as a function of cell age. *Appl Environ Microbiol*, *74*(8), 2534-2536. doi:10.1128/AEM.02402-07
- Pingoud, A., Fuxreiter, M., Pingoud, V., & Wende, W. (2005). Type II restriction endonucleases: structure and mechanism. *Cellular and Molecular Life Sciences*, *62*(6), 685-707. doi:10.1007/s00018-004-4513-1
- Pletnev, P., Osterman, I., Sergiev, P., Bogdanov, A., & Dontsova, O. (2015). Survival guide: *Escherichia coli* in the stationary phase. *Acta Naturae*, *7*(4), 22-33.
- Plunkett, G., 3rd, Rose, D. J., Durfee, T. J., & Blattner, F. R. (1999). Sequence of Shiga toxin 2 phage 933W from *Escherichia coli* O157:H7: Shiga toxin as a phage late-gene product. *J Bacteriol*, *181*(6), 1767-1778.
- Pruimboom-Brees, I. M., Morgan, T. W., Ackermann, M. R., Nystrom, E. D., Samuel, J. E., Cornick, N. A., & Moon, H. W. (2000). Cattle lack vascular receptors for *Escherichia coli* O157:H7 Shiga toxins. *Proc Natl Acad Sci U S A*, *97*(19), 10325-10329. doi:10.1073/pnas.190329997
- Rakhuba, D. V., Kolomiets, E. I., Dey, E. S., & Novik, G. I. (2010). Bacteriophage receptors, mechanisms of phage adsorption and penetration into host cell. *Pol J Microbiol*, *59*(3), 145-155.
- Ranade, K., & Poteete, A. R. (1993). Superinfection exclusion (*sieB*) genes of bacteriophages P22 and lambda. *J Bacteriol*, *175*(15), 4712-4718.
- Reissbrodt, R., Hammes, W. P., dal Bello, F., Prager, R., Fruth, A., Hantke, K., . . . Williams, P. H. (2009). Inhibition of growth of Shiga toxin-producing *Escherichia coli* by nonpathogenic *Escherichia coli*. *Fems Microbiology Letters*, *290*(1), 62-69. doi:DOI 10.1111/j.1574-6968.2008.01405.x
- Reshes, G., Vanounou, S., Fishov, I., & Feingold, M. (2008). Cell shape dynamics in *Escherichia coli*. *Biophys J*, *94*(1), 251-264. doi:10.1529/biophysj.107.104398
- Reuter, C., Alzheimer, M., Walles, H., & Oelschlaeger, T. A. (2018). An adherent mucus layer attenuates the genotoxic effect of colibactin. *Cell Microbiol*, *20*(2). doi:10.1111/cmi.12812

- Rezania, S., Amirmozaffari, N., Tabarraei, B., Jeddi-Tehrani, M., Zarei, O., Alizadeh, R., . . . Zarnani, A. H. (2011). Extraction, Purification and Characterization of Lipopolysaccharide from *Escherichia coli* and *Salmonella typhi*. *Avicenna J Med Biotechnol*, 3(1), 3-9.
- Riede, I., & Eschbach, M. L. (1986). Evidence that TraT interacts with OmpA of *Escherichia coli*. *FEBS Lett*, 205(2), 241-245.
- Riley, L. W., Remis, R. S., Helgerson, S. D., McGee, H. B., Wells, J. G., Davis, B. R., . . . Cohen, M. L. (1983). Hemorrhagic colitis associated with a rare *Escherichia coli* serotype. *N Engl J Med*, 308(12), 681-685. doi:10.1056/NEJM198303243081203
- RKI. (2011a). Abschließende Darstellung und Bewertung der epidemiologischen Erkenntnisse im EHEC O104:H4 Ausbruch Deutschland 2011. Retrieved from [https://www.rki.de/DE/Content/InfAZ/E/EHEC/EHEC\\_O104/EHEC-Abschlussbericht.pdf?\\_blob=publicationFile](https://www.rki.de/DE/Content/InfAZ/E/EHEC/EHEC_O104/EHEC-Abschlussbericht.pdf?_blob=publicationFile)
- RKI. (2011b). Abschließende Darstellung und Bewertung der epidemiologischen Erkenntnisse im EHEC O104:H4 Ausbruch, Deutschland 2011. Retrieved from [www.rki.de](http://www.rki.de) website:
- Rode, T. M., Axelsson, L., Granum, P. E., Heir, E., Holck, A., & L'Abée-Lund, T. M. (2011). High stability of Stx2 phage in food and under food-processing conditions. *Appl Environ Microbiol*, 77(15), 5336-5341. doi:10.1128/AEM.00180-11
- Rokney, A., Kobiler, O., Amir, A., Court, D. L., Stavans, J., Adhya, S., & Oppenheim, A. B. (2008). Host responses influence on the induction of lambda prophage. *Mol Microbiol*, 68(1), 29-36. doi:10.1111/j.1365-2958.2008.06119.x
- Rund, S. A., Rohde, H., Sonnenborn, U., & Oelschlaeger, T. A. (2013). Antagonistic effects of probiotic *Escherichia coli* Nissle 1917 on EHEC strains of serotype O104:H4 and O157:H7. *International Journal of Medical Microbiology*, 303(1), 1-8. doi:DOI 10.1016/j.ijmm.2012.11.006
- Schmidt, H. (2001). Shiga-toxin-converting bacteriophages. *Res Microbiol*, 152(8), 687-695.
- Schmidt, H., Bielaszewska, M., & Karch, H. (1999). Transduction of enteric *Escherichia coli* isolates with a derivative of Shiga toxin 2-encoding bacteriophage phi3538 isolated from *Escherichia coli* O157:H7. *Appl Environ Microbiol*, 65(9), 3855-3861.
- Schwechheimer, C., & Kuehn, M. J. (2015). Outer-membrane vesicles from Gram-negative bacteria: biogenesis and functions. *Nat Rev Microbiol*, 13(10), 605-619. doi:10.1038/nrmicro3525
- Schweizer, M., & Henning, U. (1977). Action of a major outer cell envelope membrane protein in conjugation of *Escherichia coli* K-12. *J Bacteriol*, 129(3), 1651-1652.

- Sender, R., Fuchs, S., & Milo, R. (2016). Revised Estimates for the Number of Human and Bacteria Cells in the Body. *PLoS Biol*, *14*(8), e1002533. doi:10.1371/journal.pbio.1002533
- Simpson, D. J., Sacher, J. C., & Szymanski, C. M. (2016). Development of an Assay for the Identification of Receptor Binding Proteins from Bacteriophages. *Viruses*, *8*(1). doi:10.3390/v8010017
- Siragusa, S., De Angelis, M., Calasso, M., Campanella, D., Minervini, F., Di Cagno, R., & Gobbetti, M. (2014). Fermentation and proteome profiles of *Lactobacillus plantarum* strains during growth under food-like conditions. *J Proteomics*, *96*, 366-380. doi:10.1016/j.jprot.2013.11.003
- Smith, D. L., James, C. E., Sergeant, M. J., Yaxian, Y., Saunders, J. R., McCarthy, A. J., & Allison, H. E. (2007). Short-tailed stx phages exploit the conserved YaeT protein to disseminate Shiga toxin genes among enterobacteria. *J Bacteriol*, *189*(20), 7223-7233. doi:10.1128/JB.00824-07
- Sommer, S., Boudsocq, F., Devoret, R., & Bailone, A. (1998). Specific RecA amino acid changes affect RecA-UmuD'C interaction. *Mol Microbiol*, *28*(2), 281-291.
- Sonnenborn, U. (2016). *Escherichia coli* strain Nissle 1917-from bench to bedside and back: history of a special *Escherichia coli* strain with probiotic properties. *Fems Microbiology Letters*, *363*(19). doi:10.1093/femsle/fnw212
- Sperandio, V., Torres, A. G., Giron, J. A., & Kaper, J. B. (2001). Quorum sensing is a global regulatory mechanism in enterohemorrhagic *Escherichia coli* O157:H7. *J Bacteriol*, *183*(17), 5187-5197.
- Stearns-Kurosawa, D. J., Collins, V., Freeman, S., Tesh, V. L., & Kurosawa, S. (2010). Distinct physiologic and inflammatory responses elicited in baboons after challenge with Shiga toxin type 1 or 2 from enterohemorrhagic *Escherichia coli*. *Infect Immun*, *78*(6), 2497-2504. doi:10.1128/IAI.01435-09
- Stern, A., & Sorek, R. (2011). The phage-host arms race: shaping the evolution of microbes. *Bioessays*, *33*(1), 43-51. doi:10.1002/bies.201000071
- Szekely, A. J., & Breitbart, M. (2016). Single-stranded DNA phages: from early molecular biology tools to recent revolutions in environmental microbiology. *Fems Microbiology Letters*, *363*(6). doi:10.1093/femsle/fnw027
- Takeda, K., & Uetake, H. (1973). In vitro interaction between phage and receptor lipopolysaccharide: a novel glycosidase associated with Salmonella phage 15. *Virology*, *52*(1), 148-159.

- Tarr, P. I., & Neill, M. A. (2001). *Escherichia coli* O157:H7. *Gastroenterol Clin North Am*, 30(3), 735-751.
- Tarr, P. I., Neill, M. A., Allen, J., Siccardi, C. J., Watkins, S. L., & Hickman, R. O. (1989). The increasing incidence of the hemolytic-uremic syndrome in King County, Washington: lack of evidence for ascertainment bias. *Am J Epidemiol*, 129(3), 582-586.
- Temin, H. M., & Mizutani, S. (1970). RNA-dependent DNA polymerase in virions of Rous sarcoma virus. *Nature*, 226(5252), 1211-1213.
- Thursby, E., & Juge, N. (2017). Introduction to the human gut microbiota. *Biochem J*, 474(11), 1823-1836. doi:10.1042/BCJ20160510
- Tilden, J., Jr., Young, W., McNamara, A. M., Custer, C., Boesel, B., Lambert-Fair, M. A., . . . Morris, J. G., Jr. (1996). A new route of transmission for *Escherichia coli*: infection from dry fermented salami. *Am J Public Health*, 86(8), 1142-1145.
- Tissier, H. (1906). Traitement des infections intestinales par la méthode de la flore bactérienne de l'intestin. *C. R. Soc. Biol.*, 60, 359-361.
- Tjaden, B., Saxena, R. M., Stolyar, S., Haynor, D. R., Kolker, E., & Rosenow, C. (2002). Transcriptome analysis of *Escherichia coli* using high-density oligonucleotide probe arrays. *Nucleic Acids Research*, 30(17), 3732-3738. doi:DOI 10.1093/nar/gkf505
- Toh, H., Oshima, K., Toyoda, A., Ogura, Y., Ooka, T., Sasamoto, H., . . . Hattori, M. (2010). Complete genome sequence of the wild-type commensal *Escherichia coli* strain SE15, belonging to phylogenetic group B2. *J Bacteriol*, 192(4), 1165-1166. doi:10.1128/JB.01543-09
- Tolosa, L., Gimenez, R., Fabrega, M. J., Alvarez, C. S., Aguilera, L., Canas, M. A., . . . Baldoma, L. (2015). The secreted autotransporter toxin (Sat) does not act as a virulence factor in the probiotic *Escherichia coli* strain Nissle 1917. *BMC Microbiol*, 15, 250. doi:10.1186/s12866-015-0591-5
- Torgersen, M. L., Lauvrak, S. U., & Sandvig, K. (2005). The A-subunit of surface-bound Shiga toxin stimulates clathrin-dependent uptake of the toxin. *Febs Journal*, 272(16), 4103-4113. doi:10.1111/j.1742-4658.2005.04835.x
- Touchon, M., Hoede, C., Tenailon, O., Barbe, V., Baeriswyl, S., Bidet, P., . . . Denamur, E. (2009). Organised genome dynamics in the *Escherichia coli* species results in highly diverse adaptive paths. *PLoS Genet*, 5(1), e1000344. doi:10.1371/journal.pgen.1000344
- Troge, A. (2012). *Studien am Flagellensystem des Escherichia coli Stammes Nissle 1917 (EcN) im Hinblick auf seine Funktion als Probiotikum*. (Dissertation), Universität Würzburg, Würzburg. Retrieved from urn:nbn:de:bvb:20-opus-74201

- Tyler, J. S., Mills, M. J., & Friedman, D. I. (2004). The operator and early promoter region of the Shiga toxin type 2-encoding bacteriophage 933W and control of toxin expression. *J Bacteriol*, *186*(22), 7670-7679. doi:10.1128/JB.186.22.7670-7679.2004
- Ulett, G. C., Valle, J., Beloin, C., Sherlock, O., Ghigo, J. M., & Schembri, M. A. (2007). Functional analysis of antigen 43 in uropathogenic *Escherichia coli* reveals a role in long-term persistence in the urinary tract. *Infect Immun*, *75*(7), 3233-3244. doi:10.1128/IAI.01952-06
- Vally, H., Hall, G., Dyda, A., Raupach, J., Knope, K., Combs, B., & Desmarchelier, P. (2012). Epidemiology of Shiga toxin producing *Escherichia coli* in Australia, 2000-2010. *BMC Public Health*, *12*, 63. doi:10.1186/1471-2458-12-63
- Vasanthakumari, R. (2007). *Textbook of Microbiology*. New Dehli: BI Publications Pvt Ltd.
- Vejborg, R. M., Friis, C., Hancock, V., Schembri, M. A., & Klemm, P. (2010). A virulent parent with probiotic progeny: comparative genomics of *Escherichia coli* strains CFT073, Nissle 1917 and ABU 83972. *Mol Genet Genomics*, *283*(5), 469-484. doi:10.1007/s00438-010-0532-9
- Vidakovic, L., Singh, P. K., Hartmann, R., Nadell, C. D., & Drescher, K. (2017). Dynamic biofilm architecture confers individual and collective mechanisms of viral protection. *Nat Microbiol*. doi:10.1038/s41564-017-0050-1
- Vlasova, A. N., Kandasamy, S., Chattha, K. S., Rajashekara, G., & Saif, L. J. (2016). Comparison of probiotic lactobacilli and bifidobacteria effects, immune responses and rotavirus vaccines and infection in different host species. *Vet Immunol Immunopathol*, *172*, 72-84. doi:10.1016/j.vetimm.2016.01.003
- Waldor, M. K., & Friedman, D. I. (2005). Phage regulatory circuits and virulence gene expression. *Curr Opin Microbiol*, *8*(4), 459-465. doi:10.1016/j.mib.2005.06.001
- Walker, G. C. (1984). Mutagenesis and inducible responses to deoxyribonucleic acid damage in *Escherichia coli*. *Microbiol Rev*, *48*(1), 60-93.
- Wassenaar, T. M. (2016). Insights from 100 Years of Research with Probiotic *E. Coli*. *Eur J Microbiol Immunol (Bp)*, *6*(3), 147-161. doi:10.1556/1886.2016.00029
- Whitfield, C., & Roberts, I. S. (1999). Structure, assembly and regulation of expression of capsules in *Escherichia coli*. *Mol Microbiol*, *31*(5), 1307-1319.
- WHO. (2001). Evaluation of health and nutritional properties of powder milk and live lactic acid bacteria. *Food and Agriculture Organization of the United Nations and World Health Organization*, 2018(23.02.).
- Retrieved from [ftp://ftp.fao.org/es/esn/food/probio\\_report\\_en.pdf](ftp://ftp.fao.org/es/esn/food/probio_report_en.pdf).

- Wilkinson, S. G. (1996). Bacterial lipopolysaccharides--themes and variations. *Prog Lipid Res*, 35(3), 283-343.
- Witkin, E. M. (1976). Ultraviolet mutagenesis and inducible DNA repair in *Escherichia coli*. *Bacteriol Rev*, 40(4), 869-907.
- Wong, C. S., Jelacic, S., Habeeb, R. L., Watkins, S. L., & Tarr, P. I. (2000). The risk of the hemolytic-uremic syndrome after antibiotic treatment of *Escherichia coli* O157:H7 infections. *N Engl J Med*, 342(26), 1930-1936. doi:10.1056/NEJM200006293422601
- Wood, T. K. (2009). Insights on *Escherichia coli* biofilm formation and inhibition from whole-transcriptome profiling. *Environ Microbiol*, 11(1), 1-15. doi:10.1111/j.1462-2920.2008.01768.x
- Wray, C., McLaren, I. M., Randall, L. P., & Pearson, G. R. (2000). Natural and experimental infection of normal cattle with *Escherichia coli* O157. *Vet Rec*, 147(3), 65-68.
- Zeng, L., & Golding, I. (2011). Following cell-fate in *E. coli* after infection by phage lambda. *J Vis Exp*(56), e3363. doi:10.3791/3363
- Zhou, K., Zhou, L., Lim, Q., Zou, R., Stephanopoulos, G., & Too, H. P. (2011). Novel reference genes for quantifying transcriptional responses of *Escherichia coli* to protein overexpression by quantitative PCR. *BMC Mol Biol*, 12, 18. doi:10.1186/1471-2199-12-18



**8. Appendix****8.1. *stx2*-prophage genes****Table 15: Genes of the *stx2*-prophage.**

<b>Locus_tag</b>	<b>Coding sequence</b>	<b>Product</b>
<i>z1423*</i>	1330282 - 1330827	trp repressor binding protein
<i>z1424</i>	1330857 - 1332191	integrase
<i>z1425</i>	1332220 - 1332519	putative excisionase
<i>z1426</i>	1332590 - 1332901	unknown protein
<i>z1428</i>	1332961 - 1333326	unknown protein
<i>z1429</i>	1333238 - 1333861	unknown protein
<i>z1430</i>	1333865 - 1334152	unknown protein
<i>z1431</i>	1334191 - 1334487	unknown protein
<i>z1432</i>	1334931 - 1335704	unknown protein
<i>z1433</i>	1336021 - 1336302	unknown protein
<i>z1434</i>	1336313 - 1336504	unknown protein
<i>z1435</i>	1336659 - 1337336	putative exonuclease
<i>z1437</i>	1337333 - 1338118	putative Bet recombination protein
<i>z1438</i>	1338124 - 1338426	putative host-nuclease inhibitor protein Gam
<i>z1439</i>	1338124 - 1338420	putative Kil protein
<i>z1440</i>	1338845 - 1339213	putative single-stranded DNA binding protein
<i>z1441</i>	1339364 - 1339834	unknown protein
<i>z1442</i>	1339893 - 1340276	putative antitermination protein N
<i>z1443</i>	1340765 - 1340929	unknown protein
<i>z1444</i>	1340932 - 1341978	putative serine/threonine kinase
<i>z1445</i>	1341972 - 1342433	unknown protein
<i>z1446</i>	1342501 - 1342842	unknown protein
<i>z1447</i>	1342903 - 1343610	putative repressor protein CI
<i>z1448</i>	1343689 - 1343916	putative regulatory protein Cro
<i>z1449</i>	1344055 - 1344351	putative regulatory protein CII
<i>z1450</i>	1344384 - 1345322	putative replication protein O

<i>z1451</i>	1345319 - 1346020	putative replication protein P
<i>z1452</i>	1346378 - 1346656	unknown protein
<i>z1453</i>	1347208 - 1347654	unknown protein
<i>z1454</i>	1347651 - 1348178	putative DNA N-6-methyltransferase
<i>z1456</i>	1348366 - 1349409	unknown protein
<i>z1457</i>	1349555 - 1350283	putative DNA-binding protein Roi
<i>z1458</i>	1350283 - 1350888	unknown protein
<i>z1459</i>	1351072 - 1351506	antitermination protein Q
<i>z1460</i>	1351809 - 1351907	unknown protein
<i>z1461</i>	1351948 - 1352023	RNA; tRNA
<i>z1462</i>	1352033 - 1352109	RNA; tRNA
<i>z1463</i>	1352123 - 1352199	RNA; tRNA
<i>z1464</i>	1352290 - 1353249	shiga-like toxin II A subunit
<i>z1465</i>	1353261 - 1353530	shiga-like toxin II B subunit
<i>z1467</i>	1356135 - 1356581	unknown protein
<i>z1468</i>	1356658 - 1396873	putative lysis protein S
<i>z1469</i>	1356878 - 1357411	putative lysozyme protein R
<i>z1471</i>	1357682 - 1358251	putative antirepressor protein Ant
<i>z1473</i>	1358405 - 1358869	putative endopeptidase Rz
<i>z1474</i>	1358901 - 1359194	putative Bor protein precursor
<i>z1475</i>	1359603 - 1360409	putative terminase small subunit
<i>z1476</i>	1360390 - 1362096	partial putative terminase large subunit
<i>z1477</i>	1362096 - 1364240	putative portal protein
<i>z1478</i>	1364398 - 1365405	unknown protein
<i>z1479</i>	1365429 - 1366643	unknown protein
<i>z1480</i>	1366699 - 1367088	unknown protein
<i>z1481</i>	1367138 - 1367599	unknown protein
<i>z1482</i>	1368146 - 1368796	unknown protein
<i>z1483</i>	1368793 - 1370730	putative tail fiber protein
<i>z1484</i>	1370693 - 1371001	unknown protein
<i>z1485</i>	1371048 - 1371329	unknown protein
<i>z1486</i>	1371546 - 1373249	unknown protein
<i>z1487</i>	1373291 - 1374514	unknown protein

## Appendix

---

<b><i>z1488</i></b>	1374813 - 1375430	unknown protein
<b><i>z1489</i></b>	1375521 - 1376255	putative outer membrane protein Lam precursor
<b><i>z1490</i></b>	1376685 - 1377086	unknown protein
<b><i>z1491</i></b>	1977180 - 1377836	unknown protein
<b><i>z1492</i></b>	1377839 - 1378285	unknown protein
<b><i>z1493</i></b>	1378295 - 1378546	unknown protein
<b><i>z1494</i></b>	1378557 - 1379822	unknown protein
<b><i>z1495</i></b>	1379853 - 1388273	unknown protein
<b><i>z1498</i></b>	1388824 - 1389168	unknown protein
<b><i>z1500</i></b>	1389734 - 1390129	unknown protein
<b><i>z1501</i></b>	1390129 - 1391028	unknown protein
<b><i>z1503</i></b>	1391294 - 1391923	unknown protein
<b><i>z1504*</i></b>	1392479 - 1392541	Amino terminal fragment of WrbA

\* genes outside of the *stx2*-phage genome

## 8.2. Prophages of EcN

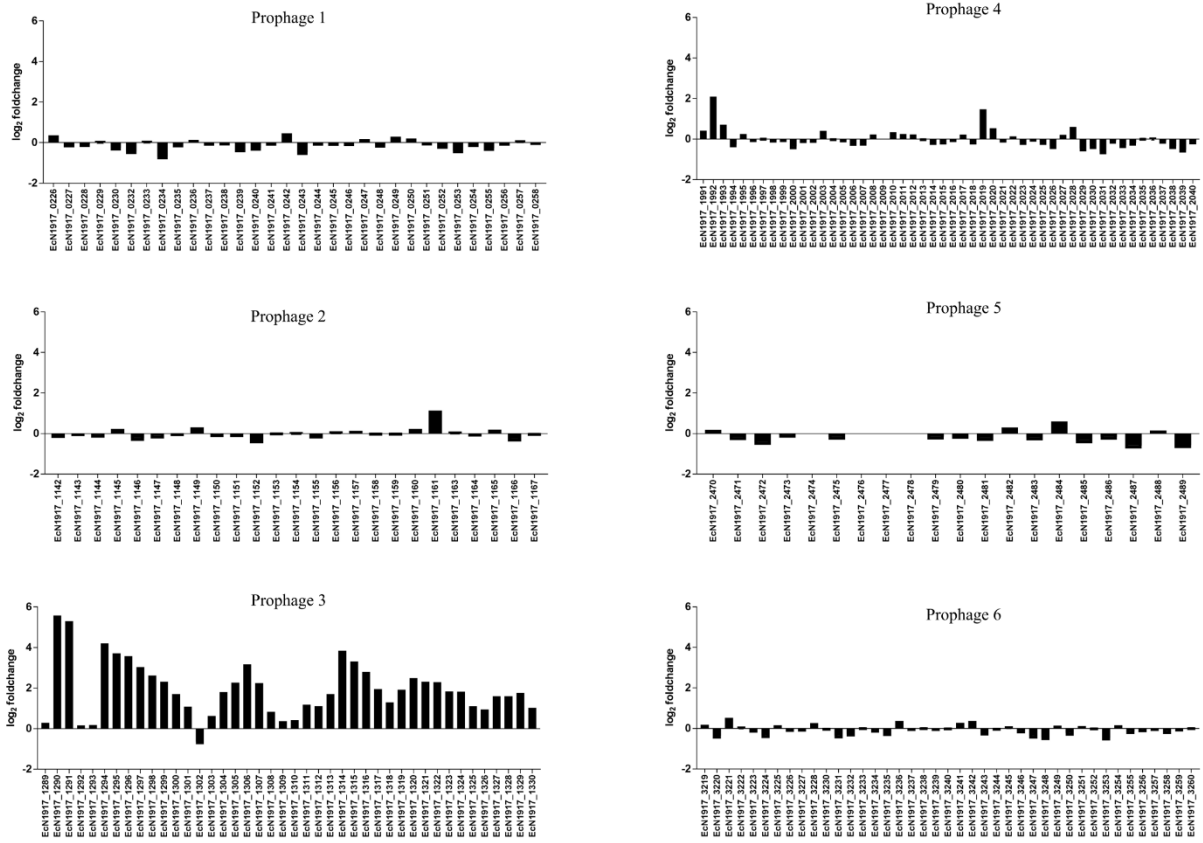


**Figure 52: Transcriptome analysis of EcN’s prophages.** log<sub>2</sub> fold changes of the gene expression of EcN’s prophages in the presence of *stx*-phages.

**8.3. YaeT protein sequence comparison**

**Table 16: Amino acid sequence comparison of the *E. coli* strains MG1655, EcN, CFT073, SE11, SE15 and IAI1.**

MG1655	MAMKLLIASLLFSSATVYGAEGFVVKDIHFEGLRVAVGAALLSMPVRTGDTVNDEDIS
EcN	MAMKLLIASLLFSSATVYGAEGFVVKDIHFEGLRVAVGAALLSMPVRTGDTVNDEDIS
CFT073	MAMKLLIASLLFSSATVYGAEGFVVKDIHFEGLRVAVGAALLSMPVRTGDTVNDEDIS
SE11	MAMKLLIASLLFSSATVYGAEGFVVKDIHFEGLRVAVGAALLSMPVRTGDTVNDEDIS
SE15	MAMKLLIASLLFSSATVYGAEGFVVKDIHFEGLRVAVGAALLSMPVRTGDTVNDEDIS
IAI1	MAMKLLIASLLFSSATVYGAEGFVVKDIHFEGLRVAVGAALLSMPVRTGDTVNDEDIS
MG1655	NTIRALFATGNFEDVRVLRDGDITLLVQVKERPTIASITFSGNKSVKDDMLKONLEASGVR
EcN	NTIRALFATGNFEDVRVLRDGDITLLVQVKERPTIASITFSGNKSVKDDMLKONLEASGVR
CFT073	NTIRALFATGNFEDVRVLRDGDITLLVQVKERPTIASITFSGNKSVKDDMLKONLEASGVR
SE11	NTIRALFATGNFEDVRVLRDGDITLLVQVKERPTIASITFSGNKSVKDDMLKONLEASGVR
SE15	NTIRALFATGNFEDVRVLRDGDITLLVQVKERPTIASITFSGNKSVKDDMLKONLEASGVR
IAI1	NTIRALFATGNFEDVRVLRDGDITLLVQVKERPTIASITFSGNKSVKDDMLKONLEASGVR
MG1655	VGESLDRITTIADIEKGLDFYYSVGKYSASVKAVVPLPRNRVLDLKLVFQEGVSAEIQQI
EcN	VGESLDRITTIADIEKGLDFYYSVGKYSASVKAVVPLPRNRVLDLKLVFQEGVSAEIQQI
CFT073	VGESLDRITTIADIEKGLDFYYSVGKYSASVKAVVPLPRNRVLDLKLVFQEGVSAEIQQI
SE11	VGESLDRITTIADIEKGLDFYYSVGKYSASVKAVVPLPRNRVLDLKLVFQEGVSAEIQQI
SE15	VGESLDRITTIADIEKGLDFYYSVGKYSASVKAVVPLPRNRVLDLKLVFQEGVSAEIQQI
IAI1	VGESLDRITTIADIEKGLDFYYSVGKYSASVKAVVPLPRNRVLDLKLVFQEGVSAEIQQI
MG1655	NIVGNHAFTTDELISHFQLRDEVPWNNVVGDRKYQKQKLAGDLETLRSYLLDRGYARFNI
EcN	NIVGNHAFTTDELISHFQLRDEVPWNNVVGDRKYQKQKLAGDLETLRSYLLDRGYARFNI
CFT073	NIVGNHAFTTDELISHFQLRDEVPWNNVVGDRKYQKQKLAGDLETLRSYLLDRGYARFNI
SE11	NIVGNHAFTTDELISHFQLRDEVPWNNVVGDRKYQKQKLAGDLETLRSYLLDRGYARFNI
SE15	NIVGNHAFTTDELISHFQLRDEVPWNNVVGDRKYQKQKLAGDLETLRSYLLDRGYARFNI
IAI1	NIVGNHAFTTDELISHFQLRDEVPWNNVVGDRKYQKQKLAGDLETLRSYLLDRGYARFNI
MG1655	DSTQVSLTPDKKGIYVTVNITEGDQYKLSGVEVSGNLAGHSAEIEQLTKIEPGEIYNGTK
EcN	DSTQVSLTPDKKGIYVTVNITEGDQYKLSGVEVSGNLAGHSAEIEQLTKIEPGEIYNGTK
CFT073	DSTQVSLTPDKKGIYVTVNITEGDQYKLSGVEVSGNLAGHSAEIEQLTKIEPGEIYNGTK
SE11	DSTQVSLTPDKKGIYVTVNITEGDQYKLSGVEVSGNLAGHSAEIEQLTKIEPGEIYNGTK
SE15	DSTQVSLTPDKKGIYVTVNITEGDQYKLSGVEVSGNLAGHSAEIEQLTKIEPGEIYNGTK
IAI1	DSTQVSLTPDKKGIYVTVNITEGDQYKLSGVEVSGNLAGHSAEIEQLTKIEPGEIYNGTK
MG1655	VTKMEDDIKLLGRYGYAYFRVQSMPEINDADKTVKLRVNVDAAGNRFYVRKIRFEGNDTS
EcN	VTKMEDDIKLLGRYGYAYFRVQSMPEINDADKTVKLRVNVDAAGNRFYVRKIRFEGNDTS
CFT073	VTKMEDDIKLLGRYGYAYFRVQSMPEINDADKTVKLRVNVDAAGNRFYVRKIRFEGNDTS
SE11	VTKMEDDIKLLGRYGYAYFRVQSMPEINDADKTVKLRVNVDAAGNRFYVRKIRFEGNDTS
SE15	VTKMEDDIKLLGRYGYAYFRVQSMPEINDADKTVKLRVNVDAAGNRFYVRKIRFEGNDTS
IAI1	VTKMEDDIKLLGRYGYAYFRVQSMPEINDADKTVKLRVNVDAAGNRFYVRKIRFEGNDTS
MG1655	KDAVLRREMRQMEGAWLGSDLVDQGKERLNRLGFFETVDTIDTQRVPGSPDQVDVYKVKKE
EcN	KDAVLRREMRQMEGAWLGSDLVDQGKERLNRLGFFETVDTIDTQRVPGSPDQVDVYKVKKE
CFT073	KDAVLRREMRQMEGAWLGSDLVDQGKERLNRLGFFETVDTIDTQRVPGSPDQVDVYKVKKE
SE11	KDAVLRREMRQMEGAWLGSDLVDQGKERLNRLGFFETVDTIDTQRVPGSPDQVDVYKVKKE
SE15	KDAVLRREMRQMEGAWLGSDLVDQGKERLNRLGFFETVDTIDTQRVPGSPDQVDVYKVKKE
IAI1	KDAVLRREMRQMEGAWLGSDLVDQGKERLNRLGFFETVDTIDTQRVPGSPDQVDVYKVKKE
MG1655	RNTGSFNFGIYGTESGVSVFQAGVQDNLWLTGTGYAVGNGTKNDYQTYAELSVINPYFTV
EcN	RNTGSFNFGIYGTESGVSVFQAGVQDNLWLTGTGYAVGNGTKNDYQTYAELSVINPYFTV
CFT073	RNTGSFNFGIYGTESGVSVFQAGVQDNLWLTGTGYAVGNGTKNDYQTYAELSVINPYFTV
SE11	RNTGSFNFGIYGTESGVSVFQAGVQDNLWLTGTGYAVGNGTKNDYQTYAELSVINPYFTV
SE15	RNTGSFNFGIYGTESGVSVFQAGVQDNLWLTGTGYAVGNGTKNDYQTYAELSVINPYFTV
IAI1	RNTGSFNFGIYGTESGVSVFQAGVQDNLWLTGTGYAVGNGTKNDYQTYAELSVINPYFTV
MG1655	DGVSLLGGRIFYNDFQADDADLSDYTNKSYGTDVTLGFFINEYNSLRAGLGYVHNSLSNMQ
EcN	DGVSLLGGRIFYNDFQADDADLSDYTNKSYGTDVTLGFFINEYNSLRAGLGYVHNSLSNMQ
CFT073	DGVSLLGGRIFYNDFQADDADLSDYTNKSYGTDVTLGFFINEYNSLRAGLGYVHNSLSNMQ
SE11	DGVSLLGGRIFYNDFQADDADLSDYTNKSYGTDVTLGFFINEYNSLRAGLGYVHNSLSNMQ
SE15	DGVSLLGGRIFYNDFQADDADLSDYTNKSYGTDVTLGFFINEYNSLRAGLGYVHNSLSNMQ
IAI1	DGVSLLGGRIFYNDFQADDADLSDYTNKSYGTDVTLGFFINEYNSLRAGLGYVHNSLSNMQ
MG1655	PQVAMWRYLYSMGEHPSTSDQDNSFKTDDFTFNYGWTYNKLDRGYFFPTDGSRVNLTGKVI
EcN	PQVAMWRYLYSMGEHPSTSDQDNSFKTDDFTFNYGWTYNKLDRGYFFPTDGSRVNLTGKVI
CFT073	PQVAMWRYLYSMGEHPSTSDQDNSFKTDDFTFNYGWTYNKLDRGYFFPTDGSRVNLTGKVI
SE11	PQVAMWRYLYSMGEHPSTSDQDNSFKTDDFTFNYGWTYNKLDRGYFFPTDGSRVNLTGKVI
SE15	PQVAMWRYLYSMGEHPSTSDQDNSFKTDDFTFNYGWTYNKLDRGYFFPTDGSRVNLTGKVI
IAI1	PQVAMWRYLYSMGEHPSTSDQDNSFKTDDFTFNYGWTYNKLDRGYFFPTDGSRVNLTGKVI
MG1655	IPGSDNEYKVTLDATATYVPIDDDHKVVVLGRTRWGYDGLGGKEMPFYENFYAGGSSTV
EcN	IPGSDNEYKVTLDATATYVPIDDDHKVVVLGRTRWGYDGLGGKEMPFYENFYAGGSSTV
CFT073	IPGSDNEYKVTLDATATYVPIDDDHKVVVLGRTRWGYDGLGGKEMPFYENFYAGGSSTV
SE11	IPGSDNEYKVTLDATATYVPIDDDHKVVVLGRTRWGYDGLGGKEMPFYENFYAGGSSTV
SE15	IPGSDNEYKVTLDATATYVPIDDDHKVVVLGRTRWGYDGLGGKEMPFYENFYAGGSSTV
IAI1	IPGSDNEYKVTLDATATYVPIDDDHKVVVLGRTRWGYDGLGGKEMPFYENFYAGGSSTV
MG1655	RGFQSNITIGPKAVYFFHQASNYDPDYDECATQDQAKDLCKSDDAVGGNAMAVASLEFII
EcN	RGFQSNITIGPKAVYFFHQASNYDPDYDECATQDQAKDLCKSDDAVGGNAMAVASLEFII
CFT073	RGFQSNITIGPKAVYFFHQASNYDPDYDECATQDQAKDLCKSDDAVGGNAMAVASLEFII
SE11	RGFQSNITIGPKAVYFFHQASNYDPDYDECATQDQAKDLCKSDDAVGGNAMAVASLEFII
SE15	RGFQSNITIGPKAVYFFHQASNYDPDYDECATQDQAKDLCKSDDAVGGNAMAVASLEFII
IAI1	RGFQSNITIGPKAVYFFHQASNYDPDYDECATQDQAKDLCKSDDAVGGNAMAVASLEFII
MG1655	PTPFI SDKYANSVRTSFFWDMGTVWDTINWSSQYSGYPDYS DPSNIRMSAGIALQWMSPL
EcN	PTPFI SDKYANSVRTSFFWDMGTVWDTINWSSQYSGYPDYS DPSNIRMSAGIALQWMSPL
CFT073	PTPFI SDKYANSVRTSFFWDMGTVWDTINWSSQYSGYPDYS DPSNIRMSAGIALQWMSPL
SE11	PTPFI SDKYANSVRTSFFWDMGTVWDTINWSSQYSGYPDYS DPSNIRMSAGIALQWMSPL
SE15	PTPFI SDKYANSVRTSFFWDMGTVWDTINWSSQYSGYPDYS DPSNIRMSAGIALQWMSPL
IAI1	PTPFI SDKYANSVRTSFFWDMGTVWDTINWSSQYSGYPDYS DPSNIRMSAGIALQWMSPL
MG1655	GPLVFSYAQPFKKYDGDKAEQFQFNIGKTIW
EcN	GPLVFSYAQPFKKYDGDKAEQFQFNIGKTIW
CFT073	GPLVFSYAQPFKKYDGDKAEQFQFNIGKTIW
SE11	GPLVFSYAQPFKKYDGDKAEQFQFNIGKTIW
SE15	GPLVFSYAQPFKKYDGDKAEQFQFNIGKTIW
IAI1	GPLVFSYAQPFKKYDGDKAEQFQFNIGKTIW

**8.4. Prophages of EcN, CFT073, SE11, SE15, IAI1 and MG1655**

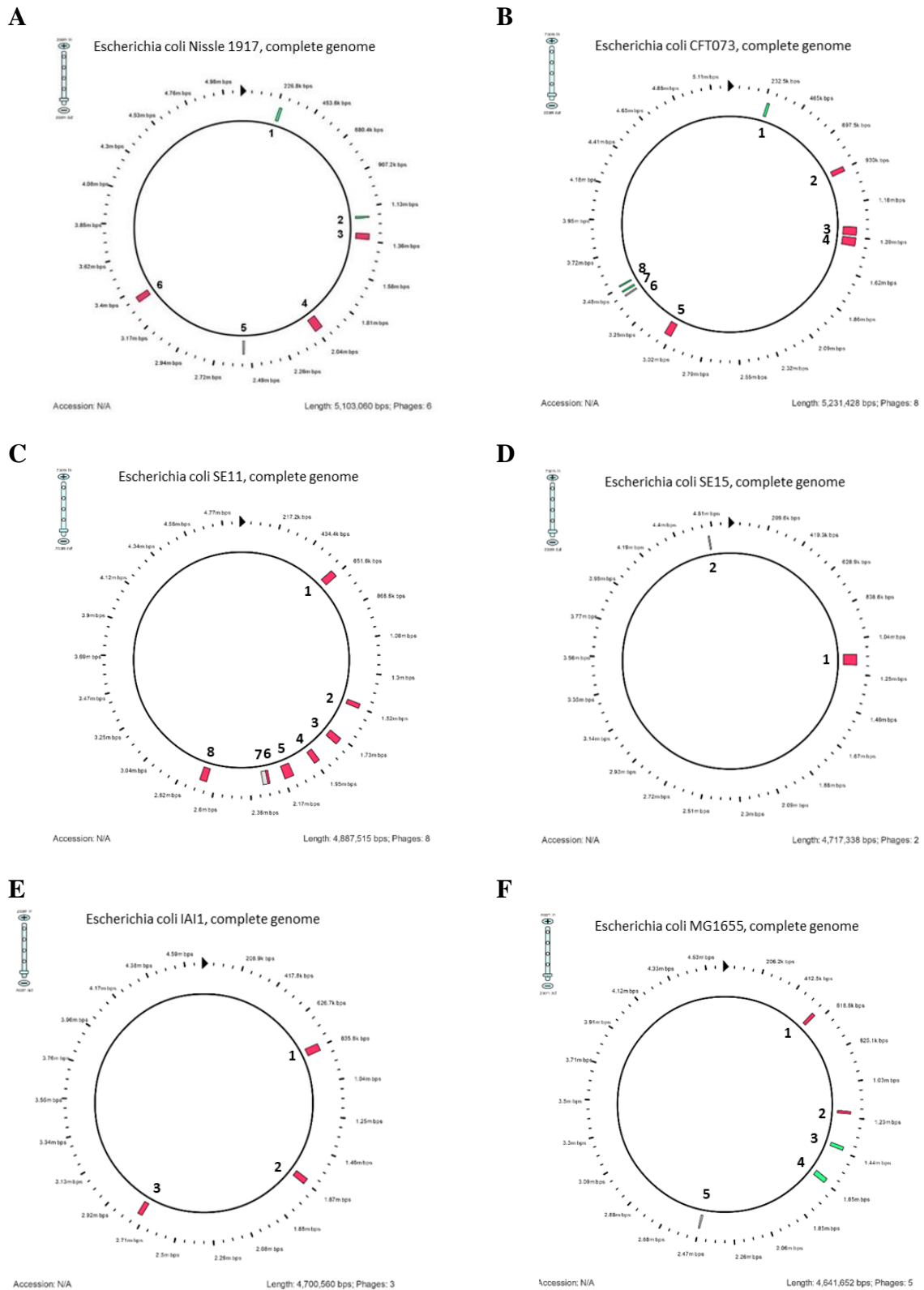


**Figure 53: PHAST prophage prediction of (A) EcN, (B) CFT073, (C) SE11, (D) SE15, (E) IAI1 and (F) MG1655. Red: intact prophage, white: incomplete prophage, green: questionable prophage.**

**Table 17: PHAST predicted prophages of EcN.** Yellow colored: lambdoid prophage.

	Completeness	Size [Kb]	CDS	Phage type
1	questionable	18.8	32	PHAGE_Klebsi_vB_KpnP_KpV475_NC_031025
2	questionable	15.1	25	PHAGE_Bacill_PfEFR_5_NC_031055
3	intact	45.5	52	PHAGE_Enterolambda_NC_001416
4	intact	59	56	PHAGE_Enteroc_1_NC_019706
5	incomplete	11.2	15	PHAGE_Enterolambda_NC_001901
6	intact	38.8	21	PHAGE_Enterolambda_NC_005856

**Table 18: PHAST predicted prophages of CFT073.** Yellow colored: lambdoid prophages.

	Completeness	Size [Kb]	CDS	Phage type
1	questionable	17.6	32	PHAGE_Klebsi_vB_KpnP_KpV475_NC_031025
2	intact	36.5	46	PHAGE_Salmon_Fels_2_NC_010463
3	intact	56.6	72	PHAGE_Enterolambda_NC_001416
4	intact	57.5	82	PHAGE_Enterolambda_NC_001416
5	intact	49.4	61	PHAGE_Enterolambda_NC_019711
6	incomplete	9.4	7	PHAGE_Stx2_c_1717_NC_011357
7	questionable	12.8	13	PHAGE_Stx2_c_1717_NC_011357
8	questionable	8.5	7	PHAGE_Stx2_c_1717_NC_011357

**Table 19: PHAST predicted prophages of SE11.** Yellow colored: lambdoid prophages.

	Completeness	Size [Kb]	CDS	Phage type
1	intact	50.3	59	PHAGE_Enterolambda_NC_001416
2	intact	30.7	35	PHAGE_Enterolambda_NC_009514
3	intact	47.6	67	PHAGE_Enterolambda_NC_001416
4	intact	39.0	52	PHAGE_Enterolambda_NC_026014
5	intact	60.1	63	PHAGE_Enterolambda_NC_001416
6	intact	19.3	23	PHAGE_Enterolambda_NC_000078
7	incomplete	30.7	22	PHAGE_Pectob_ZF40_NC_019522
8	intact	45.5	57	PHAGE_Escher_D108_NC_013594

**Table 20: PHAST predicted prophages of SE15.** Yellow colored: lambdoid prophage.

	Completeness	Size [Kb]	CDS	Phage type
1	intact	67.5	63	PHAGE_Enterolambda_NC_001416
2	incomplete	8.8	11	PHAGE_Klebsi_vB_KpnP_KpV475_NC_031025

**Table 21: PHAST predicted prophages of IAI1.** Yellow colored: lambdoid prophages.

	Completeness	Size [Kb]	CDS	Phage type
<b>1</b>	intact	48.9	53	PHAGE_Enterolambda_NC_001416
<b>2</b>	intact	37.8	46	PHAGE_Enterolambda_NC_001416
<b>3</b>	intact	31.9	41	PHAGE_SalmonSEN34_NC_028699

**Table 22: PHAST predicted prophages of MG1655.** Yellow colored: lambdoid prophage.

	Completeness	Size [Kb]	CDS	Phage type
<b>1</b>	intact	10.7	17	PHAGE_Enterolambda_NC_001416
<b>2</b>	intact	18.0	21	PHAGE_ShigelSfIV_NC_022749
<b>3</b>	questionable	23.0	28	PHAGE_ShigelPOCJ13_NC_025434
<b>4</b>	questionable	33.8	37	PHAGE_Salmon118970_sal3_NC_031940
<b>5</b>	incomplete	12.3	18	PHAGE_ShigelSfIV_NC_022749

### **8.5. *E. coli* investigation for the Type 3,4,6 Secretion Systems**

**Table 23: T346Hunter predicted T6SS genes (Martinez-Garcia et al., 2015).** -: not present.

	Core components of the T3SS	Core components of the T4SS	Core components of the T6SS
EcN	11	-	13
CFT073	11	-	13
SE11	11	-	13
SE15	11	-	13
IAI1	11	-	13
MG1655	11	-	-



**8.6. List of abbreviations**

aa	amino acid
abi	abortive infection
Ag43	adhesin antigen 43
AHL	acyl homoserine lactones
Amp	ampicillin
ATP	adenosine triphosphate
BGs	bacterial ghosts
BLAST	basic local alignment search tool
bp	base pair
°C	degree Celsius
CaCl <sub>2</sub>	calcium chloride
CDS	Coding sequence
CFUs	colony forming units
cm	centimeter
CRISPR-Cas	Clustered Regularly Interspaced Short Palindromic Repeats
d	distilled
DEAC	diffusely adherent <i>E. coli</i>
DMSO	dimethylsulfoxid
DNA	deoxyribonucleic acid
ds	double stranded
EAEC	enteroaggregative <i>E. coli</i>
ECC	Chromogenic <i>E. coli</i> coliform agar
EDTA	Ethylenediaminetetraacetic acid
EcN	<i>E. coli</i> Nissle 1917
<i>E. coli</i>	<i>Escherichia coli</i>
<i>E. coli</i> <sup>+C</sup>	<i>E. coli</i> cultured in LB medium + Cellulase
<i>E. coli</i> <sup>x</sup>	1 h, 100 °C heat killed <i>E. coli</i>
e. g.	exempli gratia
EHEC	enterohemorrhagic <i>E. coli</i>
EIEC	enteroinvasive <i>E. coli</i>
ELISA	enzyme-linked immunosorbent assay
EPEC	enteropathogenic <i>E. coli</i>

EPS	exopolysaccharides
ER	endoplasmatic reticulum
EtBr	ethidium bromide
ETEC	enterotoxigenic <i>E. coli</i>
EtOH	Ethanol
F	fimbriae
g	gram
Gb3	Globotriaosylceramide
GI	gastrointestinal tract
h	hour
H	flagellum
HCl	hydrogen chloride
H <sub>2</sub> O	water
HUS	hemolytic uremic syndrome
IPTG	Isopropyl $\beta$ -D-1-thiogalactopyranoside
K	capsule
l	liter
LB	Luria-Bertani
LPS	lipopolysaccharide
m	Milli, meter
M	Molar, Marker
$\mu$	micro
MG1655R	recombinant MG1655
min	minutes
MMC	Mitomycin C
MOI	Multiplicity of infection
MUSCLE	multiple sequence alignment
n	nano
NMEC	neonatal meningitis <i>E. coli</i>
nt	nucleotides
ns	not significant
OD	optical density
ONC	overnight culture
OMVs	outer membrane vesicles

PCR	polymerase chain reaction
pfus	plaque forming units
PHAST	PHAge Search Tool
P. I.	proteinase inhibitor cocktail
PK	proteinase K
PPA	Phage-Plaque-Assay
<i>pr</i>	phage repressor
qRT-PCR	Real-Time Quantitative Reverse Transcription PCR
r	ribosomal
R	rough LPS
RKI	Robert Koch Institute
R-M	restriction-modification
RNA	ribonucleic acid
rpm	revolutions per minute
RT	room temperature
S	smooth LPS
SD	standard deviation
<i>S. dysenteriae</i>	<i>Shigella dysenteriae</i>
sec	second
SEPEC	sepsis-associated <i>E. coli</i>
sie	superinfection exclusion
sn	supernatant
ss	single stranded
STEC	Shiga toxin producing <i>E. coli</i>
Stx	Shiga toxin
t	transfer
TAE	Tris-acetate-EDTA
TEM	transmission electron microscope
<i>trp</i>	tryptophan repressor binding gene
U	units
ud	undiluted
UPEC	uropathogenic <i>E. coli</i>
UV	ultraviolet
VLP	virus like particles

VTEC	Verotoxin producing <i>E. coli</i>
WHO	World Health Organization
x g	times gravity
*	p<0.05
**	p<0.01
***	p<0.001
****	p<0.0001

**8.7. List of figures**

<b>Figure 1: Antigenic surface structures of <i>E. coli</i>.</b> .....	9
<b>Figure 2: Phylogenetic tree of <i>E. coli</i>.</b> .....	10
<b>Figure 3: EcN's fitness factors.</b> .....	12
<b>Figure 4: Schematic figure of Shiga toxin.</b> .....	14
<b>Figure 5: Pathology of kidneys from baboons being challenged with shiga toxins.</b> .....	15
<b>Figure 6: 933W stx2-prophage regulation.</b> .....	18
<b>Figure 7: Model of a DNA bacteriophage assembly.</b> .....	20
<b>Figure 8: Bacterial lysis, lysogenization by bacteriophages.</b> .....	21
<b>Figure 9: Mechanisms to prevent phage adsorption.</b> .....	23
<b>Figure 10: 100 bp DNA Ladder.</b> .....	30
<b>Figure 11: GeneRuler 100 bp DNA Ladder.</b> .....	30
<b>Figure 12: GeneRuler 1 kb DNA Ladder.</b> .....	30
<b>Figure 13: Schematic figure of the EDL933 “insert transfer” from an insert with only LB medium or with SK22D in the well into a new insert with LB medium in the well.</b> .....	44
<b>Figure 14: Schematic instruction of agarose slab preparation.</b> .....	51
<b>Figure 15: <i>E. coli</i> colonies on ECC plates.</b> .....	53
<b>Figure 16: PCR screen to identify specific chromosomal regions of EcN and the K-12 strains.</b> .....	54
<b>Figure 17: PCR screen to identify specific chromosomal regions of EcN and CFT073.</b> ..	55
<b>Figure 18: PCR screen to identify specific chromosomal regions of EcN and the commensal control strains SE11, SE15 and IAI1.</b> .....	56
<b>Figure 19: PCR screen to identify specific chromosomal regions of the STEC strains EDL933 the 2011 outbreak strains TY3730 and TY3456 (O104:H4).</b> .....	57
<b>Figure 20: PCR screen to identify the microcin mutant SK22D.</b> .....	60
<b>Figure 21: PCR screen to identify the EcN mutants EcN<math>\Delta</math><i>bcs</i>, EcN<math>\Delta</math><i>csg</i>, EcN<math>\Delta</math><i>k5</i>.</b> .....	61
<b>Figure 22: PCR screen to identify the EcN mutants EcN<math>\Delta</math><i>fliC</i>, EcN<math>\Delta</math><i>pks</i>.</b> .....	62
<b>Figure 23: PCR screen to identify the EcN mutant EcN<math>\Delta</math><i>sat</i>.</b> .....	63
<b>Figure 24: Stx level, stx-phage titer and CFU kinetics of the EHEC strain EDL933 in mono-/co-/ and triculture.</b> .....	65
<b>Figure 25: Stx and stx-phage kinetics after MMC induction.</b> .....	67
<b>Figure 26: Stx level and stx-phage titer of <i>stx2</i> and <i>stx1</i> STEC strains in mono-/co- (1:10)/ and triculture (1:10:10) with SK22D and/or MG1655.</b> .....	69

Figure 27: <i>stx</i> -phage detection by PCR in the supernatant of the mono-/co- and tricultures.....	71
Figure 28: PCR screen to detect genes spanning the entire <i>stx2</i> -phage genome in the supernatant of the mono-/ and cocultures.....	73
Figure 29: Stx-ELISA of isolated Stx. ....	74
Figure 30: Determination of the <i>stx2a</i> stability in the absence and presence of EcN. ....	75
Figure 31: Investigation of the Stx reduction by SK22D's supernatant or heat killed SK22D.....	76
Figure 32: Stx and <i>stx</i> -phage kinetics of EDL933 in the Transwell system.....	78
Figure 33: Stx and <i>stx</i> -phage reduction efficiency of SK22D in the Transwell system....	81
Figure 34: Electron microscopy images of <i>stx</i> -phages and the <i>E. coli</i> strains EcN and MG1655.....	83
Figure 35: Bacterial lysis by <i>stx</i> -phages. ....	85
Figure 36: Identification of EcN and MG1655 <i>stx</i> -prophage lysogens.....	86
Figure 37: Analysis of the transcriptome of EcN cocultured with <i>stx</i> -phages.....	88
Figure 38: Phage Plaque Assay with MG1655 recombinant strains.. ....	90
Figure 39: <i>stx</i> -phage reduction kinetics. ....	91
Figure 40: PCR screen for the <i>stx</i> -phage localization. ....	92
Figure 41: Identification of the <i>stx</i> -phage inactivation by various <i>E. coli</i> strains.....	93
Figure 42: Investigation of the <i>stx</i> -phage inactivation agent.....	96
Figure 43: <i>stx</i> -phage inactivation by EcN surface mutants. ....	98
Figure 44: Investigation of the biofilm of EcN, CFT073 and MG1655 for <i>stx</i> -phage inactivating activities.....	101
Figure 45: Investigation of the biofilm of EcN, and the biofilm mutants EcN $\Delta$ <i>bcs</i> and EcN $\Delta$ <i>csg</i> for <i>stx</i> -phage inactivating activities. ....	102
Figure 46: SK22D protects K-12 strains from <i>stx</i> -phage infection.....	104
Figure 47: Light microscope study of the <i>E. coli</i> growth formations.....	105
Figure 48: Kinetics of MG1655 phage infection or protection by SK22D.....	109
Figure 49: Protection of MG1655 against <i>stx</i> -phage infection by various <i>E. coli</i> strains. ....	111
Figure 50: Protection of MG1655 infection by <i>stx</i> -phages from the 2011 O104:H4 outbreak strains.....	113
Figure 51: Protection of MG1655 in the Transwell system.....	115
Figure 52: Transcriptome analysis of EcN's prophages.....	154

<b>Figure 53: PHAST prophage prediction of (A) EcN, (B) CFT073, (C) SE11, (D) SE15, (E) IAI1 and (F) MG1655. ....</b>	<b>156</b>
---	------------

### **8.8. List of tables**

<b>Table 1: Laboratory equipment and materials. ....</b>	<b>27</b>
<b>Table 2: Chemicals used in this study. ....</b>	<b>28</b>
<b>Table 3: E. coli strains used in this study. ....</b>	<b>31</b>
<b>Table 4: Oligonucleotides used in this study. ....</b>	<b>33</b>
<b>Table 5: LB-medium composition. ....</b>	<b>37</b>
<b>Table 6: 0.7 % LB-Agar composition. ....</b>	<b>38</b>
<b>Table 7: 1.5 % LB-Agar composition. ....</b>	<b>38</b>
<b>Table 8: Kits used in this study. ....</b>	<b>38</b>
<b>Table 9: Transwell assay set up. ....</b>	<b>44</b>
<b>Table 10: Taq Polymerase PCR reaction. ....</b>	<b>46</b>
<b>Table 11: Phusion polymerase PCR reaction. ....</b>	<b>46</b>
<b>Table 12: Deletion or insertion regions of EcN mutants. ....</b>	<b>58</b>
<b>Table 13: Presence of EcN's lambdoid prophage genes in CFT073, the commensal strains SE11, SE15 and IAI1 and the K-12 strain MG1655. ....</b>	<b>123</b>
<b>Table 14: Biofilm components of the E. coli strains EcN, CFT073, SE11, SE15, IAI1 and MG1655. ....</b>	<b>128</b>
<b>Table 15: Genes of the <i>stx2</i>-prophage. ....</b>	<b>151</b>
<b>Table 16: Amino acid sequence comparison of the <i>E. coli</i> strains MG1655, EcN, CFT073, SE11, SE15 and IAI1. ....</b>	<b>155</b>
<b>Table 17: PHAST predicted prophages of EcN. ....</b>	<b>157</b>
<b>Table 18: PHAST predicted prophages of CFT073. ....</b>	<b>157</b>
<b>Table 19: PHAST predicted prophages of SE11. ....</b>	<b>157</b>
<b>Table 20: PHAST predicted prophages of SE15. ....</b>	<b>157</b>
<b>Table 21: PHAST predicted prophages of IAI1. ....</b>	<b>158</b>
<b>Table 22: PHAST predicted prophages of MG1655. ....</b>	<b>158</b>
<b>Table 23: T346Hunter predicted T6SS genes (Martinez-Garcia et al., 2015). ....</b>	<b>158</b>

### **8.9. Workshops**

- Biochemistry, physiology and genetics of mammalian cell culture
- Intercultural communication and cooperation
- Analyzing your market potential as a scientist
- Good Scientific Practice
- Poster Design

### **8.10. Additional Activities**

- 01.05.2016 - 01.08.2016

Mentoring of a DAAD's RISE student majoring in Food Science at the University of Wisconsin-Madison, United States.

- 17.10.2016 - 11.02.2017

University Course: „Entscheidungsorientierte Einführung in die Betriebswirtschaftslehre“

- 01.11.2016 - 01.11.2017

Member of the Organizing Committee of the 11<sup>th</sup> International GSLS Student Symposium

- 25.04.2017 - 27.04.2017

Training: „Sicherheit und Gesundheitsschutz in Laboratorien - Schwerpunkt Biologie und Gentechnik“



**8.11. Curriculum Vitae**

## Appendix

---

### Professional Experience

---

Würzburg,

Susanne Bury